

MORPHOGENESIS IN THE MOSS

*PHYSCOMITRELLA PATENS*

by

Angela Julia Russell



A thesis submitted in accordance  
with the requirements for the degree of  
Doctor of Philosophy

September 1993

Department of Genetics

University of Leeds

## ABSTRACT

A method was developed for recording the development of moss protonema using time-lapse video microscopy. This has provided a detailed record of the time-course of development from spore germination to the production of gametophores. Detailed records of the growth of primary and secondary chloronema, the transition of primary chloronema to caulonema, and the development of side-branches were obtained. Filaments were found to undergo the transition to caulonema earlier than previously thought. The majority of caulonema side-branches were found to begin as chloronema and switch to caulonema after one or two cell cycles. The early cell divisions of bud formation were found to follow a distinct pattern, which was upset by high concentrations of cytokinin and lanthanum. The response of caulonema apical cells to polarotropic light was recorded and compared to the gravitropic response.

The time-lapse studies provided the basis for the further development of the quantitative analysis of protonemal branching patterns to include second and third side-branches of a sub-apical cell, and transitional caulonema. Analysing side-branch patterns should allow the detection of developmental mechanisms underlying the determination of side-branch fate. The potential of this method for assessing the effect of hormone treatments and for analysing more precisely mutant phenotypes was explored. An analysis of bud spacing was carried out to determine if the formation of a bud on a filament was inhibitory to other buds forming on the same filament. It was found, to the contrary, that buds tended to form in clusters.

The hypothesis that the primary mode of action of cytokinin is an enhanced influx of calcium ions into the cell was investigated. Classical electrophysiology was used in order to detect any change in membrane potential suggestive of ionic fluxes in response to cytokinin treatment. No definitive changes in membrane potential were detected in response to cytokinin. This appeared to rule out the involvement of

voltage-regulated channels in cytokinin action. The effects of some inhibitors used in studies of calcium on the moss protonemal system were examined. It is suggested that the concentrations commonly used had toxic effects that were not specific to calcium channels. The ionophore A23187 was used to characterise the protonemal response to a sustained influx of calcium. Some mutant strains were found to have a differential response to the ionophore. This may mean that they have mutations affecting their calcium regulatory system.

Two new techniques of imaging calcium were used in order to detect changes in intracellular calcium in response to cytokinin. A method was developed for loading the dual wavelength fluorescent dye Indo-1 into moss protonema using iontophoretic microinjection, and intracellular calcium was imaged using ratio-image technology. Wild-type moss and some mutant strains were also successfully transformed with the gene for apoaequorin, and calcium luminescence measured in response to cold-shock and plant hormones. Some different responses to temperature shock were apparent in one of the transformed mutants. Preliminary experiments did not reveal any aequorin-dependent calcium luminescence in response to cytokinin.

## TABLE OF CONTENTS

### CHAPTER I INTRODUCTION

	page
1.1 Moss as a system for the study of development	1
1.2 The life-cycle of <i>Physcomitrella patens</i>	2
1.3 Cell signalling in plants	6
1.4 The calcium messenger system	9
1.5 Calcium in plant cell signalling	13
1.6 Cytokinin	18
1.7 Project aims	24

### CHAPTER II ANALYSIS OF PROTONEMAL DEVELOPMENT USING TIME-LAPSE VIDEO MICROSCOPY

2.1 Introduction	26
2.2 Materials and Methods	27
2.3 Results and Discussion	29
2.3.1 Development of methodology	29
2.3.2 Spore germination and the transition from primary chloronema to caulonema	30
2.3.3 Secondary chloronema	36
2.3.4 Caulonema	40
2.3.5 Mutant strains	47
2.3.6 Protoplast regeneration	47
2.3.7 Bud development	52
2.3.8 The effect of cytokinin on bud development	57
2.3.9 The effect of light on a dark-grown caulonema filament	60
2.3.10 Polarotropism and the cell cycle	65



## **CHAPTER III BRANCHING PATTERN ANALYSIS**

<b>3.1</b>	<b>Introduction</b>	<b>71</b>
<b>3.2</b>	<b>Methods</b>	<b>74</b>
<b>3.3</b>	<b>Results and Discussion</b>	<b>75</b>
<b>3.3.1</b>	<b>Time-lapse: subapical cell division</b>	<b>77</b>
<b>3.3.2</b>	<b>Side-branch development</b>	<b>77</b>
<b>3.3.3</b>	<b>Branch pattern analysis</b>	<b>79</b>
<b>3.3.4</b>	<b>Plant hormones</b>	<b>85</b>
<b>3.3.5</b>	<b>Mutants</b>	<b>94</b>
<b>3.3.6</b>	<b>Light</b>	<b>102</b>
<b>3.3.7</b>	<b>Bud spacing</b>	<b>102</b>

## **CHAPTER IV ELECTROPHYSIOLOGY AND INHIBITOR STUDY**

<b>4.1</b>	<b>Introduction</b>	<b>113</b>
<b>4.2</b>	<b>Materials and Methods</b>	<b>119</b>
<b>4.3</b>	<b>Results and Discussion</b>	<b>121</b>
<b>4.3.1</b>	<b>Electrophysiology</b>	<b>121</b>
<b>4.3.2</b>	<b>Inhibitors</b>	<b>133</b>

## **CHAPTER V CALCIUM IMAGING**

<b>5.1</b>	<b>Introduction</b>	<b>152</b>
<b>5.1.1</b>	<b>Calcium imaging using fluorescent dyes</b>	<b>152</b>
<b>5.1.2</b>	<b>Transformation with recombinant aequorin</b>	<b>154</b>
<b>5.2</b>	<b>Materials and Methods</b>	<b>157</b>
<b>5.3</b>	<b>Results and Discussion</b>	<b>163</b>
<b>5.3.1</b>	<b>Dye-loading</b>	<b>163</b>
<b>5.3.2</b>	<b>Microinjection</b>	<b>165</b>
<b>5.3.3</b>	<b>Ratio-imaging</b>	<b>169</b>
<b>5.3.4</b>	<b>Transformation</b>	<b>172</b>

**CHAPTER VI GENERAL DISCUSSION**

6.1	Time-lapse microscopy	185
6.1.1	Spore germination and protonemal development	185
6.1.2	Bud formation	188
6.1.3	Effects of cytokinin	189
6.2	Side-branch analysis	190
6.2.1	Hormones	194
6.2.2	Bud spacing	196
6.2	Mutant strains	196
6.4	Calcium and cytokinin action	197
6.4.1	Calcium imaging	197
6.4.2	Transformation with aequorin	199
6.5	Calcium and bud formation	200

**APPENDIX A**

Methods and procedures for <i>Physcomitrella patens</i>	204
---	-----

REFERENCES	209
------------	-----

## LIST OF TABLES

### CHAPTER II

Table		page
2.1	The change in growth rate and cell cycle time in relation to cell length in a filament undergoing the transition from primary chloronema to caulonema	35
2.2	A comparison of spore germination in <i>P. patens</i> and <i>F. hygrometrica</i>	39
2.3	Increase in growth rate and size of caulonema cells with age	43
2.4	The cell cycle times, length and growth rates of caulonema apical cells of different ages	45
2.5	The cell cycle times, length and growth rates of selected mutant strains	48

### CHAPTER III

Table:		
3.1	The subapical position of side-branch differentiation	78
3.2	Side-branch analysis of the first 20 cell positions of caulonema filaments of wt <i>P. patens</i>	81
3.3	Side-branch analysis of wt <i>P. patens</i>	82
3.4	Analysis of side-branches occurring in pairs on the first 20 cells of 150 filaments of wt <i>P. patens</i>	86
3.5	Side-branch analysis of cultures of wt <i>P. patens</i> treated with various concentrations of BAP and NAA	87
3.6	Side-branch analysis of <i>P. patens</i> treated with 30nM BAP	89
3.7	Side-branch analysis of <i>P. patens</i> treated with 100 nM BAP	90
3.8	Side-branch analysis of <i>P. patens</i> treated with 1µM BAP	91
3.9	Side-branch analysis of <i>P. patens</i> treated with 1µM NAA	97
3.10	Side-branch analysis of two mutant strains	99
3.11	Side-branch analysis of the mutant <i>gam-139</i>	100
3.12	Side-branch analysis of the mutant <i>nar-87</i>	101
3.13	Side-branch analysis of wt <i>P. patens</i> treated with light of 300mW	103
3.14	Analysis of buds on 445 wt filaments of <i>P. patens</i>	105
3.15	Analysis of the spacing between pairs of buds	106
3.16	Analysis of buds on filaments treated with 50µM A23187	108
3.17	Analysis of buds on filaments treated with 30µM BAP	111
3.18	Analysis of buds on filaments treated with 50µM BAP	112

### CHAPTER IV

4.1	Summary of experiments on the effects of hormones on membrane potential in <i>P. patens</i> and <i>F. hygrometrica</i>	123
4.2	The effect of the inhibitors verapamil, nifedipine and trifluoperazine on growth and cytokinin-induced bud production in <i>P. patens</i>	134

## LIST OF FIGURES

CHAPTER I		page
1.1	Cell lineage of <i>P. patens</i>	3
CHAPTER II		
2.1	Culture chamber used for time-lapse filming	28
2.2	The germination of a spore of <i>P. patens</i>	32
2.3	The growth of primary chloronema of <i>P. patens</i>	33
2.4	The growth of a filament undergoing the transition to caulonema	34
2.5	The germination of a spore of <i>F. hygrometrica</i>	38
2.6	The growth of secondary chloronema filaments	41
2.7	The growth of two transitional side-branches	42
2.8	The growth of secondary chloronema compared to secondary caulonema	44
2.9	The growth and cell cycle times of caulonema of 4 mutant strains	49
2.10	Protoplast regeneration in <i>P. patens</i>	51
2.11	Bud formation in <i>P. patens</i>	54
2.12	" " " "	56
2.13	Cytokinin induced bud formation in <i>P. patens</i>	59
2.14	The effect of light on the apical cell of a dark-grown filament	62
2.15	The growth rate of a dark-grown filament exposed to light	63
2.16	The polarotropic response of <i>P. patens</i>	66
CHAPTER III		
3.1	The well plate method of growing <i>P. patens</i>	76
3.2	The effect of subapical cell position on side-branch production	83
3.3	The effect of cell position on cytokinin-induced bud formation	93
3.4	A comparison of the effect of 1 $\mu$ M BAP on bud formation in wt <i>P. patens</i> and the gam strain bar-576	95
3.5	A comparison of low-level responses to BAP and the wt response to 1 $\mu$ M BAP	96
3.6	The spacing between pairs of buds on the first 20 cell positions of wt caulonema	107
3.7	The effect of A23187 on bud production in <i>P. patens</i>	109
3.9	Buds developing on the basal cells of side-branches and in clusters in wt <i>P. patens</i>	110a
CHAPTER IV		
4.1	The effect of BAP (1 $\mu$ M) on membrane potential in wt <i>P. patens</i>	124
4.2	The effect of NAA (20 $\mu$ M) on membrane potential in wt <i>P. patens</i>	124
4.3	The effect of BAP (1 $\mu$ M) on membrane potential in <i>F. hygrometrica</i>	125
4.4	The effect of pH on membrane potential of <i>F. hygrometrica</i>	125
4.5	The effect of BAP (10 $\mu$ M) on membrane potential in wt <i>P. patens</i>	126
4.6	The effect of DR-OPP (4 $\mu$ g/ml) on membrane potential in wt <i>P. patens</i>	127
4.7	The effect of caffeine and BAP on membrane potential in wt <i>p. patens</i>	128
4.8	The effect of BAP (5 $\mu$ M) and DR-OPP on membrane potential	



	in gam-710	129
4.9	The effect of BAP (5 $\mu$ M) on membrane potential in nar-87	129
4.10	The addition of BAP (100nM) to <i>P. patens</i>	135
4.11	The addition of verapamil (30 $\mu$ M) to <i>P. patens</i>	135
4.12	The addition of Nifedipine (20 and 40 $\mu$ M) to <i>P. patens</i>	136
4.13	The addition of Trifluoperazine to wt <i>P. patens</i>	137
4.14	Time-lapse sequence of the effect of Nifedipine	140
4.15	The effect of 500 $\mu$ M LaCl	142
4.16	The effect of 100 $\mu$ M LaCl on the growth of <i>P. patens</i>	143
4.17	The effect of 80uM LaCl on the early cell divisions of bud formation	146
4.18	The addition of 40 $\mu$ MA23187 to wt <i>P. patens</i>	148
4.19	The addition of 40 $\mu$ M A23187 to bar-1	149
4.20	The addition of 40 $\mu$ M A23187 to bar-576	149
4.21	The addition of 40 $\mu$ M A23187 to gam-710	150
4.22	The addition of 40 $\mu$ M A23187 and 1 $\mu$ M BAP to gam-710	150

## CHAPTER V

5.1	The fluorescent dual emission dye Indo-1	155
5.2	The plasmid pAQNEO1	161
5.3	Fluorescence micrographs of cells of <i>P. patens</i> after incubation in the single wavelength dye Fluo-3.	164
5.4	Caulonema filament of <i>P. patens</i> before and after microinjection with Indo-1	166
5.5	Caulonema subapical cell of <i>P. patens</i> showing dye diffusing through the cytoplasm after successful microinjection	167
5.6	Caulonema subapical cell of <i>P. patens</i> damaged by microinjection	168
5.7	Ratio image of a caulonema subapical cell	170
5.8	Ratio image of a caulonema subapical cell	171
5.9	Ratio images of caulonema subapical cells incubated for varying periods in BAP (1 $\mu$ M)	174
5.10	Western blot expression of apoaequorin	175
5.11	The stable transformation of 3 mutant strains	177
5.12	In vivo reconstitution of apoaequorin in whole cultures of <i>P. patens</i>	178
5.13	The effect of temperature-shock and BAP on calcium-dependent aequorin luminescence	179
5.14	The effect of temperature shock on calcium-dependent aequorin luminescence in three mutant strains	180
5.15	Image of calcium-dependent aequorin luminescence in response to cold-shock in wt <i>P. patens</i>	181
5.16	The effect of high pH on calcium-dependent aequorin luminescence in three mutant strains	183

## CHAPTER VI

6.1	Stylised diagram of the developmental fates of side-branches	192
-----	--	-----

## **ACKNOWLEDGEMENTS**

I would like to thank my supervisor, Professor D.J. Cove, for his advice and encouragement throughout this project. I would like to thank Celia Knight and Wolfgang Kammerer, my colleague Dave Atkinson and all my colleagues in the moss lab for their interest, assistance and discussions.

I am indebted to the Edinburgh Cell Signalling Group for using the facilities in their lab. I would like to thank Professor T. Trewavas, Nick Read, Heather and Mark Knight for their help and suggestions, and for providing pAQNEO1.

I wish to thank Dr. Dale Saunders for the use of facilities in the Botany department at York. Especially I thank Helmuth Hohmeyer for his tuition in electrophysiology.

I especially thank my son Anton for his technical assistance with the presentation of this thesis.

I acknowledge the receipt of an award from the Science and Engineering Research Council.



## LIST OF ABBREVIATIONS

ABA	abscissic acid
BAP	6-benzyl aminopurine
cAMP	cyclic adenosine 5' monophosphate
DAG	diacylglycerol
DMSO	dimethylsulphoxide
DR-OPP	thidiazuron
EPGF	epidermal growth factor
GA	gibberellic acid
HPLC	high performance liquid chromatography
IAA	indole-acetic acid
IP <sub>3</sub>	inositol triphosphate
NAA	napthalene acetic acid
nic	nicotinic acid
paba	p-Amino Benzoic acid
PEG	polyethylene glycol
sbi	side-branch initial
SRM	standard recording medium
thi	thiamine

## CHAPTER I

### INTRODUCTION

Plant morphogenesis involves a complex interaction between internal and external factors controlling growth and development. Plants exist in a fixed position in relation to the external environment, and as such are subject to continual fluctuations in light quality and quantity, temperature, pH, nutrient and water availability. All these constitute incoming signals which may influence and modulate endogenous controls of gene expression. Directional stimuli may also contribute to the morphogenetic phenotype of a plant. The study of development therefore involves all aspects of how a plant transduces the numerous signals available to it both internal and external, into the synthesis and moderation of gene products necessary for phenotypic expression at each stage of its life-cycle.

#### 1.1 Moss as a System for the Study of Development

The spores of moss give rise to filaments of single cells, which can be regarded as a "one-dimensional" growth form. In a few species of moss, protonemata develop into prothalli, a two-dimensional form, but in most, protonemata give rise directly to the leafy gametophore, the three-dimensional growth form. The protonemal phase of moss has been of interest in the study of development ever since Sironval (1947) distinguished two phases in the growth of protonema of *Funaria hygrometrica*, which he named the chloronema and caulonema, and subsequent work discovered the importance of plant hormones in the differentiation of each stage. In 1957 Gorton and Eakin demonstrated that the synthetic cytokinin kinetin supplied exogenously induces bud formation in the protonema of *Tortella caespitosa*. Since then this and other cytokinins have been found to induce buds in the majority of species of moss tested. Evidence that auxin was involved in moss development came from the work of Johri and Desai (1973) who demonstrated that

exogenous auxin induces the transition from chloronema to caulonema in a suspension culture of *F. hygrometrica*. Under these conditions, the formation of caulonema does not occur spontaneously. For both cytokinin and auxin, therefore, the hormone could be shown to control a discrete step in development at the level of the single cell. Subsequently endogenous production of most of the major classes of growth factors have been reported in mosses: auxins (Sheldrake, 1971; Ashton *et al*, 1985) cytokinins (Beutlemann, 1973; Wang *et al*, 1980) abscissic acid (Menon and Lal, 1974) and ethylene (Rowler and Bopp, 1985). As the primary mode of action of all these hormones remains unknown, their study in moss offers an alternative system to higher plants, and further enables their effects to be examined at the level of the single cell.

## 1.2 The Life Cycle of *Physcomitrella patens*

A number of reviews detail the life cycles of both *P. patens* and *F. hygrometrica* (see, for example, Bopp, 1980, 1983; Knoop, 1984 for *F. hygrometrica*, Cove, 1984, 1992; Wang *et al*, 1984 for *Physcomitrella patens*). Since this project is concerned with clarifying some aspects of these, a brief overview will be given here. Fig. 1.1 shows a cell lineage of *P. patens*, including some of the factors known to affect each developmental step. In both species, it is convenient to take as the first step in development the emergence from the spore of a single germ-tube, which establishes the polarity of the germinating spore. This has been more fully described in the case of *F. hygrometrica* (Knoop, 1984). In *F. hygrometrica* the germ-tube may be either a primary rhizoid or a chloronema (Bopp, 1980). Knoop (1984) established that the polarity of germination depends on the light conditions, high light encouraging a bipolar germination where the pale negatively phototropic germ rhizoid emerges from the shaded side of the spore simultaneously with the positively phototropic chloronema. A germ rhizoid has not been reported in *P. patens*. Gradients of calcium (Chen and Jaffe, 1979) have been reported as playing a



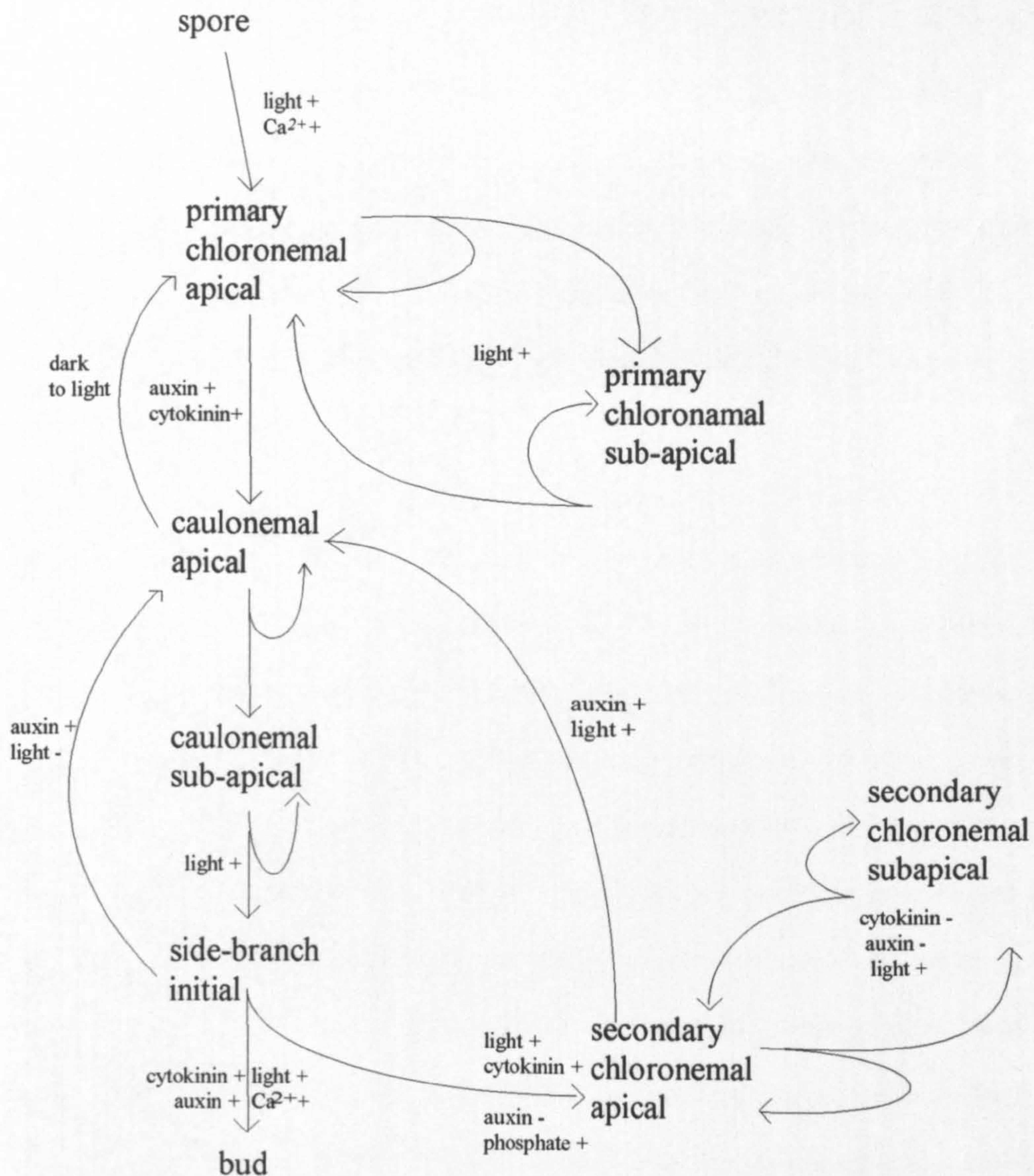


Fig.1.1 Cell lineage of *Physcomitrella patens* showing stages affected by phytohormones, light and other environmental factors.

- + the developmental step requires or is enhanced by the treatment
- the developmental step is blocked or inhibited by the treatment

From: Cove and Knight (1993)

The inclusion of light as a requirement for secondary chloronemal apical cells to undergo the transition to caulonemal apical cells is as a result of this thesis.



role in the establishment of polarity in *F. hygrometrica*. Experiments with *P. patens* have suggested that while the primary germ-tube or filament responds phototropically (Cove and Schild, 1978), the position at which it emerges from the spore is unrelated to light direction. Having reached a certain length the first filament separates from the spore by cell division either in the filament or still within the spore (Knoop, 1984).

The first protonemal cell type, known as primary chloronemata, develops from the chloroplast-rich germ tube (Knoop, 1984). In *P. patens*, these cells are slow-growing, and in a previous study were reported as dividing once approximately every 20 hours. They are distinguished cytologically by having cross walls perpendicular to the axis of growth, and being packed with round chloroplasts. Growth of the cells occurs only at the extreme apical portion of the cell, and elongation of the filament is by division of the apical cell. Subapical cells divide once or twice to produce side branches but do not undergo further elongation. Approximately a week after germination, depending on culture conditions, apical chloronema cells undergo a transition leading to the production of a new cell type, the caulonema apical cell. While the chloronema apical cell is axially unpolarised, the caulonema apical cell of *F. hygrometrica* has a highly polarised appearance which can be divided into distinct cytoplasmic zones (Schmeidel and Schnepf, 1980). Caulonema cells grow much faster than chloronema (reported growth rates are up to 40µm/h for dark-grown filaments of *P. patens* (C. Knight, unpublished data)) and divide three times more frequently, to produce highly vacuolate subapical cells, with smaller spindle-shaped chloroplasts arranged around the cell cortex.

In the light, the second cell in a chloronema filament or the third or fourth cells in a caulonema filament divide to form a side-branch. Very low levels of light are required to saturate this process (Jenkins and Cove, 1983). It is reported for *P. patens* that chloronema subapical cells only give rise to secondary chloronema side-

branches (D. McClelland, 1988). Once the main filaments have become caulonema, side-branches on the caulonema subapical cells can develop into any of three types of tissue, secondary chloronema, caulonema, or buds. For *P. patens* no previous study has established over how many cell cycles the transition from chloronema to caulonema lasts. In *F. hygrometrica* the literature differentiates more clearly a chloronemal phase where the ramifying protonema, both main filaments and side-branches, are all chloronemal, followed by a caulonemal phase where the tips of all chloronema, which includes the main filament and the side-branches, successively convert to caulonema (Knoop, 1984). This transitional phase in which the daughter cells produced by the growing tip become longer and develop fewer and smaller plastids is described by Knoop as a gradual conversion over four or five cells. Once this stage is reached the primary side-branches usually become caulonema, while second side-branches, if they occur, become secondary chloronema. Knoop (1984) also notes that it is possible to maintain the chloronema phase indefinitely at low light levels. Under these conditions, the growth of filaments remains slow, and the transition to caulonema does not occur. Knoop suggests that the differentiation of chloronema to caulonema requires the establishment of a critical rate of growth before it can occur.

Sironval (1947) working with *F. hygrometrica* reported that it was necessary for protonema to be at the caulonema phase for side-branch initials to develop into buds. In *F. hygrometrica* the development of buds is more markedly associated with the caulonema than in *P. patens*, appearing in a ring around the culture shortly after this phase is reached, and leading Bopp and Brandes (1964, in Knoop, 1984) to relate their appearance to a 'critical size' of the protonema. The time at which buds appear on a culture is very variable. Simon and Naef (1981) report the occurrence of buds on *F. hygrometrica* as early as the 4th day of culture. Buds are reported to occur in *P. patens* ca. 20 days after spore germination (McClelland, 1988).



Knoop (1984) suggests that the organisation of the protonema and its developmental stages result from a combination of factors transported from cell to cell and interactions with alterations of the substrate during culture.

*P. patens* is relatively easy to take through its life cycle in the laboratory. Once the leafy gametophore has developed, the formation of gametes can be induced by lowering the temperature to 15°C. Meiosis occurs in the diploid spore capsules resulting in approximately  $10^4$  haploid spores in each capsule.

Engel (1968) was the first to isolate mutants in the moss *P. patens*. Since then mutagenesis of spores (Ashton *et al*, 1977) and the development of somatic mutagenesis (Boyd *et al*, 1988) have resulted in the isolation of a number of mutants which are blocked at different stages of the life cycle (Knight *et al*, 1988). These have been divided into categories according to their sensitivity to hormones (Cove, 1983; Cove and Ashton, 1983). Many of these are also altered in their pattern of side-branch formation. These, combined with the ease with which it is possible to manipulate environmental conditions, provide scope for the further investigation of the factors, both endogenous and exogenous, influencing each developmental step.

### 1.3 Cell Signalling in Plants

The interrelationship of plant growth and environmental factors suggests that systems of communication from the extracellular to the intracellular compartments must exist. Small changes in calcium concentration, pH and membrane potential in response to stimuli such as light and auxins have been detected showing that plants can respond rapidly to external signals (Boss and Morre, 1989). However the molecular basis of how environmental stimuli are transduced into growth responses in plants still remains to be elucidated. In animals it has been found that a highly

conserved signalling system exists, which through receptor modification can control a diverse range of cellular processes from the rapid responses of nerve and muscle to the slower responses to circulating hormones. Taking the view that a basic eukaryotic signalling system may have emerged early in evolution, researchers in this field have used the animal model as a basis for exploring signalling in plants.

The first signal transduction system to be proposed was based on the work of Sutherland and co-workers (1968) on the role of cyclic AMP in adrenergic responses. The term 'second messenger' arose from this work. First messengers were considered to be action potentials, neurotransmitters or hormones. In the case of adrenaline, the conformation of a transduction protein (G protein) is altered to an active state, on binding with a receptor at the cell surface. The  $\alpha$ -subunit of the G protein binds GTP. This complex activates the enzyme adenyl cyclase, which generates cAMP. Cyclic-AMP in turn activates cAMP dependent protein kinase, thus phosphorylating phosphorylase kinase. This enzyme converts enzymatically inactive phosphorylase b to active phosphorylase a, thus initiating the breakdown of glycogen and the subsequent synthesis of glucose.

Initially it was thought that plant hormones too, should have a similar all embracing second messenger such as cAMP. Attempts to establish cAMP as a second messenger in plants proved unsuccessful. The presence of cAMP has been reported in plants, including *F. hygrometrica* (Handa and Johri, 1979), but neither adenylate cyclase nor cAMP-dependent protein kinase have been detected. Cyclic AMP phosphodiesterases were also reported in *F. hygrometrica* (Sharma and Johri, 1982, 1983). The role of cyclic AMP is now less certain in animal systems as the calcium messenger system has become unravelled (1.6), and elements of this system have been found to have similar phosphorylating effects on enzymes such as adenylate cyclase and phosphorylase kinase. In moss evidence was presented against cAMP having a role in the action of the plant hormone cytokinin (Schneider



*et al*, 1975).

However, because phosphorylation has an obvious integrating and amplifying function (Blowers and Trewavas, 1989), an examination of the possible role of phosphorylation in plant cell signalling is thought to be worthwhile. Protein kinases or protein phosphatases are being sought that could be sensitive to any of the known factors that vary intracellularly in plants, such as  $\text{Ca}^{2+}$ ,  $\text{K}^{+}$ ,  $\text{H}^{+}$ , membrane potential or to external signals such as light, pressure, gravity and temperature. Protein kinase or protein phosphorylation in response to many of these factors has already been found (Ranjeva and Boudet, 1987), although there has been a lack of identifiable substrates. The lack of a specific second messenger may not discount the importance of this aspect in plant cell signalling.

It is frequently debated to what extent animal and plant hormones are equivalent. The term growth factor or substance is often preferred in relation to plant hormones. In both animals and plants, a regulatory effect is mediated on target tissue at concentrations below  $10^{-6}\text{M}$ . Animal hormones are synthesised by one tissue and transported via the circulatory system, to have their effects on another tissue. Many animal hormones have been identified, ranging from simple organic ring structures such as adrenaline to small proteins such as glucagon. Each has a specific effect and is recognised by its target tissue by means of high affinity receptors. The majority of animal hormones are hydrophilic and do not cross the plasma membrane easily. They interact with specific receptors on the cell surface, which then initiate the cascades of cellular events such as those described above. The small hydrophobic steroid hormones move directly into the cytoplasm where they complex with soluble cytosolic receptors which are themselves transcription factors.

In contrast, only five classes of growth factor, either singly, or in combination,

affect many aspects of growth in plants. Plants do not have clearly defined tissues for the synthesis of growth factors, which may be synthesised throughout the plant. Although some transport of substances may occur via the vascular system, growth factors may also have their effects in their tissue of origin. Plant growth factors also interact with each other and with the environment to a great extent. Different concentrations and ratios of the same factors may induce different effects in the same tissues. Blowers and Trewavas (1989) suggest that we could view plant hormones themselves as second messengers mediating environmental influences, a sort of plant equivalent to cAMP. Although this suggestion has never been seriously incorporated into the literature on plant hormones, it is certainly inherent in some lines of research, such as the work on gradients of auxin in response to gravity (Pickard, 1985).

Plant hormones are hydrophobic or amphipathic molecules able to penetrate the plasma membrane with ease. This argues against the hypothesis that they act by means of membrane receptors (Lazarus *et al*, 1991). Blowers and Trewavas (1989) point out also that these are unlikely to have second messenger requirements unless their subsequent metabolic effects can be considered to represent second messengers. However, much research has gone into attempting to find either membrane or cytoplasmic receptors. There is some evidence that auxin binds to a membrane receptor (Hicks *et al*, 1989) and an auxin binding protein has been purified (Venis and Napier, 1990).

#### 1.4 The Calcium Messenger System

Over the last two decades, in the field of animal physiology, research on the numerous aspects of cell physiology relating to a role for the calcium ion in cell signalling has been gradually integrated into a unifying hypothesis. In the early 1970's, it was noted that in many of the cells in which there was a rise in cAMP in



response to a stimulus, there was also a rise in intracellular calcium ion concentration (Rasmussen *et al*, 1972). Also for many of the responses to occur, calcium needed to be present in the external medium. Initial attempts to discover the mechanism that linked calcium and cAMP were unsuccessful. The discovery of the calcium-binding protein calmodulin (Cheung, 1971, in Cheung 1982) was the result of exploring the regulation of phosphodiesterase, the enzyme responsible for the degradation of cAMP, and provided a link between the two. The calcium-calmodulin complex was soon found to be a mediator of many other enzymatic activities, and calcium was firmly established as an essential intermediate in 'signal-response coupling'.

Since that time the means by which cells regulate their intracellular calcium concentrations have been under intense study. It is known, for example, that elevated levels of calcium are toxic to cells if sustained over long periods and that many responses involve a transient sharp increase in calcium concentration followed by a return to normal levels, even when the response is sustained. One of the response elements activated by the calcium-calmodulin complex was found to be a calcium pump in the plasma membrane. Much research has centred round the means by which calcium enters the cytosol, the types of calcium channel and their operation by receptors (ch. 4.1).

Concurrently with this research, another area was assuming importance. As early as 1953 Hokin and Hokin discovered that the turnover of the phosphorylinositol group of phosphatidylinositol was enhanced in cells in response to a variety of stimuli (Michell, 1975). In the 1960's it was recognised that much of the inositol in eukaryote cells exists in a combined form in the phospholipids of membranes, and that many cell functions, from secretion to ATPase activity depended on an adequate supply of inositol. Only in the last decade have the elements of phosphatidylinositol metabolism been resolved into a coherent picture of their

function in the transmission of information. As in the work with cAMP, it was realised that changes in  $\text{Ca}^{2+}$  were involved. One of the reasons phosphatidylinositol was not initially considered as possessing a messenger role was the fact that secretory responses, but not the phosphatidylinositol response, could be prevented by the omission of  $\text{Ca}^{2+}$  in the medium, nor did the phosphatidylinositol response appear to be dependent on raising the intracellular levels of  $\text{Ca}^{2+}$  with ionophore. It was Michell, reviewing the experimental evidence in 1975, who put forward the hypothesis that phosphatidylinositol breakdown could “lie early on the main pathway linking receptor activation to the full spectrum of cellular responses, at a point preceding the involvement of  $\text{Ca}^{2+}$ ”.

It is now accepted that for animals the majority of signals are mediated through an initial turnover of phosphatidylinositol to generate the dual messenger system of the two second messengers inositol triphosphate ( $\text{IP}_3$ ) and diacylglycerol (DAG) (Berridge, 1993). Two major receptor families are linked to this pathway, G-protein-linked receptors and receptors that are either directly or indirectly linked by tyrosine kinase. Agonists which include acetylcholine, glutamate, light and odorants bind to receptors coupled to a GTP transducing mechanism which activates phospholipase C to hydrolyse the precursor phosphatidylinositol 4,5-bisphosphate to give  $\text{IP}_3$  and DAG. The former binds to an  $\text{IP}_3$  receptor to mobilise stored calcium and to promote an influx of external calcium, while the latter activates protein kinase C. Other agonists such as platelet-derived (PDGF) and epidermal (EGF) growth factors bind to tyrosine kinase-linked receptors linked to an ATP transducing mechanism which activates the  $\gamma$  form of phospholipase, also resulting in the production of  $\text{IP}_3$  and DAG. These receptors also activate other effectors such as the phosphatidylinositol 3-OH kinase which generates the putative lipid messenger phosphatidylinositol (3,4,5)-triphosphate ( $\text{PIP}_3$ ) and the GTPase-activating protein (GAP) that regulates the expression of the *ras* gene.



In mammals, a family of IP<sub>3</sub> receptors has now been identified (Furuichi, 1990). These represent one of the two principle intracellular calcium channels responsible for mobilising stored calcium, and are located principally in the smooth ER. The receptor contains typical membrane-spanning domains in its C-terminal region, four subunits combining to form the IP<sub>3</sub>-sensitive calcium channel. The N-terminal region containing the IP<sub>3</sub> binding site lies free in the cytoplasm. How IP<sub>3</sub> regulates calcium influx into the cell is less clear. In some cells IP<sub>3</sub> may directly activate IP<sub>3</sub> receptors in the plasma membrane. Putney (1986, in Berridge, 1993) put forward the hypothesis of 'capacitative entry', that the influx of external calcium may be regulated by a portion of the ER lying close to the plasma membrane. When calcium is drained out of these stores, the influx of calcium is switched on automatically by a putative coupling mechanism between two calcium channels, one in the ER, the other in the plasma membrane.

Calcium influx, mediated by second messengers in the manner described above, generates a different pattern of intracellular calcium dynamics from the voltage-operated calcium influxes of nerve and muscle. Recent developments in single cell imaging techniques (see ch.5.1) have revealed some of the spatio-temporal aspects of calcium signalling. It was found that many cells which responded to agonists by generating increases in cytosolic calcium concentration, displayed both temporal patterning, in terms of repetitive increases in calcium concentration (spikes), and also a recurring spatial organisation. For example, in the eggs of many species, on fertilisation a calcium-wave could be visualised using fluorescence microscopy, spreading through the cell from a specific initiation site (Jaffe, 1985). Miyazaki (1988) reported that the microinjection of IP<sub>3</sub> and guanine nucleotides into golden hamster eggs caused recurring calcium transients in a local area of the cytoplasm. Each calcium transient was accompanied by a small hyperpolarisation of the plasma membrane, which was thought to be caused by the stimulation of Ca-activated K<sup>+</sup> channels. While the first one or two Ca<sup>2+</sup> transients were independent of

extracellular calcium, subsequent ones required calcium in the medium. Miyazaki (1988) proposed that  $IP_3$  causes  $Ca^{2+}$  release from internal stores and also stimulates a pathway for elevation of  $Ca^{2+}$  permeability in the plasma membrane.

By contrast, influx of calcium through voltage operated channels creates an immediate uniform rise in calcium concentration throughout the cell. It is thought to be unlikely, however, that the  $IP_3$  pathway plays a role in the rapid voltage-regulated signalling of nerve and skeletal muscle.

### 1.5 Calcium in Plant Cell Signalling

It is generally accepted that calcium plays an essential role in mediating many cellular functions, in plants (Hepler and Wayne, 1985; Roux and Slocum, 1982). However it has been much more difficult to establish an analogous role in signal transduction to that of animals, due mainly to the difficulties of measuring calcium in plants. As in animal cells, plant cells maintain a steep gradient between extracellular and intracellular calcium of about four orders of magnitude, and therefore must possess means of regulating their intracellular calcium levels. The situation is complicated in plants by the cell wall matrix which has a potent buffering capacity for calcium, the necessity of a continual supply of calcium in the medium for many growth responses to occur, and the necessity for surface-bound calcium to stabilise the plant plasma membrane (Kauss, 1987).

Calmodulin was first isolated from plants in 1978 as a heat stable factor able to stimulate the calmodulin-deficient cAMP phosphodiesterase from bovine brain in a calcium dependent manner (Marmé, 1989). In the same year Gross and Marmé (1978) demonstrated the occurrence of ATP-dependent  $Ca^{2+}$  uptake into isolated plant membrane vesicles, and it was shown later that this could be stimulated by the addition of either purified plant or animal calmodulin (Dieter and Marmé, 1980). This was then shown to be due to calmodulin activation of a  $(Ca^{2+}+Mg^{2+})$  ATPase

(Dieter and Marme, 1981). Two elements of a putative calcium messenger system were therefore demonstrated, the possibility of calcium-regulated enzyme activity by way of a  $\text{Ca}^{2+}$ -calmodulin complex, and the means to regulate internal calcium by pumping calcium out of the cell in an energy dependent manner.

Only a few  $\text{Ca}^{2+}$ -calmodulin regulated enzymes have been discovered in plants to date.  $\text{Ca}^{2+}$ -calmodulin dependent protein kinase activity has been demonstrated in wheat embryo and zucchini, but only in plant homogenates, and nothing is known about the phosphorylated substrates, only one of which has so far been identified, the quinate:  $\text{NAD}^+$  oxidoreductase kinase from light-grown carrot cells, which reversibly converts dehydroquinate into quinate. The activation of the kinase that phosphorylates this enzyme was shown to be dependent on the presence of calcium and calmodulin in the incubating medium (Ranjeva et al, 1983). NAD kinases that are dependent on calmodulin and sensitive to calcium concentration have also been isolated (Marme, 1989). It is now clear, for both animals and plants, that not all enzymes which are regulated by calcium are calmodulin-dependent.

The possibility that the phosphatidylinositol messenger system may exist in plants is also being explored. The plasma membranes of plant cells have been found to be rich in phosphoinositides and the enzymes involved in their biosynthesis and metabolism (Boss, 1989). A calcium-dependent phospholipid-activated protein kinase has been isolated from plants, which could be analogous to the protein kinase C activated by DAG (Elliott and Skinner, 1986). This enzyme was found not to bind phorbol esters, unlike the C-type protein kinases of animal cells. Many of the difficulties associated with exploring the role of the inositol phosphates in plants are set out by Boss (1989). Phosphoinositide metabolism in plants is complex. In addition to synthesising inositol, plants can synthesise inositol hexaphosphate ( $\text{IP}_6$ ), which is utilised as a phosphate store in dormant tissue and seeds. Inositol is also metabolised to glucuronic acid, which is used in the biosynthesis of noncellulosic



wall polysaccharides, glycoproteins, gums and mucilages (Loewus and Loewus, 1983).  $\text{PIP}_2$ , the precursor of  $\text{IP}_3$ , is usually less than 1% of the total inositol-labelled lipid recovered in radio-labelling studies. Against this background, demonstration of a decrease in  $\text{PIP}_2$  and concomitant increase in  $\text{IP}_3$  is near the limits of detection of current chromatography.

In vitro studies have shown that low concentrations of  $\text{IP}_3$  added to microsome vesicles or tonoplast vesicles result in small transient changes in  $^{45}\text{Ca}^{2+}$ . Rincon and Boss (1987) demonstrated an efflux of calcium from protoplasts of wild carrot treated with  $\text{IP}_3$ . Two studies on stomatal closure in guard cells demonstrate an increase of cytoplasmic calcium preceding closure in response to the release in the cell of microinjected caged  $\text{IP}_3$  (Gilroy *et al*, 1990; Blatt *et al*, 1990). This is a fast response, with some equivalence to the animal responses studied, and allows the possibility that  $\text{IP}_3$  may act similarly as a messenger in rapid responses. Shacklock *et al* (1992) also demonstrated that photolytic release of caged  $\text{IP}_3$  induced a transient cytosolic calcium increase which preceded red light-induced swelling of etiolated protoplasts, supporting the hypothesis that phytochrome-mediated signals are transduced through calcium, and that  $\text{IP}_3$  is involved in some plant responses. There has however been no unequivocal demonstration of increased  $\text{IP}_3$  formation in any plant system. The majority of plant hormone responses take hours to days and the question of whether they use the inositide signalling pathway, or even calcium as intermediate messenger, remains entirely unresolved.

If calcium is involved in signal transduction processes in plants, this must involve effects on calcium fluxes into and out of the cell and on calcium transport mechanisms on internal membranes. Much work has gone into attempts to characterise calcium channels (see ch. 4.1). In animal cells the most clearly defined channels are voltage-operated. Receptor-operated channels have been postulated to explain  $\text{Ca}^{2+}$  influx into cells that do not possess voltage-gated calcium channels,

but direct evidence for these has been sparse, and confusion seems to exist between receptor-operated channels and second-messenger operated channels. The activation of calcium channels in the plant plasma membrane in response to physiological signals has also been postulated. Schroeder and Hagiwara (1990), again using ABA-induced stomatal closure, simultaneously measured cytosolic  $\text{Ca}^{2+}$  and ion currents across the plasma membrane of single *Vicia faba* guard cells. They found that external application of ABA produced transient repetitive increases in the cytosolic free calcium concentration accompanied by concomitantly occurring increases in an inward-directed current. Under patch-clamp conditions, depolarisation of the membrane terminated both these effects. This suggests that ABA-mediated  $\text{Ca}^{2+}$  transients are produced by passive influx of  $\text{Ca}^{2+}$  from the extracellular space through calcium-permeable channels. Reversal potentials of the ABA-induced currents showed that they were not highly selective for calcium, permitting the permeation of  $\text{K}^{+}$  also. This mechanism of activation is unlike that of receptor-ion channel complexes in animal cells when the receptor and the ion channel constitute one molecular identity. The results also deviate from the hypothesis that  $\text{Ca}^{2+}$  release from intracellular stores is the initial mechanism of guard cell closure, as suggested by  $\text{IP}_3$  work. Scheuelein *et al*, 1991, measured cytoplasmic calcium concentrations in *Dryopteris* spores and found that these changed in response to changes in extracellular calcium concentrations. This established that intracellular calcium changed according to the  $\text{Ca}^{2+}$ -gradient established between cytoplasm and extracellular medium, but could not determine whether  $\text{Ca}^{2+}$ -fluxes were mediated by specific channels or by a non-controlled passage of  $\text{Ca}^{2+}$  through the plasmalemma.

Another much studied system is gibberellin (GA)-stimulated synthesis and secretion of  $\alpha$ -amylase in barley aleurone layers (Bush *et al*, 1988, 1989). Here the situation is complicated by the requirement of  $\alpha$ -amylase for  $\text{Ca}^{2+}$  for stability and activity. However, the barley aleurone cell must maintain a high level of  $\text{Ca}^{2+}$  in the

lumen of the ER for synthesis of  $\alpha$ -amylase to occur. Bush *et al* (1989) measured the rate of  $^{45}\text{Ca}^{2+}$  transport into the ER in the presence and absence of GA, and found that it was stimulated several-fold by GA, suggesting an effect of GA on the activity of an ATP-dependent  $\text{Ca}^{2+}$  pump in the ER.

The relationship of calcium and auxin transport has been studied in the gravitropic response of coleoptiles and root tips. Slocum and Roux (1983) reported a redistribution of applied  $^{45}\text{Ca}^{2+}$  during gravitropic stimulation of coleoptiles. Bjorkman and Cleland (1991) measured the calcium activity in the apoplast of maize root tips using calcium microelectrodes and found that a gradient of calcium does develop in response to gravistimulation, and precedes curvature. The calcium gradient can be correlated with an auxin gradient developing in the opposite direction (Pickard, 1985). The mechanism by which this occurs is unclear.

Recently, Messiaen *et al* (1993) have reported a prolonged elevation of calcium in carrot protoplasts treated with cell wall oligogalacturonides that are elicitors of host defence mechanisms. The increases in intracellular calcium observed were slow and prolonged rather than transient, beginning after 5 to 10 minutes and increasing to over 1  $\mu\text{M}$  by 20 to 30 minutes. It was not possible to observe calcium changes beyond 30 minutes due to photobleaching and dye leakage. Messiaen *et al* surmise that long-term calcium elevations may be a feature of plant cells, and a possible mechanism to explain them may be inhibition of the  $\text{Ca}^{2+}$ -ATPases. However they also state that the elicitor concentration needed to induce a  $\text{Ca}^{2+}$  elevation was the same concentration that induced membrane depolarisation in tomato leaf cells, but do not examine the implications of this in terms of altering the ionic balance of a cell.



## 1.6 Cytokinin

While much is known about the metabolism of plant cytokinins, their primary modes of action remain unelucidated. In higher plants cytokinins possess a range of biological activities. In addition to their established role as a cell division factor, cytokinins interact with auxins in the induction of organ formation in tissue culture, and affect many aspects of growth, including the stimulation of chloroplast development, the differentiation of vascular tissue, the development of lateral shoots and buds, and delay of senescence. Some of these effects are paralleled in moss development.

The effect of cytokinin on cell division was studied by Szweykowska *et al* (1971, 1972), using moss protonema. They found that as well as cytokinins, compounds such as adenine and adenosine, with no bud inducing potential, also stimulated cell division in isolated apical cells of *F. hygrometrica* and *Ceratodon purpureus*. They came to the conclusion that the cell division response was non-specific, and that bud induction by cytokinin is not simply a stimulation of cell division.

In moss, the most obvious and clearly attributable effect is on the dose-dependent morphogenesis of single-celled side-branch initials into buds. There is some controversy over whether the target cell for cytokinin action is the caulonema subapical cell or the developing side-branch initial. Saunders and Hepler (1981, 1982) describe the first stage of cytokinin action in moss as the induction of division in the caulonema subapical cell to form an bud. However, they use stress conditions of phosphate-free medium to grow the filaments for experimental work, which inhibit the spontaneous formation of side-branches. This effect of cytokinin on the production of the side-branch initial may be non-specific (Szweykowska, 1971) and/or unrelated to the effect of cytokinin on budding. Alternatively, mutants of *P. patens*, which are unable to produce buds, produce normal non-bud side-branches.

This is consistent with the hypothesis that the moss has a lower concentration requirement of cytokinin for the formation of side-branch initials. Bopp and Jacob (1986) distinguish between the effect of a low concentration of cytokinin which induces side-branch initials on filaments growing in phosphate-free medium, and that of the higher concentrations which induce buds on existing initials, suggesting that these two effects of cytokinin may be unrelated, and work by means of different mechanisms. This effect of cytokinin on unbranched initials only occurs in the light. Larpent-Gourgaud (1969, in Simon and Naef, 1981) induced branching in the dark with traumatic acid treatment, and then budding with kinetin, suggesting that budding is dependent on the production of side-branch initials.

Bopp (1990) states that the number of buds induced by cytokinin is proportional to the log of the concentration between 0.1 and 10 $\mu$ M under standard conditions. If the distribution of buds is examined, at the lowest concentration, only one cell in a filament of *F. hygrometrica* responds, the cell at subapical position 6. He also demonstrated this with single isolated cells (Bopp, 1984). With increasing concentration, younger cells in the same filament respond. However, once a side-branch initial has reached a length of 80 $\mu$ M it no longer responds. He therefore came to the conclusion that the most sensitive target cell was the developing side-branch initial when it was at the sixth cell position in a filament.

Brandes and Kende (1968) showed that bud formation was reversible. If protonema were treated with cytokinin for 24 hours and then removed to fresh medium, many buds were induced, but reverted to filamentous growth after the transfer. The withdrawal of the hormone at later stages caused progressively less dedifferentiation, and no reversal could be obtained after 72 hours of cytokinin treatment.

The addition of exogenous cytokinin sets in motion a train of clearly observable



effects on the single-celled initial, and is one of the fastest and most specific observable effects of this hormone. The first steps of cytokinin action in bud induction are described by Bopp (1984) for the moss *F. hygrometrica*. After three hours the growth rate of the initial starts to slow and the tip of the cell develops a dome shape, growing in width so that the cell develops a club shape. Growth is no longer confined to the apical end of the cell as in filament growth. Bopp and Fell (1975, in Bopp 1984) demonstrated through  $^{14}\text{C}$ -glucose labelling that one of the first steps consists of an altered distribution in cell wall material. Brandes (1967) showed an enhanced formation of acridine orange stained RNA in buds and that labelled benzyladenine accumulated in caulonema cells which were at the stage of bud formation and in the newly formed buds. Schneider and Szweykowska (1974) found increases in RNase and DNase activities. An electron micrograph study by Conrad and Hepler (1986) revealed a change in the distribution of vesicle densities as bud development progressed, from a clustering of vesicles in the cell apex at bud induction to dispersal throughout the cytoplasm after the bud initial has formed. Two further studies (McCauley and Hepler, 1990, 1992) revealed that the cortical ER network is arranged in a much tighter configuration in both side-branch initials and buds than in the caulonema filament cells, and is closely associated with the cytoskeleton. Doonan *et al* (1987) compared the organisation of microtubules in side-branch initials in the presence and absence of cytokinin. In presumptive bud initials, microtubules appeared diffusely organised compared to those in branches. This suggests that some of the morphogenetic effects of cytokinin are a result of altering the organisation of the cytoskeleton.

Because a certain amount of time is required after germination of spores before it is possible to induce buds, some attempts have been made to look for the formation of specific proteins in relation to cytokinin action (Erichsen *et al*, 1977; Bopp *et al*, 1978). Attempts to isolate caulonema-specific proteins have been hampered by the difficulty of isolating the two phases of protonemal growth, and no definitive

differences have been detected.

Other attempts to isolate mRNAs in response to cytokinin treatment in moss have not so far proved successful. Some success has been achieved in other systems. Crowell *et al* (1990) reported the isolation of 20 cDNAs from cytokinin-dependent, suspension-cultured soybean cells 1 to 4 hours after the addition of cytokinin, in the presence of cycloheximide. They found that the addition of cycloheximide enhanced cytokinin-induced gene expression by causing residual levels of these mRNAs in cytokinin-starved cells to decrease and by causing the magnitude of gene induction by cytokinin to increase. Two of these cDNAs corresponded to ribosomal protein mRNAs. This lends support to the hypothesis that cytokinin stimulates growth by means of increased protein synthesis.

A primary target for cytokinin action are plastids, and many data are available on the interaction of light and cytokinin in plastid differentiation and multiplication (Reski *et al*, 1991), and references therein). The cytokinin-sensitive chloroplast mutant PC22 of *P. patens* contains one large plastid per cell, which can be stimulated to divide by the addition of cytokinin. Reski *et al* (1991) looked at the influence of exogenous cytokinin on total and plastid proteins and on steady-state levels of *rbcL*-transcripts in this mutant. They found that cytokinin promotes a transient expression of plastid polypeptides and increase of *rbcL*-transcript levels under white light conditions.

As well as in plastid development, there is interaction between cytokinin and light in the induction of moss buds. Experiments with both *P. patens* and *F. hygrometrica* have shown that cytokinin alone is not enough to induce buds on dark-grown tissue. However if cytokinin is added to medium which is first passed over light-grown tissue, this medium will induce buds on tissue grown in the dark (McClelland, 1988). This suggests that some other factor only formed in the light is



necessary in combination with cytokinin to form buds. However, some early studies do report the induction of buds in the dark. Chopra and Gupta (1967) cultured *F. hygrometrica* spores in the dark on medium containing sucrose and kinetin. They found that spores germinated after 15 days and a large number of buds differentiated after one month. On medium with kinetin but no sucrose, both spore germination and the formation of buds was delayed by several months and much reduced, but still occurred. The authors conclude that this demonstrates a non-photosynthetic role of light in the initiation of buds.

Light of different spectral quality has been found to affect the levels of free cytokinins in different tissues of potato plants (Sergeeva *et al*, 1992). Plants grown in blue light had significantly lower cytokinin content in stems and roots compared to plants grown in white light.

The means by which cytokinin initiates its effects are still unknown. It has been suggested that hormones such as cytokinin act as primary signals in the same manner as animal hormones, and may exert their effects by causing changes in calcium concentration to trigger a cascade of cellular events leading to the response. To this end research has been directed into several areas which may determine initial events in cytokinin action.

Changes in ionic fluxes at the plasma membrane in response to cytokinin have been looked for. Olah *et al* (1983) found that the  $\text{Ca}^{2+}$ -ATPase from the microsomal fraction of wheat roots is modulated by BA. Elliot and Yao (1989) reported that cytokinins influence the accumulation of  $\text{Ca}^{2+}$  in protoplasts of *Amaranthus tricolor*. Kuiper *et al* (1992) studied the effects of BA on the  $\text{Ca}^{2+}$ - and  $(\text{Ca}^{2+}+\text{Mg}^{2+})$ -ATPases of the microsomal fraction from root cells of wheat. When they compared the ATPase activities of roots supplied with BA in the growth media with those of plants which had been grown in medium without BA, they



found higher  $\text{Ca}^{2+}$ - and  $\text{Mg}^{2+}$ -ATPase activities in the BA-treated plants. However the addition of BA directly to the assay medium did not affect ATPase activity. In earlier work, they found that an extra supply of BA to plants in low nutrient medium mimicked the effects of high salts (Kuiper *et al*, 1991), and that plants grown with a high level of mineral nutrition contained higher levels of cytokinins than plants grown with a low mineral supply (Kuiper *et al*, 1989). They conclude that the action of cytokinins appears indirect in that a good mineral supply leads to increased levels of cytokinins and these in turn lead to changes in the ion transport systems.

This seems to confirm the earlier work of Kubowicz *et al* (1982) who looked at the effects of IAA and zeatin on the  $\text{Ca}^{2+}$ -ATPase of the plasmalemma of etiolated soybean hypocotyls. They found that, in each case, effects only occurred if the tissue had been preincubated in the hormone, and that direct addition of hormone had no effect on ATP-dependent  $\text{Ca}^{2+}$  uptake, concluding that hormone action appeared to be indirect.

Akerman *et al* (1983) measured calcium fluxes across the plasma membrane of isolated wheat protoplasts and found that no effect on  $^{45}\text{Ca}^{2+}$  influx into protoplasts was detectable in response to plant hormones.

In the search for a putative receptor, several cytokinin binding sites have been detected. However it has been difficult to verify their specificity experimentally and/or their involvement in growth regulation. Early work on looking for cytokinin receptors has been reviewed in Futers (1984). No definitive cytokinin receptor, either membrane or cytosolic, has as yet been identified.

A series of studies on cytokinin-induced budding in *F. hygrometrica* have been often quoted as evidence that cytokinin action is preceded by an increase in

intracellular calcium and by subsequent phosphorylation of specific proteins. Using the calcium-specific probe chlorotetracycline, Saunders and Hepler (1981) detected localised increases in  $\text{Ca}^{2+}$  at the presumptive bud site in response to cytokinin. They reported that the calcium ionophore A23187 mimicked the effect of cytokinin in causing the first stage of budding in target caulonema subapical cells (Saunders and Hepler, 1982). Studies with the calcium channel inhibitors verapamil and Lanthanum (Saunders and Hepler, 1983) suggested that an external source of calcium was necessary for cytokinin-induced budding to occur. The application of the dihydropyridine agonists, (+202-791) and CGP 28392, was reported to induce bud initials on target cells, including the tip cell (Conrad and Hepler, 1988).

Conrad and Hepler (1986) reported that the inclusion of myo-inositol in the culture medium completely reversed inhibition of budding by Lithium, which inhibits the conversion of  $\text{IP}_3$  to inositol. Talbot and Saunders (1986) detected micromolar levels of  $\text{IP}_3$  in *F. hygrometrica* and determined fluctuations in  $\text{IP}_3$  concentrations over a 48 hour incubation period in BA. However, these two pieces of work have been published only in abstract form. Zbell *et al* (1989) detected a saturable and high affinity binding of [ $^{35}\text{S}$ ]  $\text{GTP}\gamma\text{S}$  in preliminary experiments when microsomal membranes of *F. hygrometrica* were incubated with the tracer in the absence and presence of 100 $\mu\text{M}$  GTP. It remains unclear whether these binding sites have any specific function in the signal transduction of any phytohormone.

Much of this work requires qualification in terms of the techniques used. This will be discussed more fully in chapters 4 and 5 where related techniques have been used with *P. patens*.

## 1.7 Project Aims

This project is concerned with exploring further the factors involved in the transitions from one cell type to another in the moss protonema. Several approaches



have been taken. Firstly, some aspects of the early protonemal growth from spore germination remain unclear. In *P. patens* it is unclear over how many cell cycles the change from chloronema to caulonema occurs, how long the primary chloronema growth phase lasts and whether there is a difference between primary and secondary chloronema. This project undertook to clarify these details and to provide a detailed description of early protonemal development. Secondly, the production of side-branches allows the potential for assaying the effect of environmental factors on the development of each cell type. To this end, it was necessary to develop a means of quantifying side-branch growth. This method could then be used to explore endogenous factors by assaying mutant phenotypes. The third approach looks specifically at the role of cytokinin in inducing a proportion of side-branch initials at the one-dimensional stage to undergo the transition to three-dimensional growth. It is possible that the primary mode of action of cytokinin is as a signal molecule, and that having been secreted into the substrate, cytokinin acts on membrane receptors, inducing a cascade of intracellular changes analogous to those elucidated in animal systems. In this case, one of the first events should be a transient rise in intracellular calcium. This possibility was explored using a range of techniques which includes the use of inhibitors, electrophysiology and calcium imaging.



## CHAPTER II

### ANALYSIS OF PROTONEMAL DEVELOPMENT USING TIME-LAPSE VIDEO MICROSCOPY

#### 2.1 Introduction

Time-lapse video microscopy has the potential to be a powerful tool in the study of development. While light and electron microscope studies provide descriptive data on cells as static entities, it is possible with time-lapse microscopy to follow the dynamic aspects of cell growth and development. Temporal gaps are frequently found between stimuli and responses and knowledge of these can be an important factor in forming hypotheses about cellular mechanisms.

Time-lapse has been used successfully to study the gravitropic response of dark-grown filaments in *Physcomitrella patens* (Knight and Cove, 1988), and *Ceratodon purpureus* (Schwuchow et al, 1990) using infra-red illumination and an infra-red sensitive T.V. camera. However using this technique it is only possible to observe filaments for a limited time-period. In the high light levels used routinely for the growth of *P. patens*, cultures dry very quickly and development tends to be abnormal in the restricted conditions of the growth chamber (Knight and Cove, 1988). When grown in the light using standard culture techniques protonemal filaments tend to spiral and grow out of the plane of focus. For the purpose of studying protonemal development in the light it was necessary to devise a method of culturing the moss so that it was constrained in a single plane of focus without adversely affecting its growth and development.

One aim of this study was to obtain more accurate data on the protonemal stages of moss development, patterns of side-branch development, growth rates, the transitions from one cell type to another, and the effects of environmental factors such as light and hormones on growth and development.

Time-lapse studies of the gravitropic response revealed a relationship between the

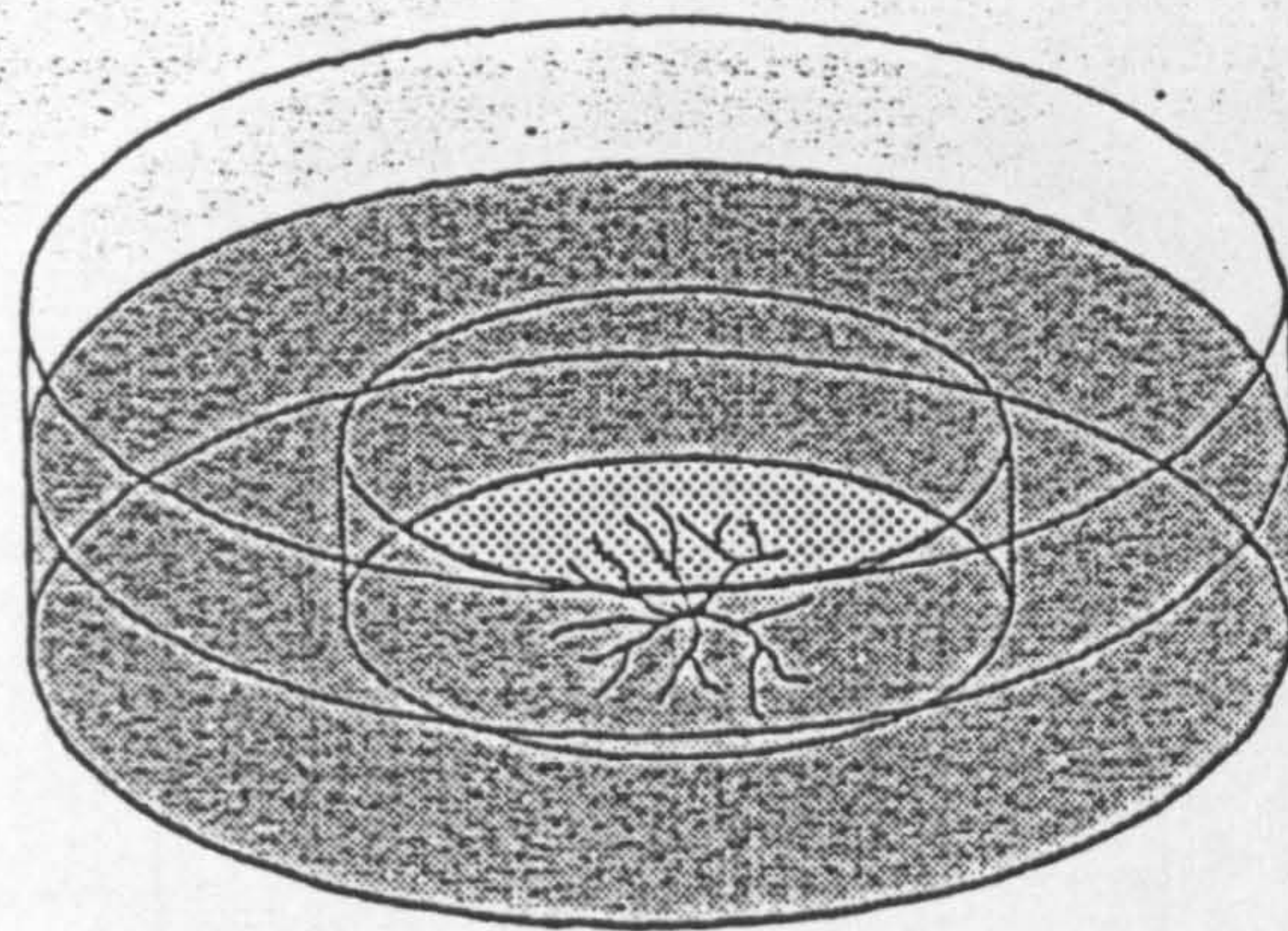
progression of the response and the cell cycle (Knight and Cove, 1991). During nuclear division negatively gravitropic growth was curtailed and a transitory reversal in the polarity of growth observed. Two possible explanations for this phenomenon have been advanced. First, that the nucleus may have a direct role in gravity perception by acting as part of a strain gauge, which can only be maintained while the nuclear membrane is intact. The second reason may be because some structural component of the cell such as a cytoskeletal element is required both to bring about changes in the direction of apical extension and also for nuclear and cell division. The gravitropic response would be curtailed because of competition for this component during division. Looking at other responses involving a change in the direction of apical growth may yield fresh clues concerning these hypotheses, and a further aim of this study was therefore to develop a means of filming the polarotropic response of protonemal filaments to determine if this too is curtailed during nuclear division.

## 2.2 Materials and methods

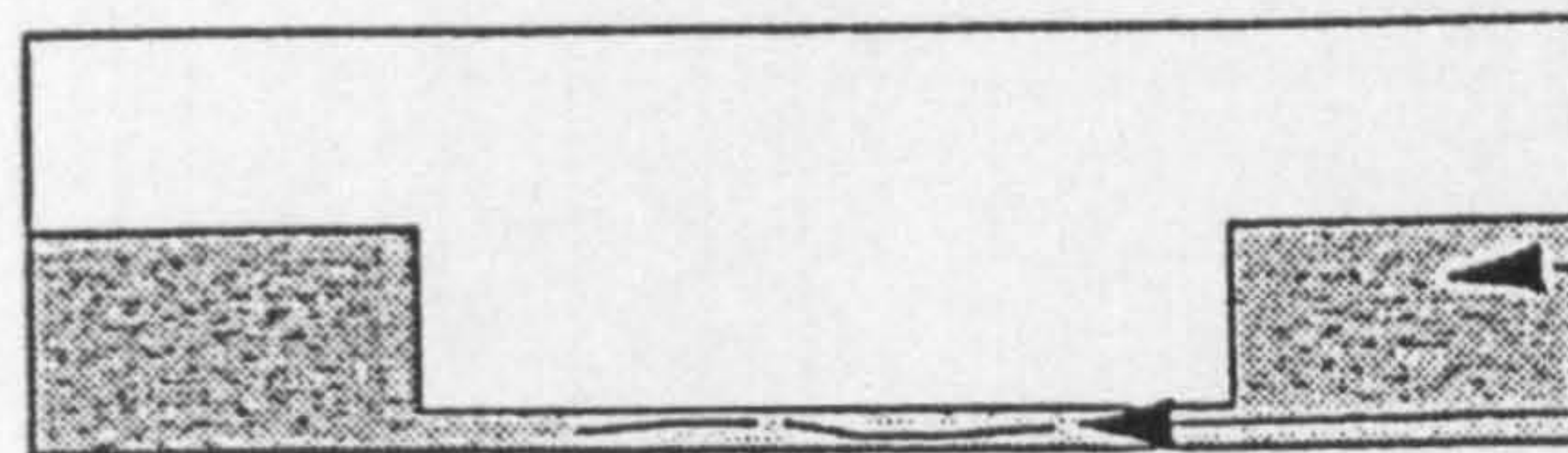
A culture chamber designed for observation and filming under the microscope is shown in fig. 2.1. The chamber is prepared as follows: liquid nutrient agar medium (ca. 9 to 10mls) is pipetted into the base of a 90mm sterile petri dish to a depth of approximately 1mm and allowed to set. A glass coverslip (22mm x 22mm), sterilised by flaming in alcohol, is placed in the centre of the petri-dish and covered with a further layer of agar to an approximate depth of 5 mm. When this is set the coverslip is lifted out by cutting through the agar with a flamed spatula to leave a layer of thin agar medium surrounded by deep agar. Protonemal fragments are sterilely inoculated into the centre of the agar well. The surrounding deeper agar prevents the cultures drying. Petri-dishes are incubated under white light at 21°C. For the purpose of filming, spores require a further drop of sterile agar to cover them so that they are embedded in agar.

The chamber is placed on the stage of a Leitz diavert inverted microscope





isodiametric view



agar medium  
culture

cross section

Fig. 2.1 A culture chamber designed for filming the moss.



(Wetzlar, Germany). Filaments embedded in the agar are observed using a CCD camera (Sony, model XC711P). The camera is linked to a time-lapse video recorder (Mitsubishi, HS-480E) into which a time-date recorder is fitted. The images are displayed on a video monitor (Sony).

Growth rates were calculated following standardisation of the video output by means of a standard graticule.

Polarised light was introduced to the cultures by attaching a lens to the base of the light tube of the microscope. A black cloth was placed over the microscope plus culture to screen out surrounding non-polarised light.

## **2.3 Results and discussion**

While the moss has been extensively used as a system for the study of morphogenetic changes at the cellular level (ch. 1.1), reports in the literature on the different cell types and the transitions between them have been based on light microscope analysis of isolated cells or filaments at selected time intervals. Because secondary side-branch growth quickly obscures the first filaments, uncertainties have remained about the growth rates, cell cycle times and length of existence of the early cell types. For the first time the use of time-lapse microscopy has been developed to provide a detailed record of the growth and associated morphogenetic changes of moss from spore germination to the early formation of gametophores.

### **2.3.1 Development of methodology**

Several methods of observing cultures growing under the microscope were tried. The culture chamber and microscope set up described in Knight and Cove (1988) were used initially. This method, though successful for filming protonema in the dark, proved to be unsuitable for filming developmental processes in the light for long periods. The thin layer of agar in the culture chamber tended to dry more quickly in

the light and the microscope required constant focusing.

The advantages of the protocol described in section 2.2 is that cultures can be filmed for over a week at a time. Little focusing is required. Two of the main disadvantages are that the light intensity cannot be altered consistently, and added substances such as hormones or inhibitors cannot be washed through. With more specialised equipment both these disadvantages could be overcome.

### 2.3.2 Spore germination and the transition from primary chloronema to caulonema

The germination of a spore of *P. patens* and the development of primary chloronema is illustrated in the sequence of pictures in Fig. 2.2.

Observations of many spores confirm the results of the films, that spore germination in *Physcomitrella* is bipolar, or multipolar. Fig. 2.2-2, where the spore coat is opening, reveals the existence of a cell division in the germ cell. An early step in germination is a division of the spore, creating two cells. Each cell then produces a filament, so that spore germination in *P. patens* can be described as bipolar. These two primary chloronema are extremely slow growing, initially growing at less than 1  $\mu\text{m/h}$ . For the first 60 hours, growth in each filament is intermittent (fig. 2.3). The first filament undergoes 2 cell divisions at 20 hour intervals, before stopping growing entirely. The second filament has a period after the first cell division, in which no growth occurs, and does not divide again for 40 hours. During the subsequent cell cycle, in this case 26 hours, growth increases from less than 1  $\mu\text{m/h}$  to 2.6  $\mu\text{m/h}$ .

Once the two primary filaments have divided from the original cells, these cells begin to put out further filaments, rather in the manner of subapical cells. Each cell puts out two initials at intervals (Fig. 2.2, 3-4). The third filament produced is unlike the other two in having a faster growth rate from the start. This filament does not grow and divide intermittently, but gradually increases its growth rate and cell cycle time concurrently over a period of 6 cell cycles. By the 7th cell cycle growth is 15  $\mu\text{m/h}$  and the cell cycle time is 9 hourly. By this stage the filament is clearly

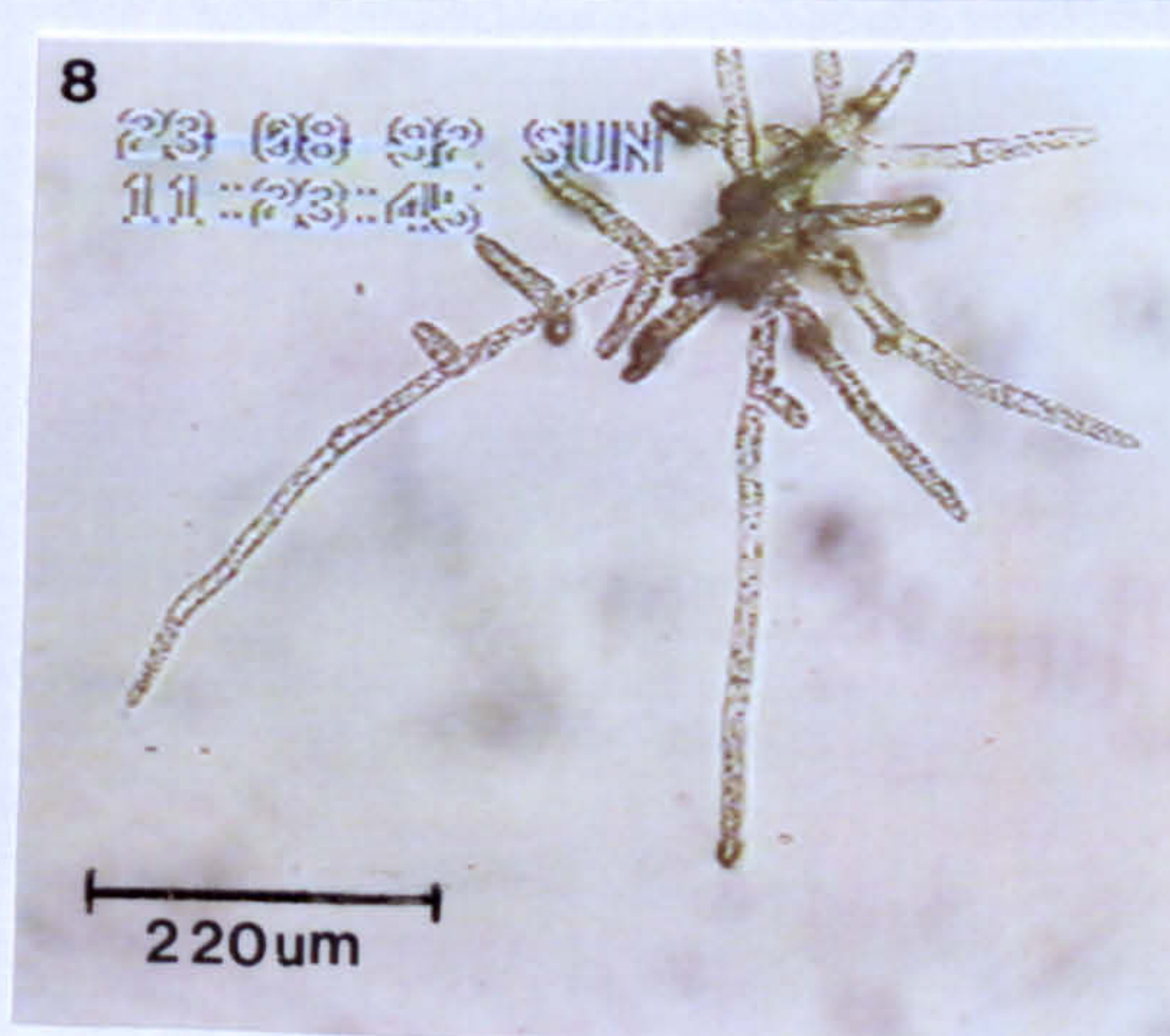
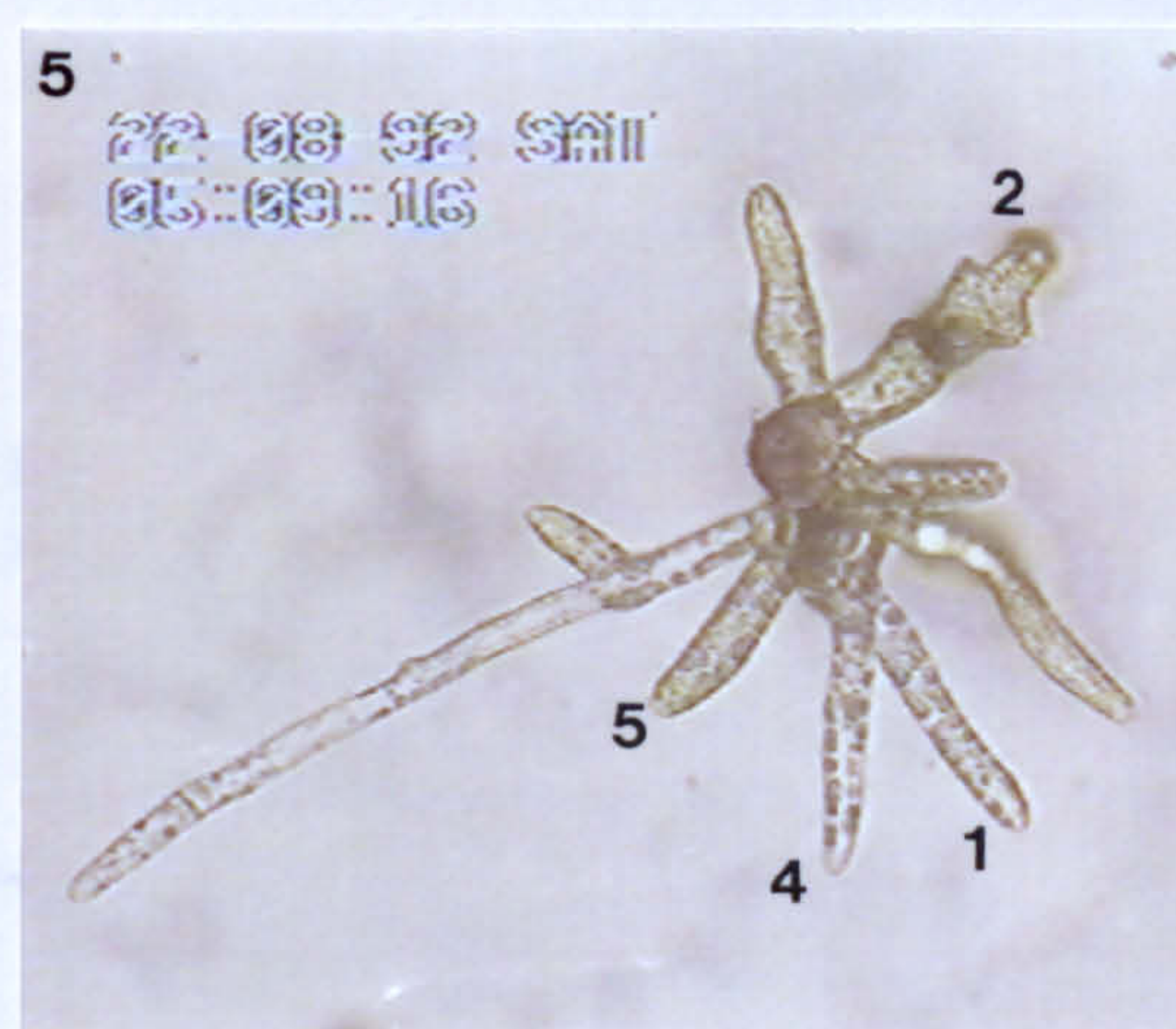
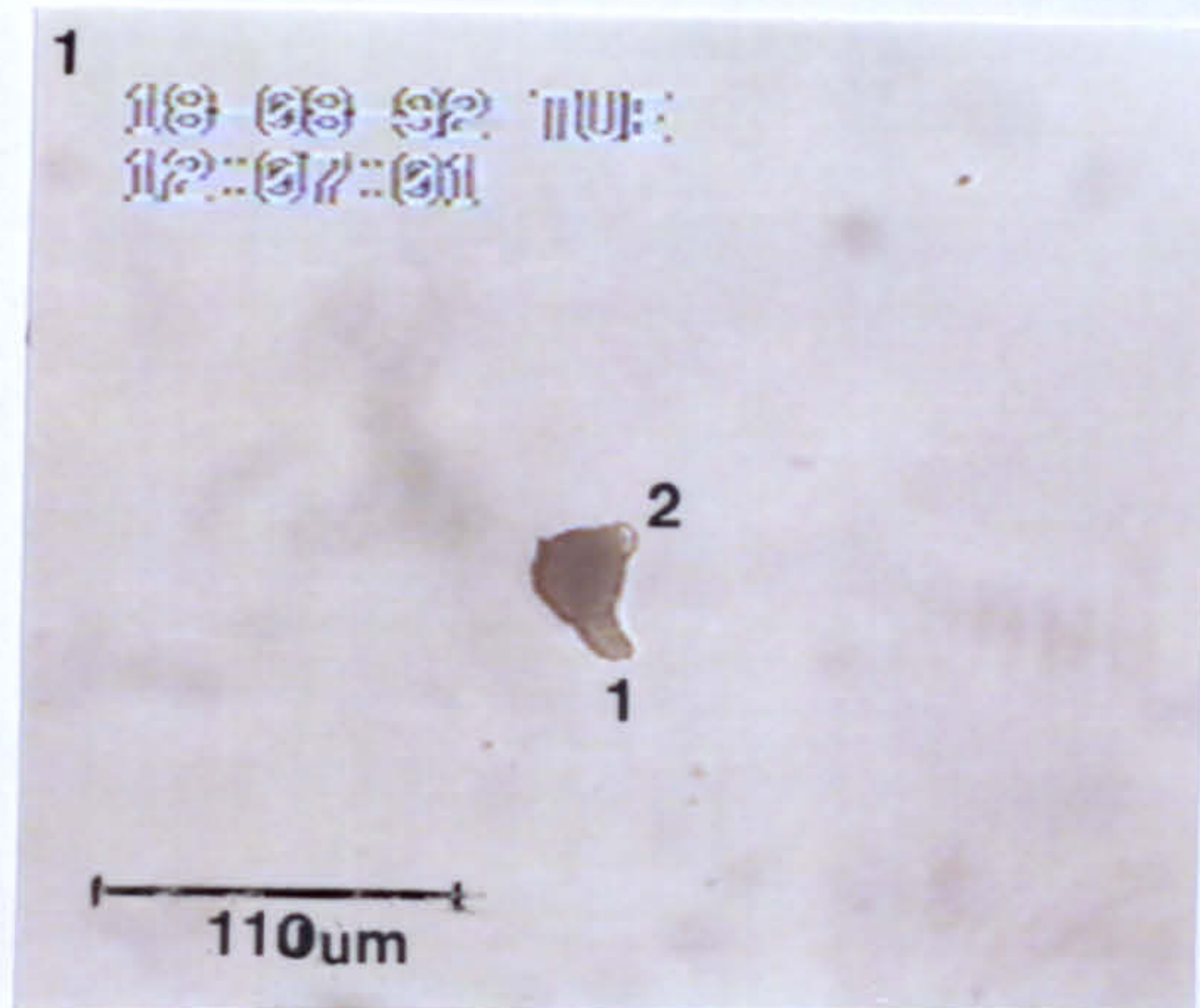


Fig. 2.2 The germination of a spore of *P. patens*.

Spores were plated on 15.08.92. Filming began at 10.30 a.m. on 18.08.

- 1      1.5 hours after the start of filming: the spore has produced two primary filaments, 1 and 2.
- 2      20 hours after the start of filming, ca. 25 hours after their origination, filaments 1 and 2 undergo their first cell division (arrows). The spore coat has slipped back to reveal a possible cell division the germ cell (middle arrow).
- 3      24 hours later, filament 2 divides a second time (arrow). Filament 1 has temporarily stopped growing. Both filaments have produced two side-branches from the basal cell of the first division. One of these (filament 3) is growing faster than the others from the beginning.
- 4      3 days after the start of filming: filament 1 has restarted growth, while filament 2 has now stopped growing. Filament 3 is growing as a transitional filament. The remaining filaments are growing as chloronema.
- 5      4 days after the start of filming: filaments 1 and 4 are beginning to increase their rate of growth, and assume a slightly caulonemal appearance. The apex of the apical cells is becoming clear and more pointed in appearance and the apical cells are appearing more vacuolated.
- 6      A caulonema side-branch has taken over growth in filament 2. Filament 5 has stopped growing.
- 7&8    5 days after the start of filming: filament 6 has undergone the transition to caulonema within a single cell cycle. The caulonema phase of growth is firmly established. All primary filaments have either switched to caulonema or stopped growing.







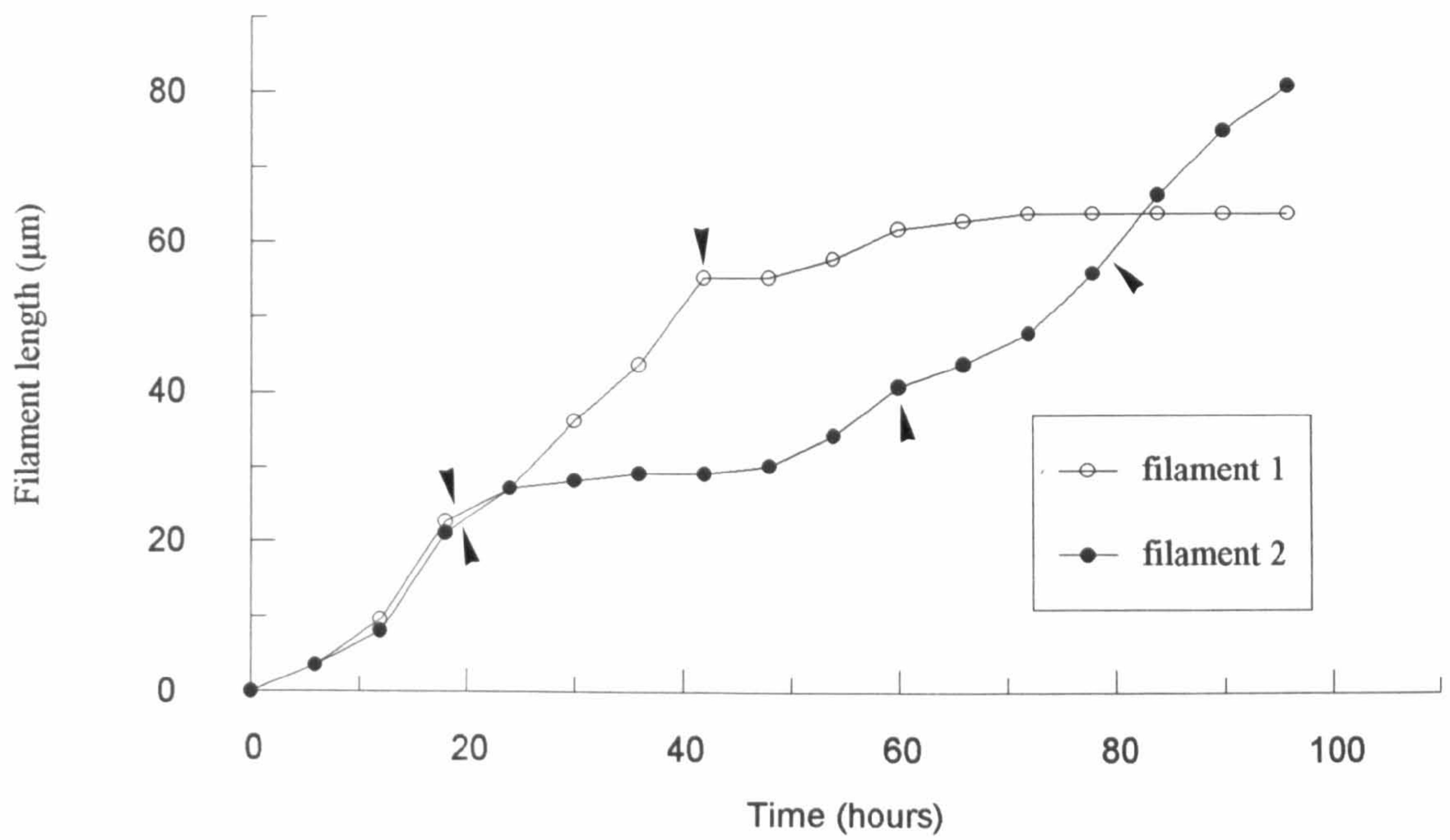


Fig. 2.3 The growth of primary chloronemata immediately following spore germination. Filaments 1 and 2 are illustrated in fig. 2.2. Arrows indicate cell divisions.

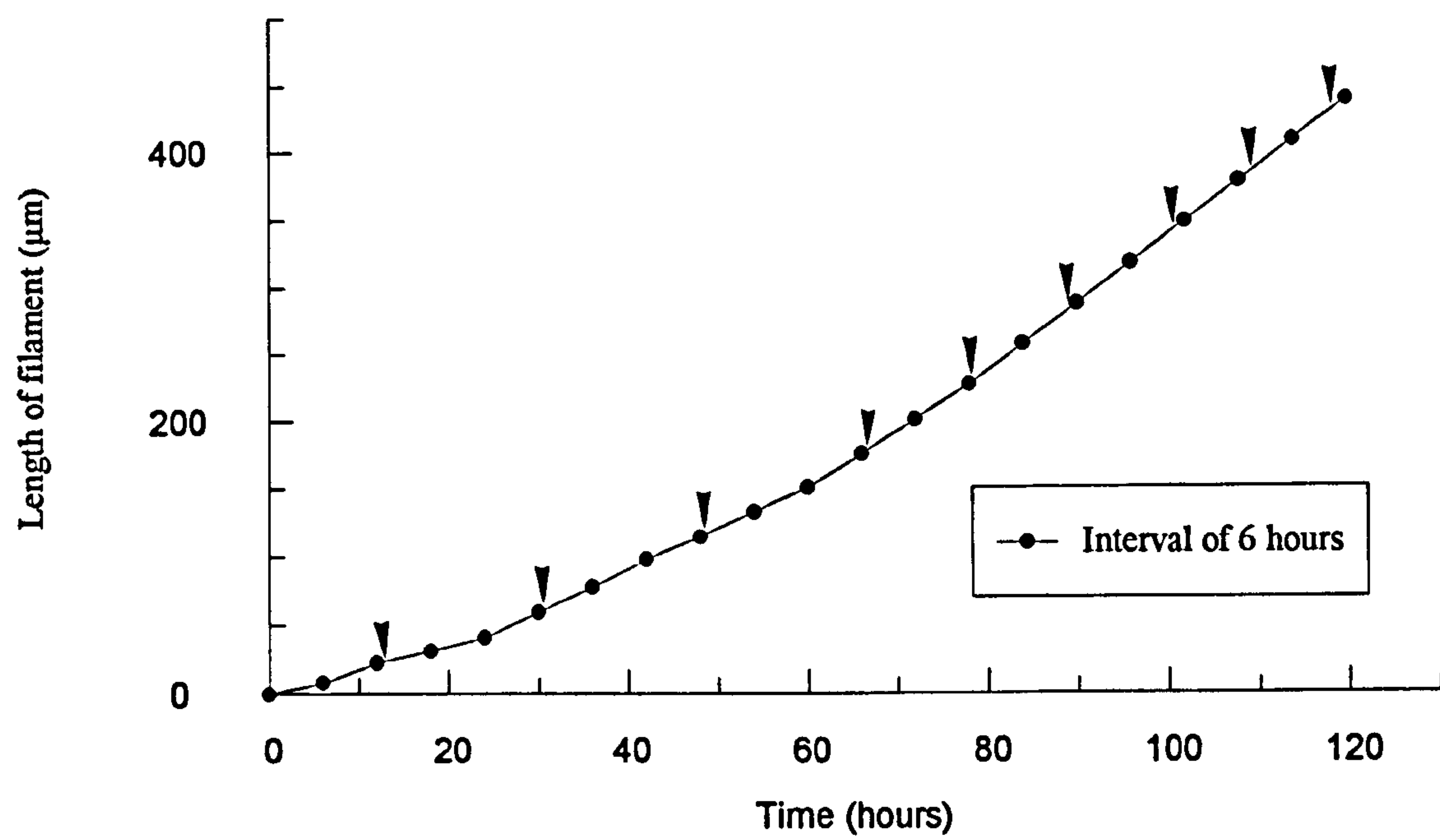


Fig. 2.4 The growth of a filament undergoing the transition to caulonema following spore germination. This is filament 3 in fig. 2.2. Arrows indicate cell divisions.



Table 2.1      The change in growth rate and cell cycle time in relation to cell length in a filament undergoing a transition from primary chloronema to caulonema.

Apical cell division	Average growth rate (µm/h)	Cell cycle time (hours)	Subapical cell length (µm)
1	2 - 4	14	60
2	3.5	20	72
3	4	18	72
4	5.5	16	90
5	6.5	14	90
6	10	12	120
7	12	9	105

caulonemal. This is illustrated in fig. 2.4 and table 2.1.

Over the period of transition the cell lengths increase gradually from 72  $\mu\text{m}$  at the 2nd and 3rd cells to 105  $\mu\text{m}$  by the 7th cell (table 2.1). This compares with 150-200  $\mu\text{m}$  as the length of a mature caulonema cell. The decrease in the cell cycle time concurrent with the increase in growth rate suggests that the regulation of the cell cycle is a factor in the regulation of cell length.

The transition from chloronema to caulonema can occur within a single cell cycle (Fig. 2.2, 7). Filament 6 undergoes two 20 to 24 hour cell cycles as a chloronema filament. The next cell division has an oblique cell wall and the apical cell has all the features of a caulonema cell. In this case there has been no extended transitional phase. Fig. 2.2, 8 shows that five days after germination all six original filaments have either switched to caulonema filaments or stopped growing. No primary chloronema filament has undergone more than two 20 hour cell cycles. Primary chloronema growth can be said to continue for up to 5 days after germination. From then on the role of chloronema is taken over by secondary chloronema arising from side-branch initials.

Fig. 2.5 shows a film sequence of a germinating spore of *F. hygrometrica*. Table 2.2 details the differences between the two species. The establishment of polarity is a clearer feature of spore germination in *F. hygrometrica*. In the majority of cases the primary rhizoid and first filament emerge sequentially. The first cell division is within the first filament, outside the germ cell. However in *P. patens*, where it appears that an early cell division within the spore divides the germ cell into two, one cell appears to be further advanced than the other, and this may be to do with the establishment of an early polar axis.

### 2.3.3 Secondary chloronema

It has been difficult to obtain a consistent picture of secondary chloronema arising from side-branch initials. Side-branches developing as chloronema filaments tend to

Fig. 2.5 The germination of a spore of *Funaria hygrometrica*.

Spores were plated on 14.05.93. Filming began at 20.00h on 15.05.93.

- 1 At the start of filming, the spore appears assymetrical. The assymetry is unrelated to the formation of a polar axis. An oil body (arrow) is visible in the spore.
- 2 6.5 hours after the start of filming: the spore has put out the first protrusion, which will be the primary rhizoid.
- 3 25.5 hours after the start of filming: the spore forms the first filament, at right angles to the rhizoid.
- 4 14 hours later, the first cell division (arrow) occurs within the filament. Primary chloronemal growth increases steadily, in contrast to the slow and intermittent growth of *P. patens*.
- 5 54 hours after the primary rhizoid was initiated. The rhizoid has a fast growth rate, but straight cross walls (arrow). In this case, the formation of an oblique cell wall is unrelated to the filament achieving a critical growth rate.
- 6 2 days after its inception, the primary chloronema is beginning to assume a caulonemal appearance at the tip of the apical cell.
- 7 18.5 hours later, 4 days after germination, caulonemal growth is established, and the characteristic oblique cell walls can be seen (arrows). No further filaments arise from the spore germ cell.



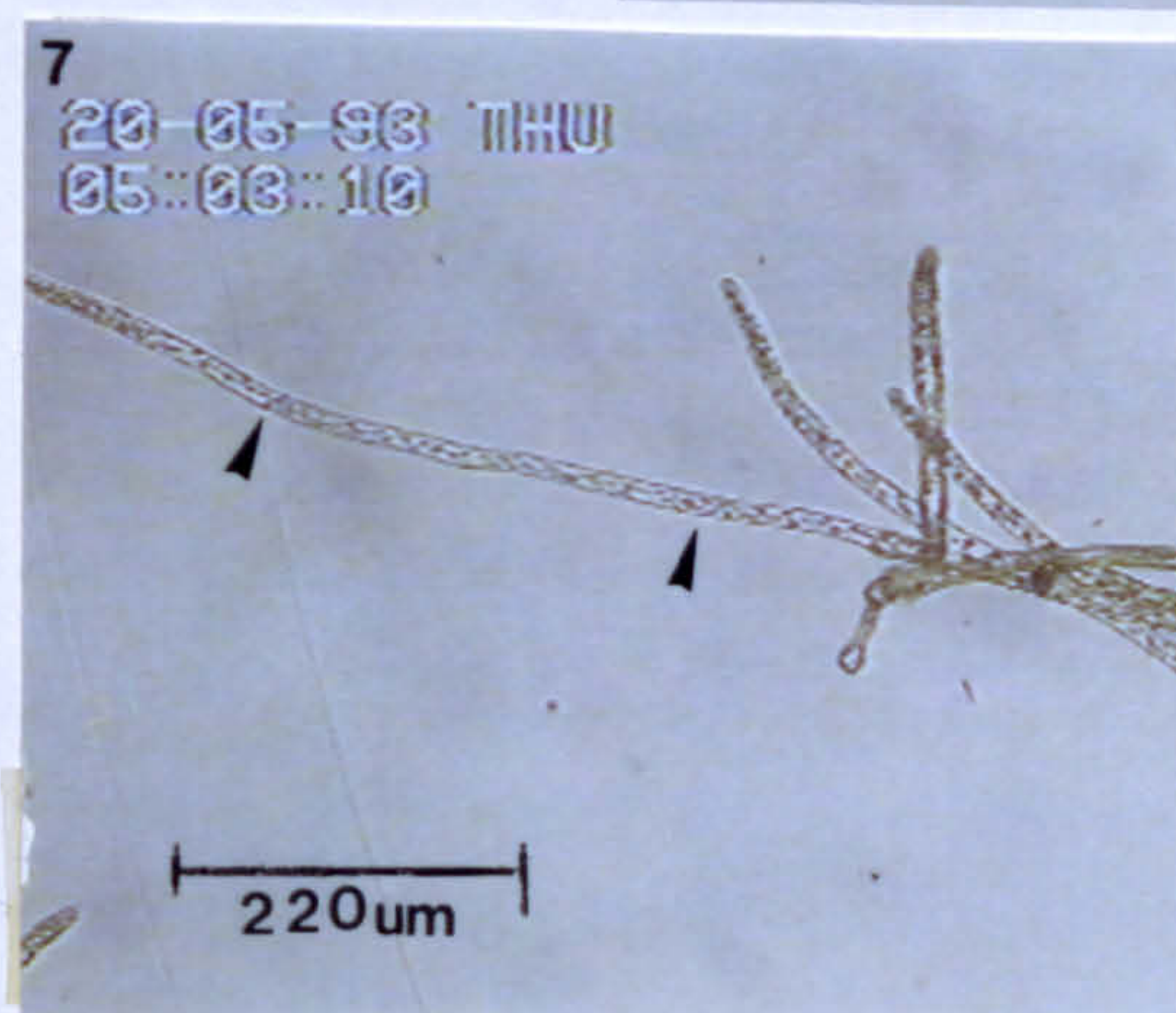
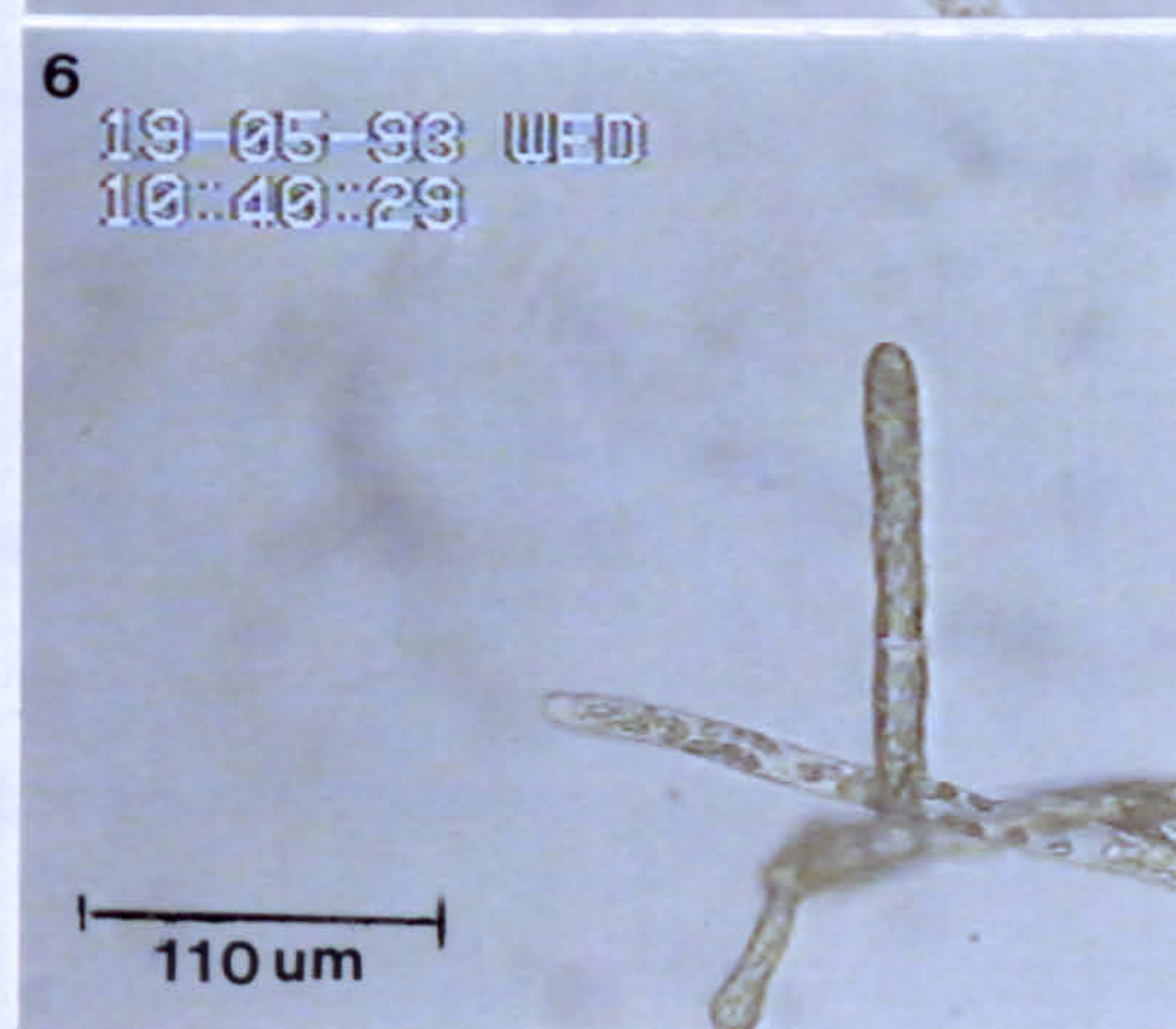
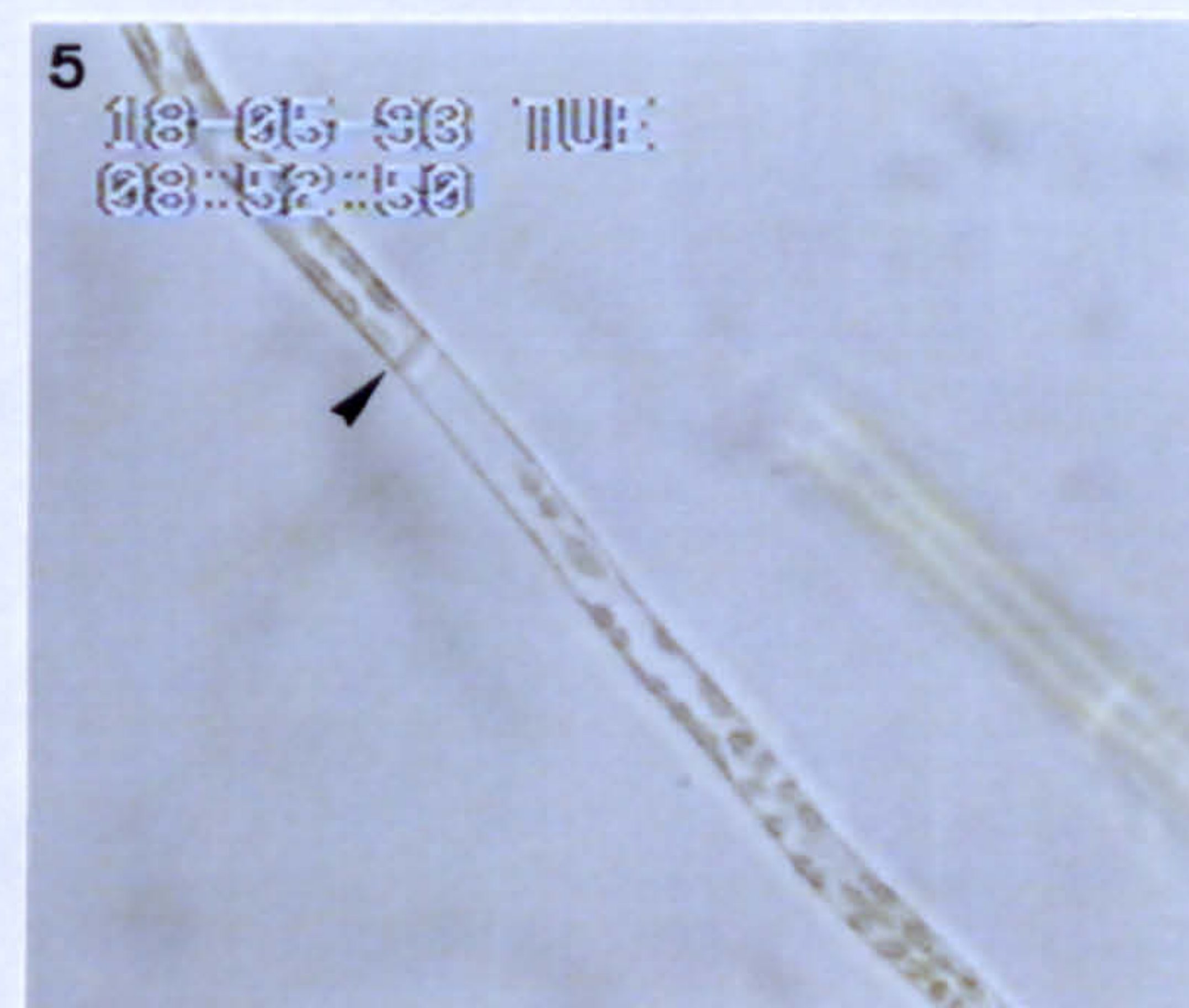
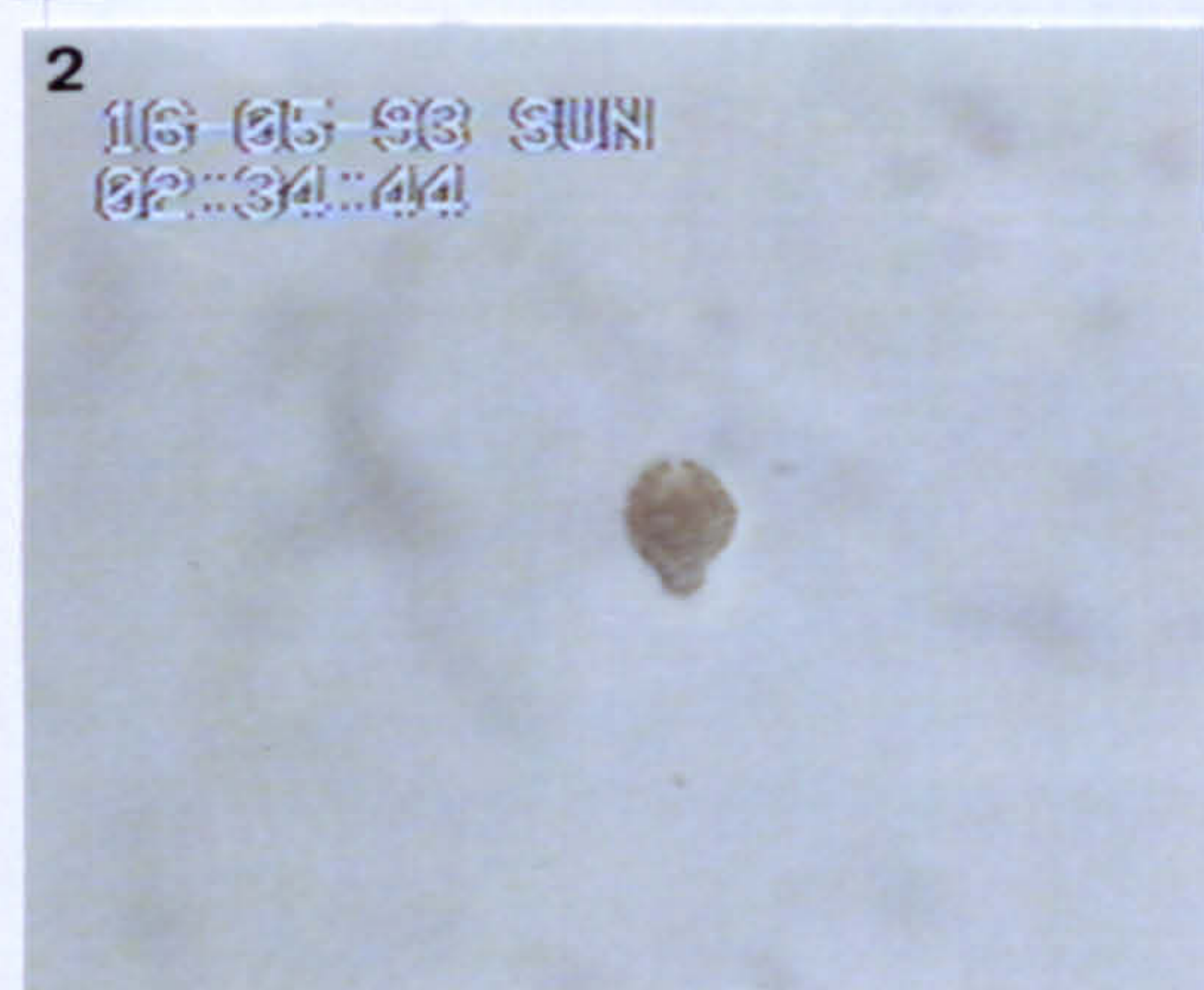
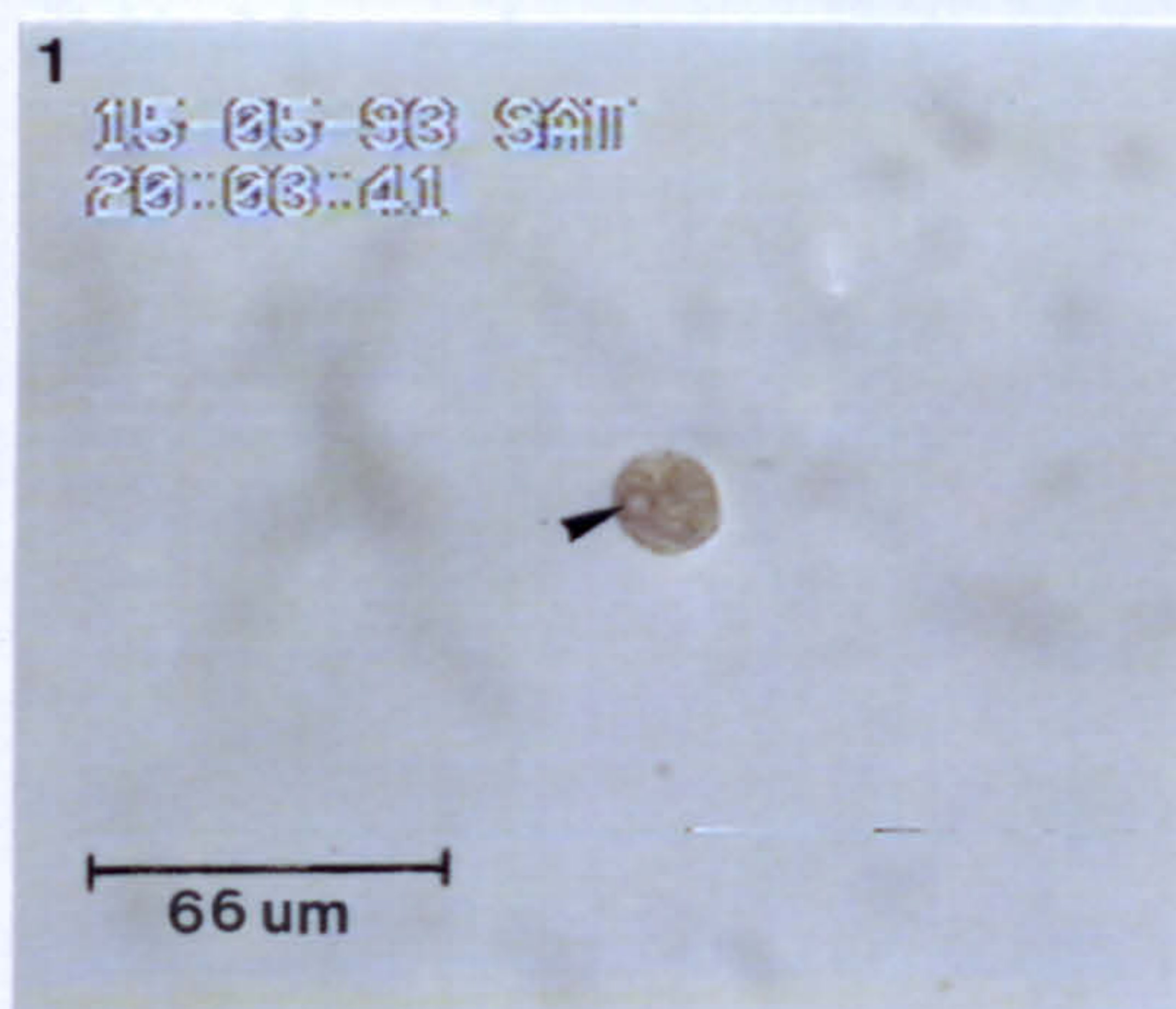




Table 2.2      A comparison of spore germination between *P. patens* and *F. hygrometrica*

<i>Physcomitrella patens</i>	<i>Funaria hygrometrica</i>
Multipolar or bipolar	Polar
First event: cell division of germ cell	No cell division in germ cell detectable. First event production of germ rhizoid
One primary filament from each cell	One primary filament
Further filaments from 2 basal germ cells	No further filaments from germ cell. All further filaments develop as side-branches.
Not all primary filaments grow at equal rates. One filament grows faster from start.	
All primary chloronema switch to caulonema or stop growing by 5 days after germination.	
The switch from primary chloronema to caulonema may take several cell divisions (up to six recorded) or only one.	The switch occurs over several cell divisions
Primary chloronema cell cycle not less than 20 hours	Primary chloronema cell cycle may be as short as six hours.



grow upwards towards the light out of the medium and out of the plane of focus. By two or three days they are overgrown by adjacent side-branches and caulonema filaments. These factors curtail filming for any length of time. However Fig. 2.6 illustrates three chloronemal side-branches filmed for periods ranging from 40-60 hours. In no case could the second cell division be seen due to overgrowth of other filaments. Filament 3 grows at  $1.5 \mu\text{m/h}$  for the first 17 hours, increases its growth rate to a maximum  $4.5\mu\text{m/h}$  for the subsequent 19 hours and then stops growth entirely, in a similar manner to primary chloronema. In all cases, the growth rate is sometimes intermittent, undergoing brief periods of slow growth or sudden increases in growth, as in primary chloronema.

It would appear that primary and secondary chloronema are very similar, except that secondary chloronema have a higher growth rate initially. In each case the transition to a caulonema mode of growth may occur over several cell cycles or within a single cell cycle. As in the case of primary chloronema, after 2 cell cycles the growth rate of secondary chloronema begins to increase into a transitional phase or stop.

The development of both primary and secondary chloronema is highly sensitive to light intensity. Primary chloronema can be maintained for an indefinite period under conditions of low light intensity. At light intensities below  $700 \text{ mWm}^{-2}\text{s}^{-1}$  the switch to caulonema does not occur. At certain light intensities a point of the transitional phase of secondary chloronema may be maintained indefinitely, so that for example all filaments are growing at a rate of ca.  $6\text{-}10 \mu\text{m/h}$  with a cell cycle time of 10 hours. A higher light intensity may maintain existing caulonema growth but inhibit chloronema side-branches from switching to caulonema.

#### 2.3.4 Caulonema

By approximately five days after germination a spore is surrounded by a radial growth of primary caulonema filaments. At this stage the average growth rate is 12-

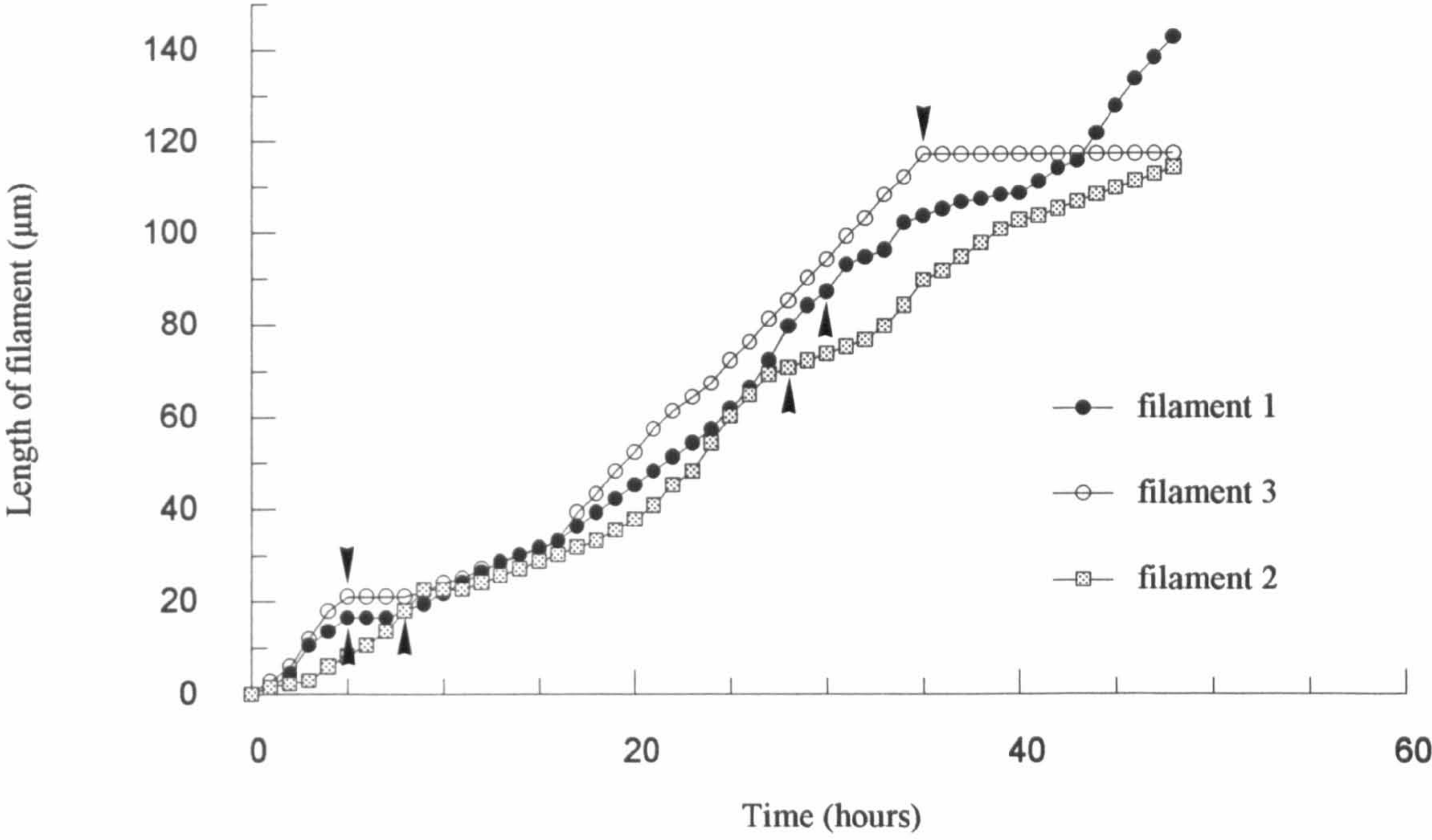


Fig. 2.6 The growth of three secondary chloronema filaments. Arrows indicate cell division. Filament 3 stops growing after 35 hours. Filament 1 begins to increase its growth rate after 40 hours.



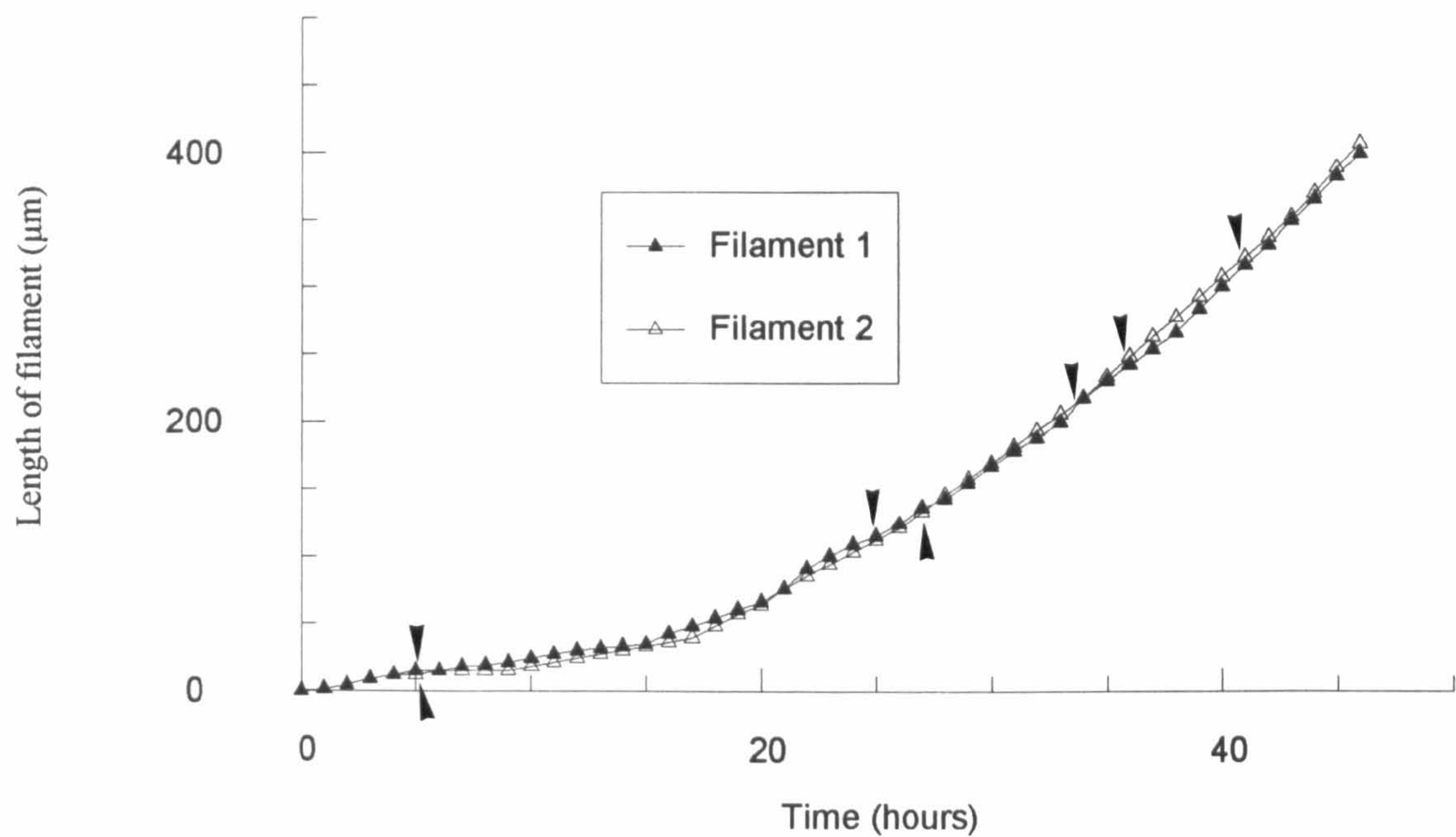


Fig. 2.7 The growth rates and cell cycle times of two side-branch filaments undergoing the transition from chloronema to caulonema. Arrows indicate cell divisions. After the first cell division the growth rate begins to increase and the cell division time to decrease, indicating that the chloronema apical cells are undergoing the transition to caulonema apical cells.

Table 2.3      Increase of growth rate and size with age of caulonemal cells from regenerating tissue innocula.

Time after inoculation (days)	Growth rate (µm/h)	Cell length (µm)	Cell diameter (µm)	Cell volume (µm³)	Cell cycle time (h)
3	14.5	127	13.5	18,250	8.8
4	21	142	13.5	20,300	6.8
5	26	157	15	25,500	6.0
6	28.5	172	15	30,500	6.0
7	28.5	172	16.5	36,900	6.0
8	29	176	16.5	37,500	6.1
9	31	180	16.5	38,500	5.8
10	31	180	16.5	38,500	5.8
11	31	187	16.5	40,000	6.1



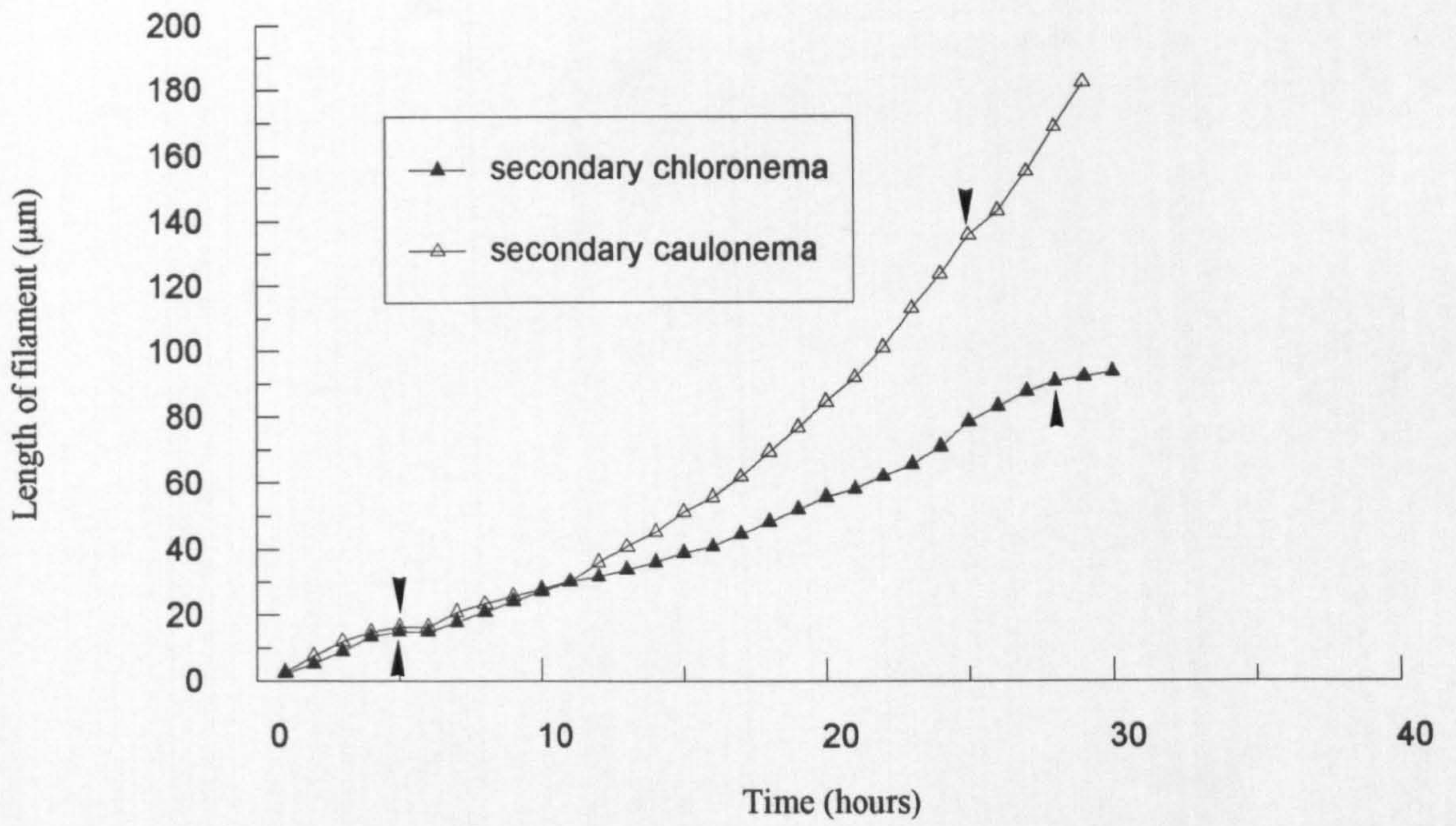


Fig. 2.8 The growth and cell cycle times of two side-branches, one secondary chloronema, the other secondary caulonema. Arrows indicate cell divisions.



Table 2.4      The cell cycle times, length and growth rate of caulonema apical cells of different ages. The cell division time was measured from the first appearance of the cell wall. Cell length refers to the length of the apical cell immediately after cell division.

Days after inoculation	Growth rate (µm/h)	Cell cycle time (h)	Cell length
8	24.6	5.3	129
		6.0	153
		6.3	150
		7.0	168
9	31	5.3	165
		6.0	189
		6.0	177
11	33	5.5	177
		5.5	183
12	26	6.0	150
		6.0	156
		6.0	153
		6.0	156
		6.0	156
15	27	6.0	174
		7.0	192
		7.0	174
16		8.3	210
		7.3	198
		7.0	186
		6.5	165
21	27	6.5	174
		6.5	174
		6.5	174
42	40	6.0	240
		6.3	222
		5.0	204
		5.5	234



15  $\mu\text{m}$ , the cell length 100-120  $\mu\text{m}$ , the cell cycle time ca. 8-9 hours. A relationship between growth rate, cell length and cell cycle time is apparent in table 2.1. As the filament develops, growth rate and cell length increase and cell cycle time decreases. Once the cell cycle time is ca. 8-9 hours the characteristic oblique cell wall of a caulonema filament appears. Table 2.3 also examines the relationship between growth rate and cell length with age of filament in this case in regenerating tissue innocula. It is not possible to compare directly the development of caulonema filaments from regenerating tissue to those of spores as the age and hormone content of tissue innocula may influence subsequent regeneration and development. Three days after subculture, caulonema filaments are clearly apparent and a primary chloronema phase may not exist as in spore germination or protoplast regeneration. However, whether developing from primary chloronema or side-branches from tissue innocula, a caulonema filament undergoes a progressive increase in growth rate and therefore the length of its cells over the first few days of growth. The increase in growth rate is most noticeable over the first two days when the growth rate of the majority of filaments increases from ca. 14  $\mu\text{m}/\text{h}$  to a maximum 30  $\mu\text{m}/\text{h}$ . A difficulty in comparing filaments from tissue of different ages is that the age of the filament undergoing filming may not be related to the age of the tissue as it may have developed from a side-branch initial at any time since subculture. However by 11 days after subculture (table 2.3) the maximum growth rate had increased to 34  $\mu\text{m}/\text{h}$  and the cell length to 187  $\mu\text{m}$ . The results presented in table 2.4 suggest that this growth rate remains stable for at least the next two to three weeks. For a six-week old colony the maximum growth rate was found to have increased to 41  $\mu\text{m}/\text{h}$  resulting in a maximum cell length of 240  $\mu\text{m}$ . The cell cycle time did not decrease below 5 hours. This is approaching the growth rate and cell length of the larger faster growing filaments of *Funaria hygrometrica*.

### 2.3.5 Mutant strains

Many mutant strains, although apparently producing normally growing caulonema while deficient in bud or gametophore production, have altered cell cycle times and/or growth rates. A few selected strains were filmed in order to characterise them more fully, and to examine the range of these two characteristics within which phenotypically normal caulonema can exist. Also to reveal strains which may be mutant in aspects of the cell cycle. Mutant strains which did not produce gametophores (*gam*), and which were either resistant to (*bar*), or sensitive to, cytokinin were chosen for analysis. Two gametophore overproducers (*ove*) were also included, one of them also deficient in the production of chloronemal side-branches.

The results of these films are shown in fig. 2.9 and Table 2.5. The two cytokinin-responsive *gam* mutants, *gam*-139 and *gam*-710, show the closest to normal wild-type caulonemal growth in terms of growth rate and cell cycle time, although both have less obviously polarised apical cells. The *gam* auxin-resistant *nar*-87 can also be repaired by the addition of cytokinin, but exhibits a high degree of variation in cell cycle time and growth rate. The length of the cell appears to be dependent on both factors to equal degree. Between the different strains, cell length is a more constant factor than cell cycle time. The two strains with the slowest growth rate, *bar*-1, and *ove*-405, both have the longest cell cycles. However, control growth rates of the auxotrophic strains from which the mutants were derived are necessary in order to confirm these observations.

### 2.3.6 Protoplast regeneration

In order to compare spore germination with other forms of regeneration, in particular protoplast regeneration, protoplasts were filmed ca. 4 days after culture on 9% mannitol. The sequence of pictures in Fig. 2.10 illustrate the early stages in protoplast regeneration. These appear to be very similar to the first events in spore



Table 2.5      The cell cycle times, cell length and growth rate of caulonema apical cells of selected mutant strains grown under standard conditions

Mutant strain	Growth rate (μ/h)	Cell cycle time (h)	Cell length (μm)
<i>gam</i> -139	27-30	7.16	186
		8.16	183
		8.16	153
<i>nar</i> -87	15-27	5.0	105
		7.16	120
		5.6	105
		7.16	150
		7.0	114
<i>bar</i> -576	21-24	9.8	210
		9.0	189
		9.3	192
		9.0	189
<i>gam</i> -710	21	7.16	186
		8.16	183
		8.16	153
<i>bar</i> -1	15	11.0	180
		10.0	150
		10.0	165
<i>ove</i> -405	12-15	12.0	126
		11.0	108
		16.0	165

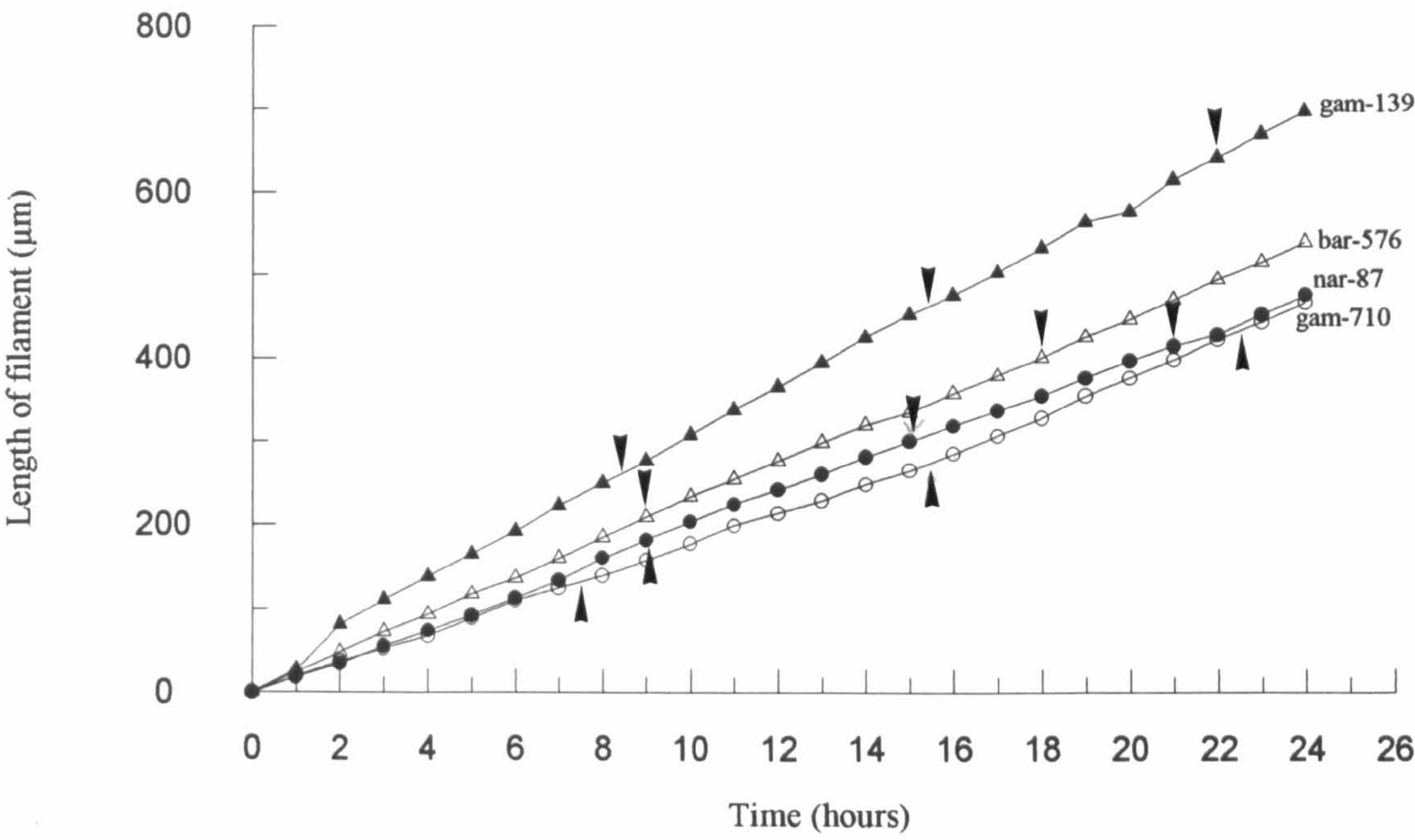


Fig. 2.9 The growth and cell cycle times of caulonema of four mutants. Arrows indicate cell division.

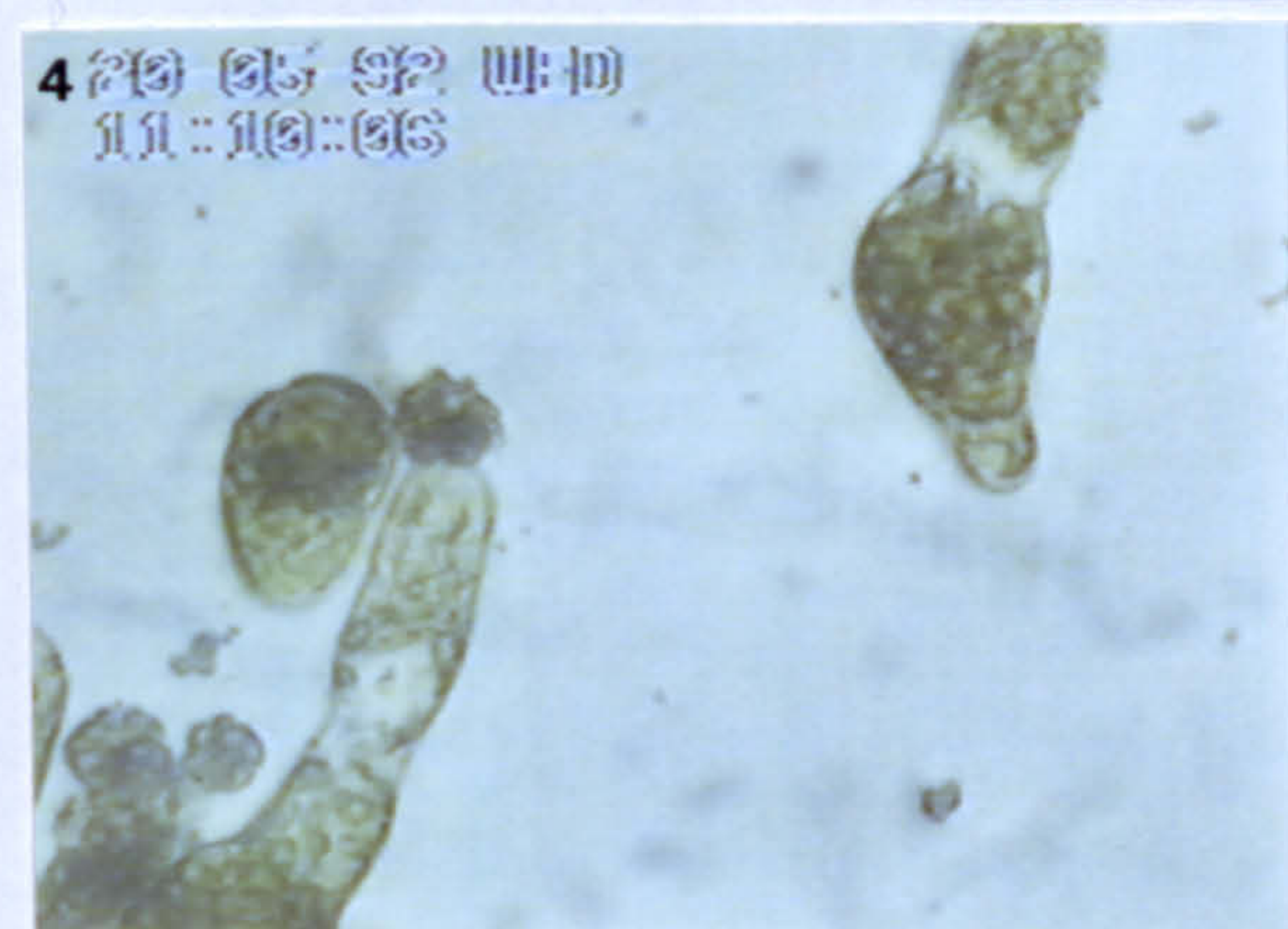
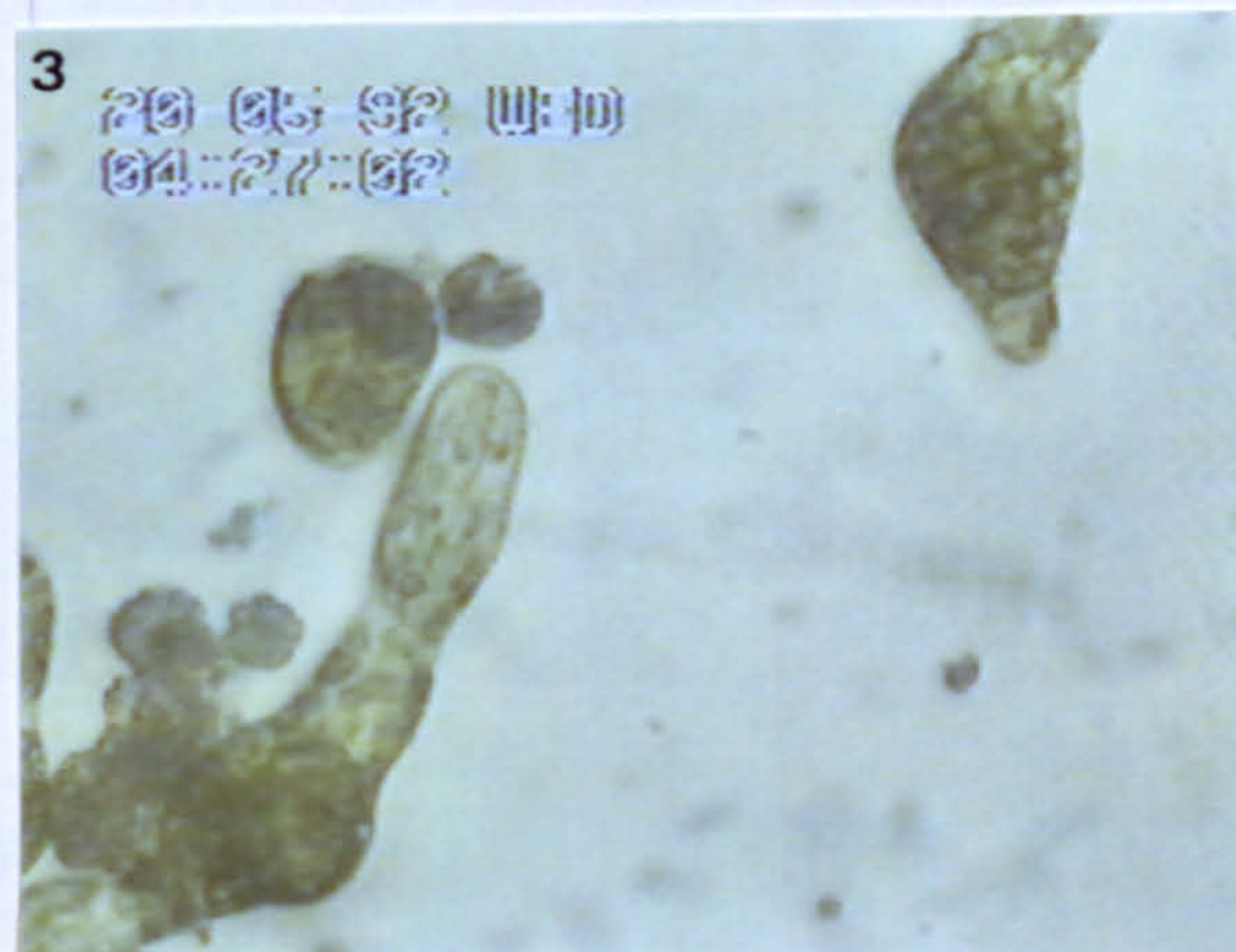
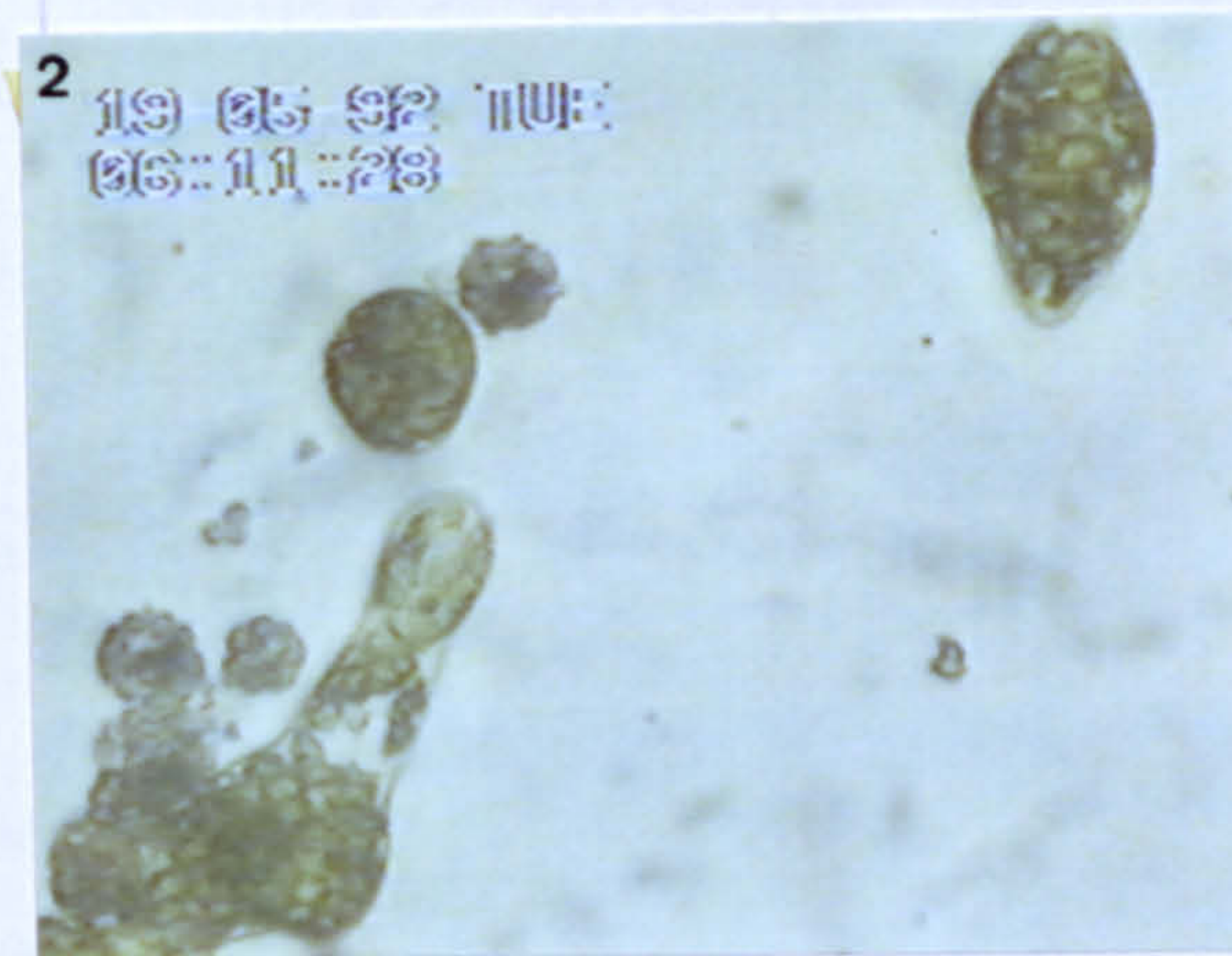


**Fig. 2.10 The regeneration of protoplasts**

Protoplasts were plated on 9% mannitol on 14.5.92. Filming began at 14.30 on 18.5.92.

- 1 At the start of filming, protoplast 2 has formed the first protrusion. Protoplasts regenerate at different rates over a 4 or 5 day period.
- 2 15.5 hours after the start of filming: protoplast 2 is forming a slight pear shape with a clear membranous area just visible at the base. protoplast 1 has produced a filament at each end.
- 3 38 hours after the start of filming: protoplast 2 undergoes cell division within the protoplast (arrow).
- 4 42.5 hours after the start of filming. The first filament is formed in protoplast 2. Arrow indicates the cell division occurring in the second filament of protoplast 1.







germination. At the point where the first filament will protrude the protoplast becomes slightly but noticeably pear-shaped (2.10, 2). The first event to happen is therefore the establishment of a polar axis. At this magnification (x320) a clear membranous area is just visible. The next step is for the cell to divide parallel to the pear-shaped membranous clearing (2.10, 3). This appears to be equivalent to the initial (hidden) division of the spore. As in the spore filaments are pushed out at opposite ends of the two cells created by the initial division. These are chloronema and have a similarly slow growth rate to the primary chloronema of the spore.

### 2.3.7 Bud development

The earliest it has so far been possible to film a developing bud is shortly before the first cell division. The sequence of pictures in fig. 2.11 show a bud developing as a second side-branch initial at the 10th subapical cell position. The culture in this film has not had hormone added to it. The occurrence of buds as second side-branches and as pairs is not an unusual event (see ch. 3). Second side-branches normally arise when the subapical cell is at the 6th or 7th position. Assuming the cell cycle of the apical cell is 6 hours, this bud initial would have been developing for ca. 24 hours. Fig. 2.11, 1) shows the nucleus in a slightly acentric position with more chloroplasts on the lower side of the initial which will eventually form the leaf initial cell. The subsequent cell division divides the initial into two distinct regions, one with the majority of chloroplasts, the other relatively chloroplast-free. A feature of the developing bud initial is the assymetrical development of the cell walls before the first division. A slight bulge on one side corresponds to the position at which the first rhizoid will form. On the opposite side of the initial an indentation marks a point of attachment of the future oblique cell wall and divides the cell into stalk and leaf regions.

The second and third cell divisions occur synchronously (Fig. 2.11, 3) ca. 6 hours later. The division of the upper chloroplast-poor zone divides this portion of the initial into rhizoid initial cell and stalk. These two cells do not undergo further divisions as

**Fig. 2.11 Bud formation in *P. patens*.**

Filming began at 14.00h on 8.03.91. The bud initial is at the 10th cell position of the caulonema filament, and is developing from the second side-branch initial of the subapical cell.

- 1      1 hour after the start of filming: the nucleus can be clearly seen in the centre of the initial (arrow), shortly before the first cell division of the initial.
- 2      2 hours after the start of filming: the first cell division of the bud initial divides the initial into two distinct regions, one with more chloroplasts than the other.
- 3      Ca. 5.5h later, 2 second cell divisions occur (arrows). The initial now consists of 4 cells.
- 4      24 hours after the start of filming: cell 1 has become the stalk of the bud. Cell 2 forms the first rhizoid. Cells 3 and 4 divide to form further rhizoid cells and leaf initial cells. The gametophore forms from cells 3 and 4.
- 5-8    Further divisions occur around the initial. Cells towards the base of the bud form further rhizoids. Cells at the upper end of the bud form leaf initials. Arrows indicate the leaf initials.



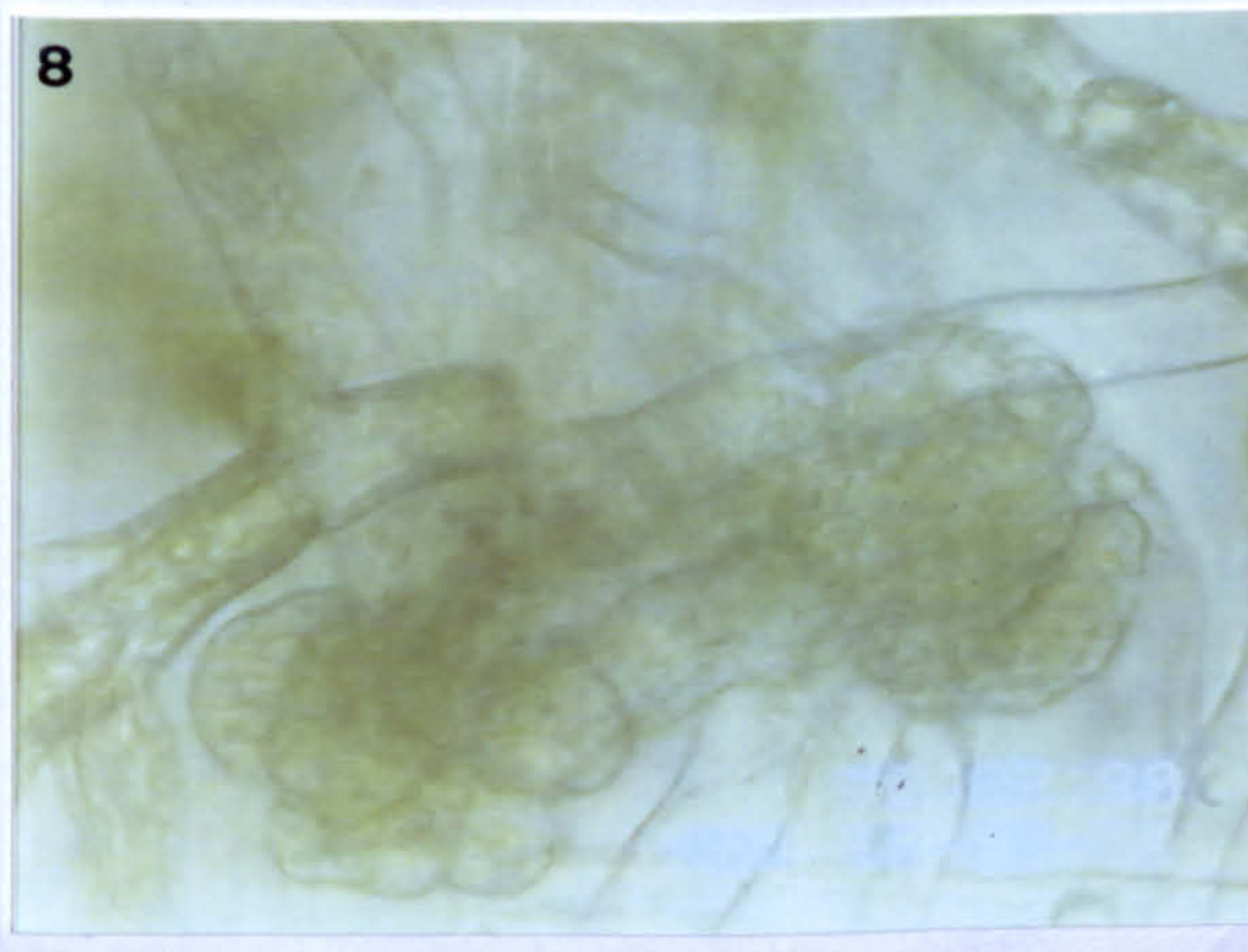
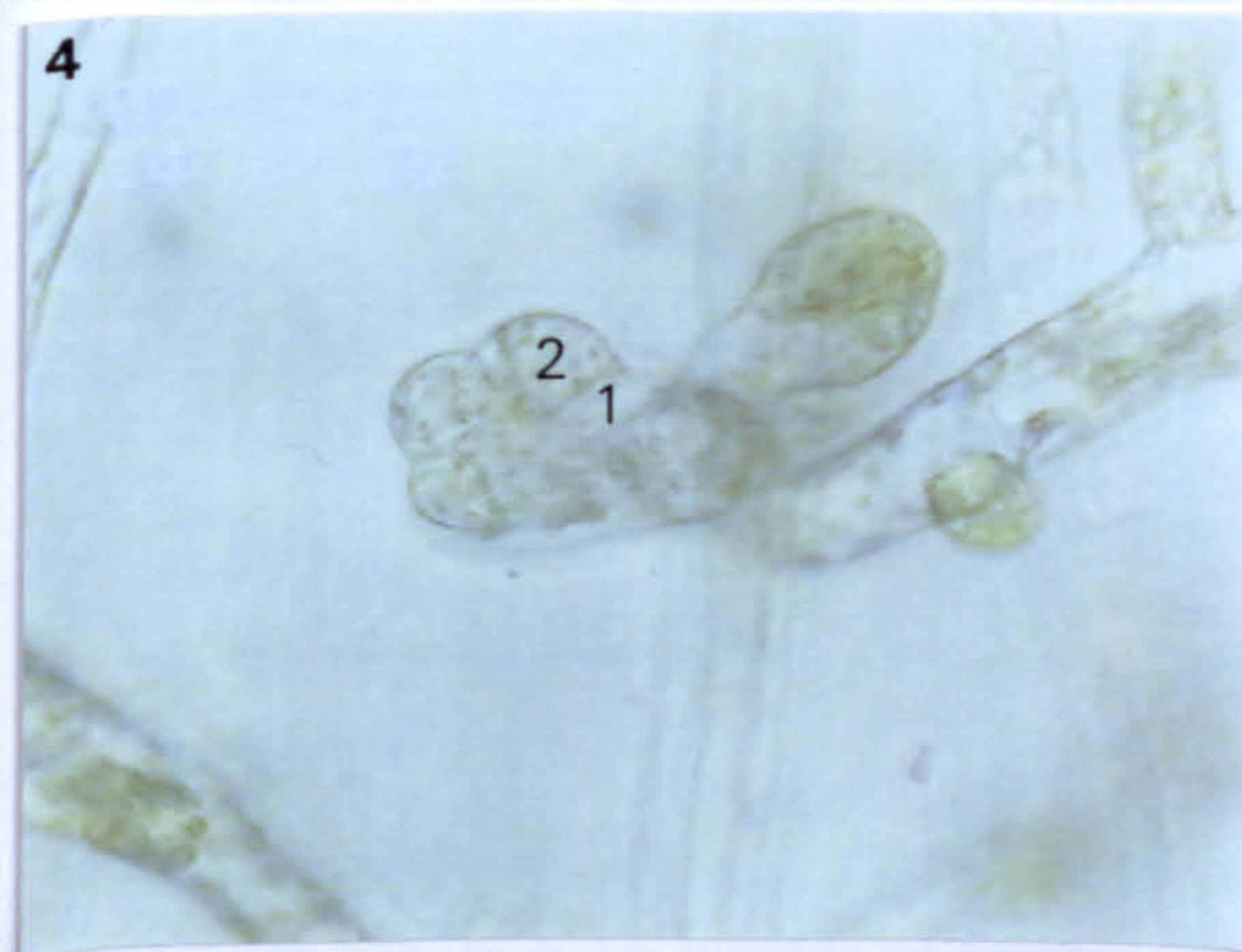
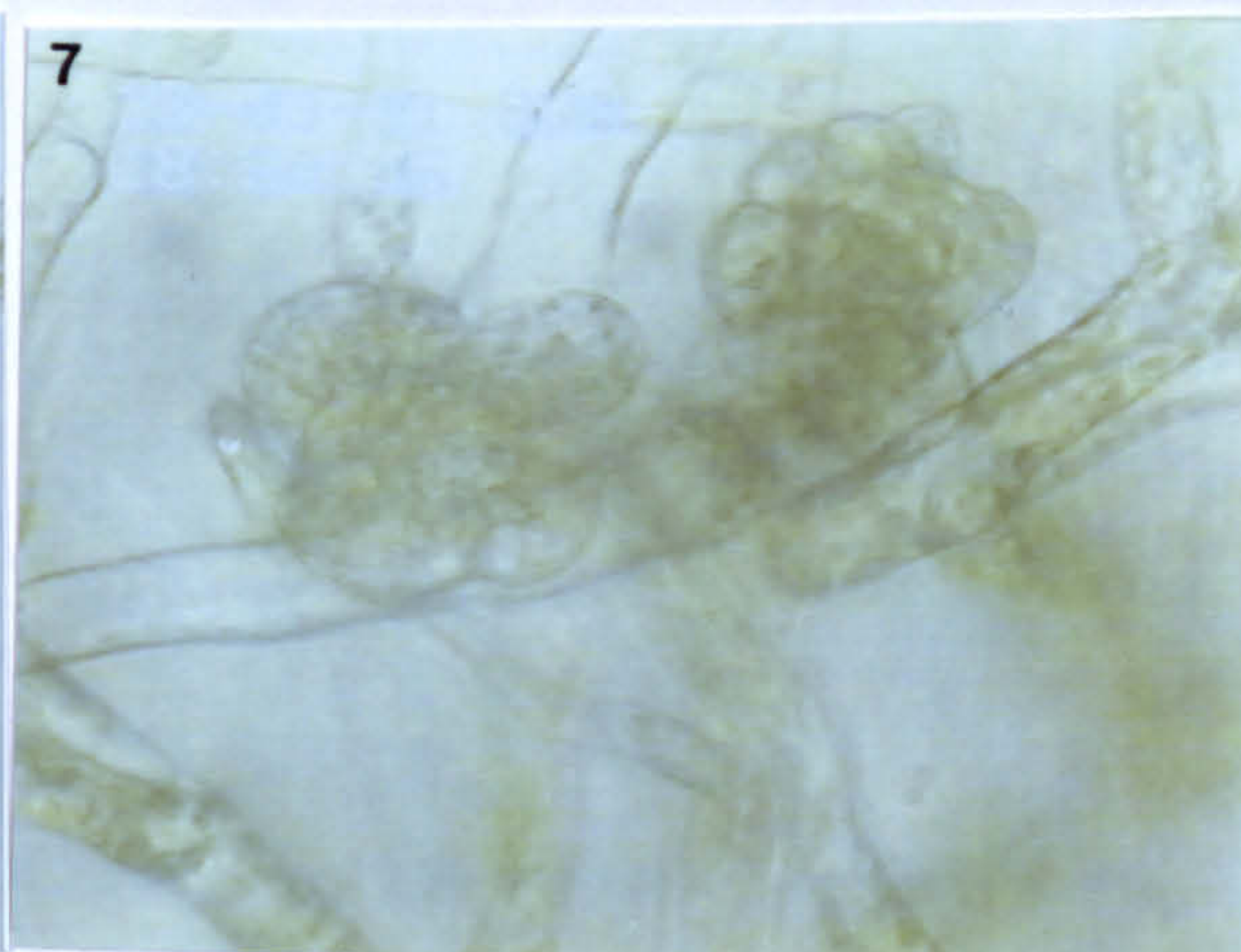
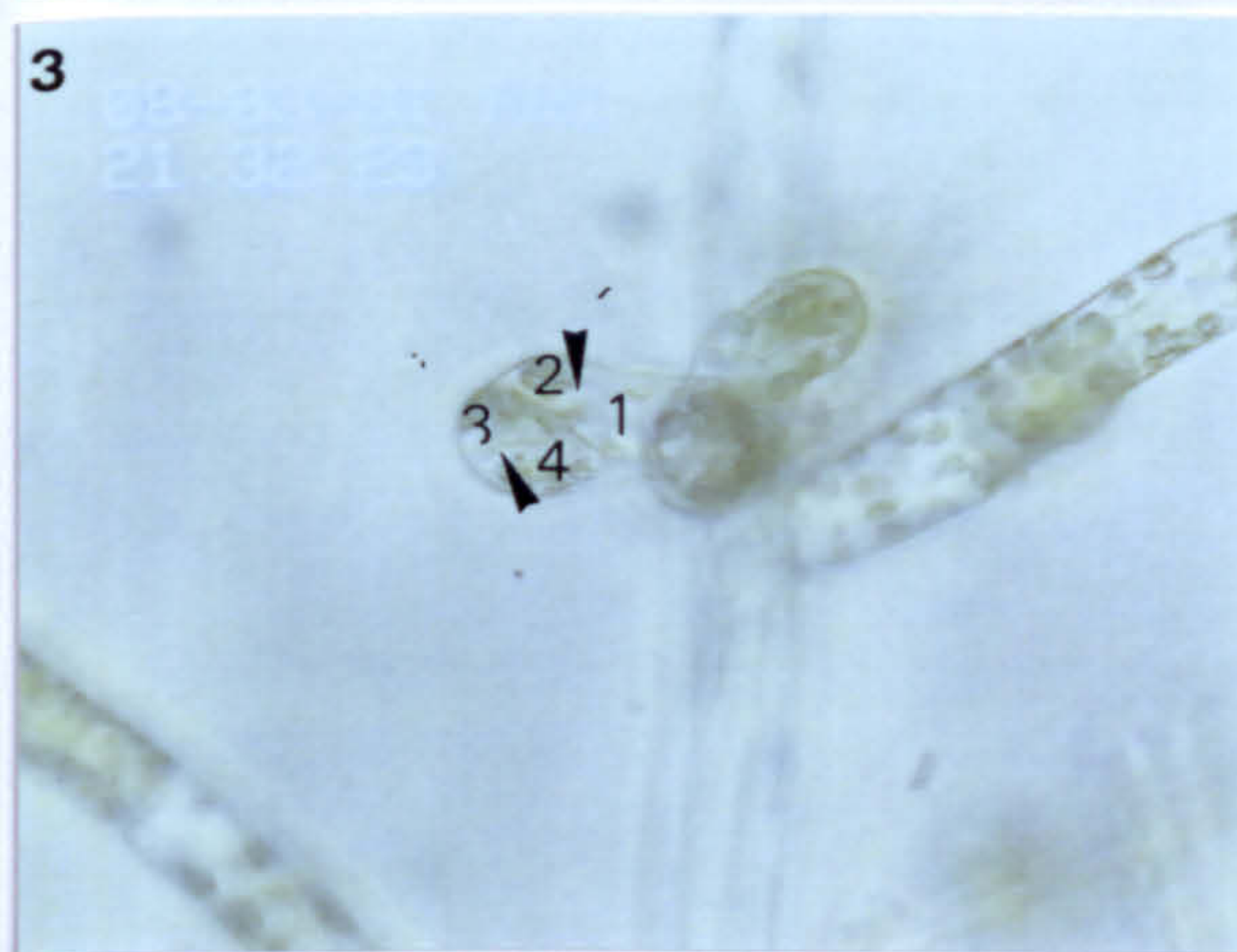
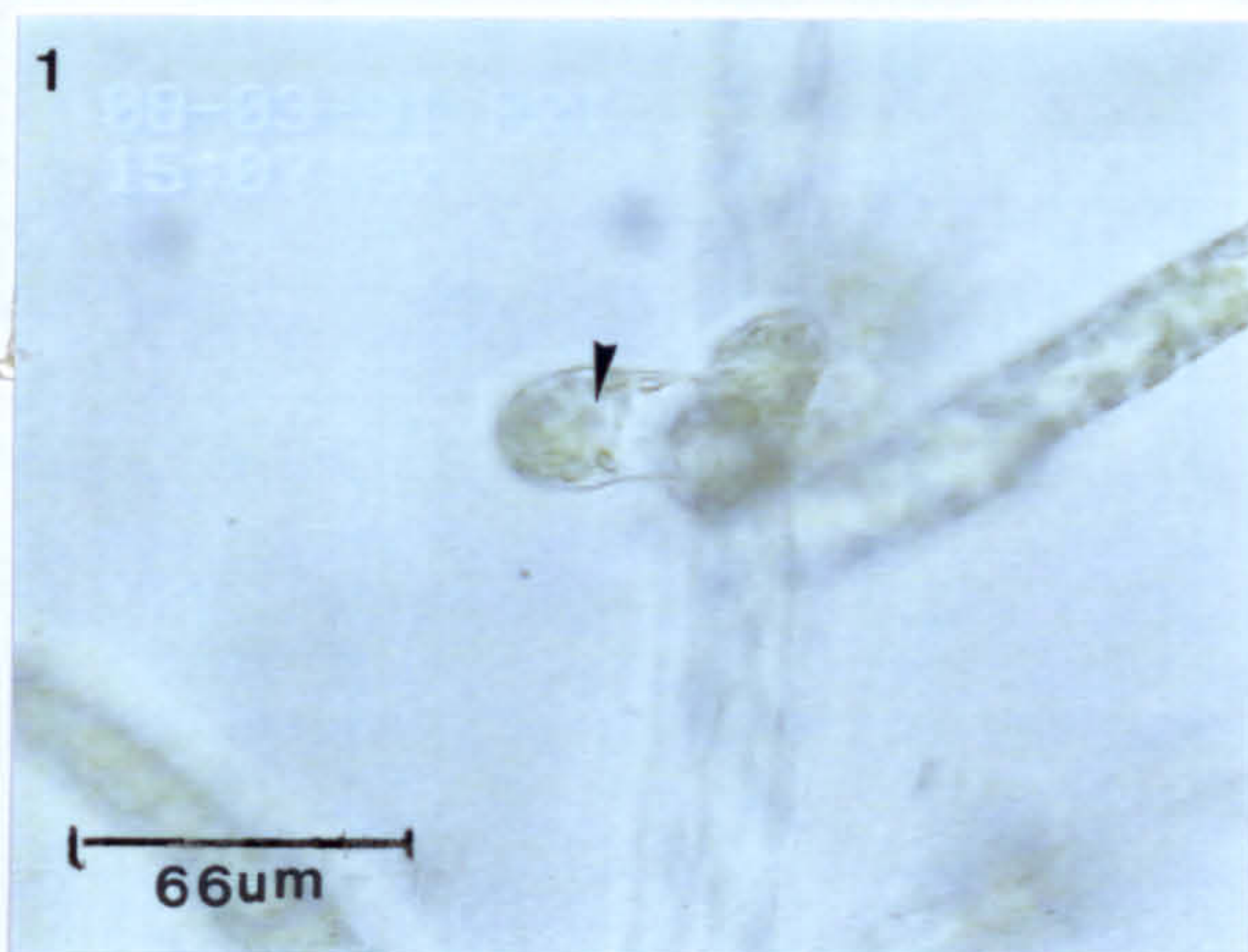


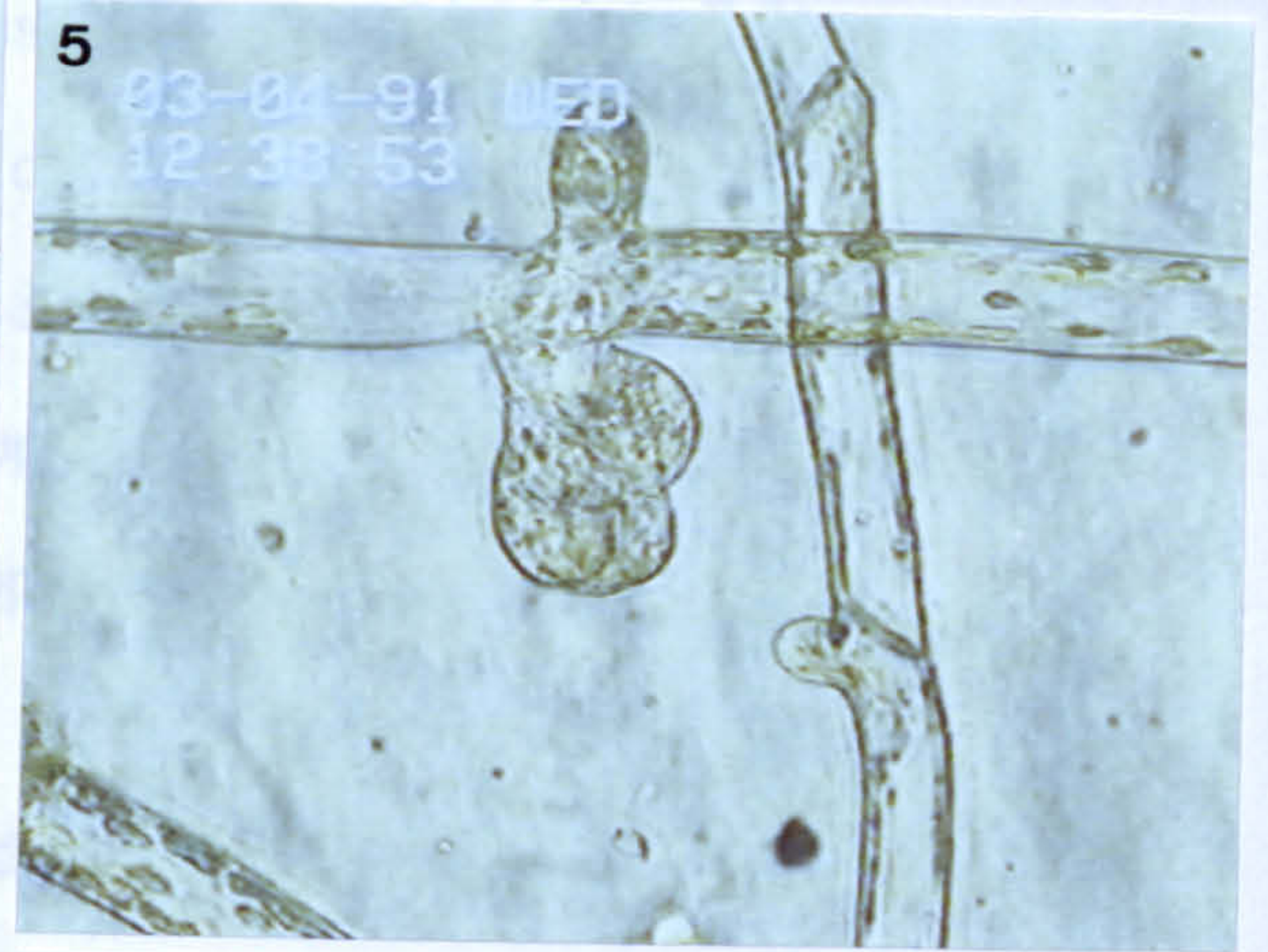
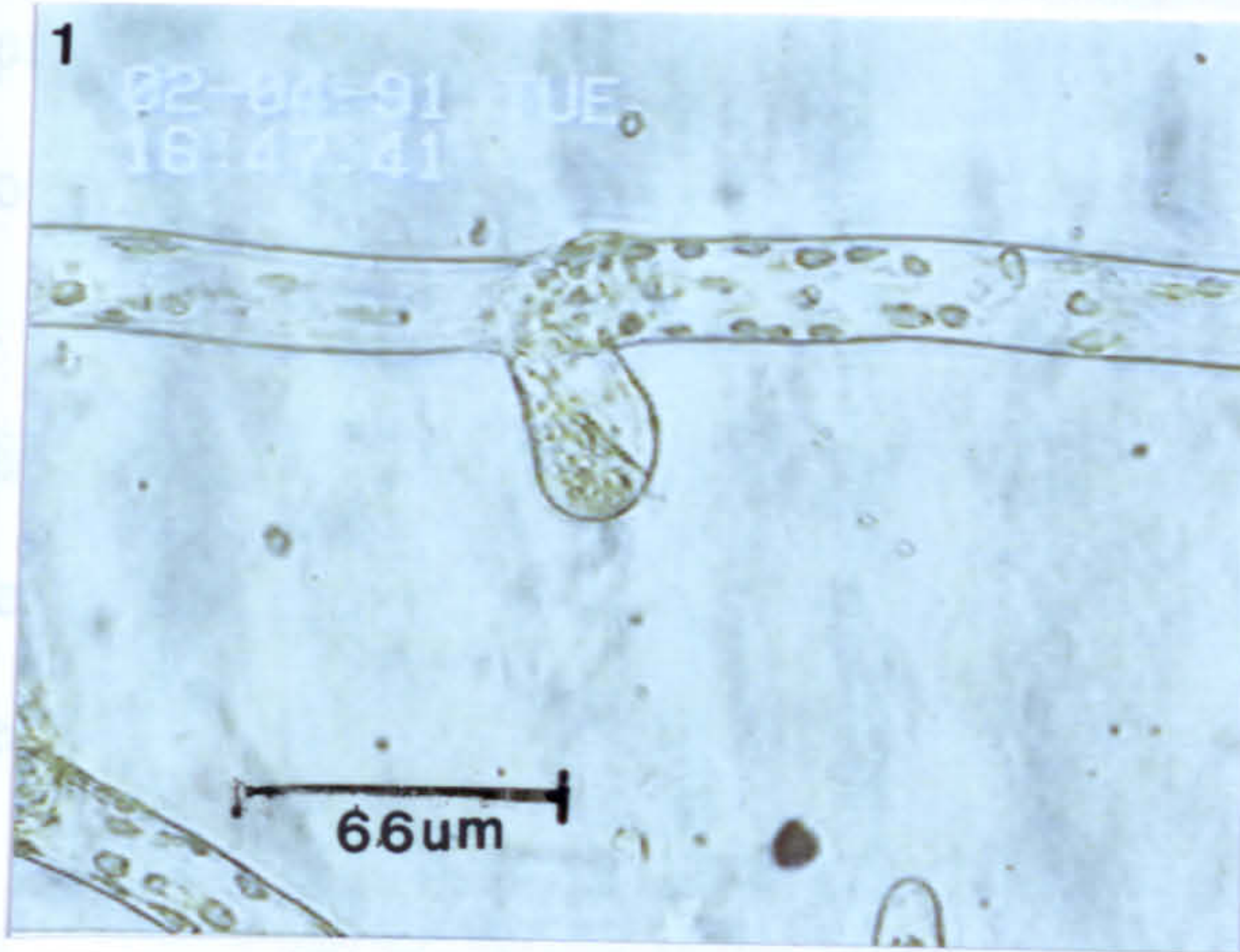


**Fig. 2.12 Bud formation in *P. patens*.**

**A second film of a bud forming from an initial in an untreated culture of *P. patens*. Filming began at ca 16.40 on 2.4.91. The initial is on a subapical caulonema cell at the seventh cell position from the apex.**

- 1        The first division of the initial into chloroplast-rich and chloroplast-poor regions can be clearly seen.**
- 3&4    From the 4-celled stage of the bud, cells 1 and 2 again form the stalk and first rhizoid.**
- 5-8    The rest of the gametophore develops from cells 3 and 4.**





the side branch initials and form separate bud initials.



part of the initial. The lower cell directly opposite the rhizoid initial (cell 3) appears to undergo further divisions as in fig. 2.12. The cells toward the stalk appear to create a 'meristematic area' producing more rhizoid initials. The upper cells continue to divide producing the first leaf initial. Cell 4 opposite the stalk area (Fig. 2.11, 4-8), referred to as the tetrahedral apical cell, also appears to expand and divide to create a leaf initial.

Fig. 2.12 is another filmed sequence of bud formation. Here the division of the initial cell into a chloroplast-free and chloroplast-rich zone is even clearer. Out of the four cells created by the first two cell divisions two are clearly determinate, the stalk area and the rhizoid initial. The whole of the gametophore forms from the two indeterminate cells resulting from division of the original chloroplast-rich cell.

### 2.3.8 The effect of cytokinin on bud development

The effect of cytokinin on the early patterns of cell division in bud development can be seen in fig. 2.13. BAP (1 $\mu$ M) has been added to the culture at the start of filming. The cells in fig. 2.13 (1) are at cell positions 4, 5 and 6. An early effect of cytokinin at this concentration is to cause the first cell division of the initial to occur within the subapical cell, rather than parallel to its cell walls. The growth of the initials is not slower than the growth of chloronema initials, so that an inhibition of polar growth is not immediately apparent. However, the cells increase in width as well as length, so that there is a switch from polar growth to overall growth. Even with time-lapse, it is not easy to assess the exact time that this occurs. Shortly before the first cell division, the vacuole expands to create the stalk region, as in natural bud formation. From thereon the early cell divisions do not follow any pattern. The cells of the bud initial divide independently to form callus rather than as a unit to form rhizoid and leaf initials. At this concentration cytokinin inhibits the formation of rhizoids completely. Outgrowths of cells which could be equivalent to rhizoid initials react to cytokinin in the same manner as side-branch initials and form separate bud initials.

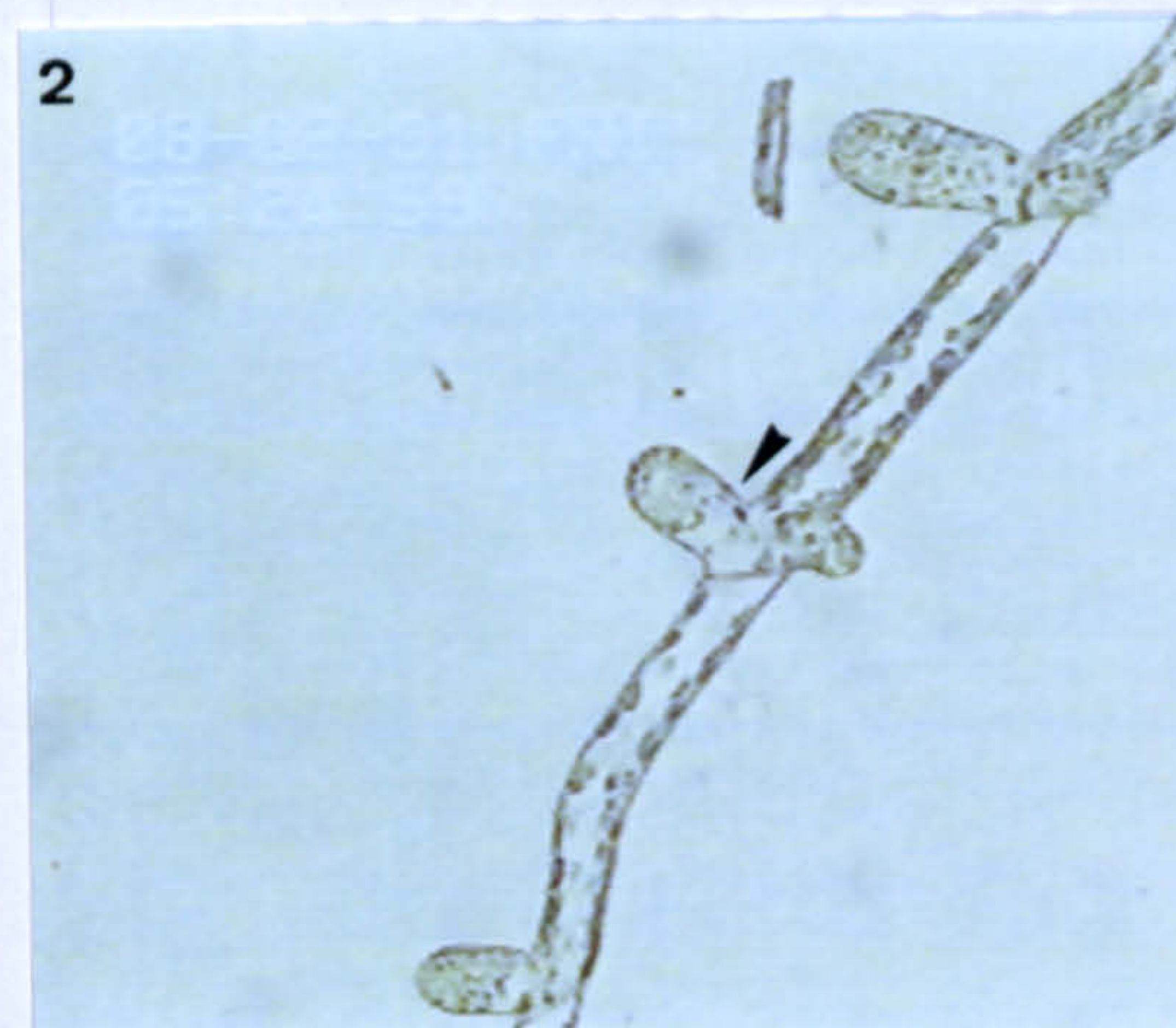
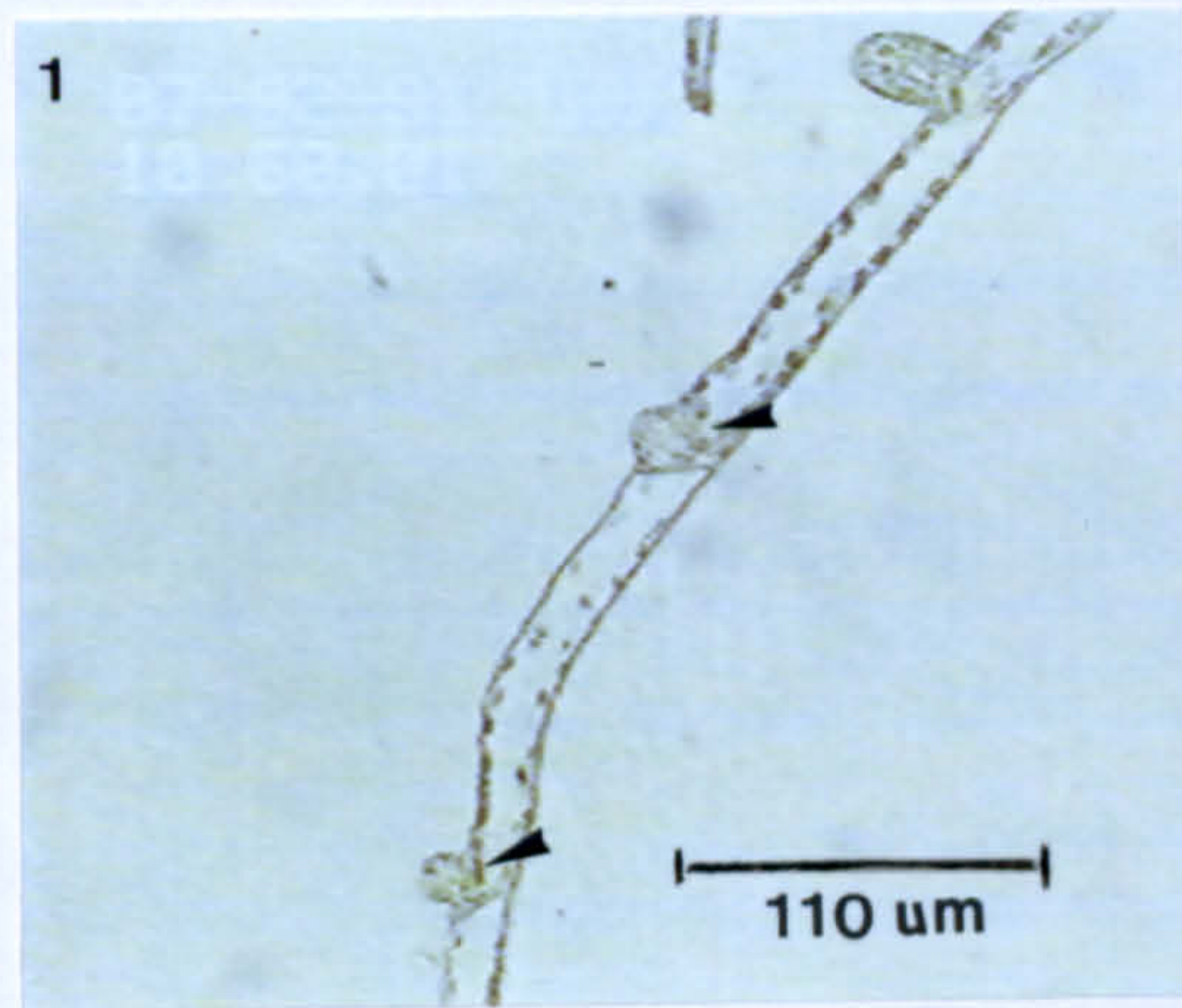


**Fig. 2.13 Cytokinin-induced bud formation in *P. patens*.**

Filming began at ca 20.15 on 6.2.91. BAP (1 $\mu$ M) was added at the start of filming. The initials are on subapical cells at cell positions 3, 4 and 5 from the apex at the start of filming.

- 1      15 hours after the start of filming: the side-branch initials have formed normally, but the cell walls dividing initials 1 and 2 from the parent subapical cells have formed within the subapical cell (arrows) rather than parallel to the walls of the subapical cell.
- 2      32 hours after the start of filming: the first stage of bud formation, the expansion of the vacuole to form the stalk region (arrow), is the same as in untreated bud formation.
- 3      49 hours after the start of filming. The growth of the first 3 initials is not slower than chloronemal polar growth. However, the cells have undergone increases in width, as well as length, and disorganised cell divisions have occurred. The apical cell of a caulonema filament is not induced to swell by BAP. Arrow indicates cell division in the 4th initial.
- 4      63 hours after the start of filming. Cytokinin has induced initials to form disorganised callus buds. The production of rhizoids is inhibited.







The growth of filaments exhibiting established polar growth at the time of application of the hormone is not immediately affected. As Bopp (1984) recorded, side-branches over ca. 80  $\mu\text{m}$  in length continue to grow as filaments. However after approximately 3 days, all filamentous growth, including that of the apical cell, is inhibited at concentrations of 1  $\mu\text{M}$  cytokinin.

As well as inhibiting cell polar growth, cytokinin appears to encourage chloroplast division. Fig. 2.13, 2,3 shows the increase in chloroplast numbers in the subapical cells of the caulonema filament.

### 2.3.9 The effect of light on a dark-grown caulonema filament

When a dark-grown culture is exposed to the light, there appears to be intense branching activity in the manner of regeneration or spore germination. Each filament produces side-branches which spread in all directions so that the tip of every filament appears to be forming a separate focus of regeneration.

To study this process in more detail a culture was grown in the dark for 6 days. The effect of sudden exposure to high light on one of the filaments of this culture was filmed over a period of three days (fig. 2. 14, 1-8). The culture was placed in light at the beginning of filming.

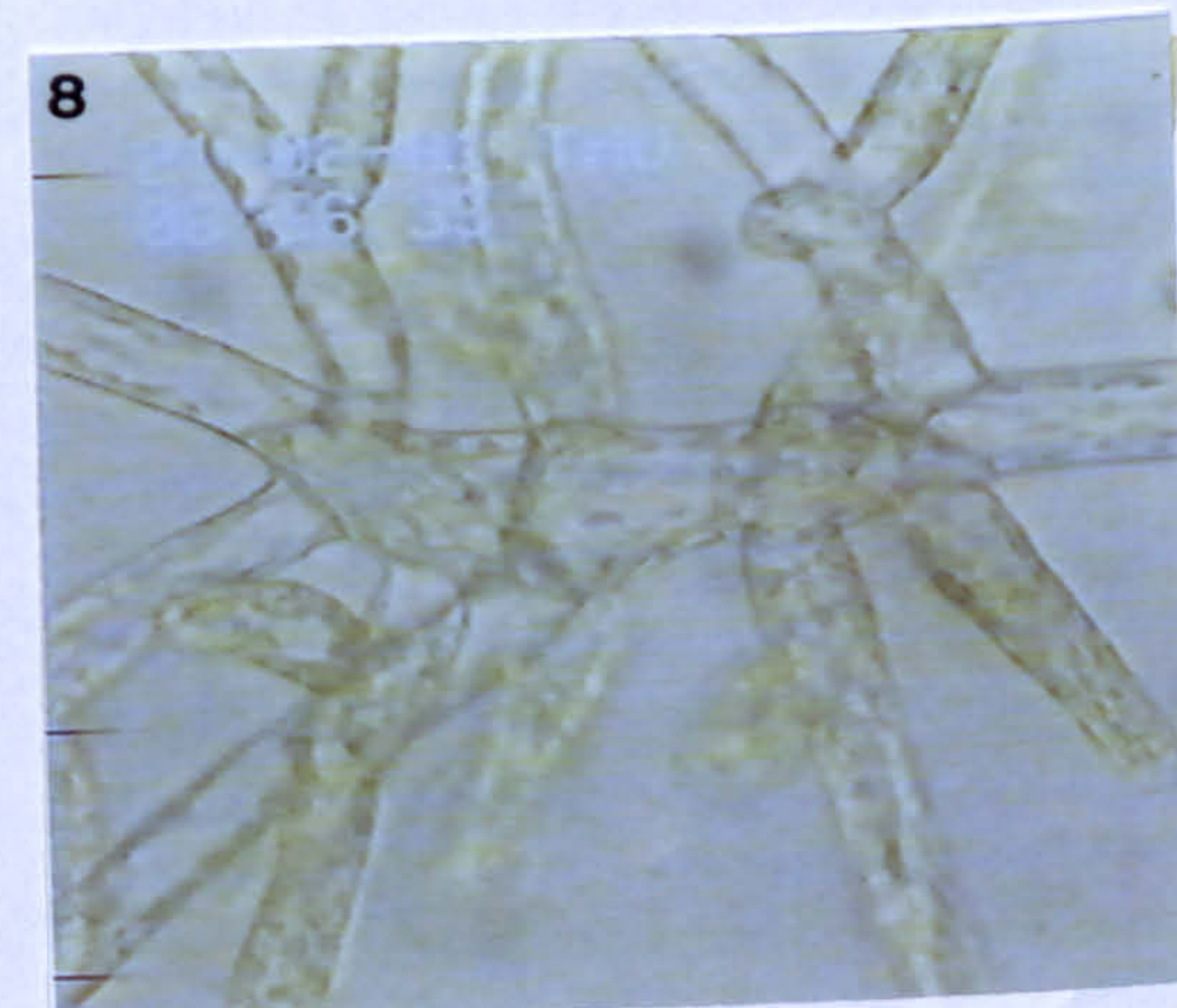
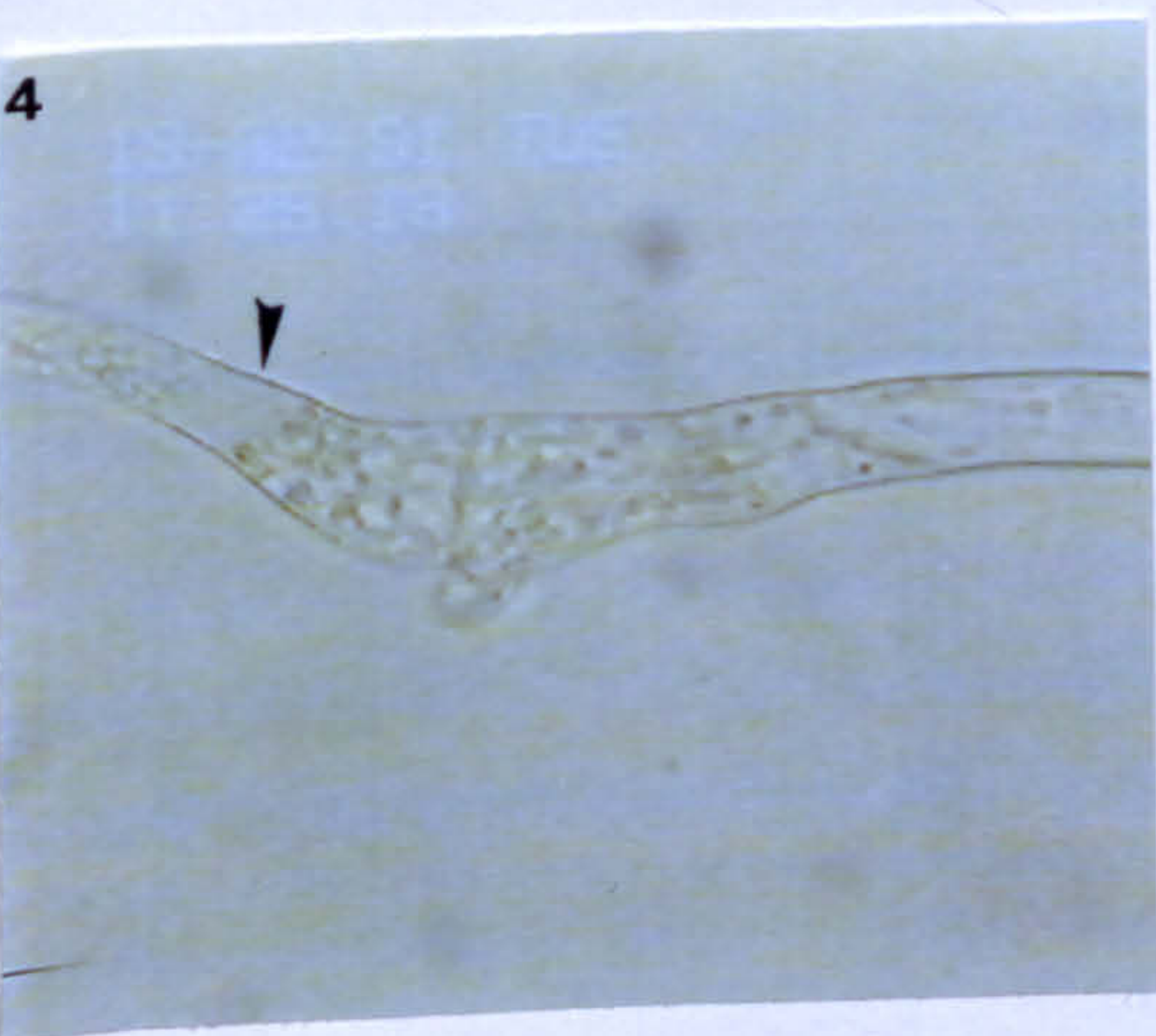
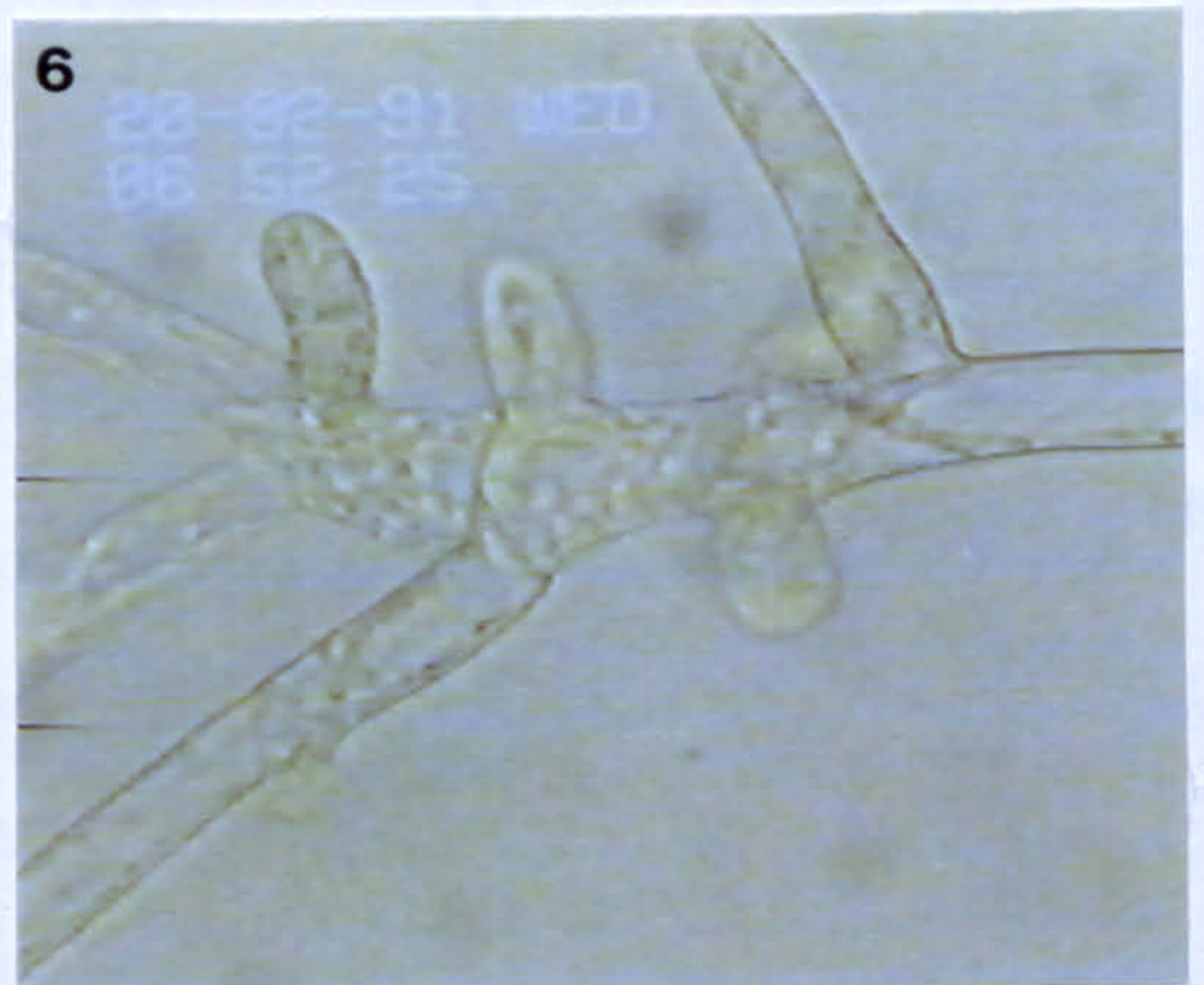
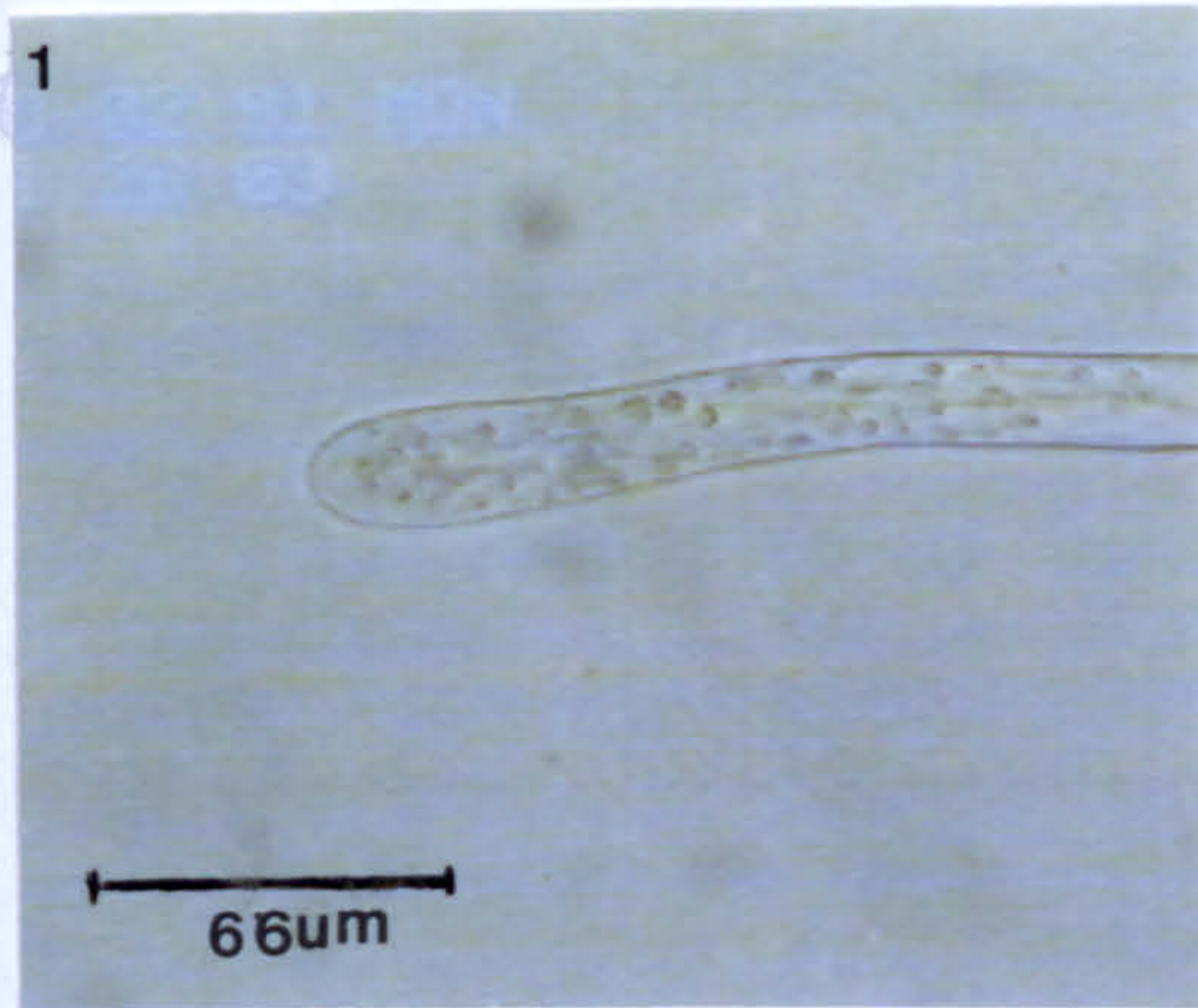
The first observable effect is an almost immediate swelling of the apex of the filament. Dark grown filaments grow at an average rate of 40  $\mu\text{m}/\text{h}$  (Knight and Cove, 1988). The growth rate on exposure to light initially slows to 15  $\mu\text{m}/\text{h}$ , then to 6  $\mu\text{m}/\text{h}$  in the first 3 hours. Four hours after exposure to light the first cell division occurs, as the apical cell continues to swell (Fig. 2.14, 2). The apical cell divides again 6 hours later (2.14, 3). At ca. the same time a further division occurs in the subapical cell (2.14, 3). A further division of the apical cell occurs after another 6-hour period (2.14, 3). Thus over a 16 hour period 4 cell divisions have occurred creating 3 swollen central cells. These produce side-branch initials in the manner of subapical cells (2.14, 5-8), each producing side-branches more or less in synchrony

**Fig. 2.14 The effect of exposure to light on a filament grown in the dark**

**Filming began at 18.50 on 18.2.91.**

- 1      2.5 hours after the start of filming, the apex of the caulonema apical cell is beginning to swell.**
- 2      4.5 hours after the start of filming, the apical cell divides (arrow).**
- 3      6 hours later, the apical cell and subapical cell divide at the same time (arrows).**
- 4      6 hours later, a further cell division of the apical cell (arrow) occurs. A caulonema side-branch initial has been produced by the subapical cell which was the apical cell at the time of exposure to light.**
- 5-8    22.5 hours after the start of filming, and exposure to light. The four subapical cells are producing side-branches synchronously. Subapical cells 1, 2 and 3 divide 3 times to produce 3 side-branches each.**







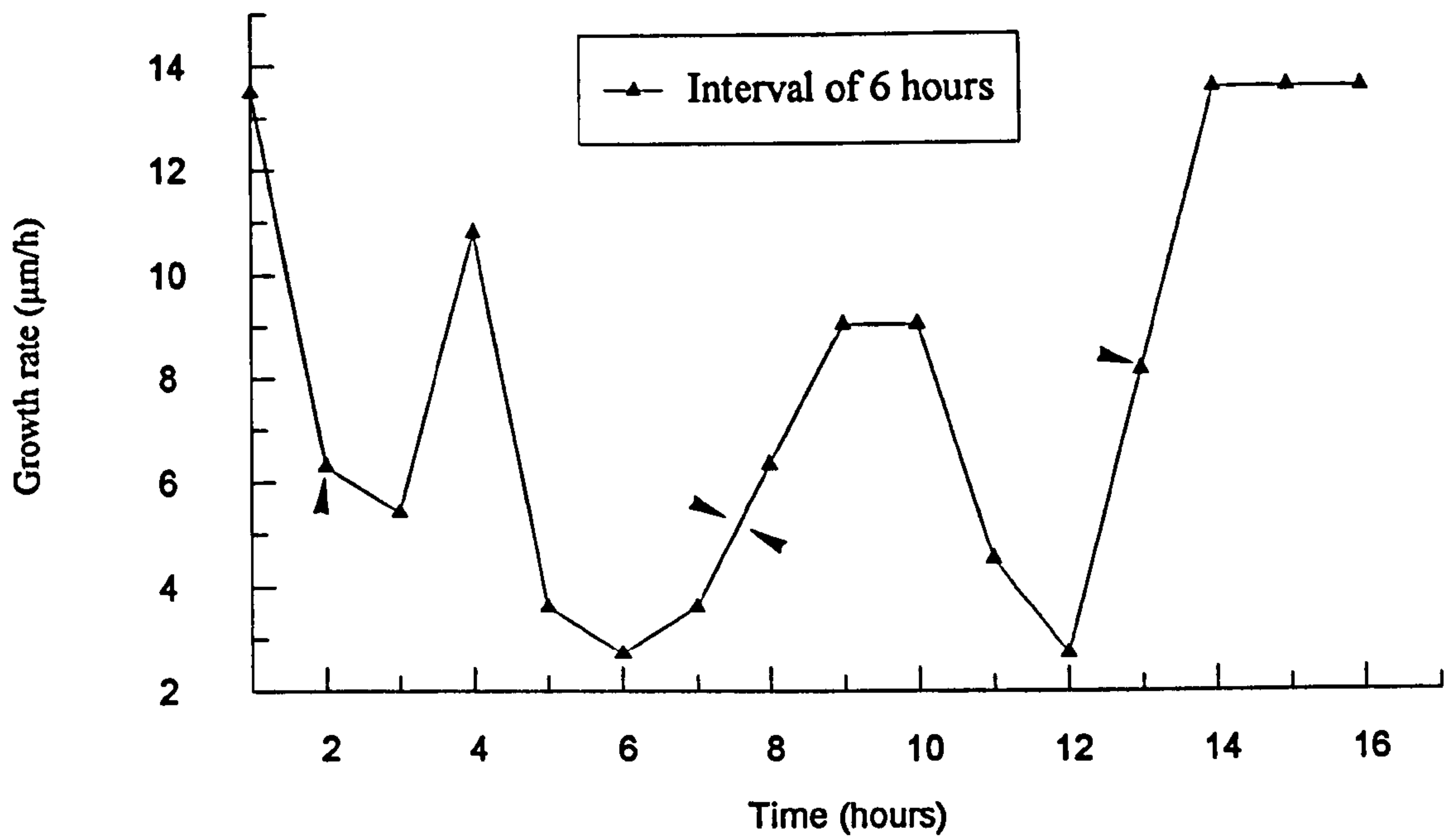


Fig. 2.15 The effect of exposure to light on the growth rate of a dark-grown filament. Arrows indicate cell divisions.



over the subsequent 30 hours. The first side-branch initial produced is a caulonema filament, reflecting the loss of apical dominance of the main caulonema apical cell. It was noted that for the majority of filaments exposed to light in this manner, at least one of the side-branch initials develops into a bud. It was also noted that subapical cells further down the filament did not divide to produce side-branch initials in response to light. During the first 16 hours of exposure to light the growth rate is highly fluctuating (fig. 2.15).

The first effect of light therefore is an increase in overall growth and mitotic activity to create cells that could be considered to be analagous to spores or protoplasts. The production of side-branches may also be analogous to the behaviour of the two cells of the spore, which also appear to produce 3 side-branches each (in this case primary filaments). There is a difference in that the side-branches can be secondary caulonema or buds. This may be due to a build up of substances in the dark-grown caulonema filaments that are unable to react with substances normally produced in light. While analogous to spore germination, or protoplast regeneration, this process is not entirely equivalent.

The increase in mitotic activity and apical swelling may relate to the occurrence of action potentials which are generated in response to an exposure of light. The work of Hohmeyer and Sanders at York (unpublished data) suggests that the first stage of an action potential may be an influx of calcium ions. Unlike the budding response to cytokinin which is reversible (Brandes and Kende, 1968), it is possible to produce side-branch initials on dark-grown caulonema filaments with a brief flash of light (Doonan, 1983). The possibility that the formation of side-branches is controlled by phytochrome has been demonstrated (Larpen and Jacques, 1971, in Simon and Naef, 1981). Hartmann and Pfaffmann (1990) reported transient increase levels of IP<sub>3</sub> in protonemal cells of *Ceratodon purpurea* after irradiation of tissue incubated in darkness with different light programmes, and suggested that the phytochrome-mediated phototropic response could be linked to the phosphatidylinositol signal transduction pathway.

### 2.3.10 Polarotropism and the cell cycle

The majority of apical caulonema cells respond to polarised light by growing parallel to the E-vector (fig. 2. 16). This may result in a change in the direction of growth of filaments if a culture is reoriented with respect to the plane of light. Not all filaments respond to the directional change immediately or in the same manner. In many filaments there is a considerable delay in the onset of the response. However 48 hours after reorientation the majority of filaments in a culture are growing parallel to the new E-vector.

In order to characterise this response in more detail, and to compare it to the gravitropic response, individual filaments were filmed in more detail. The results of these films are shown in the graphs of figs. 2.17-19.

The response to a 90° reorientation appears to follow a similar pattern in all filaments filmed. There is an initial delay of 15 to 25 minutes followed by a sharp change in the direction of growth of ca. 30 to 40 degrees. This is followed by a 10 to 20 degree reversal of growth which is then maintained for up to 200 minutes after reorientation. The stepwise nature of the response can be seen in some detail as the next turn in growth direction takes the filament to 50 or 60 degrees, followed by another reversal. Occasionally a filament may only turn 45 degrees towards a 90 degree reorientation.

However, unlike the reverse bend of the gravitropic response, the reversal in growth direction does not appear to be related to the cell cycle. Where mitosis occurs in the middle of the response there is not necessarily an associated reversal of growth. Fig. 2.17 shows two filaments undergoing a progressive turn throughout the whole of mitosis. In the two cases where mitosis occurs within the first hour of the response (fig.2.18) there is an increased delay from 20 minutes to 40 minutes before the first change in direction of the apical cell. As the apical cells respond at different times after the introduction of polarised light, it is difficult to be certain this delay is due to mitosis. Fig. 2.19 shows two filaments where a small reversal of the bending response



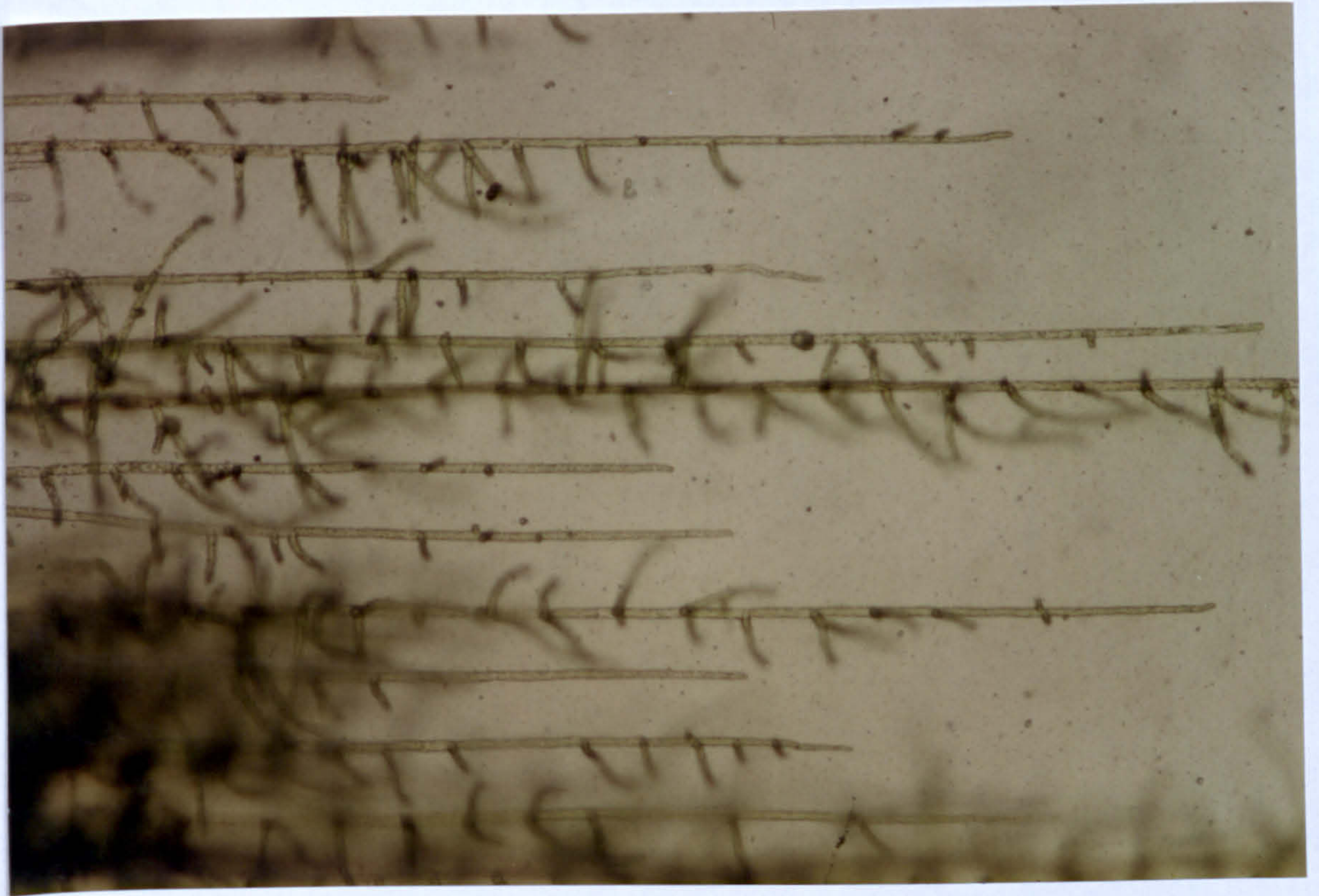
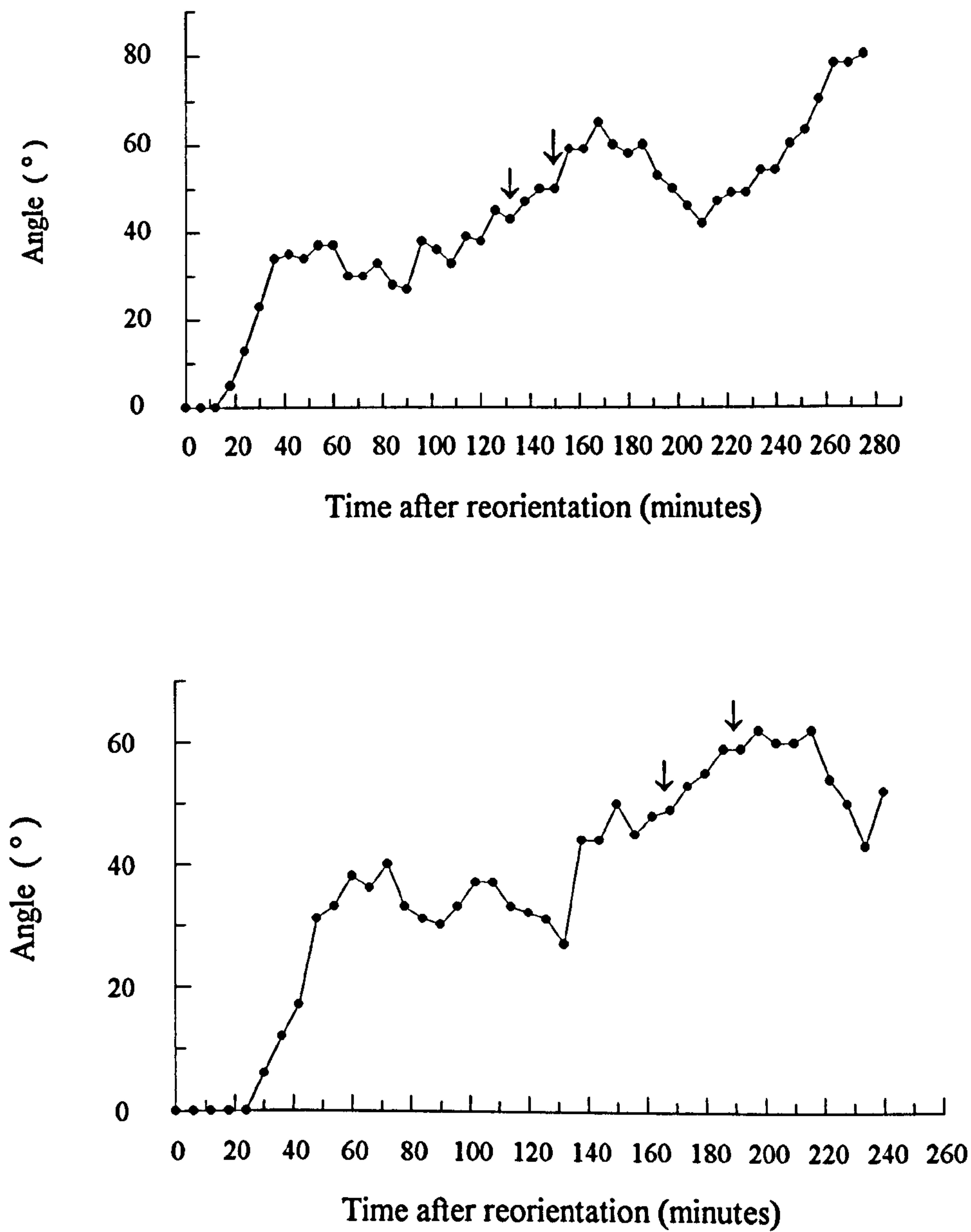


Fig. 2.16 Filaments of *P. patens* growing parallel to the E-vector in white plane-polarised light.





**Fig. 2.17**      The response of caulonema filaments to a 90° reorientation to the E vector.

Arrows indicate the beginning and end of mitosis. In each case mitosis occurred in the second phase of the bending response. There is no indication of a reversal of the response during mitosis.



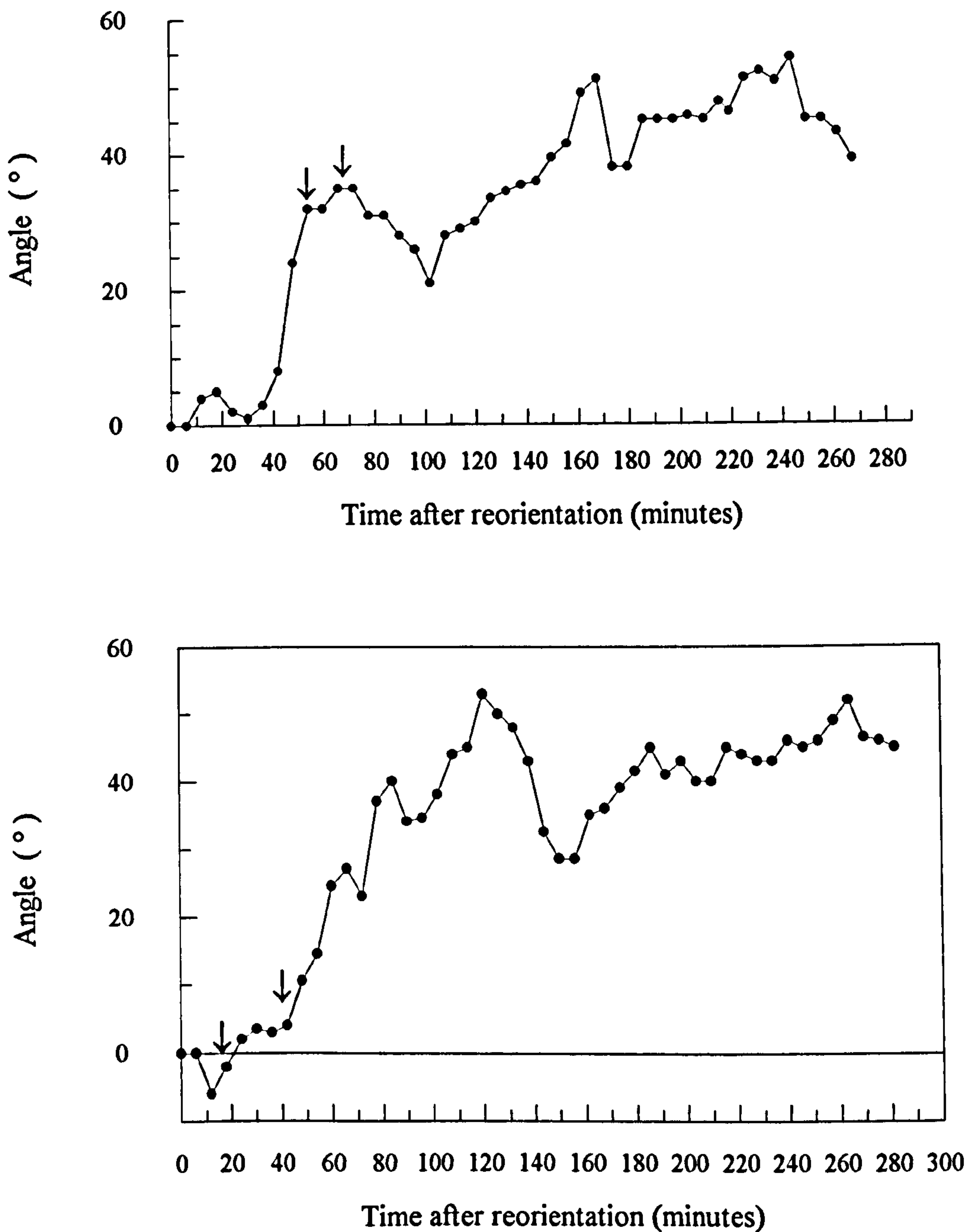


Fig. 2.18

The response of caulonema filaments to a 45° reorientation to the E vector.

Arrows indicate the beginning and end of mitosis. Mitosis occurred near the beginning of the response. There is an indication of a delay in the start of the first phase of the response.

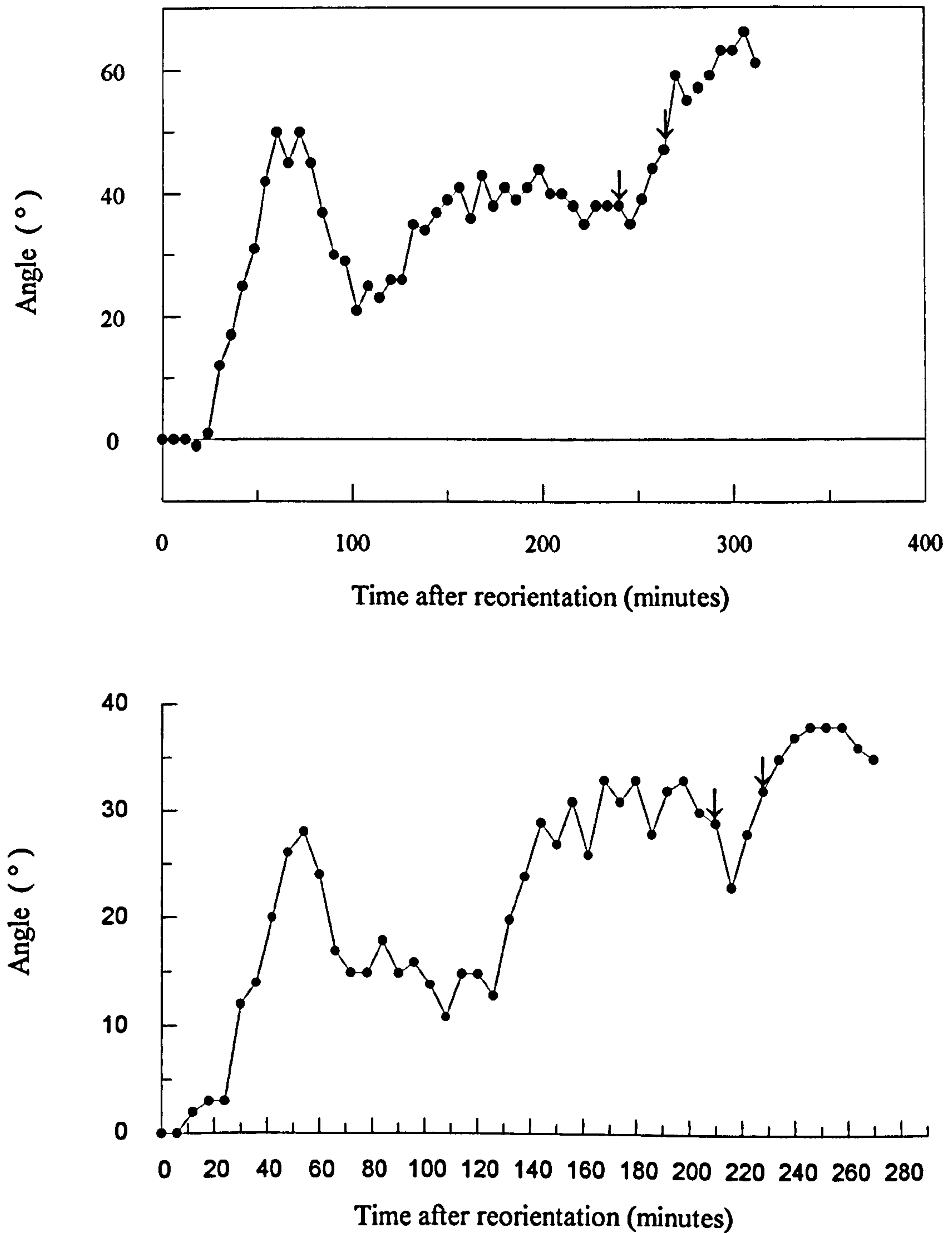


Fig. 2.19

The response of caulonema filaments to a 90° reorientation to the E vector.

Arrows indicate the beginning and end of mitosis. Each filament undergoes a small reversal of bending during mitosis. This is comparable to the normal movement of the apex of the tip cell during growth.



occurs during mitosis. However, this is not greater than the normal bending movement shown by the apical cells as they grow.

The change in directional growth of an apical cell in response to plane polarised light is clearly under the influence of a different set of regulatory factors to that of the response to gravity. The probable involvement of phytochrome may elicit a separate chain of signal-transduction events, which are membrane-related. However the growth response itself must involve common processes such as the redirection of cell wall and plasma membrane components. As this is unimpaired during mitosis in polarotropic bending, it would seem that cytoskeletal elements involved in these processes are maintained during formation of the spindle. This points to the possibility of the nucleus having a role in graviperception, which is impaired on breakdown of the nuclear membrane. This does not discount the hypothesis that cytoskeletal elements necessary for gravity detection are sequestered at this time. Specific populations of cytoskeletal elements might exist for different cell functions such as orientation of tip growth and gravity detection.

## CHAPTER III

### BRANCHING PATTERN ANALYSIS

#### 3.1 Introduction

Subapical cells of caulonemal filaments divide to form side-branches in a regular manner as they age and their position changes in relation to the growing apical cell. The early stages of side branch formation of several species of *Funariales* have been studied in detail using the light and electron microscope (Schmeidel and Schnepf, 1979a; Jensen, 1981; Yoshida and Yamamoto, 1982).

In all cases branch formation is initiated as a localised swelling at the distal end of the subapical cell when in the 3rd or 4th cell position from the apex. Schmeidel and Schnepf (1979a) report that in *Funaria hygrometrica* the developing initial pierces the cell wall of the mother cell and is not simply an extension of that cell wall. There is a progressive shift of chloroplasts towards and into the developing protrusion accompanied by an increase in chloroplast total number. When the protrusion achieves a certain size or at a certain time after its formation the nucleus migrates to the distal end of the cell and across to the base of the branch, where cell division occurs. Jensen (1981) reports that in *Physcomitrium turbinatum*, the subapical cell in the third position from the apex divides to produce a side branch initial at the same time as the apical cell divides so that the third cell then becomes the fourth cell from the apex of the caulonema filament. At the time of division the majority of chloroplasts are located in the branch initial at the distal end of the cell. Schmeidel and Schnepf (1979b) conclude from experiments with inhibitors of apical cell growth that this process depends on the developmental time or cell cycle of the subapical cell itself, rather than the position of the cell in relation to the apex.



Beyond these descriptions of subapical cell division, the further differentiation of the initial into a particular side-branch type has been less well documented. Previous research has produced the following classification of side-branch fate: a subapical cell may divide to produce:

1. An initial that develops no further.
2. A secondary chloronemal filament.
3. A secondary caulonemal filament.
4. A bud which develops into the moss gametophore.

The point at which the decision is made to develop in one of these alternative fates and how far the factors which influence this are endogenous or external are still unclear. Many studies have described the development of a side-branch initial into a bud under the influence of exogenously-added cytokinins. However in this case the developmental decision is artificially induced at a particular time. Yoshida and Yamamoto (1982) report that in *Physcomitrium sphaericum* differentiation into either a bud or a lateral filament occurs on the eighth or ninth cell position from the apical cell. They conclude that the position of side-branch differentiation is determined strictly by the number of cells from the tip of the filament. However this is in conflict with the results of Schmeidel and Schnepf (1979b), also the authors do not specify their criteria for determining differentiation.

McClelland (1988) also suggested that the differentiation of initials into a particular side-branch type may be influenced by their position on a filament relative to the apical cell. He proposed the hypothesis that initials may go through a window of development. If an initial does not develop into a chloronema filament at a certain subapical cell position, it will become either a caulonema or a bud. Similarly, if an initial fails to become a filamentous side branch it will become a bud. This raised the question of whether buds developed directly from newly formed initials or from initials that did not immediately differentiate, or subapical cells that did not divide in the normal way in the first few subapical positions.

The overall morphology of the moss colony with its ramifications of protonema interspersed with gametophores is determined by the morphogenesis of side-branch initials and the proportions of each type into which they develop. This project aimed to study protonemal morphology for the following reasons:

1. To look for any underlying pattern in protonemal development which might suggest hypotheses of developmental mechanisms.
2. To assess the effects of exogenous treatments such as phytohormones and light.
3. To provide a means of analysing mutant phenotypes more precisely.

In order to analyse branching patterns it is necessary to develop a method of analysing side-branch fate quantitatively. A major difficulty in performing a quantitative analysis of this sort on a standard petri-dish culture is the crowding of filaments and their overgrowth by developing gametophores, so that it is difficult to analyse more than ten to fourteen subapical cell positions and then only on selected filaments. The initial stage of this study therefore developed a method by which side-branch fate could be quantitatively determined.

It was also necessary to define the subapical position at which side-branch initials differentiated into either filamentous side-branch types or buds. This does not relate to the concept of whether differentiation is dependent on position or not (Schmeidel and Schnepf, 1979b). In normally growing cultures, by the time the fate of a side-branch is clearly established, i.e. it has undergone one or two cell divisions, it is several cell positions further back from the apex than at its initiation, as the subapical cell continues to grow and divide. As side-branches are scored further than the ninth or tenth cell position, it is necessary to know the point at which their differentiation into a particular branch type occurred. Once a side-branch is formed, its development is independent of the main filament, so in this work, position is intended as a convenient marker of time, not as a definitive statement of the stage of development of a side-branch.



Much speculation has centred around the question of whether the production of buds is completely random or whether some developmental mechanism exists that allows a spacing of buds at regular intervals along a filament, or within a culture. Bopp (1961) reported that as the protonema develop radially from a spore, buds are produced at a given distance from the spore. Accordingly buds on a protonema appear to be positioned in a ring around the spore. He called this a "Hexenring". Other studies suggested that the majority of filaments produce only one bud. These observations have lead to the suggestion that the moss has some mechanism to space bud production. Spacing of buds suggests an hypothesis that once a bud has been produced some inhibitory substance is produced preventing adjacent initials from becoming buds. Alternatively a random production of buds suggests the build-up and response to a critical substance which accumulates either in the cell or in the medium. A further aim of this study was therefore to answer the question of the spacing of buds by an analysis of the position of buds along a filament and their overall spacing in a colony.

The effect of growth substances and the role of calcium on this aspect of developmental fate was also explored.

### **3.2 Methods**

The methods used for analysing branching patterns were adapted from those used for time-lapse microscopy.

Cultures were inoculated into the centre of a well plate, prepared as for time-lapse microscopy. The plates were kept at a temperature of around 20°C to avoid drying of the thin layer of agar, and to encourage spreading growth of the filaments.

Filaments were analysed when the cultures were 17 to 20 days old. For the branching pattern analysis, side-branches were recorded for the first 20 cell positions along a filament. Between 10 and 30 filaments were recorded on a single culture. Filaments were scored using the Olympus light microscope (x10).

Time-lapse video microscopy was used to analyse side-branch development and to define the position at which side-branches differentiated.

Hormones, at the required concentration, were flooded over the thin layer of agar in which the cultures were growing.

For the bud spacing analysis, 10 adjacent filaments were scored for each of a number of separate cultures. The first 30 cell positions were scored and positions 9 to 30 inclusive were analysed.

The statistical significance of the data was tested using chi-squared analysis. For the side-branch data, data from replica experiments were tested for heterogeneity by  $n \times k$  contingency chi-squared analysis before being combined. For the bud spacing data, expected values were calculated using probability theory. The probability ( $p$ ) of a subapical cell producing a bud was calculated from the total numbers of buds and filaments. The hypothesis was tested that buds form randomly along a filament. The expected values for each filament producing from 0 to 6 buds according to this hypothesis were calculated using the figure obtained for  $p$ .

Yates continuity correction was used where expected values were less than 5.

### **3.3 Results and discussion**

Of the several methods of growing protonemal tissue, the well plate method was chosen for the branching analysis (fig. 3.1). This technique allowed filaments to be visualised clearly for the first twenty to thirty subapical positions. Nutrient depletion of the thin layer of agar sometimes presented a problem. Cultures could normally be identified as growing abnormally under standard conditions by a decrease in side-branch production leading to an increase in unbranched subapical cells, subapical cells with only one side-branch and side-branch development arrested at the initial stage. When additional growth substances were added these effects were less easy to distinguish. Cultures could normally be grown in this manner for up to 21 days.



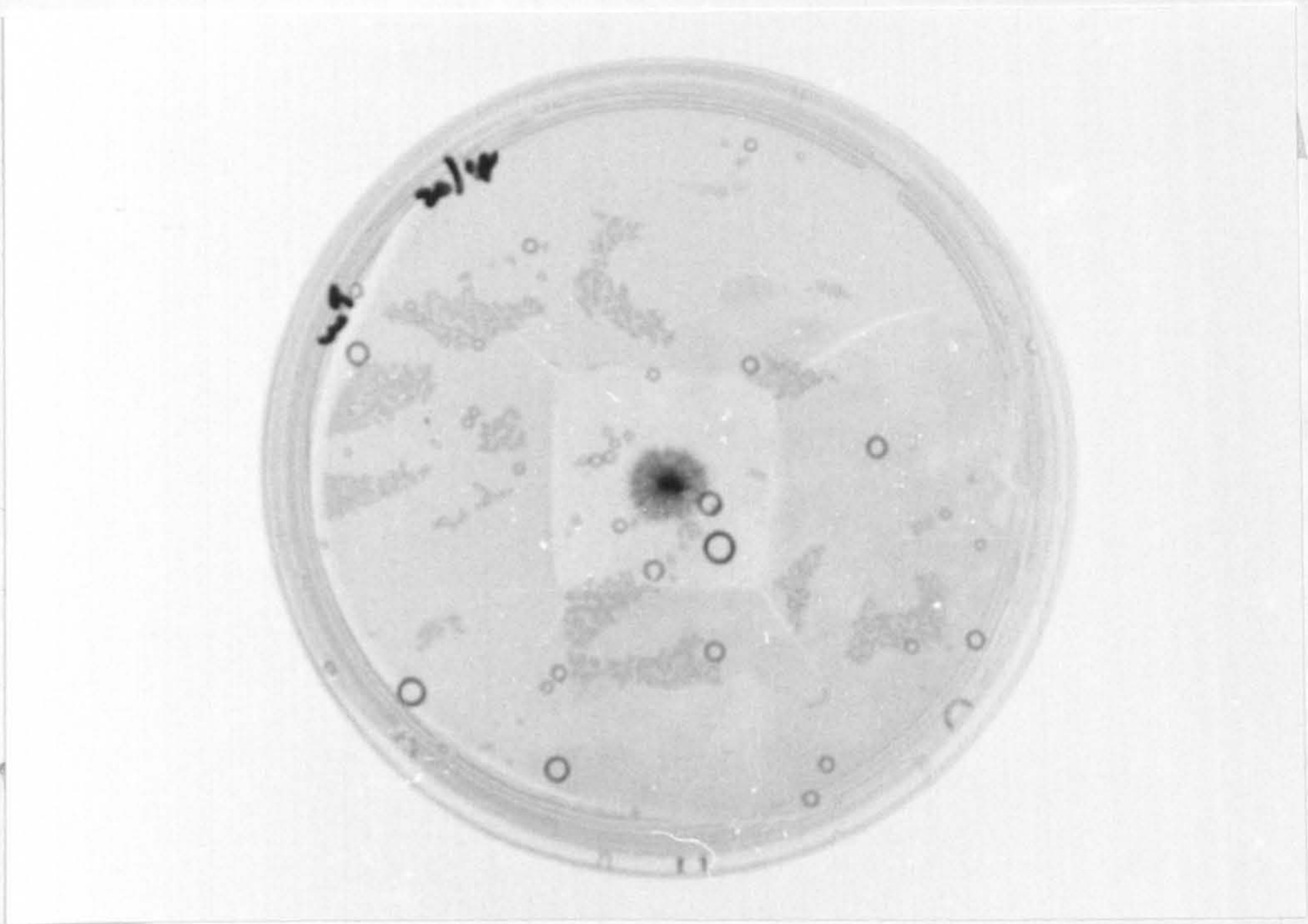


Fig.3.1 The well plate method of growing *P. patens*.

This method of growing *P. patens* was used in order to carry out a side-branch analysis. in the thin layer of agar in the base of the petri dish, the filaments spread out and grow in a single plane of focus.



### 3.3.1 Time-lapse: subapical cell division

Side-branch initial formation was filmed using time-lapse microscopy.

The first sign of a protrusion at the distal end of the subapical caulonema cell occurred normally approximately 5 to 10 hours after the division of the apical cell which gave rise to the subapical cell. In the majority of cases, but not all, this is coincident with a second division of the apical cell so that the subapical cell forming the initial is in the 3rd cell position of the filament. Cell division, dividing the initial from the mother cell occurs 4 hours after the production of the protrusion, within the same apical cell cycle, while the subapical cell is still in the 2nd subapical position.

One hour before division, the nucleus begins to move towards the distal end of the cell at a rate of  $9\mu\text{m/h}$ , surrounded by a circle of cytoplasm and chloroplasts. Ten minutes before division, the nucleus plus surrounding chloroplasts begins to move rapidly to the base of the protrusion (approximately  $21\mu\text{m}$  in 10 minutes) where cell division occurs.

### 3.3.2 Side-branch development

The differentiation of side-branch initials into each type of side-branch was filmed.

Differences between the side-branch types may become apparent at a very early stage. Table 3.1 details the cell positions along a filament at which the first cell divisions of the developing side-branch occur, under standard conditions of growth. By the time of their division from the subapical cell, 4 hours after their inception, initials that will develop into caulonemal side-branches can already be distinguished by their length, which is greater (ca  $21\mu\text{m}$ ) than that of a bud or chloronema initial. Chloronemal initials are ca.  $15\text{-}20\mu\text{m}$  in length at this stage of development, and have a rounded appearance, frequently with many chloroplasts closely adpressed to the cell wall. However, many initials are less distinct at this stage - it is still unclear if these are the intermediate caulonemal type. It is not generally possible to distinguish a bud



Table 3.1

Side-branch differentiation under standard conditions of growth in *P. patens*.

Side-branch fate	Cell position				length of side-branch at 1st div. (μm)
	protrusion formation	cell division of initial	1st div. of side-branch	side-branch fate visible	
caulonema	3–4	3–4	6–7	5	135
chloronema	3–4	3–4	6–7	6–7	60–80
transitional caulonema	3–4	3–4	6–7	9	80–100
bud	3–4	3–4	7	5	45

clearly until the subapical cell which produced it is in the fifth position. By this stage the assymetrical club-shape is developing. Buds do not develop from initials that are clearly chloronemal.

The first cell division of the side branch occurs approximately 17 to 24 hours after the division which gave rise to it. While this appears to be a developmentally-controlled event unrelated to the division of the filament apical cell (3.1), under standard conditions, it will be at the sixth or seventh cell position along the filament, or when the apical cell has undergone a further 3 or 4 cell divisions. Some caulonema revert to chloronemal growth, and slow or cease growth. In this case the first side-branch division may occur on the 4th or 5th subapical position.

While the cell cycle time of the first cell of the side-branch appears to be invariant, the length of the side-branch at the first cell division varies considerably. So it is at the point of the first division of the side-branch that it is possible to define clearly the developmental fate to which the initial has become committed.

Secondary caulonemal side-branches increase their rate of growth during the first cell cycle to achieve a length of approximately 135 $\mu$ m at this division. Chloronemal side-branches continue to grow at 2-3  $\mu$ m/h so that they are 60-80  $\mu$ m long at the first division. Buds, on the other hand, initially grow faster than chloronema but by the time of the first cell division have slowed their rate of linear growth to approximately 1 $\mu$ m/h, and developed their characteristic club shape. The developing side-branch initial therefore expresses its developmental pathway by its rate of growth during the first cell cycle, beginning shortly after the cell division which cuts it off from the subapical parent cell.

The further development of initials into side-branches has been described in Ch. 2.

### 3.3.3 Branch pattern analysis

Preliminary analyses of side-branch fate encountered difficulty in distinguishing secondary chloronema from secondary caulonema. The use of time-lapse microscopy



clarified the distinction between these two filamentous branch types. It was clear that the majority of secondary caulonema could not be distinguished until the side-branch had undergone a second cell division. For the first side-branch produced by a subapical cell, this occurs when the subapical cell is in the 9th cell position along the filament. Time-lapse filming identified these caulonema as going through a chloronemal growth phase before switching to caulonema, rather in the manner of primary chloronema. As these made up a large proportion of caulonema in the steady state proportions of side-branch types, it was decided to include them in the analysis as such, rather than score the side-branch as the original basal cell type (McClelland, 1988). They were therefore included as a third filamentous cell type, that of intermediate or transitional caulonema, to distinguish them from those side-branches that are clearly caulonema from inception.

Present analyses also differ from previous analyses in including the second and third side-branches from the same subapical cell.

An analysis of the first 20 cells from 30 filaments from each of 5 independent cultures of the wild-type, grown under standard conditions is given in Table 3.2. A contingency chi-squared analysis shows that these samples do not differ significantly in their side-branch fates. These 150 filaments were therefore treated together as a control. However, chi-squared analysis revealed significant heterogeneity of the number of subapical cells undergoing a second cell division to produce 2 side-branches, so the data is less reliable as a control for this aspect of the analysis.

Table 3.3 analyses side-branch fate against filament cell position, and hence subapical cell age, for these 150 filaments.

The results show that, under standard conditions, by the 5th cell position, equivalent to 20-24 hour age of the subapical cell, 98% of subapical cells have undergone 1 cell division leading to a side-branch initial (fig. 3.2). Less than 1% of subapical cells remain unbranched. Approximately 40% of cells undergo a further cell division. This occurs when the subapical cell is in cell position 6 to 8 along the

Table 3.2

Side-branch analysis of the first 20 cells of 30 filaments from 5 independent cultures of wt *P. patens* grown under standard conditions.

Culture	No. of cells with				Side-branches as:					Total
	0	1	2	3	initials	chl	caul	chl-caul	buds	
	side-branches									
1	86	309	204	1	150	484	8	70	8	720
2	76	298	224	2	173	508	4	57	10	752
3	71	348	179	2	184	480	5	35	8	712
4	78	376	146	0	145	466	6	37	14	668
5	84	359	156	1	150	450	5	61	8	674
Total	395	1690	909	6	802	2388	28	260	48	3526
Total %	13.2	56.3	30.3	0.2	22.7	67.7	0.79	7.4	1.4	

Chi-square analysis:

het  $\chi^2_{12} = 38.79$      $p < 0.1\%$

het  $\chi^2_{16} = 27.18$      $p = 5\%$

Chi-square analysis including the control results of table 3.5:

het  $\chi^2_{15} = 39.16$      $p < 0.1\%$

het  $\chi^2_{20} = 29.57$     ns



Table 3.3

Side-branch analysis of wild-type *P. patens*.The percentage of each branch type at subapical positions 1-20 in 150 filaments.

Subapical cell	% with 2 branches	unbra	sbi	chl	caul	chl-caul	bud
1	0	100	0	0	0	0	0
2	0	100	0	0	0	0	0
3	0	50	50	0	0	0	0
4	0	8	92	0	0	0	0
5	4	2	96.8	1.3	0	0	0
6	23	1	85.9	10.8	1.6	0	0.5
7	36	0	41.7	57.4	0.5	0	0.5
8	42	0.5	31.6	62.7	1.4	3.3	0.9
9	36	0	22.5	71.6	0.5	4.4	1
10	42	0	16.4	75	0.9	7.5	0
11	38	0.5	5.8	80.7	1	10.6	1.4
12	37	0	4.3	78.8	1.4	12.5	2.9
13	40	0	2.4	81.6	1.4	14.2	0.5
14	43	0	0.9	83.7	0.5	14	0.5
15	49	0	0.9	83.5	0.9	12.9	1.8
16	47	0.5	0.9	86.9	1.8	7.2	2.7
17	44	0	1.9	84.2	0.5	11.1	2.3
18	43	0	2.8	83.8	0.9	9.3	3.2
19	42	0	1.4	89	0	6.6	2.8
20	39	0	0.5	91	0	7.7	1

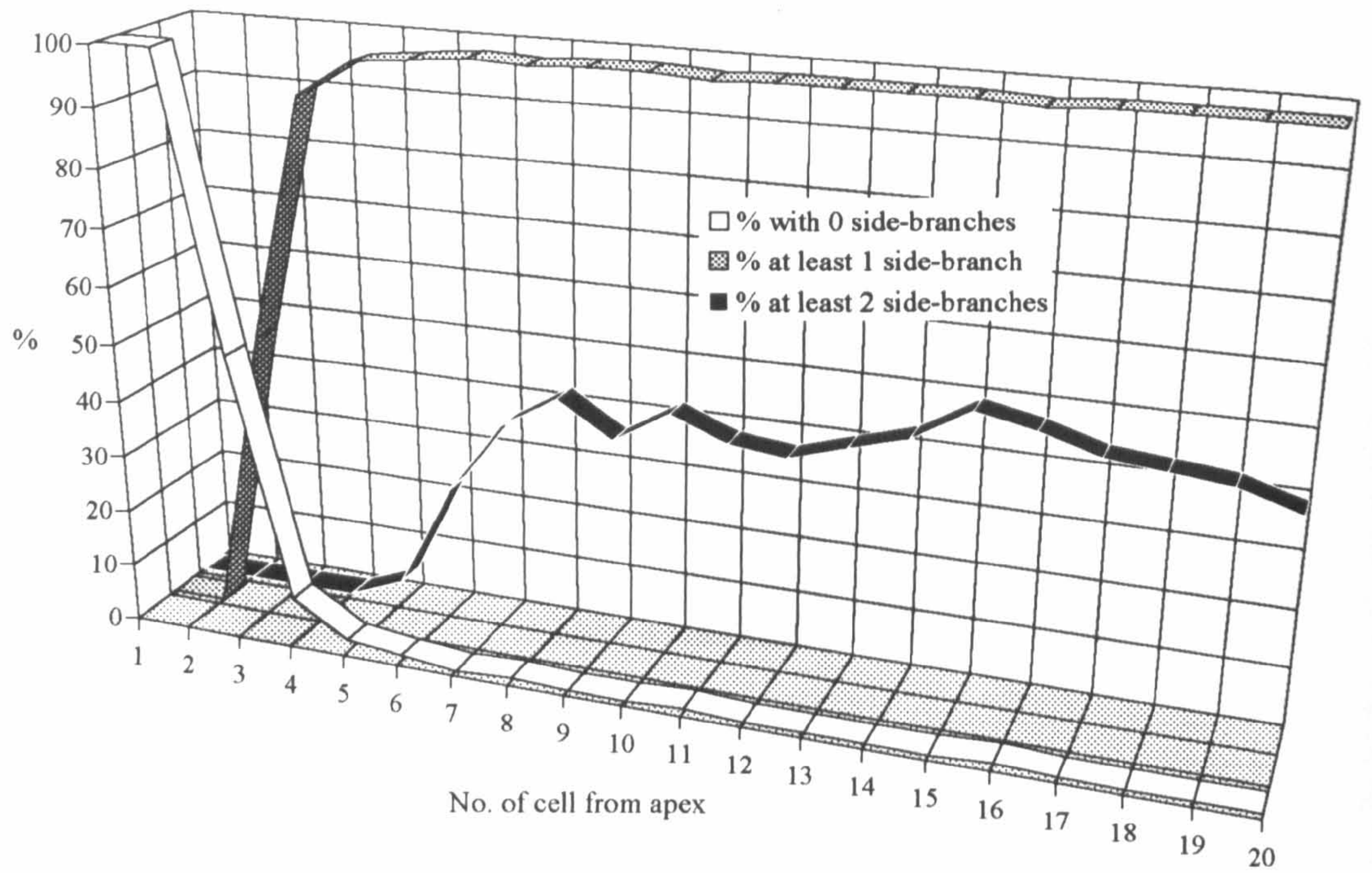


Fig 3.2 Effect of cell position/cell age on side-branch production.



filament, about 3 apical cell divisions (approximately 18h) after the first apical division. By the 7th cell position, the number of cells undergoing 2 cell divisions has reached a steady state. The percentage of cells undergoing a third division is less than 1%.

From the analysis of branch type and cell position, it can be seen that the numbers of side-branch initials peaks at cell positions 5 and 6 (fig. 3.2). This is before the cell division of the first side-branch and after the initiation of a second side-branch initial. At cell position 7 the number of side-branch initials has dropped by half, reflecting the first cell division of the first side-branch. The remaining 41.7% initials reflects those cells giving rise to a second side-branch, minus the steady state number of initials that do not develop further. As with first side-branches, the second initial also divides after approximately 20-24 hours, or 4 further divisions of the apical cell, therefore at subapical position 10 or 11.

By the 11th cell position the second side-branch has undergone the first cell division defining its developmental fate. The relationship of the fate of the second side branch to that of the first is discussed below. By the 11th cell position the filament is therefore at a steady state and the proportions of each side-branch will not change except a small proportion of chloronema may undergo a later transition to caulonema.

The proportions of each type of side-branch are given in Table 3.3. These proportions vary a little from previous analyses. A lower proportion of unbranched cells and caulonema were found. Less than 1% of initials give rise to side-branches that were caulonema from the start. By far the majority of initials give rise to secondary chloronema (70%). The most variable quantity is the number of chloronema switching to caulonema. These make up the major proportion of caulonemal side-branches (10.6% of all branches, x% of caulonema). Buds form an average 2% of side-branches at each position. The first buds appear at the same cell position as chloronema. The increase after cell 10 reflects the second side-branch.

During the course of the analysis, it was found that buds originated from two sources: the caulonema subapical cell, where either the first, or subsequent side-

branch initials could develop into buds, and also the basal cell of filamentous side-branches (fig. 3.8a). Not all side-branches produce compound branching, and those which do not, retain the capacity to develop an initial resulting in a bud. The proportion of buds increases at the 11th cell position, as a result of buds developing from second side-branch initials and then remains stable for buds originating as side-branch initials directly from the caulonema subapical cell. From the 13th cell position the proportions of buds increase if buds on the basal cells of side-branches are included.

Table 3.4 analyses the relationship between pairs of side-branches. For those cells which divide more than once the question was asked, does the first side-branch influence the developmental fate of the second?. When scoring filaments, it was not possible to be sure which side-branch was produced first, so for this analysis, the hypothesis was set up that side-branches were randomly associated, that is did not influence each other's fate. The expected values for the random occurrence of each combination of side-branch type correlated well with those observed ( $X^2=11.73$ ,  $df=9$ ), suggesting that side-branch fate is an independent event for each subapical cell division, and that there is no communication between pairs of side-branches produced from a single subapical cell. This differs from Knoop's observation for *F. hygrometrica* that the second side-branches tend to be chloronema (Knoop, 1984).

#### 3.3.4 Plant hormones

Table 3.5 contains the results of an analysis of the first 20 cells of 30 filaments from cultures treated with various concentrations of BAP and NAA.

#### Cytokinin

The results obtained show significant differences in the proportions of side-branch types obtained with progressively increasing concentrations of BAP. A concentration



Table 3.4

Analysis of side-branches occuring in pairs on the first 20 cells of 150 filaments of wild-type *P. patens*.

Side-branch:		Number of observed pairs	Number of expected pairs
1	2		
chl	chl	441	448.8
chl	trans	141	123.7
chl	bud	27	27.7
chl	caul	16	17.1
bud	trans	2	3.8
bud	caul	2	0.5
bud	bud	1	0.4
trans	caul	2	2.3
trans	trans	1	8.5
caul	caul	0	0.2

Table 3.5

Side-branch analysis of the first 20 cells of 30 filaments from cultures of wt *P. patens* treated with various concentrations of BAP and NAA.

Treatment	No. of cells with				Side-branches as:					Total
	0	1	2	3	initials	chl	caul	chl-		
	side-branches							caul	buds	
Control	78	344	176	2	150	485	8	47	12	702
30nM BAP	88	361	151	0	155	441	4	44	19	663
100 nM BAP	93	401	105	1	162	353	1	16	82	614
1μM BAP	151	352	95	2	85	292	0	16	155	548
1μM NAA	72	381	147	0	169	438	7	56	5	675

Chi<sup>2</sup> analysis of each treatment with the control culture

Comparison of control vs:	Side-branch no. (df=2)	Side-branch fate (df=4)
30nM BAP	4.92 ns	4.07 ns
100nM BAP	23.90 p<0.1%	88.60 p<0.1%
1µM BAP	47.60 p<0.1%	195.60 p<0.1%
1µM NAA	6.73 p<5%>1%	6.73 ns



of 1  $\mu$ M BAP saturates the budding response.

With the increase in the number of buds, there is a concurrent decrease in the number of all three other branch types. There is also a decrease, significant at the two higher concentrations of BAP, in the number of subapical cells giving rise to two side-branches, and an increase in the number giving rise to no side-branches at all.

BAP significantly reduced the number of caulonema side-branches produced at higher concentrations. Over the region of the filaments producing initials at the time of application, the number of buds is dramatically increased. At 1  $\mu$ M BAP there are no caulonema, even transitional, in this region. The proportions of chloronema are very much reduced and chloronema growth is inhibited in existing side-branches. However chloronema formation is not completely inhibited as is the case for caulonema. The number of unbranched cells occurring in the region of filaments immediately subsequent to BAP application increases with increasing hormone concentration. It is possible that a cell division factor is used up in the increased bud production of the previous subapical cells, as after 2 or 3 cells the ability to divide appears to return. The side-branches produced subsequently are chloronema.

Tables 3.6, 3.7 and 3.8 analyse side-branch fate against filament cell position for the three concentrations of BAP used.

The cultures were analysed 3 days (72h) after the addition of hormone. Under standard conditions, assuming a 6 hour cell cycle, the apical cell at the time of application of the hormone would have been at a position now occupied by cell 12 or 13 at the time of scoring the filaments. At 30nM BAP the maximum increases in the number of buds are at cell positions 15 and 16, which would have been cell positions 2 to 4 at the time of hormone application, and at positions 18 and 20, corresponding to positions 6 and 8, and probably representing bud production from the second initial produced by these cells. The percentages of buds at each cell position are low, so that the overall effect of 30nM BAP is not significant compared to the control, but the detailed analysis of cell position has revealed a possible effect on a particular stage of development of a side-branch.

Table 3.6

Side-branch analysis of *P. patens* after 3 days treatment with 30nM BAP. The percentage of each branch type at subapical positions 1-20 in 30 filaments.

Subapical cell	unbra	% with 2 branches	sbi	chl	caul	chl-caul	bud
1	100	0	0	0	0	0	0
2	100	0	0	0	0	0	0
3	70	0	30	0	0	0	0
4	10	0	90	0	0	0	0
5	3.3	0	96.6	0	0	0	0
6	2.9	13	94	2.9	0	0	0
7	0	20	52.8	47.2	0	0	0
8	0	43	37.2	60.5	2	2.3	0
9	0	27	18.4	73.7	2.6	5.3	0
10	2.5	33	15	75	0	5	2.5
11	0	23	5.4	78.4	5.4	5.4	5.4
12	0	27	0	89.5	2.9	5.9	2.9
13	0	33	5	85	0	7.5	2.5
14	2.3	43	2.3	72	0	16.3	7
15	0	30	0	82	0	12.5	10.3
16	0	40	7	71.4	0	16.7	4.8
17	0	43	0	97.7	0	2.3	0
18	0	37	2.4	80.5	0	12.2	4.9
19	0	37	2.4	90.2	0	4.9	2.4
20	0	53	2.2	78.3	0	19.4	4.3



Table 3.7

Side-branch analysis of *P. patens* after 3 days treatment with 100nM BAP. The percentage of each branch type at subapical positions 1-20 in 30 filaments.

Subapical cell	% with 2 branches	unbra	sbi	chl	caul	chl-caul	bud
1	0	100	0	0	0	0	0
2	0	100	0	0	0	0	0
3	0	46.7	53.3	0	0	0	0
4	0	13.3	86.7	0	0	0	0
5	17	2.9	97	0	0	0	0
6	27	2.6	89.5	7.9	0	0	0
7	20	2.7	61	36	0	0	0
8	10	15	18	66.7	0	0	0
9	13	5.9	8.8	85.3	0	0	0
10	27	5.3	7.9	84.2	0	0	2.6
11	10	9	6	69.7	0	0	15
12	13	0	8.8	58.8	0	0	32.4
13	20	0	8.3	47.2	0	0	44.4
14	17	0	11.4	51.4	0	0	37.1
15	13	0	2.9	58.8	2.9	5.8	29.4
16	23	0	5.4	86.5	0	0	8.1
17	43	0	2.3	79.1	0	4.6	13.9
18	37	0	2.4	70.7	0	7.3	19.5
19	37	0	2.3	69.8	0	11.6	16.3
20	23	0	0	83.8	0	10.8	5.4

Table 3.8

Side-branch analysis of *P. patens* after 3 days treatment with 1 $\mu$ M BAP. The percentage of each branch type at subapical positions 1-20 in 30 filaments.

Subapical cell	% with 2 branches	unbra	sbi	chl	caul	chl-caul	bud
1	0	100	0	0	0	0	0
2	0	87	13	0	0	0	0
3	0	33	60	7	0	0	0
4	6	43	34	25	0	0	0
5	0	70	27	3	0	0	0
6	0	77	23	0	0	0	0
7	0	50	43	0	0	0	7
8	3	33	13	6	0	0	48
9	17	3	6	9	0	0	83
10	17	3	5	10	0	0	81
11	23	3	3	24	0	0	70
12	27	0	8	50	0	0	42
13	40	0	12	64	0	0	24
14	33	0	5	70	0	0	25
15	23	0	5	77	0	0	18
16	23	0	3	76	0	8	14
17	27	0	3	76	0	10.5	10.5
18	27	0	3	87	0	10.5	0
19	23	0	0	92	0	5	3
20	27	0	0	92	0	8	0



The addition of 1 $\mu$ M BAP to cultures led to somewhat different results from those of McClelland (1988). Firstly, it was found that while initially the growth of the apical caulonemal cell was unaffected, over a period of three days the apical cell reduced its growth rate, gradually becoming chloronemal, before stopping growth altogether. This makes it more difficult to extrapolate back to an effect of BAP on a particular subapical cell position at the time of application. In the case of the two higher concentrations of BAP, there is a correlation between an increase in buds and high proportion of unbranched cells. Time-lapse microscopy has shown that while the subapical cell produced by division of the apical cell at the time of application, responds to the hormone by dividing in the normal manner to produce a bud, subsequent divisions of the apical cells give rise to subapical cells which either did not divide, or, at lower concentrations of BAP, produced chloronema side-branches. This can give a clue to the apical cell position at the time of application of the hormone. Tables 3.7 and 3.8 show that the unbranched cells begin at position 11 (100nM BAP) and 8 (1 $\mu$ M BAP). These positions reflect the increasing inhibition of growth of the higher concentrations of BAP. It is therefore likely that positions 11 (100nM BAP) and 8 (1 $\mu$ M BAP) correspond to the position of the majority of apical cells at the time of hormone application. In each case, these are the first cell positions where high numbers of buds form. These data suggest that the most sensitive cells to high concentrations of cytokinin are the first four cell positions at the time of application. Two of these, cell positions 3 and 4, should already have formed initials. This data is analysed further in fig. 3.3. It can be seen that the highest number of buds are at cell positions 14 and 15 (30nMBAP), 13 and 14 (100nM BAP) and 9, 10 and 11 (1 $\mu$ M BAP). In each case this is likely to correspond to cell positions 2, 3 and 4 at the time of application of the hormone.

For all three concentrations of BAP high numbers of buds are formed from side-branch initials in a span of approximately 10 cell positions. This covers the range of responsiveness of first and second side-branch initials.

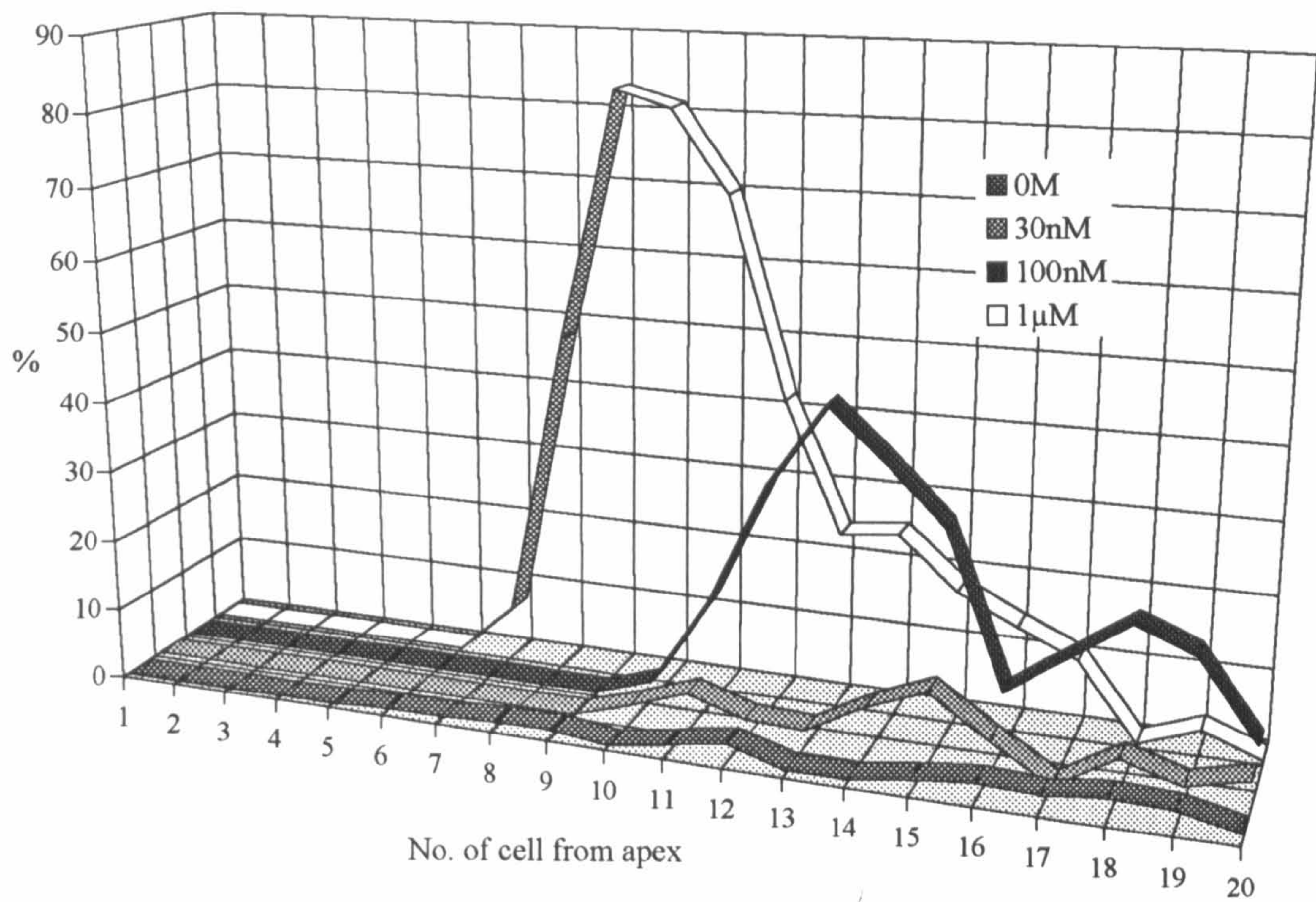


Fig. 3.3 Effect of cell position on cytokinin-induced bud formation.



The response to BAP was further analysed using two mutant strains. The mutant *bar-576* was found to respond to BAP, but with considerably lower sensitivity than wild-type. Fig. 3.4 analyses this response in terms of subapical cell position. Fig. 3.5 compares the response of *bar-576* to 1µM BAP, the response of wild-type to 30nM and 1µM BAP, and the untreated gametophyte-overproducing mutant *gam-139*. The results suggest that the lower the concentration of BAP, the less likely the effect will be on specific subapical positions.

### Auxin

The effects of the addition of 1µM NAA on side-branch production are also shown in Table 3.5. No significant change in the overall proportions of side-branch type was detected (table 3.9). However as in the case of 1µM BAP, this concentration of hormone resulted in an inhibition of growth. Time-lapse photography revealed that the growth of the main filaments was reduced to approximately half their previous rate 10 hours after the addition of the hormone, and the filaments became chloronemal. Chloronemal side-branch growth was also inhibited. This study also found a significant reduction in the number of buds.

### 3.3.5 Mutants

Two mutants were initially selected to test the utility of branching analysis for the detailed analysis of phenotype.

The mutant *gam-139* had originally been classified as a strain unable to produce buds except in the presence of exogenous cytokinin, however the analysis (table 3.10) revealed that this mutant produced an increased number of small buds, the

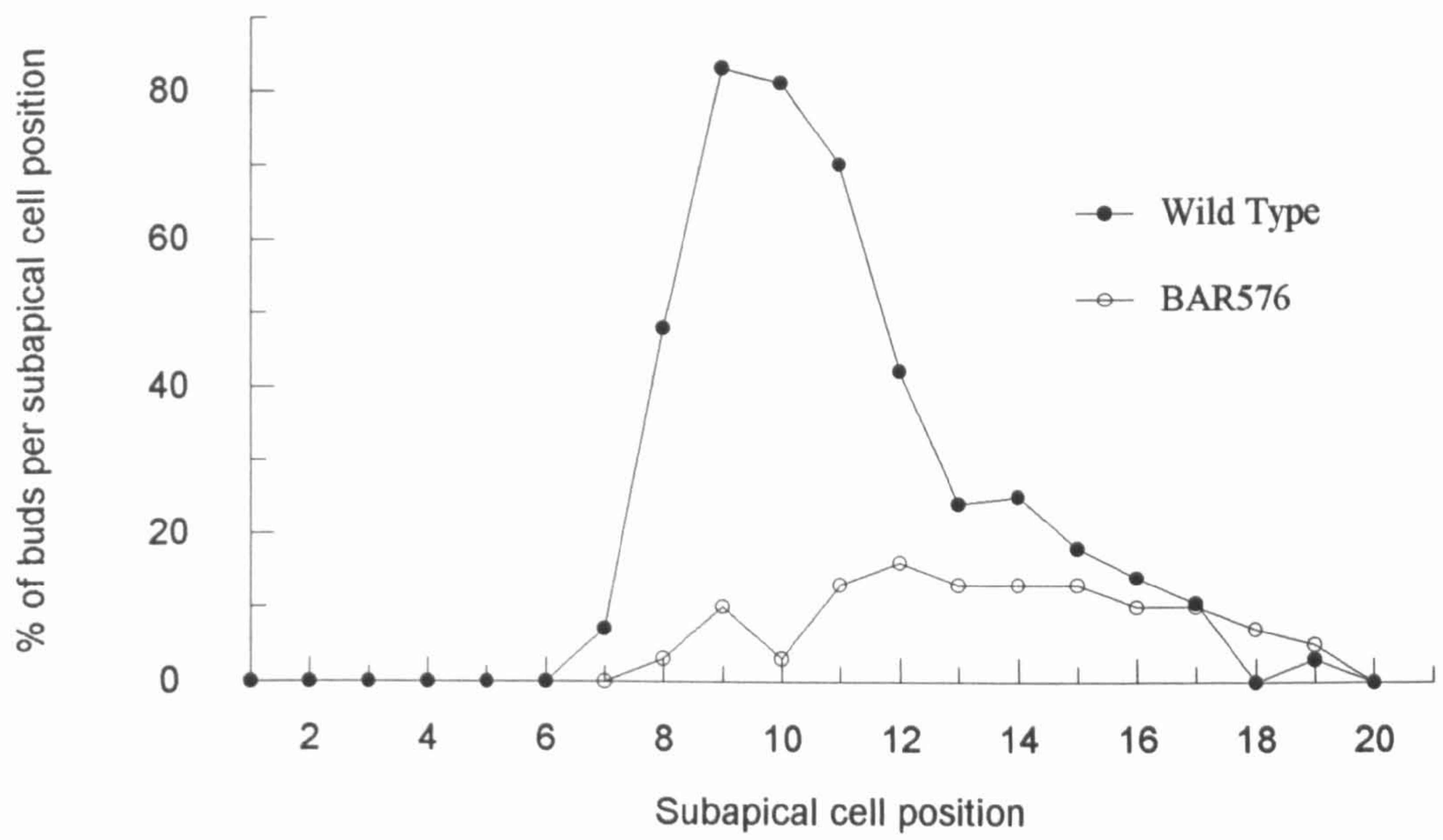


Fig. 3.4 A comparison of the effect of  $1\mu\text{M}$  BAP on bud-formation in wild-type and the gam-minus strain BAR576.



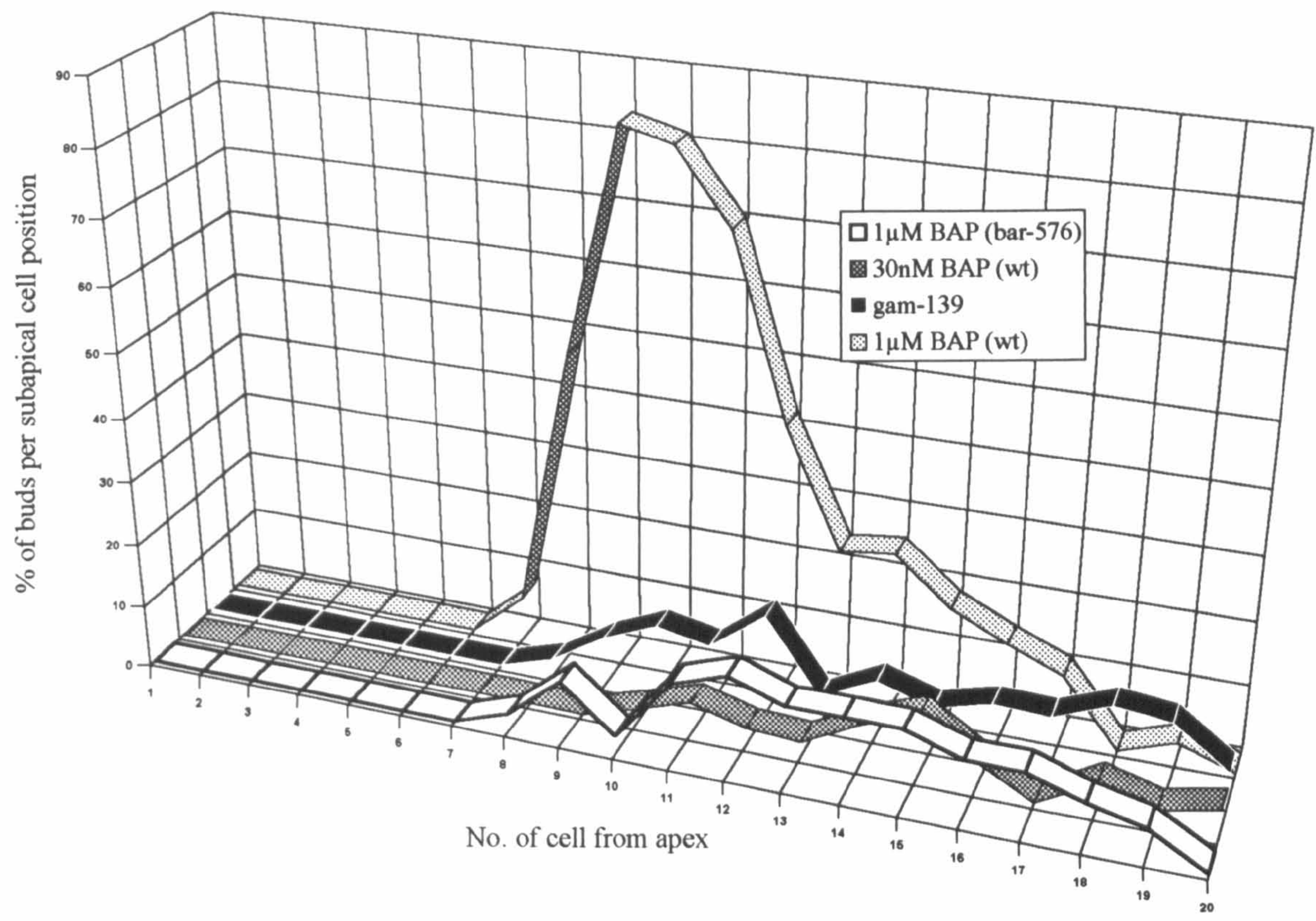


Fig. 3.5 A comparison of low-level responses to BAP to each other, and to the wild-type response to 1μM BAP. The mutant strain *gam-139* is untreated. BAP (1μM) was added to the mutant strain *bar-576* and to wild-type. BAP (30nM) was added to wild-type.

Table 3.9

Side-branch analysis of *P. patens* after 3 days treatment with 1 μM NAA. The percentage of each branch type at subapical positions 1-20 in 30 filaments.

Subapical cell	unbra	% with 2 branches	sbi	chl	caul	chl-caul	bud
1	100	0	0	0	0	0	0
2	100	0	0	0	0	0	0
3	36.7	0	63.3	0	0	0	0
4	3.2	3	96.8	0	0	0	0
5	0	17	97.1	2.9	0	0	0
6	0	43	76.7	20.9	2.3	0	0
7	0	37	46.3	53.7	0	0	0
8	0	37	31.7	58.5	4.8	2.4	2.4
9	0	40	23.8	69	0	4.8	2.4
10	0	27	10.5	78.9	0	10.5	0
11	0	30	2.5	84.6	0	12.8	0
12	0	23	2.7	83.8	2.7	10.8	0
13	0	27	2.6	86.8	0	10.5	0
14	0	27	0	84.2	2.6	13.2	0
15	0	27	0	71.1	2.6	23.7	5.3
16	0	37	2.4	90.2	0	7.3	0
17	0	33	0	82.5	0	15	2.5
18	0	30	0	89.7	0	10.2	0
19	0	37	7.3	82.9	2.4	7.3	0
20	0	17	0	80	0	17.1	2.9



development of which was blocked before leaf production. The number of buds is equivalent to a low concentration of BAP. The mutant also shows a similar reduction in the number of cells undergoing two divisions to that observed with low concentrations of BAP. The analysis of this particular mutant is complicated by the fact that the side-branch initial appears to undergo 2 cell divisions in quick succession giving the appearance of 2 side-branches from the initial rather than the distal end of the subapical cell. The number of chloronema undergoing the transition to caulonema appears to be significantly reduced. However in this mutant the basal cell of the side-branch may give rise to caulonema as well as to buds.

The mutant *nar-87* does not normally produce buds, but can be induced to produce buds by the addition of cytokinin. Two hypotheses have been proposed concerning the possible nature of the mutation. It has been suggested that this mutant is deficient in cytokinin synthesis. However it is also possible to induce buds with DR-OPP, a phenylurea, which might act by suppressing the activity of cytokinin oxidase. The possibility exists that this mutant overproduces cytokinin oxidase. The results of the side-branch analysis (table 3.11) reveal that as well as no buds, no caulonema are produced directly from side-branch initials. There is a significant increase in the number of subapical cells undergoing two and three cell divisions. A small proportion may even undergo 4 cell divisions. An average 70% of subapical cells undergo at least 2 cell divisions. The first division of a subapical cell is delayed by one cell position. At the third cell position, 90% of subapical cells remain undivided. The first two cell divisions of the subapical cell occur in quick succession. The second cell division may occur as early as the 4th cell position. By the 8th cell position, the maximum number of cells dividing twice has been reached. A further 6% of subapical cells undergo a third cell division. Side-branch development, however, is inhibited. There is also a significant increase in the number of side-branch initials that undergo no further development, remaining at the one cell stage. The majority of these result from the second and third cell divisions of the subapical cell. Chloronemal side-branch development is slow. It is extremely difficult to observe the position of the first cell

Table 3.10

Side-branch analysis of the first 20 cells of 30 filaments from 2 mutants of *P. patens*.

Treatment	No. of cells with				Side-branches as:					Total
	0	1	2	3	initials	chl	caul	chl-caul	buds	
	side-branches									
<i>gam</i> -139	65	399	135	1	134	479	10	12	37	672
<i>nar</i> -87	90	176	303	20	474	373	0	9	1	857

$\chi^2$  analysis of each mutant with wild-type control (table 1 total and table 4 control)

Comparison of control vs.	side-branch no.		side-branch fate	
	(df=3)		(df=4)	
<i>gam</i> -139	21.3	p<0.1%	80.8	p<0.1%
<i>nar</i> -87	211.3	p<0.1%	401.5	p<0.1%



Table 3.11

Side-branch analysis of the mutant GAM139. The percentage of each branch type at subapical positions 1-20 in 30 filaments.

Subapical cell	unbra	% with 2 branches	sbi	chl	caul	chl-caul	bud
1	100	0	0	0	0	0	0
2	100	0	0	0	0	0	0
3	16.6	0	83.3	0	0	0	0
4	0	0	100	0	0	0	0
5	0	0	93.3	6.6	0	0	0
6	0	7	65.6	34.4	0	0	0
7	0	17	25.7	71.4	2.9	0	0
8	0	23	18.9	75.7	2.7	0	2.7
9	0	27	7.9	84.2	0	2.6	7.9
10	0	47	6.8	77.3	4.5	2.3	11.4
11	0	37	2.4	78	4.9	4.9	9.8
12	0	43	2.3	79	2.3	2.3	16.3
13	0	33	5	85	0	5	5
14	0	43	4.7	83.7	2.3	0	9.3
15	0	43	0	88.9	2.2	6.6	6.6
16	0	47	2.3	81.8	2.3	4.5	9
17	0	27	2.6	92	0	0	8.6
18	0	10	0	90	0	0	12
19	0	20	0	88.9	0	0	11
20	0	27	0	95	0	0	5

Table 3.12

Side-branch analysis of the mutant *nar-87*. The percentage of each branch type at subapical positions 1-20 in 30 filaments.

Subapical cell	% with 2 branches	% 3 cells	unbra	sbi	chl	chl-caul	bud
1	0	0	100	0	0	0	0
2	0	0	100	0	0	0	0
3	0	0	90	10	0	0	0
4	3	0	10	90	0	0	0
5	16	0	0	100	0	0	0
6	36	3	0	95	5	0	0
7	50	0	0	87	13	0	0
8	73	0	0	81	19	0	0
9	73	3	0	74	26	0	0
10	70	0	0	63	37	0	0
11	70	3	0	53	47	0	0
12	67	7	0	47	51	2	0
13	63	7	0	45	52	2	2
14	67	3	0	33	62	6	0
15	67	13	0	31	67	2	0
16	77	7	0	33	65	2	0
17	70	10	0	41	59	0	0
18	72	3	0	37	61	2	0
19	75	0	0	37	62	4	0
20	74	7	0	35	65	0	0



division of the side-branch, resulting in error in the percentage of chloronema at cell positions 5, 6 and 7.

The high percentage of cells undergoing a second division suggests that this mutant may be an overproducer of a cell division factor, alternatively an underproducer of an inhibitor of cell division.

### 3.3.6 Light

Cultures growing in low light conditions were difficult to analyse, as the caulonema apical cells tended to revert to chloronema and grow at the same rate as the side-branches. This resulted in a spreading culture with main filaments and side-branches intermingled and difficult to distinguish. Fig. 3.13 shows the results of an analysis of a culture growing at  $300\text{mW m}^{-2}$ . An average 21% of subapical cells branch twice, compared to 40% of subapical cells in cultures growing under high light. A high proportion (*ca.* 20%) remain unbranched throughout the filament. Caulonema side-branches are completely absent. While at lower light intensities, on medium containing sucrose, filaments only produce caulonema side-branches, at intermediate light intensities (*ca.*  $100\text{-}700\text{ mW m}^{-2}$ ) chloronemal side-branches do not undergo the transition to caulonemata. It appears that light is necessary for the switch from chloronema to caulonema to occur.

### 3.3.7 Bud spacing

A total of 445 filaments were scored for numbers of buds per filament in order to examine the spacing of buds along a filament in *P. patens*.

The proportion of cells giving rise to a bud was taken as the probability of each cell position giving rise to a bud. The probability increases to 18 days then remains constant. For buds forming on side-branch initials only, the proportion of buds is in line with that found in the control cultures of the branching analysis (1.9%). When

Table 3.13

Side-branch analysis of wild-type *P. patens* grown under light intensity of 300mW m<sup>-2</sup>.  
30 filament sample.

Subapical cell	% with 2 branches	unbra	sbi	chl	caul	chl- caul	bud
1	0	100	0	0	0	0	0
2	0	100	0	0	0	0	0
3	0	30	100	0	0	0	0
4	10	20	59	41	0	0	0
5	13	6	25	75	0	0	0
6	33	13	23	78	0	0	0
7	20	23	16	84	0	0	0
8	30	6	11	89	0	0	0
9	30	23	19	78	0	0	3
10	27	27	13	87	0	0	0
11	40	13	16	89	0	0	0
12	27	10	6	94	0	0	0
13	40	23	14	86	0	0	0
14	36	27	9	91	0	0	0
15	23	20	10	90	0	0	0
16	20	27	7	93	0	0	0
17	23	33	15	81	0	0	3
18	30	20	6	93	0	0	0
19	16	30	13	85	0	0	0
20	10	40	5	95	0	0	0



buds forming on the basal cells of side branches are included, the proportion is doubled to an average 4%.

The hypothesis was tested that buds form randomly along a filament. The probability of each cell position forming a bud was used to generate the expected values for use in a chi-squared analysis.

The results of this analysis are shown in Table 3.14. When only buds forming directly from side-branch initials are analysed, bud distribution is random ( $X^2=0.75$ ). However, when all buds on a culture are analysed, bud distribution is not random ( $X^2=94$ ,  $p<0.1\%$ ), indicating that bud formation from the first cell of a side-branch is influenced by the buds already formed directly from initials. The results reveal an excess of budless filaments, also an excess of multibud filaments. There is a deficiency of filaments with 1 and 2 buds. The detailed analysis of spacing between buds (table 3.15 and fig. 3.6) reveals that when more than one bud forms on a filament, the second bud tends to be formed close to a pre-existing bud. There are an excess of buds with 5 or less cell positions between them. It may therefore be concluded, that in *P. patens*, the probability of an individual side-branch initial producing a bud is not affected by the development of a bud from other side-branch initials on the filament. However, the subsequent formation of buds from the first cells of filaments is neither random nor spaced, but positions are favoured close to pre-existing buds.

All experimental treatments (Tables 3.16-18) were analysed in a similar manner.

Cultures were treated with several different concentrations of the ionophore A23187. The results of these experiments are discussed more fully in ch. 4. Treatment with 50 $\mu$ M A23187 resulted in an increased number of buds. This treatment is therefore analysed in this section in terms of the spacing of buds. When the results are analysed in terms of the numbers of buds on each filament, a random distribution is suggested (table 3.16). However the analysis of subapical position (fig. 3.7) shows that buds form preferentially at specific cell positions. Cell positions 9 and 10 have the highest numbers of buds. The cultures were analysed 4 days after the addition of ionophore. Due to the effect on growth (see ch. 4), it is not possible to extrapolate

Table 3.14

Analysis of buds on 445 wild-type filaments of *P. patens* grown under standard conditions, covering subapical positions 9-30.

Buds as side-branch initials

No. buds.	0	1	2	3	4	p
No. obs. fils	250	150	36	4	5	0.0260
No.exp. fils	249.6	146.2	40.9	7.3	0.9	

$\chi^2_3=0.75$  (ns)

All buds

No. buds.	0	1	2	3	4	5	6	7	p
No. obs. fils	230	134	44	16	14	4	2	1	0.0373
No. exp. fils	192.9	164.3	66.8	17.2	—————3.8—————				

$\chi^2_4=94$  (p<0.1%)



Table 3.15

Analysis of the spacing between pairs of buds on 445 wild-type filaments covering subapical position 9–30 grown under standard conditions.

No. cells between pairs	Total pairs		Sbi	
	obs.	exp.	obs.	exp.
0	38	21.58	9	5.81
1	27	20.55	5	5.52
2	26	19.52	5	5.25
3	28	18.50	8	4.98
4	26	16.70	10	4.70
5	23	16.44	7	4.42
6	16	15.41	3	4.15
7	11	14.39	2	3.87
8	7	13.36	2	3.59
9	11	12.33	5	3.32
10	4	11.30	2	3.04
11	1	10.28	1	2.76
12	1	9.24	0	2.50
13	1	8.22	0	2.21
14	0	7.19	0	1.94
15	0	6.17	0	1.66
16	0	5.14	0	1.38
17	1	4.11	1	1.12
18	0	3.08	0	0.83
19	0	2.06	0	—
20	2	1.03	0	—

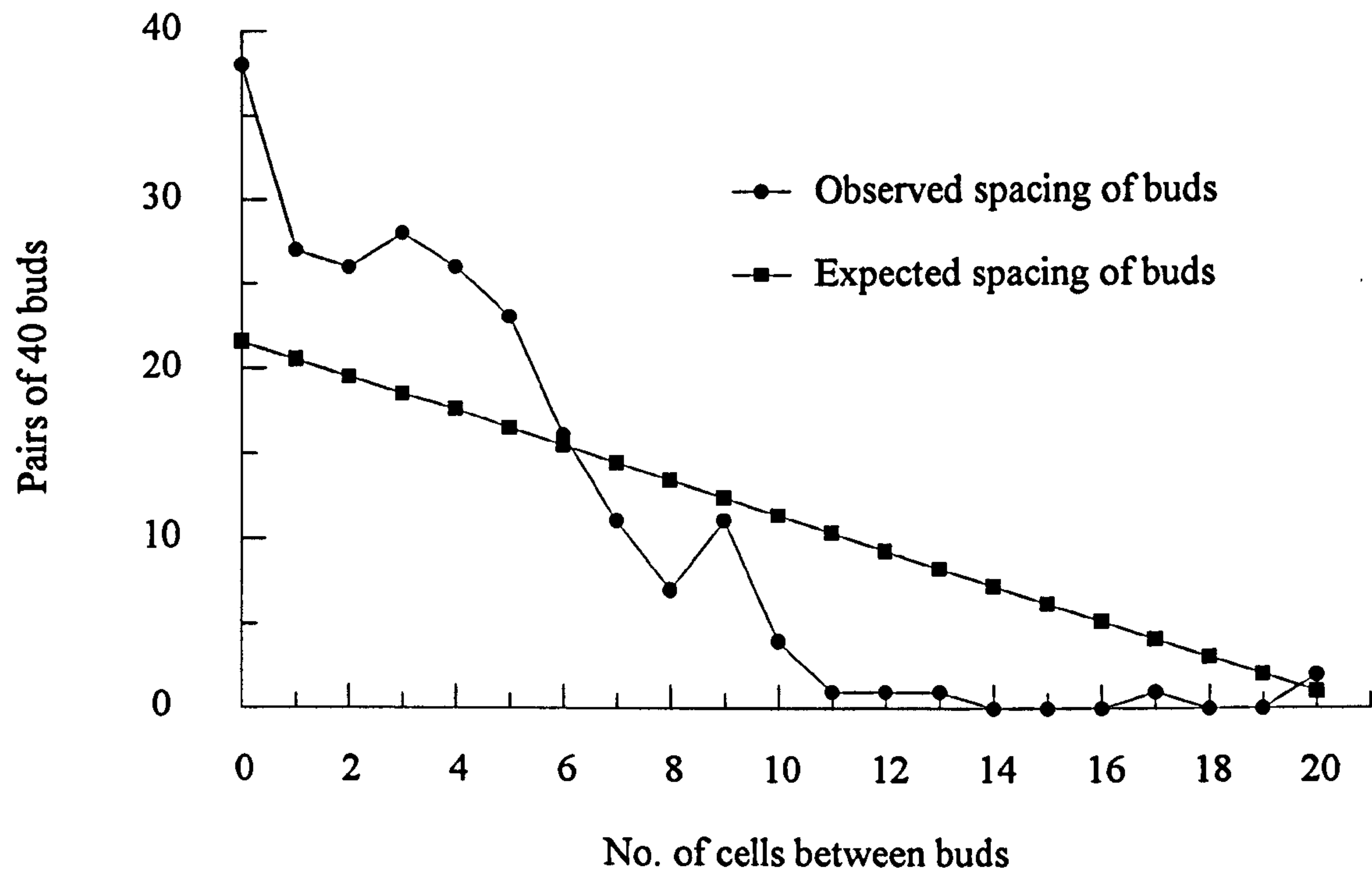


Fig 3.6 The spacing between pairs of buds on the first 20 cell positions of wild-type caulonema.



Table 3.16

Analysis of buds on 50 wild-type filaments treated for 3 days with 50μM A23187.

Buds as side-branch initials

No. buds	0	1	2	3	p
No. obs. fils	7	24	16	3	0.0866
No. exp. fils	12.84	18.27	12.14	6.75	

$\chi^2_3=7.76$  (p<5%, >1%)

All buds

No. buds	0	1	2	3	4	5	6	7	p
No. obs. fils	6	20	15	6	1	1	0	1	0.1120
No. exp. fils	8.42	15.92	14.06	7.68	3.93				

$\chi^2_4=2.22$  (ns)

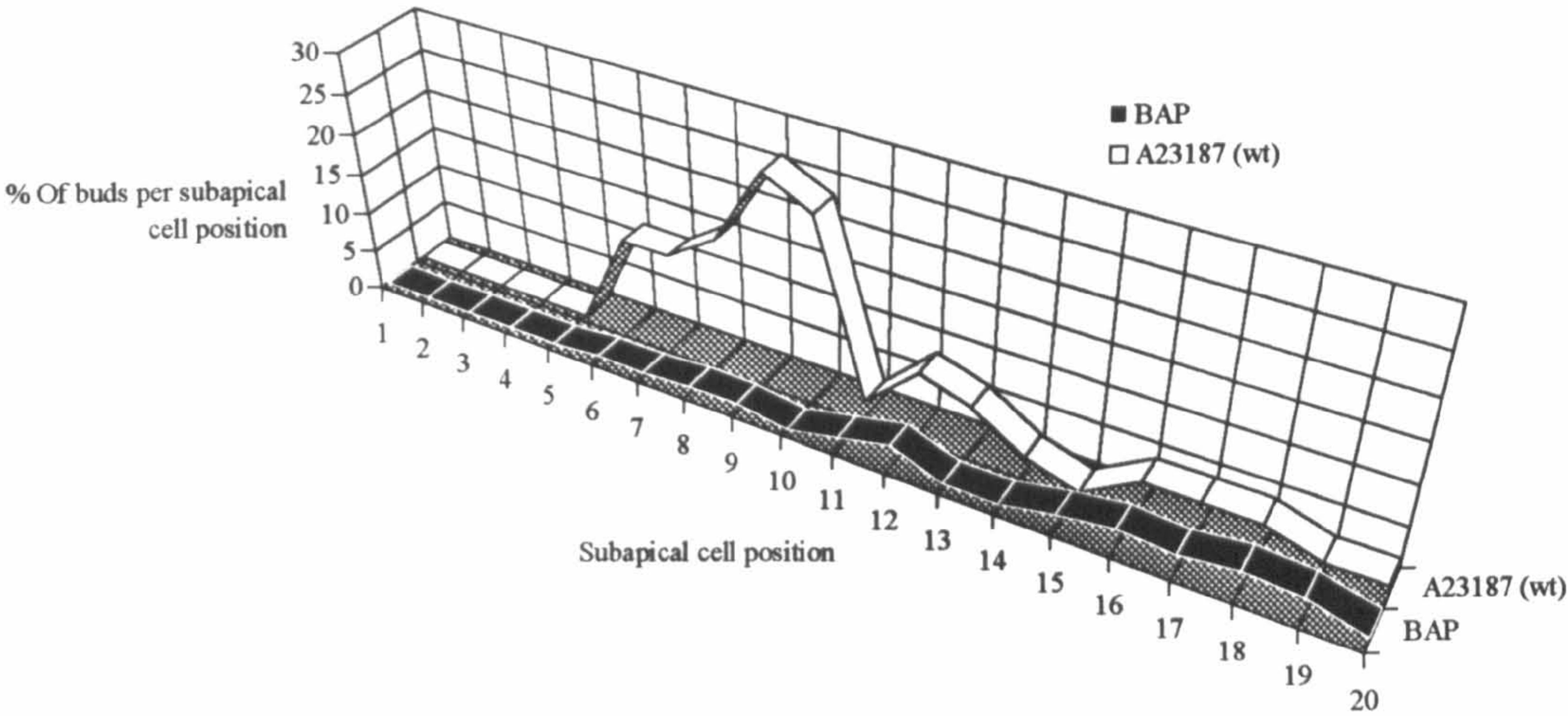


Fig 3.7 A comparison of the effect of 30nM BAP and 50μM A23187 on bud production in wild-type *P. patens*.



back to the cell position at the time of the addition of the ionophore. However, as discussed in ch. 4, time-lapse film of this treatment suggests that the effect of A23187 in producing buds is not on existing initials, but on the initials that form subsequent to the treatment.

An analysis of 30nM BAP (table 3.17) does not suggest any difference to the wild-type distribution of buds. At 50nM BAP (table 3.18) chi-squared analysis shows the distribution of buds to be non-random. Higher concentrations of BAP could not be analysed due to the saturation of budding. Increasing concentrations of BAP appear to increase the non-random clustering of buds. This will be discussed more fully in chapter VI.



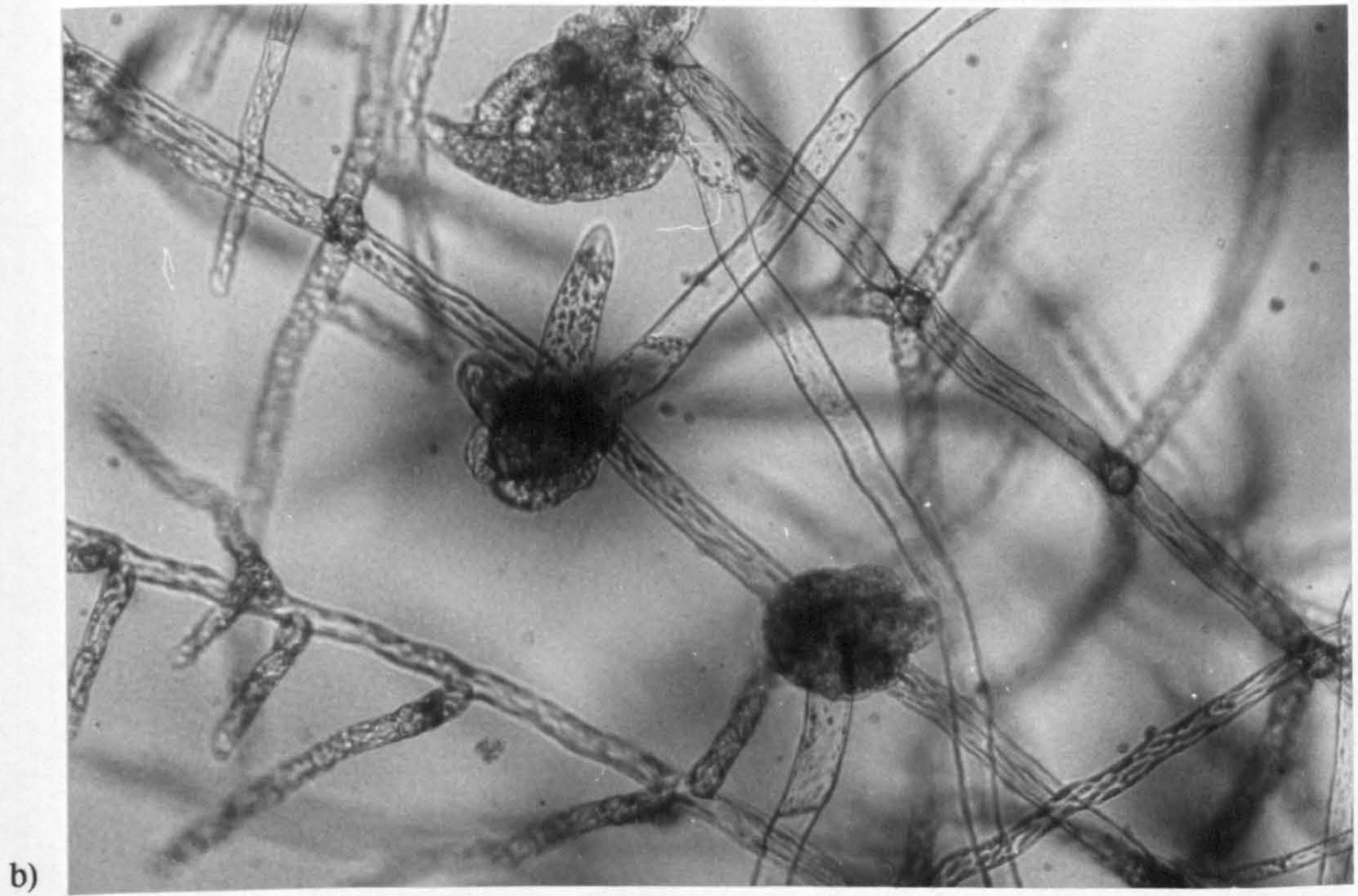
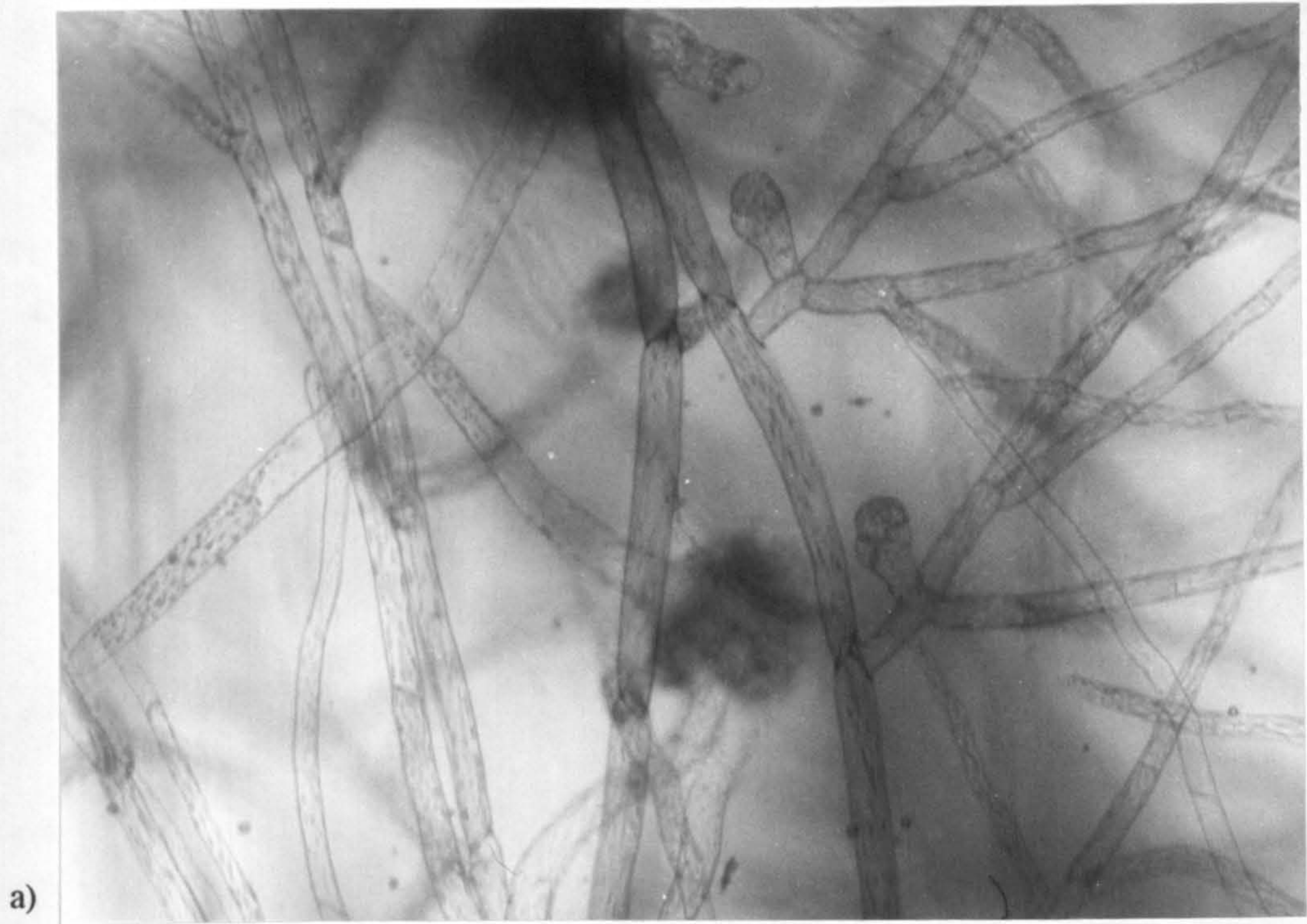


Fig. 3.8 Buds developing on the basal cells of side-branches a) and in clusters b) in wild-type *P. patens*.





Table 3.18

Analysis of buds on 130 wild-type filaments treated for 3 days with 50nM BAP.

Buds as side-branch initials

No. buds	0	1	2	3	4	5	p
No. obs. fils	41	32	24	17	9	5	0.1231
No. exp. fils	26.9	45.3	34.9	16.3	—6.6—		

$\chi^2_4=23.03$  (p<0.1%)

All Buds

No. buds	0	1	2	3	4	5	6	7	8	p
No. obs. fils	38	24	27	17	12	8	1	0	1	0.1481
No. exp. fils	19	39.6	37.9	21.9	8.6	—3.0—				

$\chi^2_5=44.8$  (p<0.1%)



## CHAPTER IV

### ELECTROPHYSIOLOGY AND INHIBITOR STUDY

#### 1. Introduction

The maintenance of a membrane potential difference across the plasma membrane is an essential feature of plant cell organisation, regulating the uptake and transport of nutrients and ions. The main component of the membrane potential ( $\Delta\Psi$ ), which is strongly negative inside with respect to the extracellular environment, is an electrogenic pump which is an outwardly directed  $H^+$ -ATPase. This generates an electrochemical gradient of protons to drive transport of solutes in antiport or symport with  $H^+$ . Passive diffusion pathways make up the rest of the membrane potential. These are largely attributable to  $K^+$ ,  $Cl^-$  and  $Ca^{2+}$ , but include a contribution from other anions and charged molecules.

The flow of any particular ion species  $i$  across the membrane either by diffusion or via a channel is driven by its electrochemical gradient  $\Delta\mu_i$ . The gradient contains two physical forces expressed by an electric (voltage) and a concentration gradient term, and has units of free energy ( $J\ mol^{-1}$ ). This relation is described by the following equation:

$$\Delta\mu_i = RT \ln(C_i^o/C_i^i) + z_i F \Delta\Psi$$

where  $R$  is the gas constant,  $T$  the temperature in degrees Kelvin,  $z$  the charge of ion  $i$ ,  $F$  the Faraday constant,  $c^o$  and  $c^i$  the chemical concentrations of the ion  $i$  inside and outside the cell and  $\Delta\Psi$  the electrical potential difference. When the electrical and concentration gradient terms just balance each other the electrochemical gradient  $\Delta\mu_i$  is zero and there is no net flux of the ion  $i$  across the membrane. Under this condition the electrical potential difference resides at the equilibrium potential of the ion and the relation to the concentration gradient is described by a form of the Nernst equation:

$$\Delta\Psi_i = RT/z_i F \cdot \ln(C_i^o/C_i^i)$$

After inserting the actual numerical values for  $R$ ,  $F$  and replacing the natural logarithm  $\ln$  by  $2.303 \lg$ , where  $\lg$  is the logarithm to the base 10, the equation becomes:

$$\Delta\Psi_i = 59/z_i \cdot \lg(C_i^o/C_i^i)$$

The contribution of, for example,  $\text{Ca}^{2+}$  to  $\Delta\Psi$  can therefore be estimated for any given concentration:

$$\Delta\Psi = 59/2 \cdot \lg(C_i^o/C_i^i)$$

Therefore at an external concentration of 1 mM  $\text{Ca}^{2+}$  and an internal activity of 100nM, the equilibrium potential of  $\text{Ca}^{2+}$  will be  $59/2 \log_{10} 10^{-3}/10^{-7} = +118\text{mV}$ . Since  $\Delta\Psi$  is normally well negative of this value (e.g.  $-150\text{mV}$ ), there is a strong inward driving force for  $\text{Ca}^{2+}$  entry, equal to  $270\text{mV}$  ( $27\text{kJ/mol}$ ). An increase in calcium influx across the plasma membrane would therefore increase the positive component of the potential leading to depolarisation. The size of the depolarisation is dependent on a range of factors such as the relationship between the current generated and the resistivity of the membrane, and the effect of an increase in  $[\text{Ca}^{2+}]_i$  on membrane permeability to other ions such as  $\text{K}^+$ .

In animal cells ionic fluxes across the membrane have been found to be an essential component of many signal transduction processes (see ch.1). The primary mode of action of many hormones and neurotransmitters is the regulation of protein ion channels, through voltage changes and/or receptors. In view of the role of calcium, particular attention has been paid to elucidating the nature of calcium channels. Animal physiologists have defined calcium-specific channels on the basis of the binding and inhibitory activity of a number of drugs found to be specific for calcium channel activity in nerve, muscle and endocrine tissue. Three main types of channel have been defined on the basis of their possible regulation. Voltage-operated channels (VOCs) exist in a number of excitable tissues, where an initial depolarisation caused, for example by an influx of sodium ions, opens calcium channels, thus increasing the depolarisation and leading to the propagation of action potentials. The term receptor-



operated channels (ROCs) was initially devised to include all calcium channels not opened by depolarisation but as a consequence of agonist stimulation. These include ROCs *sensu stricto* in which it is thought receptor and channel function coexist in a linked unit, e.g. the nicotinic acetylcholine receptor, and a range of second messenger-operated calcium channels (SMOCs) in which it is thought that permeability of the membrane to calcium is a secondary consequence of second messenger generation of a rise in intracellular calcium from internal sources. This group is linked to the inositol triphosphate signal transduction pathway. Some ROCs also may be partly voltage-regulated but operating at lower voltages and not necessarily producing action potentials.

The only channels clearly defined as a result of drug action are the L (longlasting) VOCs with high thresholds and low inactivation, found both in excitable and non-excitable tissue (Bean, 1989). These are the target of the organic inhibitors, the dihydropyridines. These include the compounds BAYK8644, (-)PN202-791, nifedipine and nitrendipine. Other types of VOC, e.g. low-threshold T and N-type VOCs are less sensitive to these compounds. The phenylalkylamine series of channel blockers, which include verapamil and its methoxy derivative D-600, also block L-type VOCs more effectively than T channels. Both types of organic inhibitor have been found to block slow calcium channels in skeletal muscle (Bean, 1989).

Calcium channels are clearly present in plant tissue and uptake of calcium is necessary for normal function and growth of plant cells. Recent advances in patch clamping have revealed both stretch and voltage sensitivity of these channels (Tester, 1990). However direct evidence of voltage dependent regulation by agonists in a manner analogous to the VOCs of animal tissue is lacking (Schroeder and Thuleau, 1991). Several studies have attempted to define plant calcium channels using the dihydropyridine and phenylalkylamine drugs. Not surprisingly these have produced conflicting results.

Graziana *et al* (1988) found no effect of nifedipine, nitrendipine, or (+)PN-200-110 at up to 100uM on  $^{45}\text{Ca}^{2+}$  influxes into carrot protoplasts. Conversely, Shiina and Tazawa (1987) and Zherelova (1989) measured an inhibition of inward current during the action potential of *Nitellopsis obtusa* upon addition of 100μM Nifedipine and several other dihydropyridines. However they noted a variability of sensitivity in different cultures with some cells unaffected. Tester and MacRobbie (1990) tested a range of these drugs using the action potential of *Chara corallina*, where the initial phase of the depolarisation is known to be caused by an influx of calcium. They included nifedipine and (-)-202-791, which inhibit and (+)-202-791 and Bay K8644, which usually stimulate  $\text{Ca}^{2+}$  currents in animal systems. In all four cases they found no effect at concentrations normally used by animal physiologists ( $10^{-9}$  to  $10^{-7}$ ). All four inhibited the action potential at concentrations  $10^{-6}$  to  $10^{-4}$ , with inhibition increasing with concentration and always reversible. Low concentrations of  $\text{La}^{3+}$  had no effect, But 100μM resulted in an irreversible reduction of calcium influx.

Similarly, Graziana *et al* (1988) found inhibition of  $^{45}\text{Ca}^{2+}$  influxes into carrot protoplasts by verapamil, whereas Tretyn (1987) in other systems, found no effects or small effects with high concentrations. However verapamil has been found to bind to plant membranes, and Harvey *et al* (1989) have partially purified a verapamil-binding protein with a likely molecular weight of 169 kDa.

The majority of work on calcium influxes in plants has been done with isolated protoplasts, and is therefore divorced from any developmental process. The extent to which calcium influxes are involved in agonist-stimulated signal transduction processes in plants is still very much a matter for conjecture (see ch. 1).

Some progress has been made in elucidating the primary mode of action of auxin, in terms of ion fluxes. Felle *et al* (1991) and Tretyn *et al* (1991) have used classical electrophysiology to examine the response of *Zea mays* coleoptiles and root hairs to auxin. Tretyn *et al* (1991) come to the conclusion that both hyperpolarisation and depolarisation observed in response to various concentrations of IAA are the result of



receptor-mediated effects on the  $H^+$ ATPase. Although calcium fluctuates they do not think this is a primary result of receptor activation. Felle *et al* (1991) conclude that in *Zea mays* coleoptiles IAA has a direct effect on membrane transport and propose an influx carrier which co-transport IAA<sup>-</sup> with  $nH^+$ .

The primary mode of action of cytokinin remains unelucidated (Ch. 1). Hepler and Saunders and coworkers, working with cytokinin-induced budding in *Funaria hygrometrica* have put forward the hypothesis that the first effect of this hormone is an influx of calcium across the plasma membrane, in a manner directly analogous to hormone activity in animal cells. Conrad and Hepler (1988) examined the effects of the dihydropyridines nifedipine and (-)-202-791 on BA-induced budding, despite calcium influxes being assumed rather than measured, and found nearly 100% inhibition of BA action at concentrations of 100  $\mu$ M. They reported stimulation of budding with (+)-202-791 and CGP 28392. However the pictures of supposed buds in response to these 'agonists' do not bear any resemblance to either normal or cytokinin-induced buds, rather to an unspecific effect on the growth of moss filaments. The authors suggest on the basis of these experiments that cytokinin induces the budding response by increasing calcium entry through voltage-operated channels. This conflicts with the result of Tester and MacRobbie (1990), in which (+)-202-791 had an inhibitory effect on calcium channel activity.

Saunders and Hepler (1983) also looked at the effects of verapamil, D600 and  $La^{3+}$  on bud development. They found that all three blocked BA action, however again at high concentrations. Markmann-Mulisch and Bopp (1987) criticised this study on the grounds that the concentration of  $LaCl_3$  needed for 100% inhibition of BA action is also inhibitory to growth in general, resulting in a diminished number of sites able to bear a bud. Saunders and Hepler (1983), however, state that the results with  $La^{3+}$  give unambiguous support for the idea that  $Ca^{2+}$  required for bud formation comes from outside the cell.

Saunders (1986) investigated changes in electrical current across the plasma

membrane of *F. hygrometrica* in response to BA, using the non-intrusive vibrating microelectrode developed by Jaffe and Nuccitelli (1974). She reported that after cytokinin treatment, inward current increases twofold along the length of the cell, from 0.25 to 0.7  $\mu\text{A}/\text{cm}^2$  at the distal end of target cells by ten minutes after treatment. The current continued to rise reaching 1  $\mu\text{A}/\text{cm}^2$  by 30 minutes, and did not drop back to resting level until 10 to 24 hours after BA application. The drop in current was noted as the initial outgrowth of the presumptive bud initial became apparent. Current at the nuclear zones and proximal ends also increased immediately after cytokinin treatment, but then fell to resting levels or below within 30 to 60 minutes.

Recently Jaffe and coworkers have developed a  $\text{Ca}^{2+}$  selective vibrating microelectrode (Kuhntreiber and Jaffe, 1990). Saunders (1992) measured an increase in  $\text{Ca}^{2+}$  influx at the surface of caulonema cells from less than 0.02  $\text{pmol}\cdot\text{cm}^2\cdot\text{s}^{-1}$  to more than 1.3  $\text{pmol}\cdot\text{cm}^{-2}\cdot\text{s}^{-1}$  at the presumptive bud site. The calcium influx remains high for at least several hours after BAP treatment and is responsible for at least half the total current detected at the developing bud site. No growth conditions are given for this experiment. Kuhntreiber and Jaffe (1990) report that the probe does not function well in concentrations of calcium above 10 $\mu\text{M}$ .

Parsons *et al* (1989) sought to investigate the claim that the action of cytokinin results in an opening of membrane calcium channels, and the alternative claim put forward by Marre *et al* (1974) that the primary action of cytokinin is to stimulate the primary proton pump. Rapid changes in membrane transport in response to cytokinin application were studied in heterotrophic suspension-cultured callus of soybean using electrophysiological techniques. They found that 2 $\mu\text{M}$  kinetin (N<sup>6</sup>-furfurylaminopurine) elicited membrane hyperpolarisation of  $\pm 13\text{mV}$ . It appeared therefore that cytokinin had an activating effect on the electrogenic pump. However, hormonally inactive but chemically related compounds also elicited membrane hyperpolarisation, whereas hormonally active N<sup>9</sup> substituted cytokinins and N, N-diphenylurea failed to stimulate electrogenesis, so that it was unlikely the hormonal



effect on electrogenesis was directly related to transduction of the cytokinin signal. These authors did not discount a small influx of  $\text{Ca}^{2+}$  which might be at the limit of resolution of the technique and masked by the effect on the proton pump. Membrane conductivities and resistance were not measured.

The aim of the study described here was to look for any current associated with the action of cytokinin on moss using classical electrophysiology. The following work was done in conjunction with Helmuth Hohmeyer at York University.

Moss is a highly suitable organism for standard electrophysiological techniques. The cells are large so that it is not difficult to insert microelectrodes. Protonemal filaments can be induced to grow in parallel rows under low light conditions, so that they are optimally suited for impalement. Protonema grown in this manner have been used for the study of the light-induced action potential (H. Hohmeyer, A. Tretyn and D. Sanders, unpublished data) using techniques adapted from electrophysiological work with *Neurospora crassa*.

Protonema in standard media maintain a steady-state plasma membrane potential of around -171 mV interior negative (H. Hohmeyer, unpublished data). In the absence of calcium the potential depolarises to -50 mV.

This study also aimed to look at the effects on growth of some of the commonly used calcium channel inhibitors, and the calcium ionophore A23187.

## **4.2 Materials and Methods**

To obtain caulonema filaments suitable for microelectrode impalements, protonemal tissue was inoculated in the centre of 90mm plastic Petri dishes containing agar-solidified medium covered with cellophane discs which had been roughened using emery paper. The cultures were kept at 25° under continuous white light for 2 to 3 days to establish growth, and then transferred to a chamber in which the growing filaments were exposed to an unidirectional source of dim white light

( $0.1\text{Wm}^2$ ). This induced them to grow towards the light source in straight parallel rows, attached to the cellophane disc. Prior to an experiment, the filaments were embedded on the cellophane with a thin layer of hand-warm agar medium (SRM, see below, plus 1.2% agarose, Sigma type VII, 'low gelling temperature').

### Measurement of membrane potential

All operations were observed with an inverted microscope (Nikon Diaphot) using bright-field, long working distance 40x objective. Positioning of the microelectrodes was performed using Huxley-Goodfellow HG-3000 micromanipulators (Goodfellow metals, Cambridge, U.K.). All equipment for observation and micro-manipulation was contained in a Faraday cage mounted on a vibration isolation table.

Microelectrodes were fabricated from filamented borosilicate glass capillaries (outside diam. = 1.0mm; inside diam. = 0.58mm; Hilgenberg glass, Germany) using a vertical electrode puller (Narashige PE-2, Tokyo, Japan). The micropipettes were back-filled with 0.1 M KCl and connected to an Ag-AgCl half cell in contact with 0.1M KCl in a microelectrode holder (MEH1SF, World Precision Instruments, Newhaven, U.S.A.). Microelectrode tips were less than  $0.5\mu\text{m}$  in diameter, with a typical resistance of  $90\mu\Omega$  when measured in a 1M KCl circuit.

The microelectrode holder and half-cell was connected directly to the amplifier probe of an FD-223 electrometer amplifier, input impedance  $10^{15}\Omega$  (World Precision Instruments). Recordings were made referenced to a 1 M KCl-agar salt bridge. Measurements were monitored using a chart recorder (Rikadenki, Tokyo, Japan).

### Recording media

The composition of the standard recording media (SRM) was: (concentrations in mM)  $\text{K}_2\text{SO}_4$  (0.2), NaCl (1.0),  $\text{CaSO}_4$  (1.0), MES (5.0), adjusted to pH 7.0 with



Tris. Impaled filaments were continuously superfused with medium at  $10\text{ml}\cdot\text{min}^{-1}$  via a four-way distribution valve (Omnifit, Cambridge, U.K.), which enabled solution changes to reach the recording chamber within *ca.* 5s.

Desired volumes of stock solutions of hormones were given to SRM before pH adjustment.

### Inhibitor treatments

Cultures grown on solid ABC medium containing sucrose (appendix A) in 50mm petri-dishes were incubated in open ended boxes in broad spectrum white light provided by fluorescent tubes at an intensity of  $100\text{mW m}^{-2}$  at the end of the box. Inhibitors were added at a concentration a factor of 10 higher than that required, to take into account the volume of medium in the petri-dish (*ca.* 10 ml). After addition of the inhibitor the cultures were left to stand for *ca.* 1 hour to allow the solution to filter into the agar, before being put back into the boxes at a  $90^\circ$  reorientation to their former position. The point at which the filaments turned to grow towards the light could then be used as a reference point to measure growth.

For experiments with inhibitors using the well plate method, the agar surrounding the culture growing in the well was cut away, and solutions of inhibitor were added to the correct concentration to allow for a  $10 \times 10 \times 1$  mm volume of agar.

## 4.3 Results and Discussion

This work was performed in the laboratory of Prof. D. Sanders in collaboration with Dr. H. Hohmeyer. Dr. Hohmeyer taught me the technique of membrane potential measurement, and did some of the initial measurements. All cultures of *Funaria hygrometrica*, and mutant strains of *P. patens*, were prepared for experimental work at Leeds. Membrane potential measurements of *F. hygrometrica* were taken for the

first time during the course of this study, by both Dr. Hohmeyer and myself. The current-voltage measurements necessary for the calculations of currents were done by Dr. Hohmeyer.

In electrophysiological terms there appears to be little difference between *P. patens* and *F. hygrometrica*. The average membrane potential is very similar.  $\Delta\Psi$  equals  $-171\pm15\text{mV}$  (S.D; 22 counts) for *F. hygrometrica* as compared to  $-174\pm18\text{mV}$  (S.D; 263 counts) for *P. patens*. The average membrane conductivity is also similar,  $3.2\pm0.5\cdot10^{-6}\text{ S}\cdot\text{cm}^{-2}$  for *P. patens*,  $4.9\pm1.4\cdot10^{-6}\text{ S}\cdot\text{cm}^{-2}$  for *F. hygrometrica* although more variable in *F. hygrometrica*, with a range from 1.0 to  $10.5\cdot10^{-6}\text{ S}\cdot\text{cm}^{-2}$  (H. Hohmeyer, unpublished data). *F. hygrometrica* has one advantage over *P. patens* for electrophysiological work in that it makes fewer side-branches and appears to be more cable-like (H. Hohmeyer, unpublished data). This is significant in electrophysiological work, as current may be lost as it travels into and through side-branches.

Table 4.1 summarises the experiments performed using both *P. patens* and *F. hygrometrica*.

When cytokinin (1-100  $\mu\text{M}$ ) was added to the perfusing medium, in the majority of cases there was no detectable change to the membrane potential (figs 4.1 to 4.7). Where there was a hyperpolarisation or depolarisation these were slight, and probably reflected the fact that the basal potential was not entirely steady. In the case of *F. hygrometrica* (fig. 4.2b) the hyperpolarisation was found to be the result of a pH difference of the perfusing medium of 0.2, showing that the membrane potential is extremely sensitive to pH changes. Fig.4.3 shows the addition of 10  $\mu\text{M}$  BAP to wild-type *P. patens* after 30 minutes of steady membrane potential in standard recording medium (SRM). There was no change in  $\Delta\Psi$  even after this length of time. These results do not immediately suggest that cytokinin has any effect on membrane currents.



Table 4.1    Summary of experiments on the effects of BAP, NAA and DR-OPP on membrane potential in *P. patens* and *F. hygrometrica*.

Treatment			Response	Initial ΔΨ (mV)
WT	BAP	1μM	none	-190
		1μM	none	-135
		1μM	none	-180
		1μM	none	-170
		1μM	none	-185
		1μM	hyperpolarisation	-160-185
		10μM	none	-155
		10μM	none	-150
		10μM	depolarisation	-155
		100μM	none	-155
		100μM	depolarisation	-185
	i6-Ade	10μM	none	-155
			none	-160
	DR-OPP	4μg/ml	none	- 165-160
		4μg/ml	none	-160
	CAFFEINE 20mM BAP 1μM		depolarisation stops recovery	-190
	NAA	20μM	none	-135
		20μM	none	-165
		20μM	none	-160
		20μM	depolarisation	-120
NAR-87	BAP	5μM	none	-160
BAR-1	BAP	5μM	none	
GAM-710	BAP	1μM	none	-165
		5μM	none	-180
		5μM	depolarisation	-185
		5μM	none	-145
	DR-OPP	4μg/ml	none	-175
		4μg/ml	none	-165
FUNARIA	BAP	1μM	none	-185
		1μM	none	-197
		1μM	none	-157
		1μM	none	-199
		1μM	none	-175
		1μM	none	-180

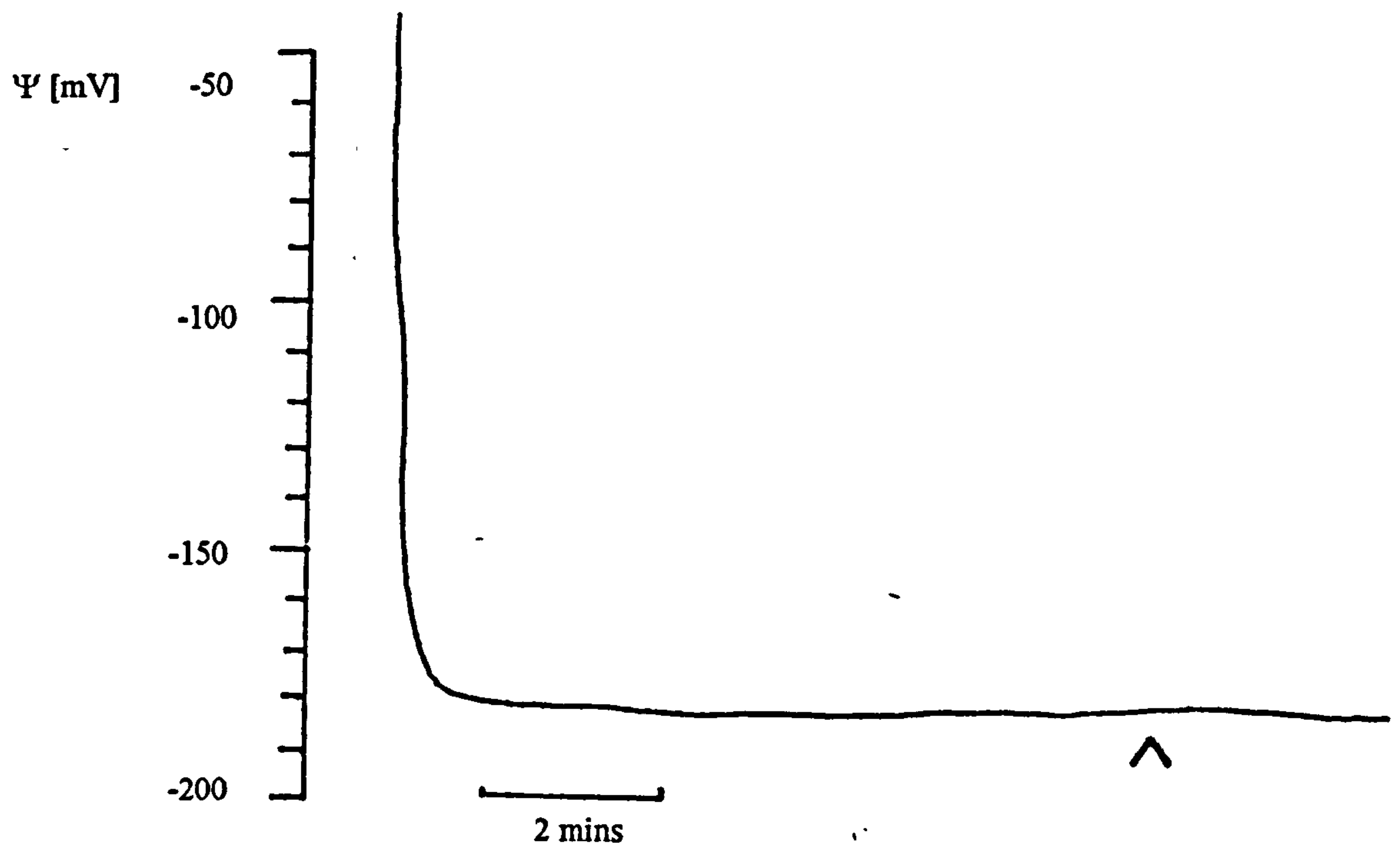


Fig. 4.1 The effect of BAP (1  $\mu$ M) on membrane potential in wild-type *P. patens*. Arrow indicates application.

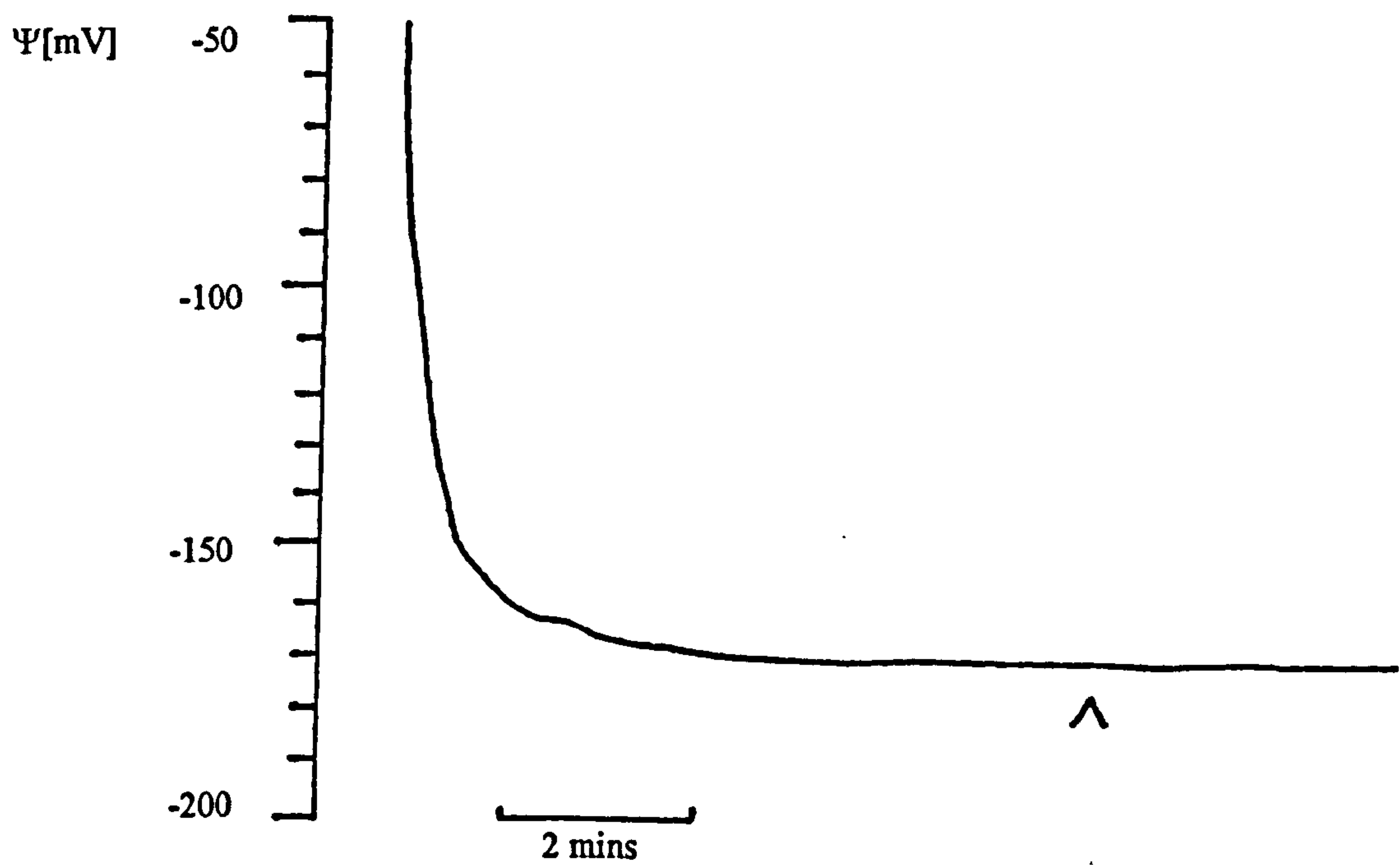


Fig. 4.2 The effect of NAA (20  $\mu$ M) on membrane potential in wild-type *P. patens*. Arrow indicates application.



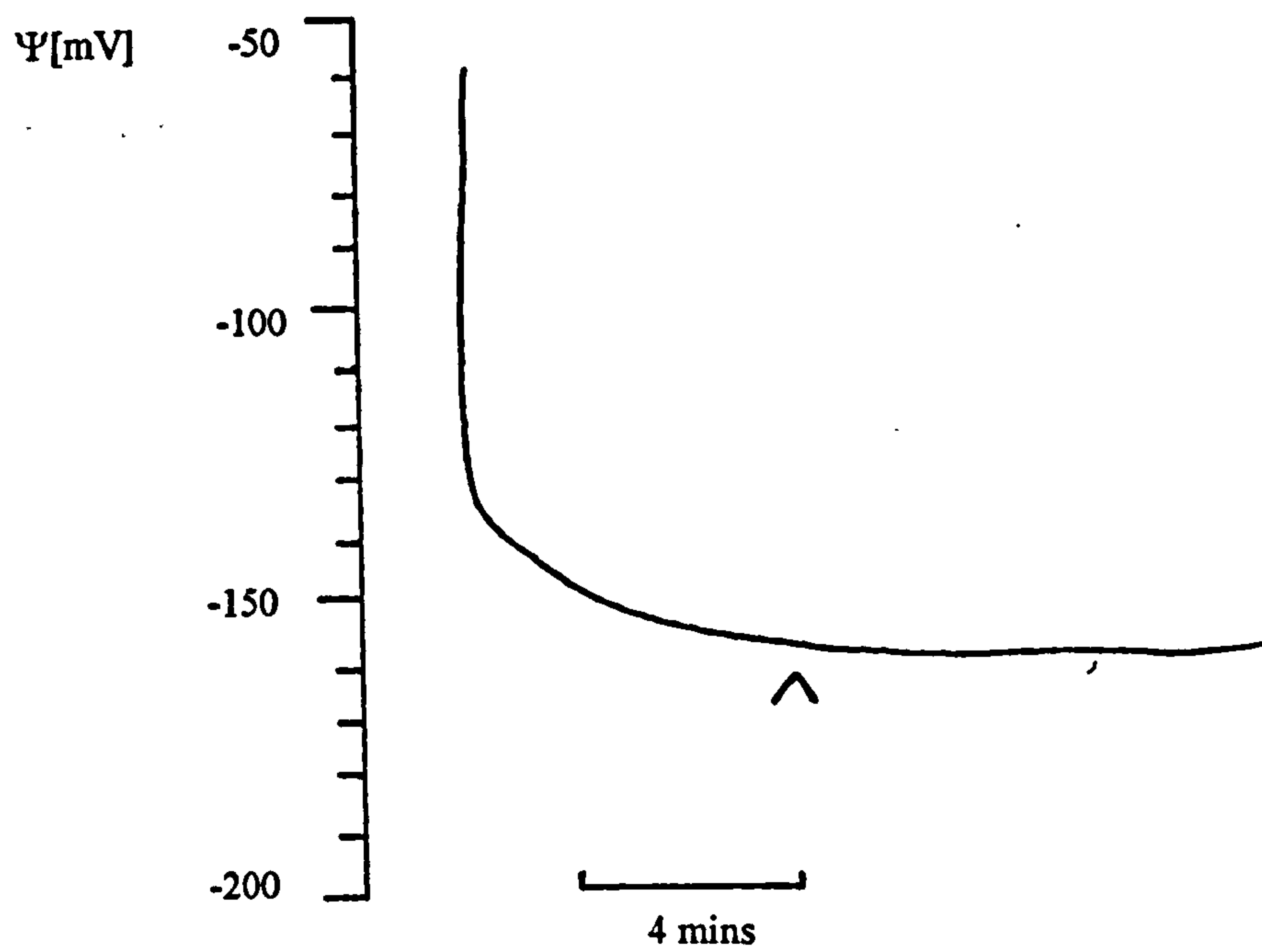


Fig. 4.3 The effect of BAP ( $1\mu\text{M}$ ) on the membrane potential of *F. hygrometrica*. Arrow indicates application.

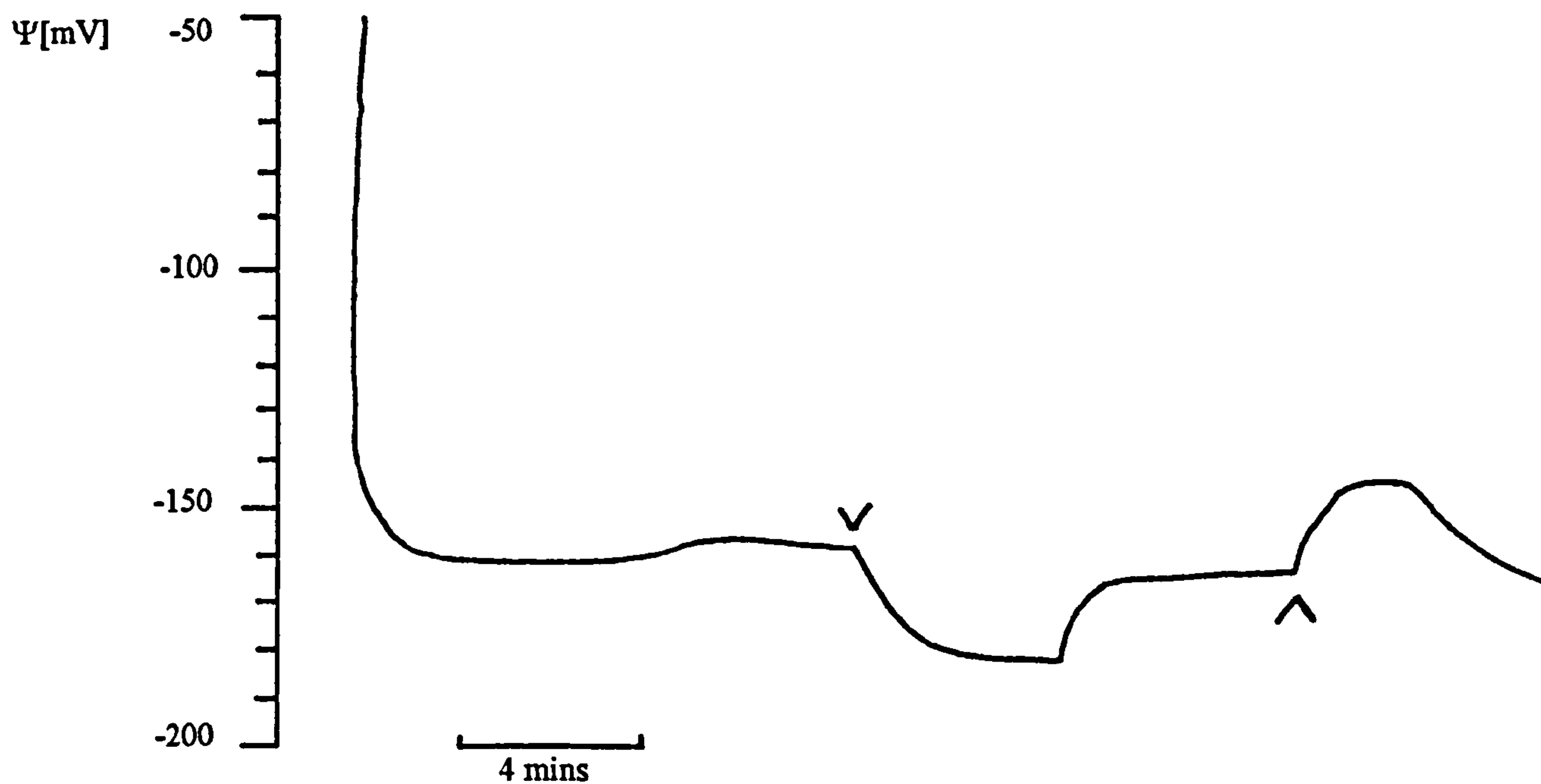


Fig. 4.4 The effect of pH on the membrane potential of *F. hygrometrica*, incubated in SRM (pH 7.2). First arrow: application of BAP ( $1\mu\text{M}$ ; pH 7.0). Second arrow: application of SRM.

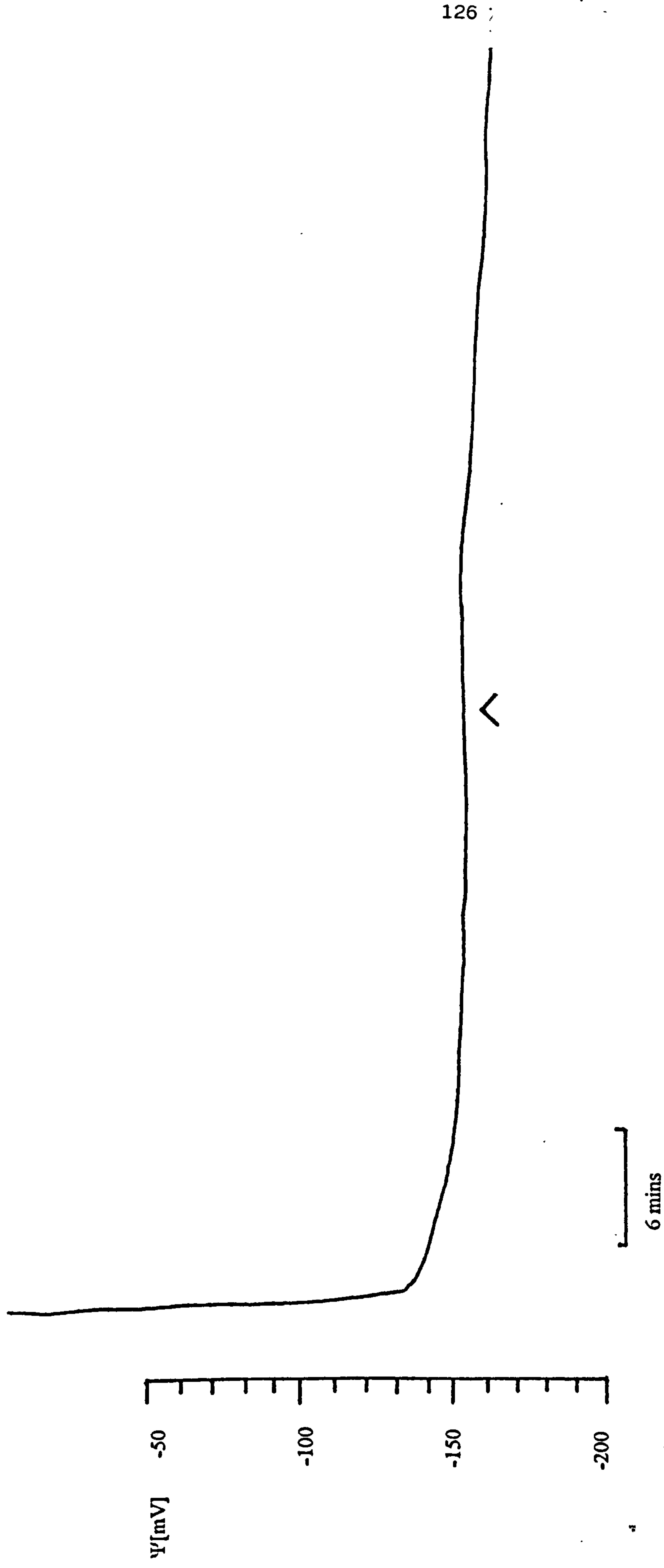
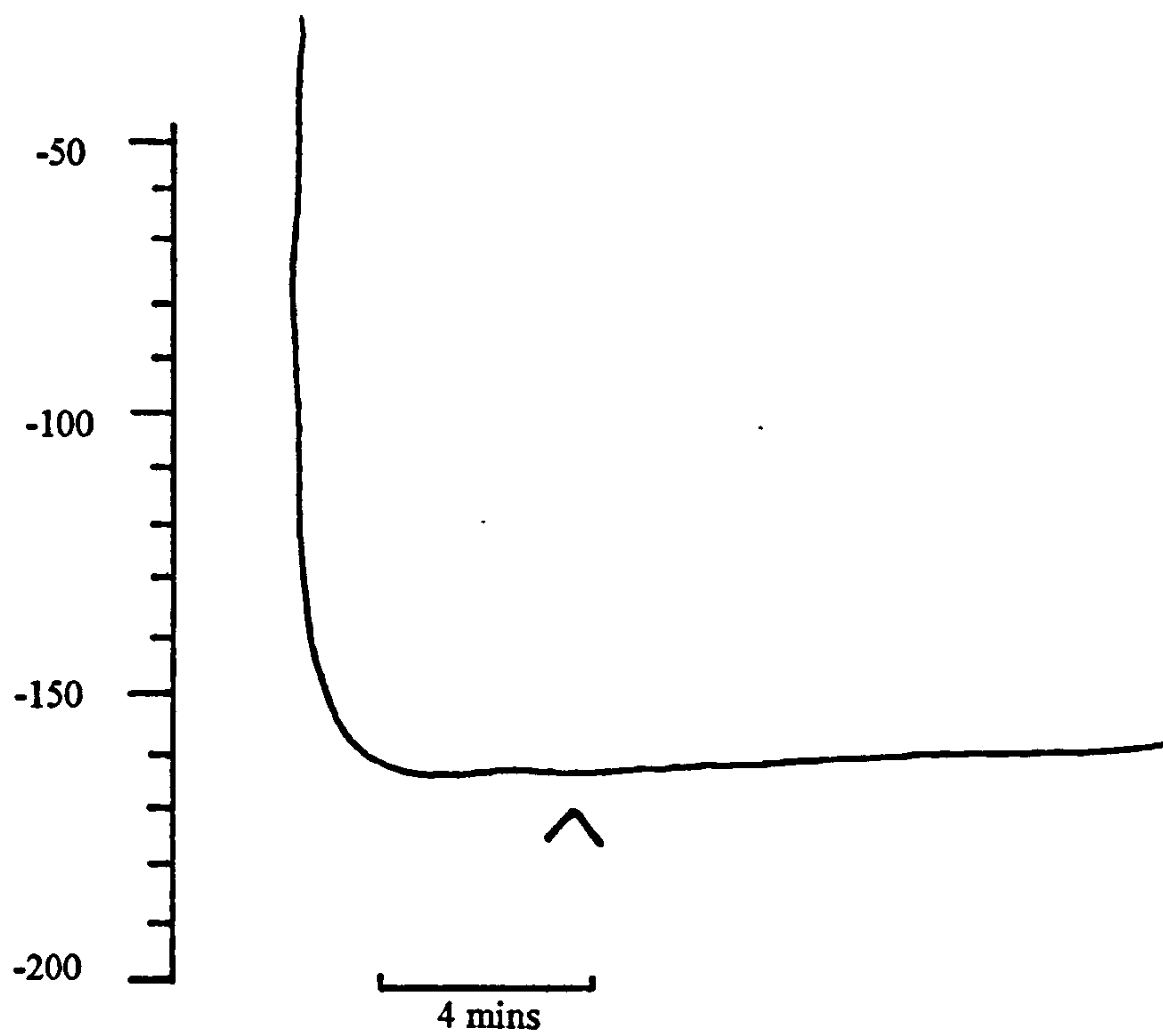
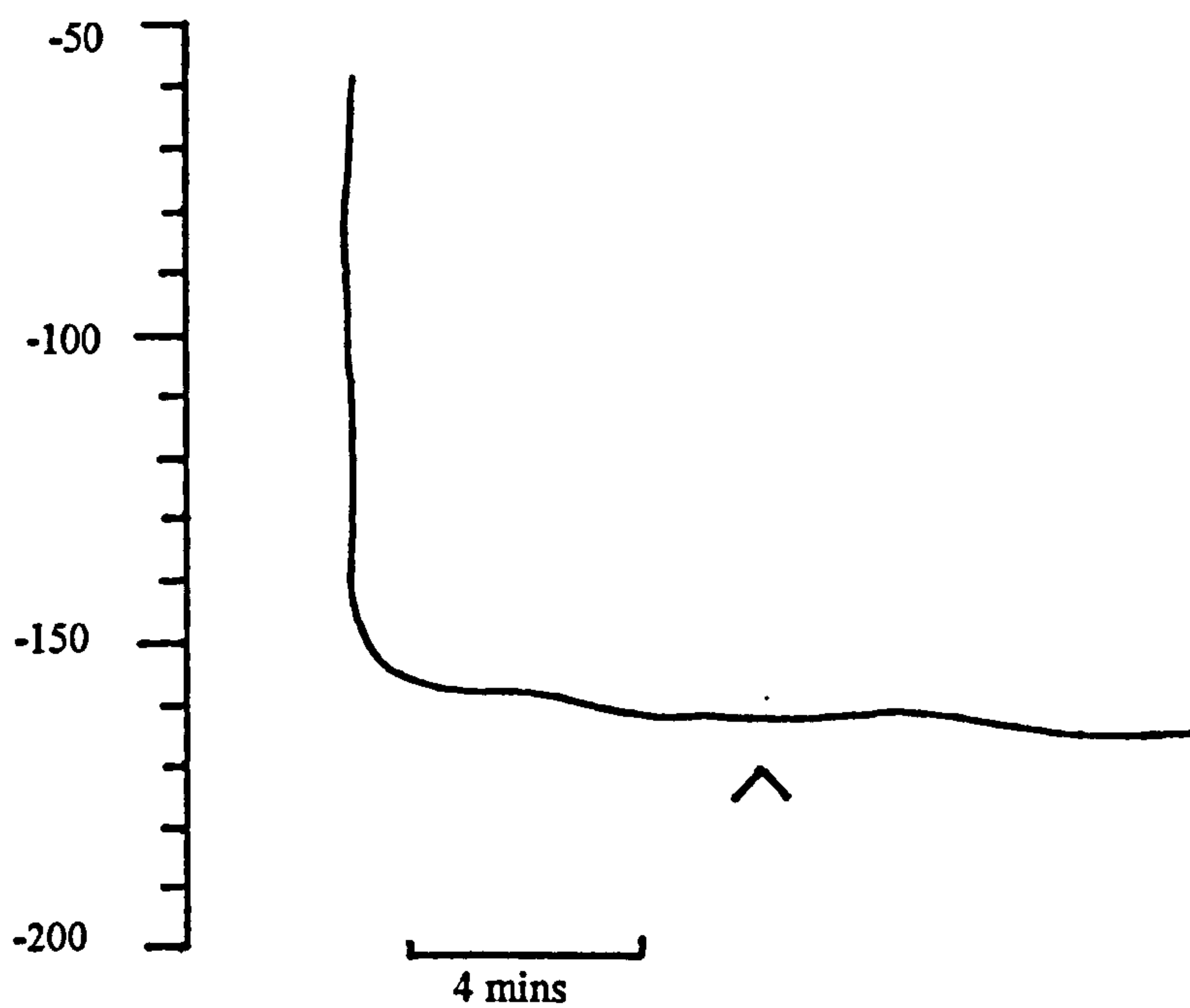


Fig. 4.5 Wild-type *P. patens* incubated in SRM. BAP (10  $\mu$ M) was added after 30 minutes steady membrane potential. No change in potential was observed for 20 minutes.





a) A slight depolarisation is observed.



b) No change in membrane potential is observed.

Fig. 4.6 The effect of DR-OPP ( $4\mu\text{g/ml}$ ) on the membrane potential of wild-type *P. patens*. Arrow indicates application.

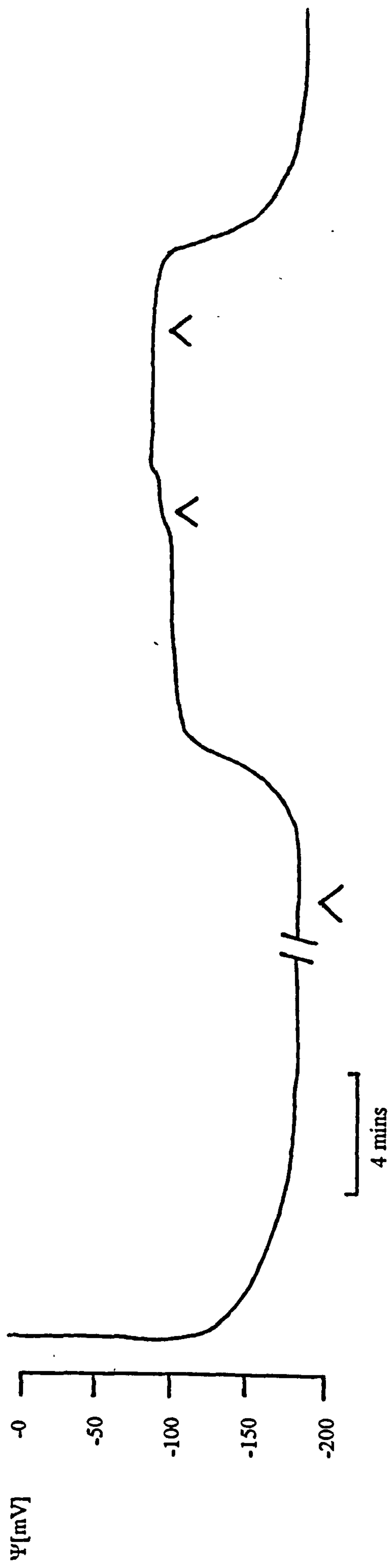


Fig. 4.7 Wild-type *P. patens* incubated in SRM. Caffeine (first arrow) caused depolarisation. SRM which included BAP ( $1\mu\text{M}$ ) (2nd arrow) inhibited recovery. After the removal of BAP from the SRM (third arrow) recovery began after 90 seconds.



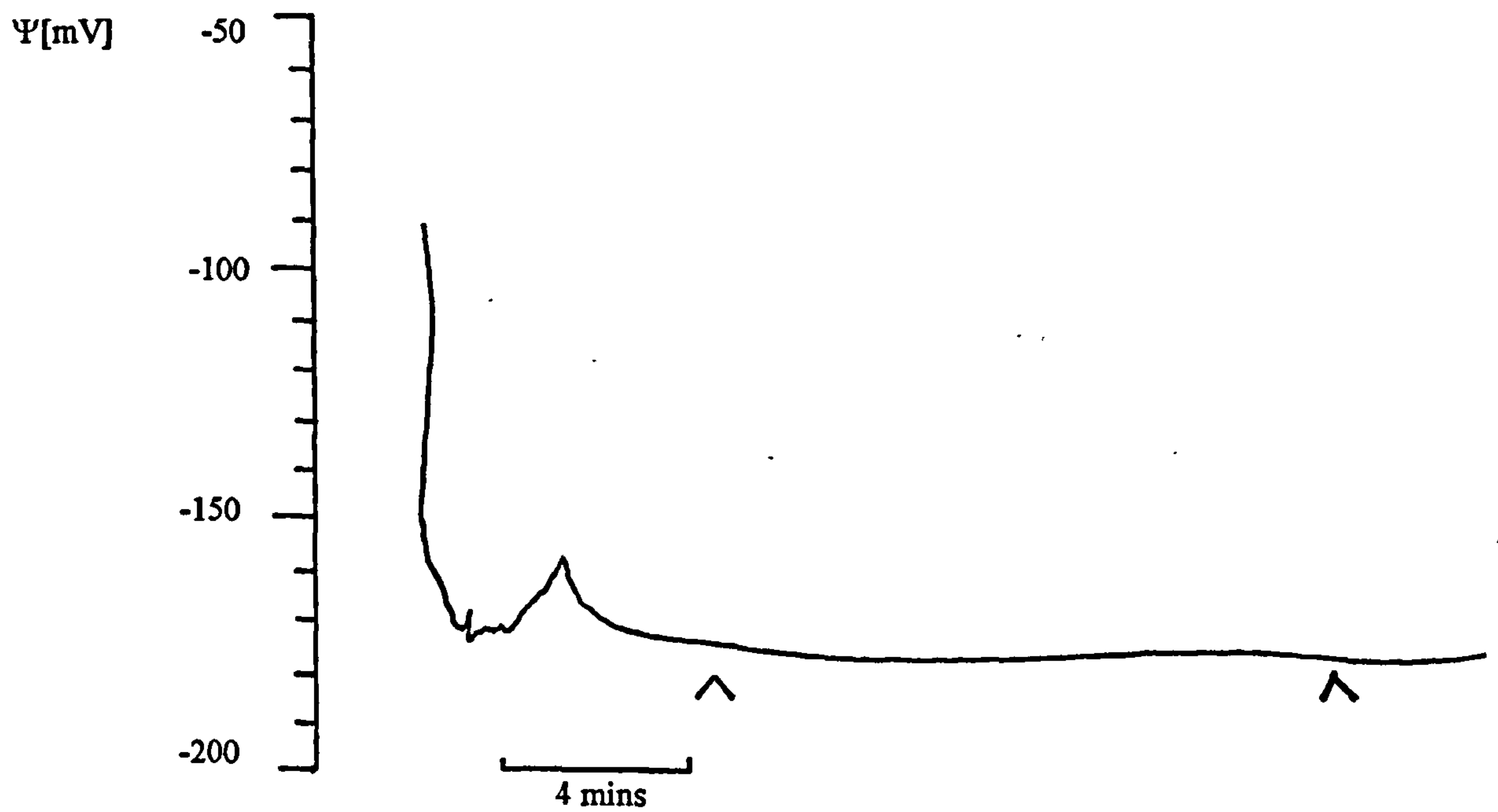


Fig. 4.8 The effect of BAP (5  $\mu$ M) (first arrow) and DR-OPP (4  $\mu$ g/ml) (second arrow) on the membrane potential of the mutant GAM710.

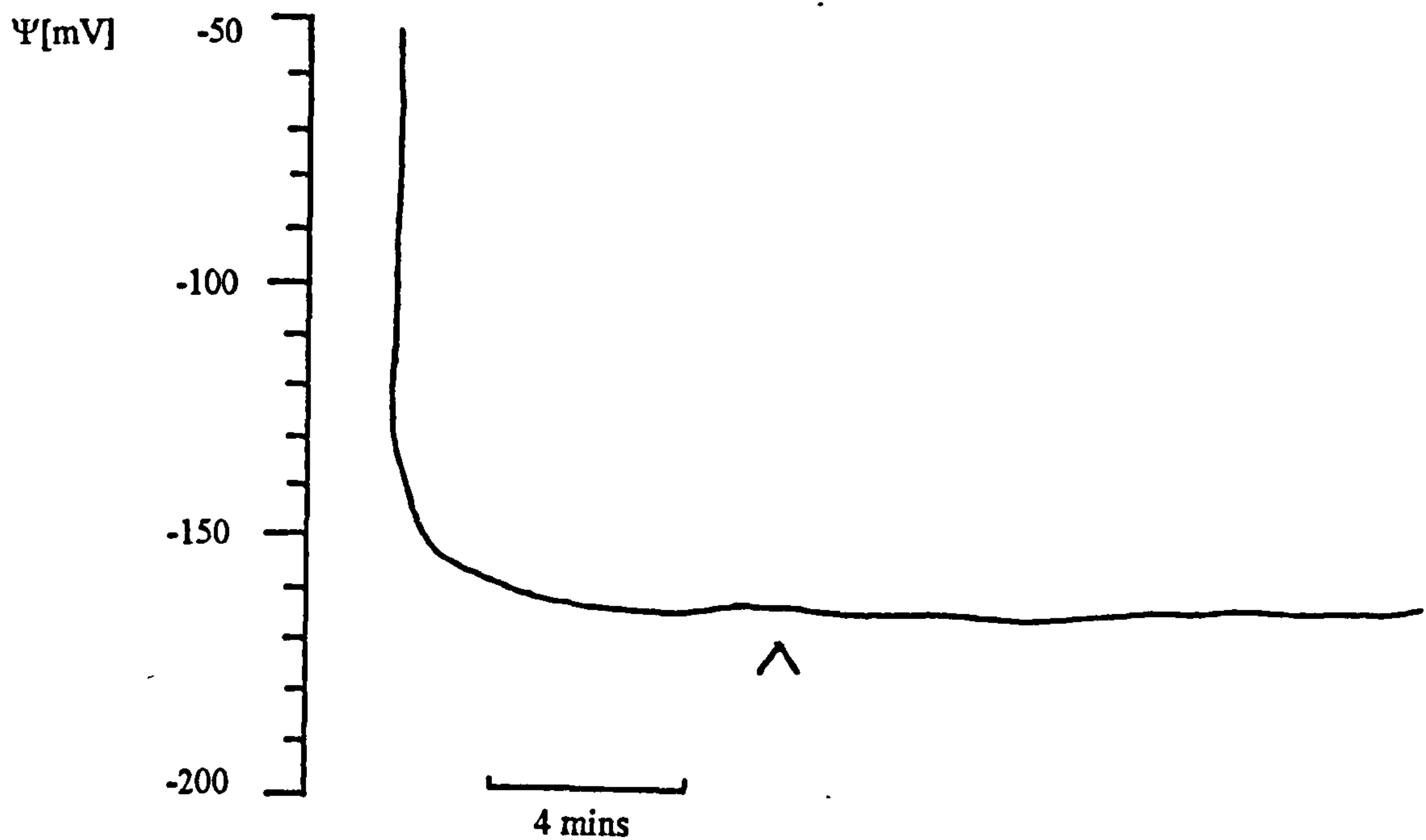


Fig. 4.9 The effect of BAP (5  $\mu$ M) on the membrane potential of the mutant NAR087. Arrow indicates application.

One interesting result was that the addition of 1 $\mu$ M BAP to SRM stopped the recovery of the potential from a depolarisation caused by caffeine (fig.4.5). There was a slight increase in the depolarisation, although this may have been coincidental. Once the perfusing medium was altered back to SRM without BAP, recovery began after 90 seconds.

None of the mutants tested showed any immediate response to BAP. However with all the mutants it was extremely difficult to obtain successful impalements. They grew more slowly than wild type moss, consequently the side-branches were more spreading and intrusive.

In order to translate the current measurements of Saunders (1986) into possible change in  $\Delta\Psi$ , it was necessary to obtain a figure for membrane resistance. A series of current/voltage readings (I/V curves) were taken for both *P. patens* and *F. hygrometrica* (H. Hohmeyer, unpublished data). These yielded the conductance figures quoted above. As conductance is the reciprocal of resistance, these also give figures for membrane resistance. As conventionally the current is described as positively charged and inwardly directed, an increase in current should lead to a depolarisation. Since the I/V relationship of *P. patens* and *F. hygrometrica* approximates to linearity, the degree of depolarisation can be estimated by Ohm's law:

$$\Delta V = \Delta I / \Delta g$$

in which  $\Delta I$  equals the theoretical change of membrane current due to cytokinin treatment and  $g$  the mean membrane conductance.

Saunders (1986) measured current at three points along the caulonemal subapical cell after the addition of cytokinin, the basal region, nuclear region and distal end. The smallest measurement was at the basal end of the cell. This still yielded a twofold increase in current, so that it can be assumed that the addition of cytokinin lead to at least a twofold increase in current along the length of the cell. Taking the basal measurement:



$$\Delta V = 0.52 - 0.25 / 4.9 \text{ } \mu\text{A}\cdot\text{cm}^{-2} / \mu\text{s}\cdot\text{cm}^{-2} = 50\text{mV (} F. \text{ hygrometrica)}$$

$$\text{or } \Delta V = 0.52 - 0.25 / 3.2 \text{ } \mu\text{A}\cdot\text{cm}^{-2} / \mu\text{s}\cdot\text{cm}^{-2} = 78\text{mV (} P. \text{ patens)}$$

This expected change is as much as occurs in light-evoked action potentials. Changes of these magnitudes should easily be recorded using standard electrophysiological techniques. Even taking the greatest measured conductance of  $10.5 \cdot 10^{-6} \text{ S cm}^{-2}$ , a depolarisation of 23 mV should be recorded. These results therefore represent a significant discrepancy with the data published by Saunders (1986).

It was found (H. hohmeyer, unpublished data) that during the taking of I/V curves, in four experiments with *F. hygrometrica* a depolarisation on treatment with 5  $\mu\text{M}$  6-BAP was recorded. However these were small (15-35 mV) and not maintained or increased. They occurred instantly, not after 5 minutes, or any delay that would suggest receptor operation. The corresponding I/V curves are inconclusive, two showing increase and two showing decrease of membrane conductance at the resting membrane potential (H. Hohmeyer, unpublished data).

Saunders (1992) reported that cytokinin induces an increase in  $\text{Ca}^{2+}$  influx at the cell surface from less than  $0.02 \text{ pmol}\cdot\text{cm}^{-2}\cdot\text{s}^{-1}$  to more than  $1.3 \text{ pmol}\cdot\text{cm}^{-2}\cdot\text{s}^{-1}$  at the developing bud site. This should result in a change in  $\Delta\Psi$  able to be recorded using standard electrophysiological techniques. First the calcium flux is converted into current using the Faraday constant  $F = 96489 \text{ A}\cdot\text{s}\cdot\text{mol}^{-1}$ :

$$(1.3 \cdot 10^{-12} - 0.02 \cdot 10^{-12}) \cdot 96489 \text{ mol A s/cm}^2 \cdot \text{s}\cdot\text{mol} = 1.235 \cdot 10^{-7} \text{ A cm}^{-2}$$

As above, Ohm's law in the form of  $\Delta V = \Delta I/g$  gives:

$$\Delta V = 1.235 \cdot 10^{-7} / 4.9 \cdot 10^{-6} \text{ A cm}^{-2} / \text{cm}^2 \cdot \text{s} = 25\text{mV (} F. \text{ hygrometrica)}$$

$$\Delta V = 1.235 \cdot 10^{-7} / 3.2 \cdot 10^{-6} \text{ A cm}^{-2} / \text{cm}^2 \cdot \text{s} = 38\text{mV (} P. \text{ patens)}$$

Saunders (1992) states that this accounts for half the inward current. So the measured depolarisation would in fact be double those figures. According to our calculations based on the previous measurements of inward current at the distal end of the cell (Saunders, 1986), it would account for between 1/3 and 1/4 of inward current after 5 minutes, only an 1/8th of current after 1 hour.

The results of this classical electrophysiological approach, therefore, do not give

any immediate indication that the action of cytokinin on existing side-branch initials or subapical cells affects ion fluxes in a voltage-dependent manner. The only result suggestive that ion fluxes are affected in some way is the inhibition of recovery from caffeine-induced depolarisation. This requires further investigation. The depolarisations that occurred during the taking of I/V curves (H. Hoymeyer, unpublished data) also render the results inconclusive.

If a consistent change in  $\Delta\Psi$  had been found, it would have been possible to explore its nature with inhibitors of calcium fluxes. As this was not the case, it was not possible to test the action of inhibitors of any type of ion or channel directly.

Many of Saunders' experiments were carried out on protonema grown in phosphate-free medium. As Markmann-Mulisch and Bopp (1987) point out, the response of *F. hygrometrica* to cytokinin is, under certain conditions, a two-phase response. When grown in medium containing no phosphate, subapical cells of *F. hygrometrica* do not divide to produce side-branch initials. The stimulation of side-branch initial production by cytokinin in the absence of phosphate is a different response to the stimulation of existing initials to develop into buds (see ch. I, 1.7). It is possible that these two responses represent two different modes of action of cytokinin. Unfortunately it was difficult to obtain a steady potential on protonema grown in phosphate-free medium. In the time available it was not possible to see if the addition of cytokinin in these conditions resulted in any changes of potential suggestive of calcium influx. These experiments therefore relate to the response of existing side-branch initials to cytokinin. Successful measurements of membrane potential were obtained for both filament sub-apical cells and side-branch initial cells. No difference to the response to cytokinin was found for either type of cell.

It is also impossible to test the effect of the absence of calcium on ion fluxes and currents, as this condition results in membrane depolarisation and therefore altered membrane permeabilities.

These results appear to rule out any large-scale immediate influx of calcium through voltage-sensitive channels. Small slow influxes of calcium would still result in



altered membrane permeabilities which should be picked up in I/V curves as consistent increases or decreases in conductance. Although changes were recorded, these were not consistent.

Recent developments in the field of patch clamping may make it possible to examine whether cytokinin has any effect on ion fluxes across the membrane, using isolated protoplasts. K. Schumacker (unpublished data) found an increase in  $^{45}\text{Ca}^{2+}$  flux into protoplasts of *P. patens* in response to the addition of cytokinin. This is contrary to the previous result of Akerman *et al* (1983), who found no effect of kinetin ( $10^{-6}\text{M}$ ) on  $^{45}\text{Ca}^{2+}$  influx into wheat protoplasts. The results of Parsons *et al* (1989) show that in studies on cytokinin and membrane transport, it is important to test inactive analogues of cytokinin to be sure that any response is linked to biological activity.

#### 4.3.2 Inhibitors

Two calcium channel inhibitors, nifedipine and verapamil, commonly used in studies of plants, were tested for their effects on growth, as well as their effects on cytokinin-induced budding. The calmodulin inhibitor trifluoperazine, was also tested.

The effects on growth of concentrations of nifedipine and lanthanum reported as being inhibitory to budding were recorded using time-lapse microscopy. The effects of the ionophore, A23187, were also filmed.

Table 4.2 examines the relationship between the number of buds per filament and the number of cells in the filament since the beginning of the treatment. The results of this experiment show that for each inhibitor, the highest concentrations used affected the growth of the filaments as well as the number of buds (figs. 4.10-13). In the case of nifedipine, a reduction of buds occurs concurrently with a reduction in growth. Verapamil affects growth before it affects the number of buds.

In animal cells these two inhibitors are specific for L-type channels at submicromolar concentrations. In plants it is generally necessary to use

Table 4.2    The effect of three calcium channel inhibitors on cytokinin-induced bud-  
production and apical cell growth.

Treatment		Buds per filament (n=30)	Cells since reorientation
6-BAP	1μM	2.4	4.7
Nifedipine	10μM	2.0	5.6
+ 1μM BAP	20μM	1.9	4.0
	30μM	1.1	5.1
	40μM	0	2.0
Verapamil	1μM	1.8	5.4
+ 1μM BAP	10μM	1.2	3.8
	30μM	1.6	3.3
Trifluoperazine	1μM	2.1	6.2
+ 1μM BAP	10μM	1.0	4.5
	20μM	0.7	3.8



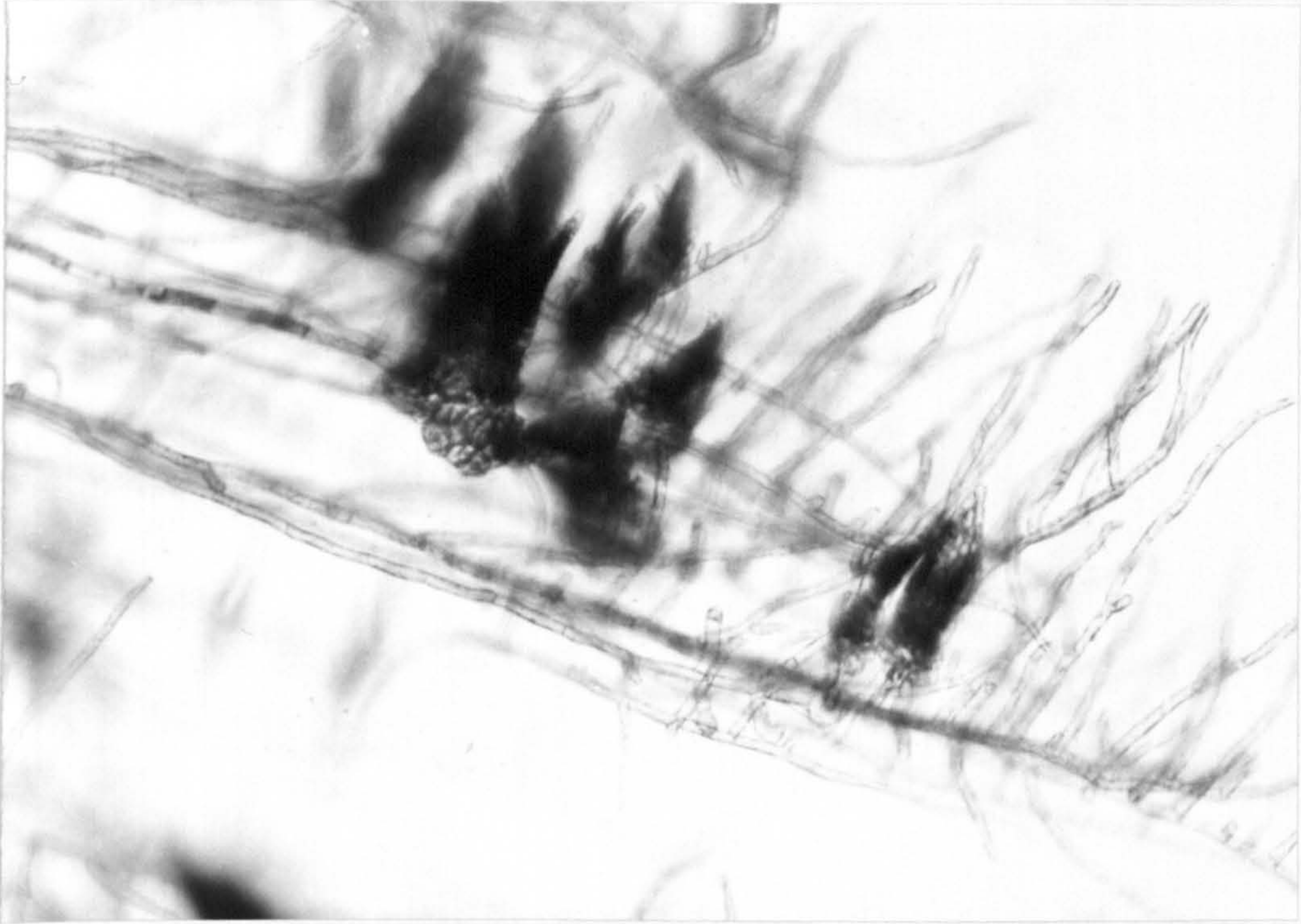


Fig. 4.10 The addition of BAP (100nM) to *P. patens*.  
Every side-branch initial at the time of application has become a gametophore.  
Subsequent subapical cells do not produce initials.

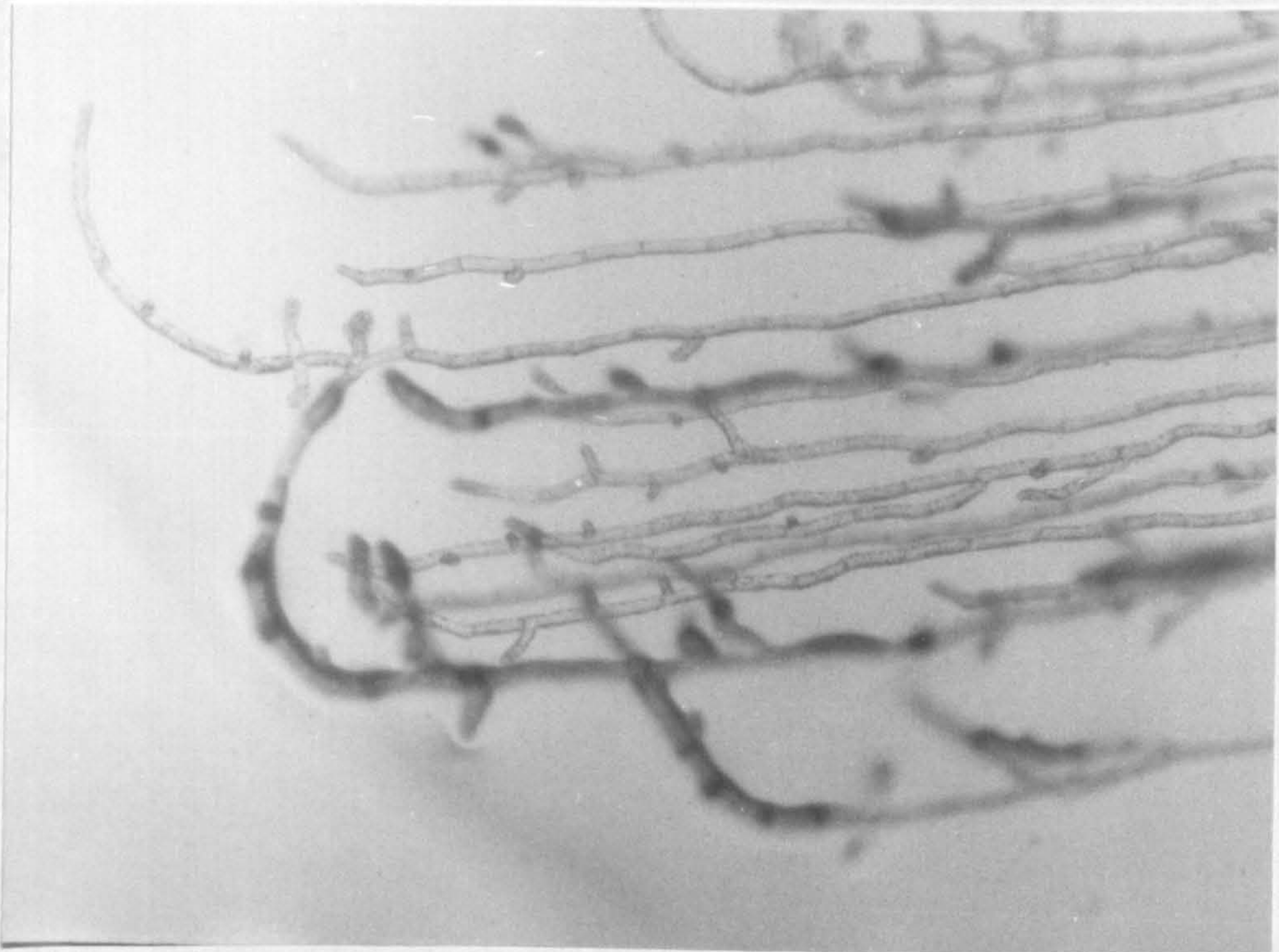
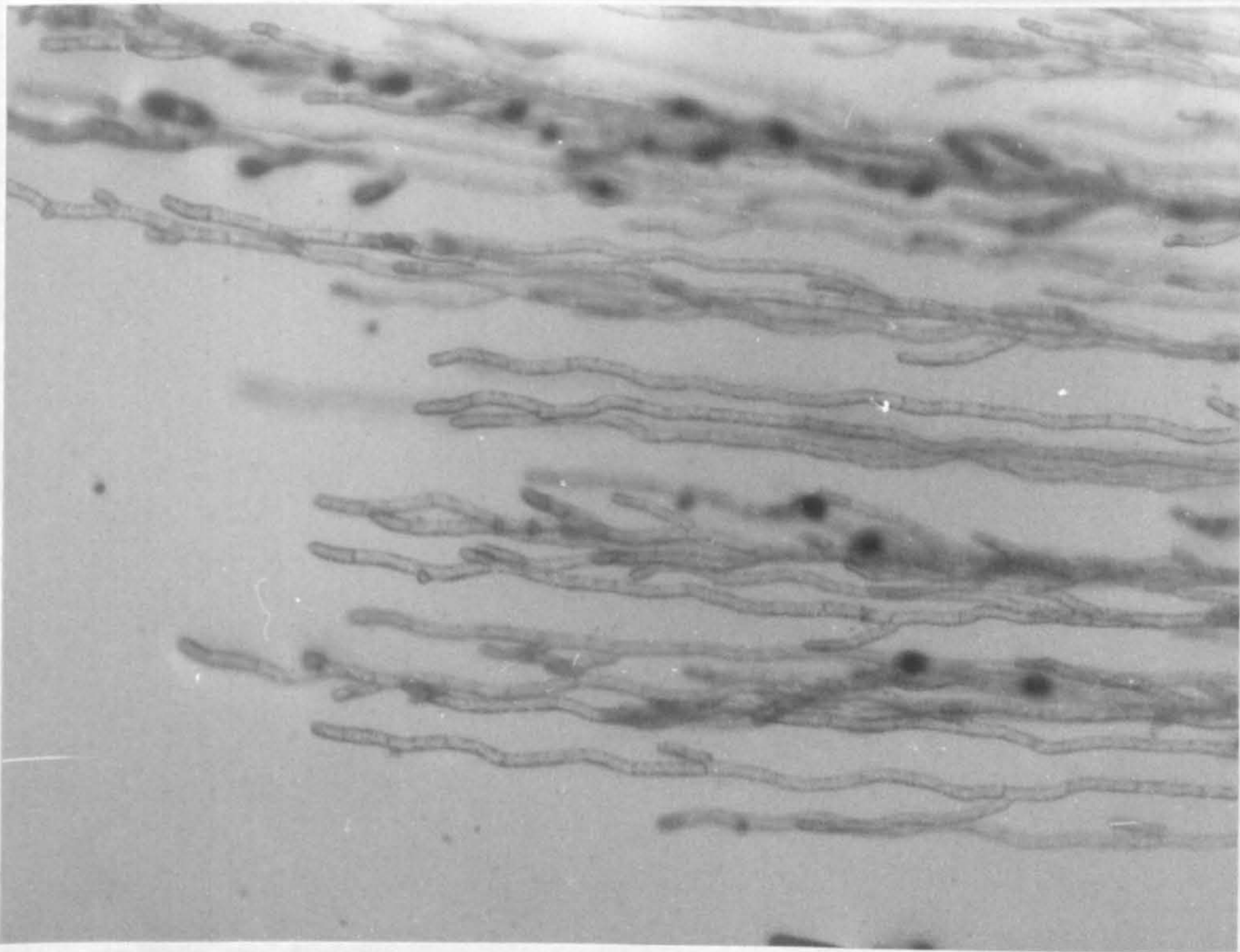


Fig. 4.11 The addition of verapamil (30μM) and BAP (1μM) to *P. patens*.  
Many filaments have stopped growing. Some side-branch initials still give rise to buds.





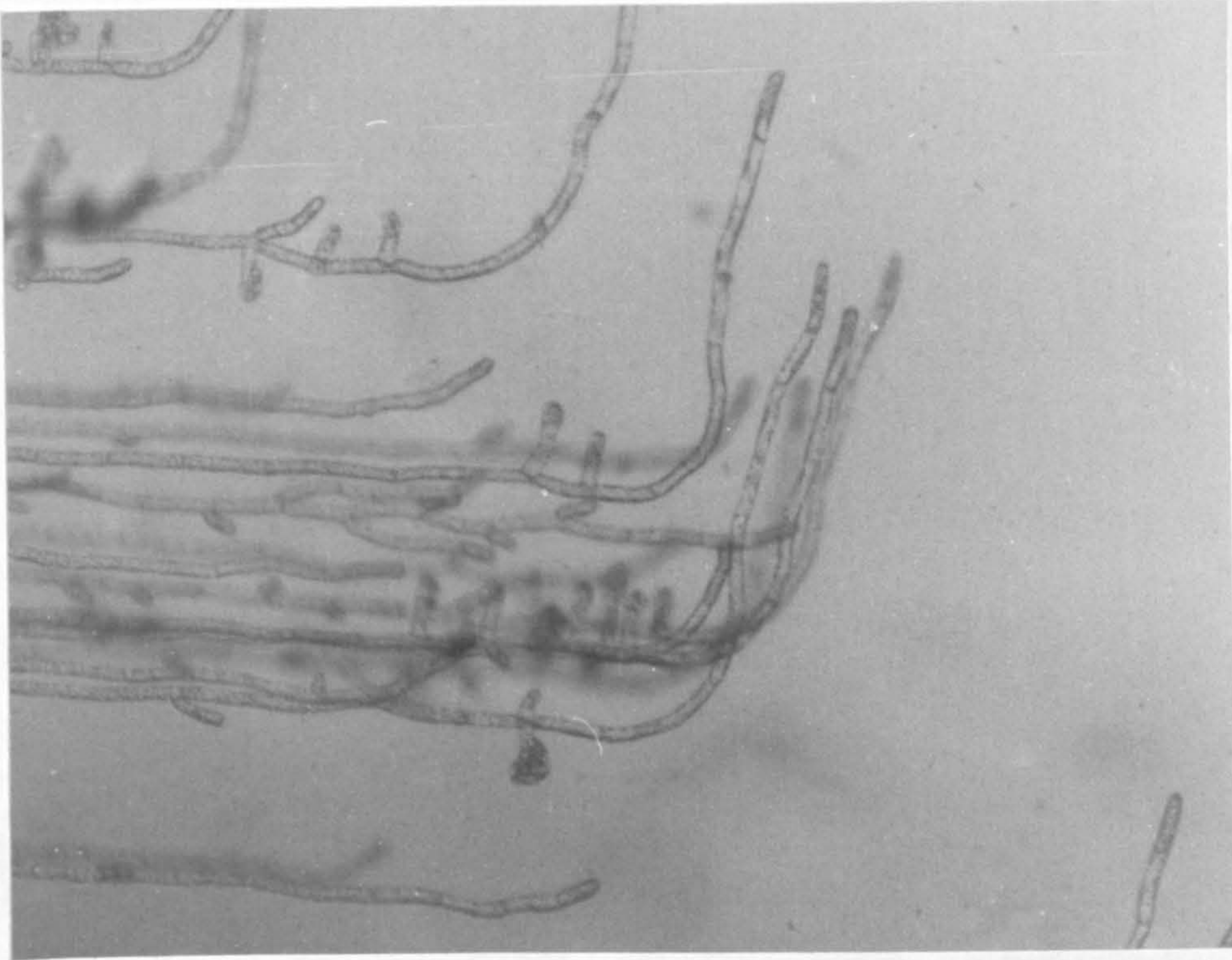
a) 20 $\mu$ M nifedipine



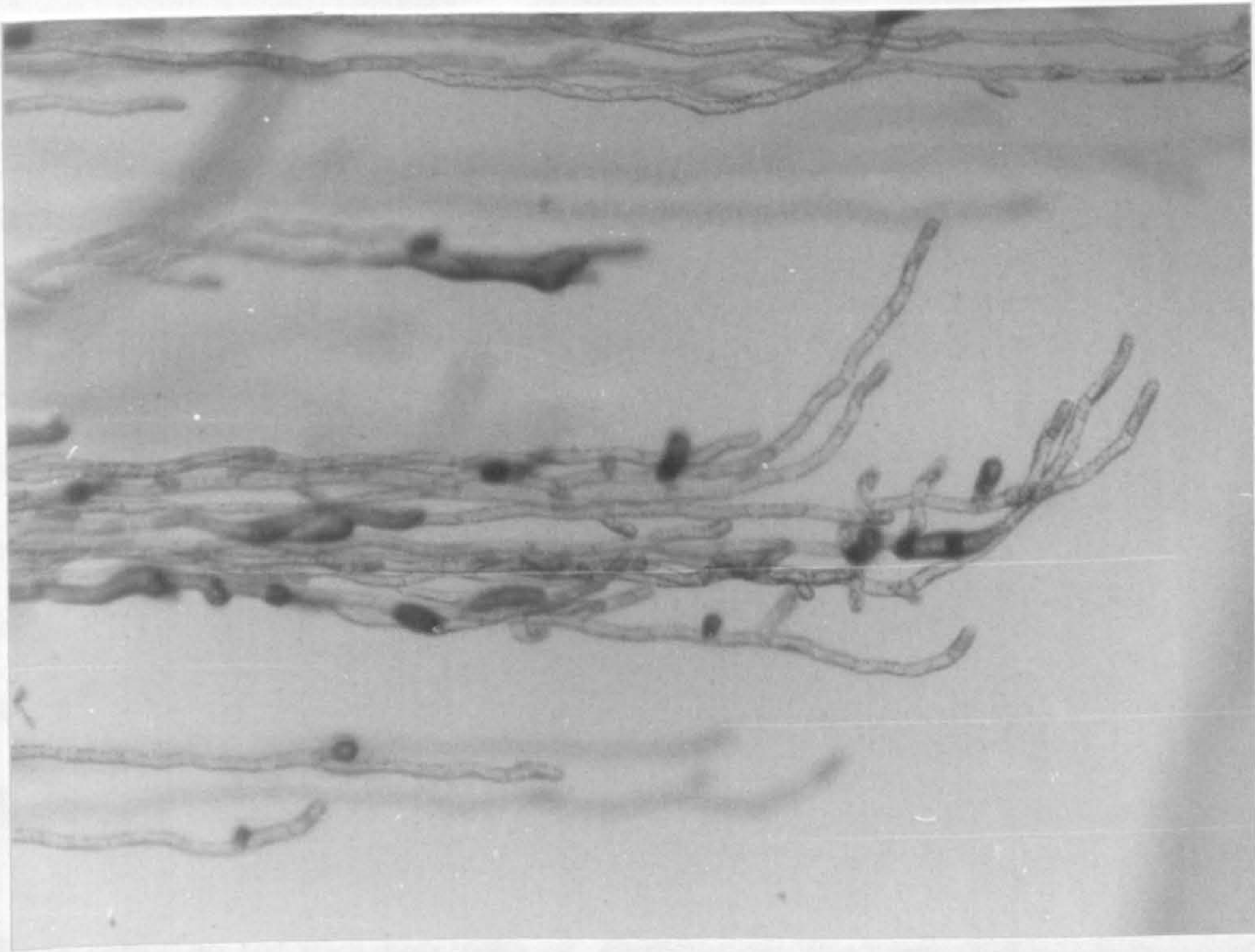
b) 40 $\mu$ M nifedipine

Fig. 4.12 The effect of nifedipine on apical cell growth and cytokinin-induced bud production in *P. patens*.





a) 10 $\mu$ M Trifluoperazine



b) 20 $\mu$ M Trifluoperazine

Fig. 4.13 The effect of trifluoperazine on apical cell growth and cytokinin-induced bud production in *P. patens*.



concentrations of one or two orders of magnitude higher to achieve an inhibitory effect. Non-specific effects of these compounds at the concentrations found to be inhibitory have been reported for several plant species (Foisner, 1990; Grotha, 1986). Wacker and Schnepf (1990) looked at the effects of nifedipine and verapamil on tip growth in *F. hygrometrica*, and reported a range of effects, which included slowing of growth, tip swelling and apical wall thickenings. The formation of callose, considered to be a calcium-dependent process in soybean suspension cells (Kauss, 1987), was found in response to incubation of the liverwort *Riella* in verapamil (Grotha, 1986).

These factors make it difficult to establish whether an inhibitory effect of nifedipine or verapamil on cytokinin-induced budding is an effect on a calcium-transport process such as L-type channels, as suggested by Ranjeva *et al* (1992), or an effect on general calcium-dependent growth, or some other toxic effect.

Fig. 4.14 shows the effect of 100 $\mu$ M nifedipine on a caulonema filament of *P. patens*. Over a period of 6 hours the growth rate slows to 4 $\mu$ m/h. During this time, the tip swells, and the apical cell polarity is lost. Surprisingly, the initial that appears on this cell develops into a bud (fig.4.14-8). The previous cell reacted to the loss of apical dominance and formed a leading caulonema filament. Both these characteristics may also occur in response to A23187 (see below) and light, and are therefore suggestive of an increase in intracellular calcium. It is possible that at this concentration nifedipine causes membrane perturbations that lead to an influx of calcium, rather than inhibition of calcium entry. It is interesting that in this case, apical growth ceases during mitosis, and the tip swells at this time.

A similar physiological response to nifedipine at a concentration of 100 $\mu$ M has been reported for root-hair cells of *Arabidopsis thaliana* (Schiefelbein *et al*, 1992). The tips of the root hairs swelled, and growth stopped. This was put down to an inhibition of calcium entry through plasma-membrane Ca<sup>2+</sup>-channels. The results of this thesis suggest this may be a toxic affect of nifedipine at this concentration.



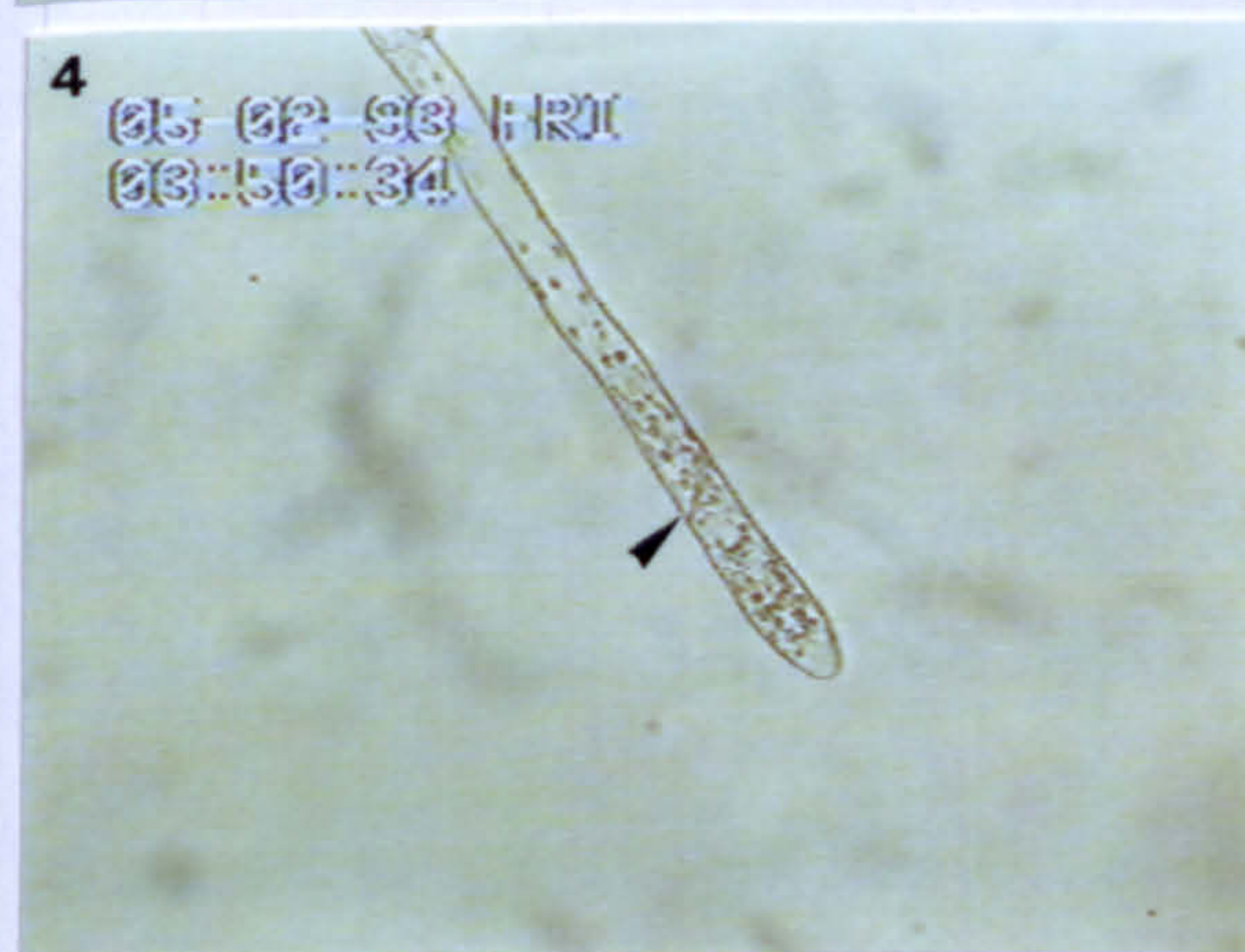
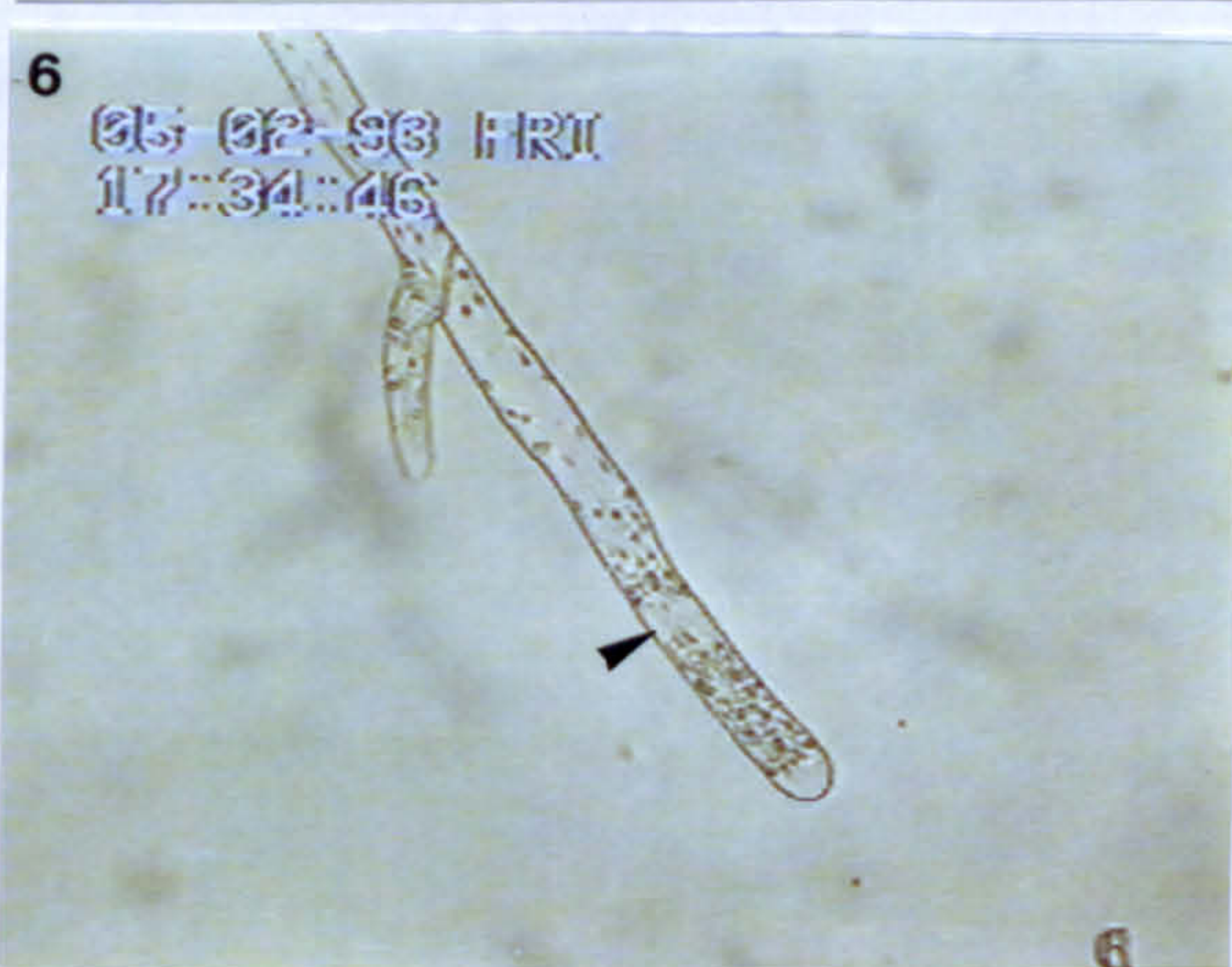
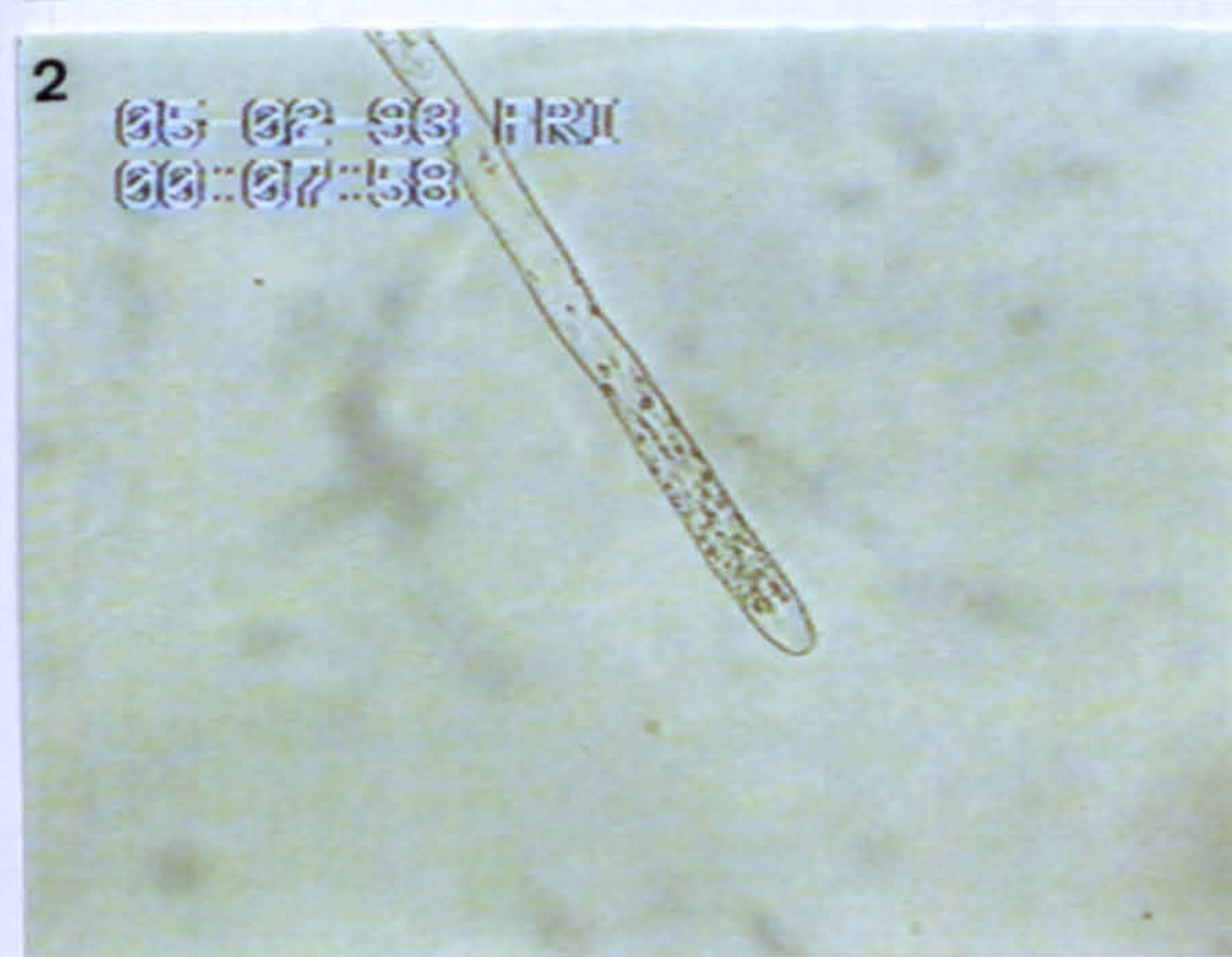
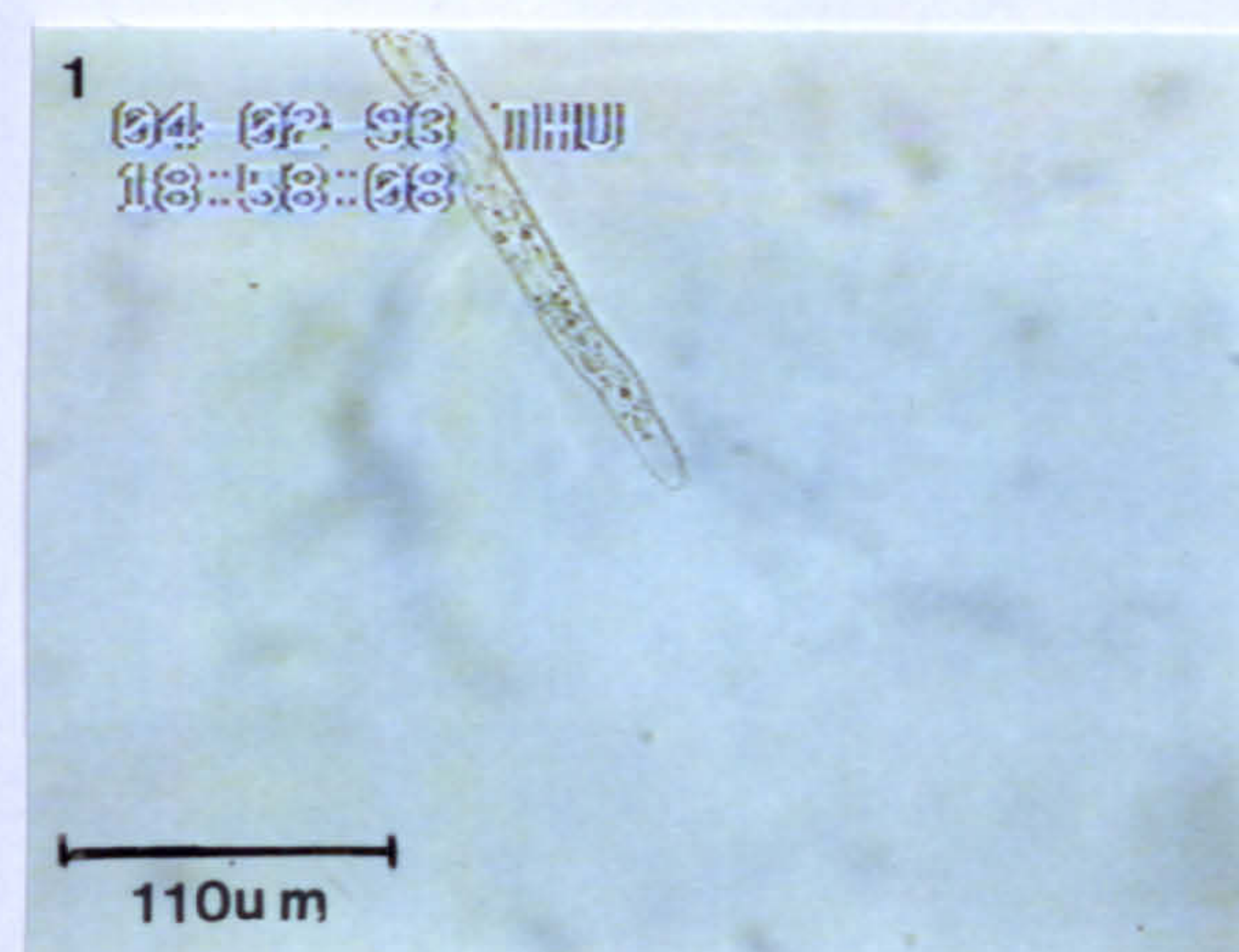
**Fig. 4.14 The effect of Nifedipine (100 $\mu$ M) on tip growth.**

Filming began at ca. 18.30h on 4.2.93. Nifedipine was added at the start of filming.

- 1-2 Over the first 6 hours, the apical cell slows its growth rate, and swells.
- 3 7 hours after the start of filming, the apical cell divides (arrow). During cell division the apex of the apical cell swells further, and growth stops.
- 4 Despite the slowing of growth, the oblique cell wall is not affected (arrow). 2 hours after mitosis, the apex of the apical cell has recovered somewhat, and growth has resumed.
- 5 Ca. 6.5 hours after mitosis, a side-branch initial is produced that takes over caulonemal growth from the tip cell (6). The growth of this side branch is not affected in the same manner as the apical cell.
- 6 16 hours after the first division, a second cell division occurs (arrow). The apex of the apical cell again swells and growth stops. The cell cycle time has lengthened as though to take into account the reduced growth rate.
- 7-8 A side-branch initial is produced which becomes a bud. Each cell produces two side-branches.

Nifedipine at this concentration has complex effects on growth, but does not inhibit either bud formation or side-branches.







The result shown in fig 4.14 of the effect of nifedipine differs from the result of the experiment shown in table 4.2. There are two possible reasons for this: the experiments of table 4.2 were performed at light levels of below  $100 \text{ mWm}^{-2}\text{s}^{-1}$ . Also, the concentration of inhibitor was added to cultures growing in agar at a concentration of a factor of 10 higher than the stated concentration to allow for the amount of agar in the petri dish. Both these factors could affect the outcome of the experiment.

The results of experiments with lanthanum confirm the conclusions of Markmann-Mulisch and Bopp (1987), that the high concentrations of lanthanum necessary to inhibit bud formation ( $10^{-4}$  to  $10^{-3}$ ) cause damage to growth by external calcium deprivation. It was found in this study that  $\text{LaCl}_3$  did not inhibit cytokinin-induced budding below concentrations of  $500\mu\text{M}$ .

Fig. 4.15 shows the effect of  $500\mu\text{M}$   $\text{LaCl}_3$  and  $1\mu\text{M}$  BAP on the growth of a caulonema filament. The immediate effect is a reduction in the growth rate of about half to  $15\mu\text{m}$  in the first hour after application. It will be recalled (see ch. 2) that  $1\mu\text{M}$  BAP alone has no immediate effect on the growth rate of caulonema apical cells. The filament then stops growing entirely for 13 hours. Growth resumes, but at the reduced rate of  $9\mu\text{m/h}$ . Three hours after the resumption of growth a cell division occurs with a strongly oblique cell wall, despite the reduced growth rate. After a further 16 hours, the filament again stops growing almost entirely (maximum growth rate:  $1\mu\text{m/h}$ ). The side-branches also ceased growth at the same time as the main filament. When they resumed growth, they did not develop into buds, but continued to grow as chloronema.

At concentrations of  $\text{LaCl}_3$  of  $100\mu\text{M}$  and less, the addition of  $1\mu\text{M}$  BAP resulted in bud formation. The effect on growth of  $100\mu\text{M}$   $\text{LaCl}_3$  alone was investigated. Fig. 4.16 illustrates the effect of this concentration of  $\text{LaCl}_3$  caulonemal growth, and side

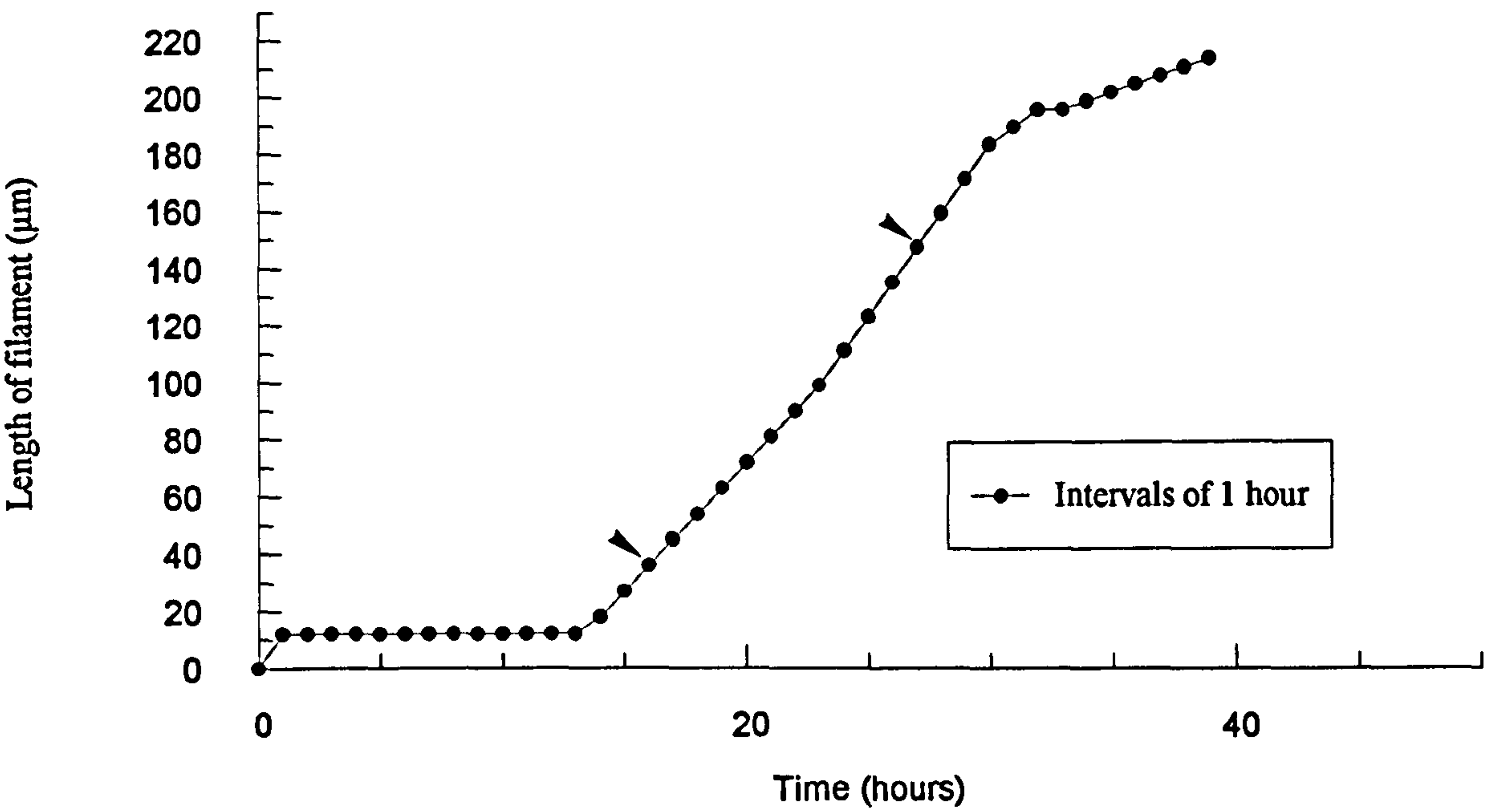


Fig. 4.15 The effect on caulonemal growth of adding 500μM LaCl and 1μM BAP at time 0 hours. Arrows indicate cell divisions.



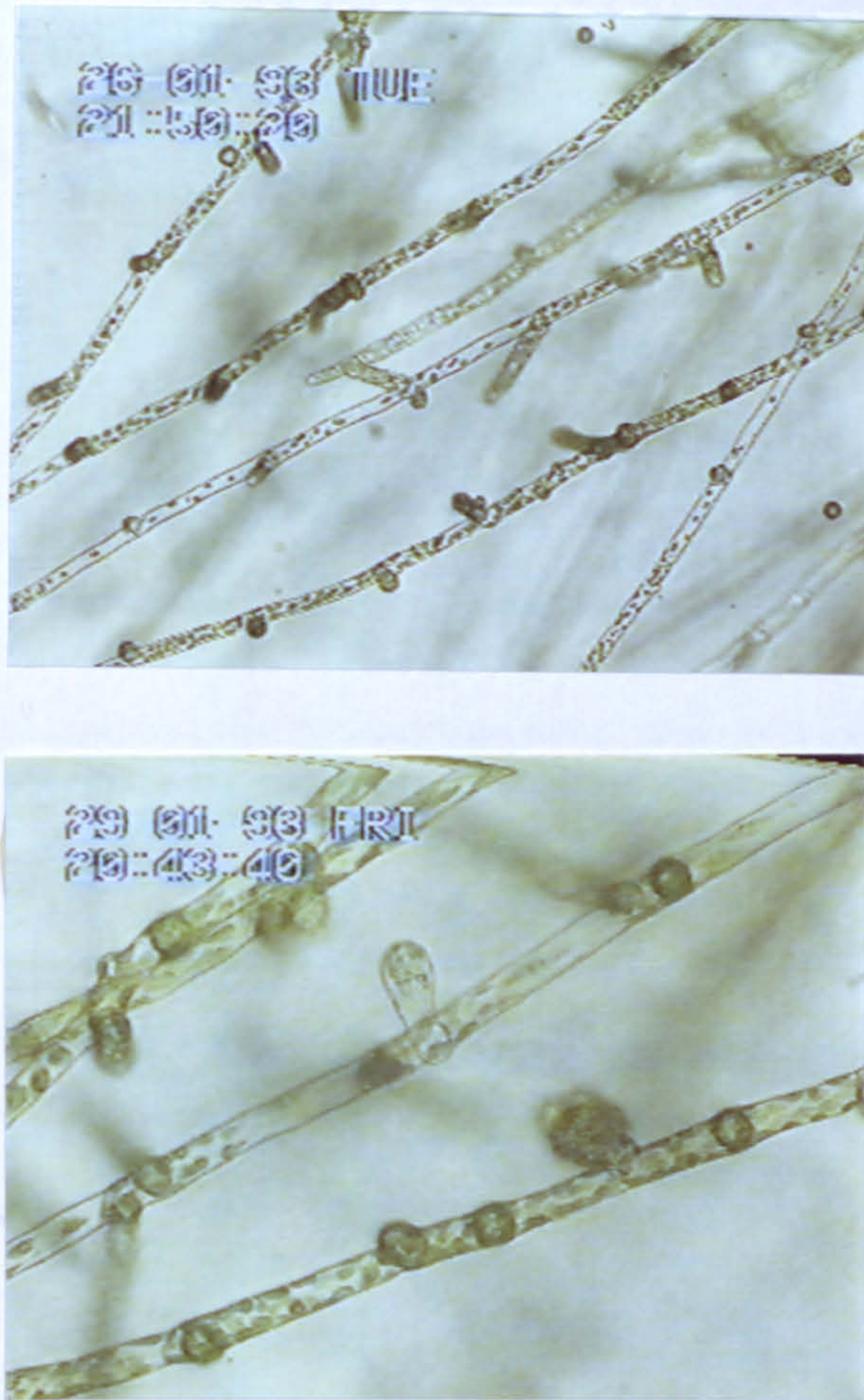


Fig. 4.16 The effect of  $100\mu\text{M}$   $\text{LaCl}_3$  on tip growth.

The growth of side-branches is more severely affected than the growth of apical cells. Subapical cell division is not inhibited. The formation of natural buds is not entirely inhibited.



branch production. The growth of the main caulonema filaments is initially unaffected. Approximately 9 hours after application, the growth rate begins to slow gradually, to ca. 18 $\mu$ m/h. The effect of lanthanum on the formation of side-branches was more severe. Many side branches did not develop beyond the one cell stage. Those that did grew very slowly, and remained chloronemal. The formation of natural buds was not inhibited by lanthanum at this concentration (fig. 4.16-3), but their development did not follow the normal pattern.

Fig. 4.17 shows the effect of 80 $\mu$ M LaCl<sub>3</sub> on a developing bud initial. At the start of filming, the bud is at the 7th subapical position, shortly before the first cell division. Instead of the oblique division characteristic of a natural bud, the plane of division is altered so that the cell wall runs across the initial. The second cell division is at right angles to the first. A further cell division parallels the first. There is no apparent stalk or rhizoid cell (fig. 4.17-3). However, although this pattern of cell division is very different from that seen in an untreated bud, subsequent development does result in the formation of a leafy gametophore. The growth of rhizoids, when they appear, does not appear to be affected by this concentration of lanthanum in the same way as filamentous side-branches.

The most sensitive cells to inhibition by lanthanum appear to be the side-branch initials. The inhibition of cytokinin-induced budding requires a higher concentration of lanthanum than the concentration needed to retard the growth of side-branch initials, but at concentrations that retard growth, natural budding is not inhibited. It is therefore difficult to conclude that the inhibition of cytokinin-induced budding by high concentrations of LaCl<sub>3</sub> is an effect of the a direct effect on a cytokinin-induced calcium influx, but may instead be due to a non-specific inhibition of growth.

The ionophore A23187 (Reed and Lardy, 1992) was added to cultures of wild-type *P. patens* and several mutant strains (fig. 4.18-22). The same concentrations of ionophore had differing effects on the mutants. At concentrations of 10-50 $\mu$ M wild-type caulonema filaments reacted by a slowing of growth and tip swelling. The effect

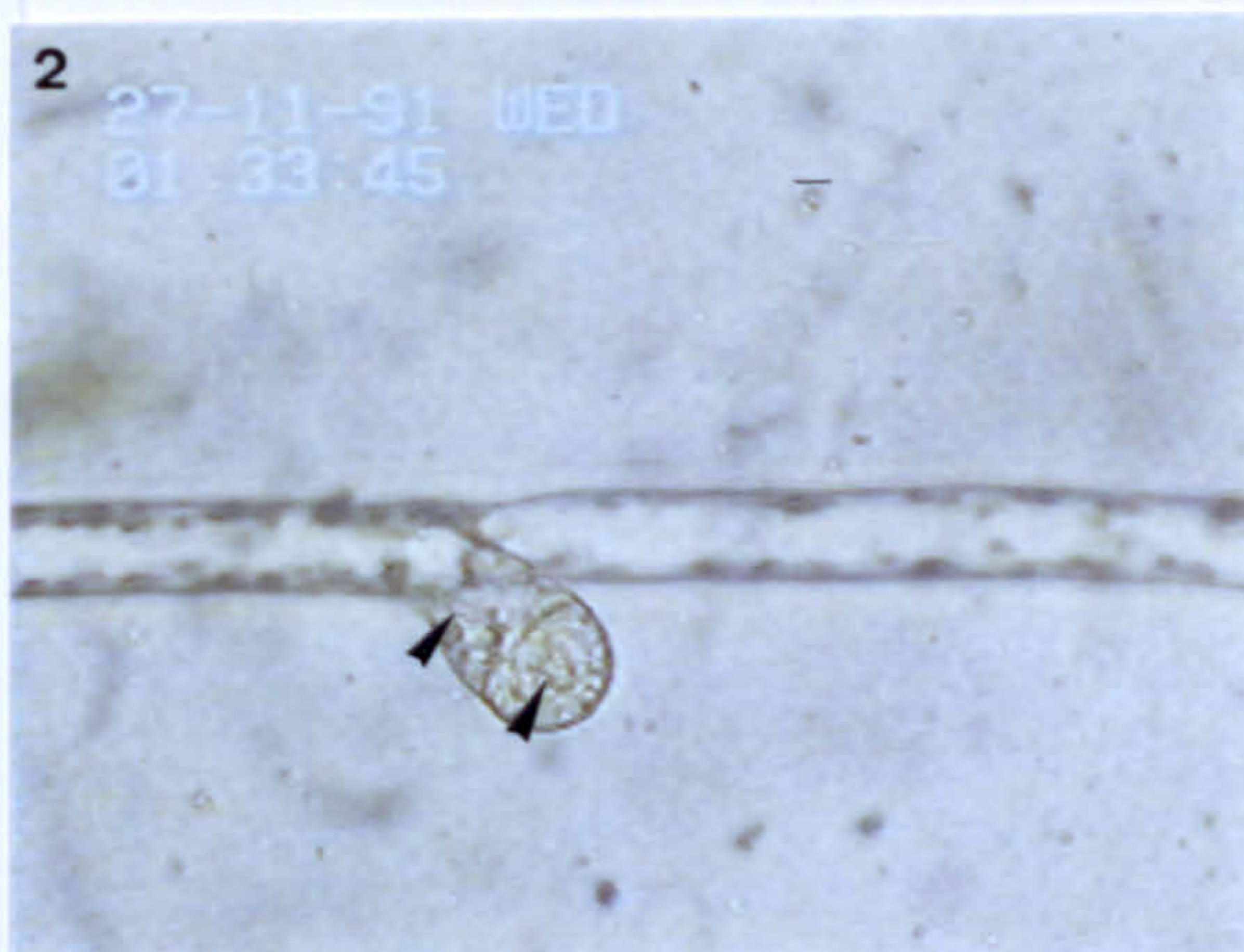


**Fig. 4.17** The effect of 80 $\mu$ M LaCl<sub>3</sub> on the early cell divisions of bud formation.

Filming began ca. 17.00h on 26.11.91.

- 1** 17.50 - the first cell division (arrow) is occurring transverse to the axis of growth of the developing bud rather than oblique.
- 2** The second cell division (arrows) has occurred at ca. 22.00h and is transverse to the first.
- 3** 16.5 hours after the first cell division. An abnormal pattern of transverse cell divisions has occurred. Arrows indicate the cell walls.
- 4** Ca. 31 hours after the start of filming. Despite the early abnormal pattern of divisions, the lower cells are giving rise to rhizoids and the upper cells give rise to leaf initials (arrowed).







was more marked with increasing concentration. The gam mutants *bar-1*, *nar-87*, and *bar-576* reacted strongly to the ionophore (figs. 4.19-22). The gam mutant *gam-710*, although cytokinin sensitive, reacted to a high concentration of ionophore only by a slowing of growth. There was no marked tip swelling, in this mutant. However, when BAP (1 $\mu$ M) was added in conjunction with the ionophore, this mutant responded in the same manner as the wild-type (fig. 4.22). This experiment needs to be repeated before conclusions can be drawn, but, as with the experiment with caffeine (fig. 4.7), BAP appeared to enhance the effect of an agent that causes calcium influx into cells.

These experiments suggest the possibility that some of these mutant strains are calcium channel mutants, or mutant in their response to increased intracellular concentrations of calcium. This will be further discussed in ch. VI.

In the wild-type moss, in some cases, from three to five days after the addition of the ionophore, a ring of buds was noticeable around the cultures, at approximately the position on filaments where the ionophore was added (fig. 4.18). The introduction of light to cultures grown in the dark can have a similar effect. The sudden introduction of light results in an action potential. Studies in York suggest that the first phase of depolarisation of the action potential is brought about by an influx of calcium.

It appears that agents that cause a sustained rise in calcium, such as A23187, can induce buds in filaments that are competent to produce a bud. However, this effect occurs over a period of 2 to 5 days, and affects a minority of side-branch initials. The effect appears to be on the caulonema subapical cell which produces the initial, rather than on the initial itself.

Where similar effects to that induced by A23187 occur in response to other agents, such as light or nifedipine, this is suggestive of a rise in intracellular calcium.

These experiments show that the results of experiments using high concentrations of inhibitors on the moss protonemal system need to be interpreted with caution. Different conditions of growth may lead to different results. High concentrations of



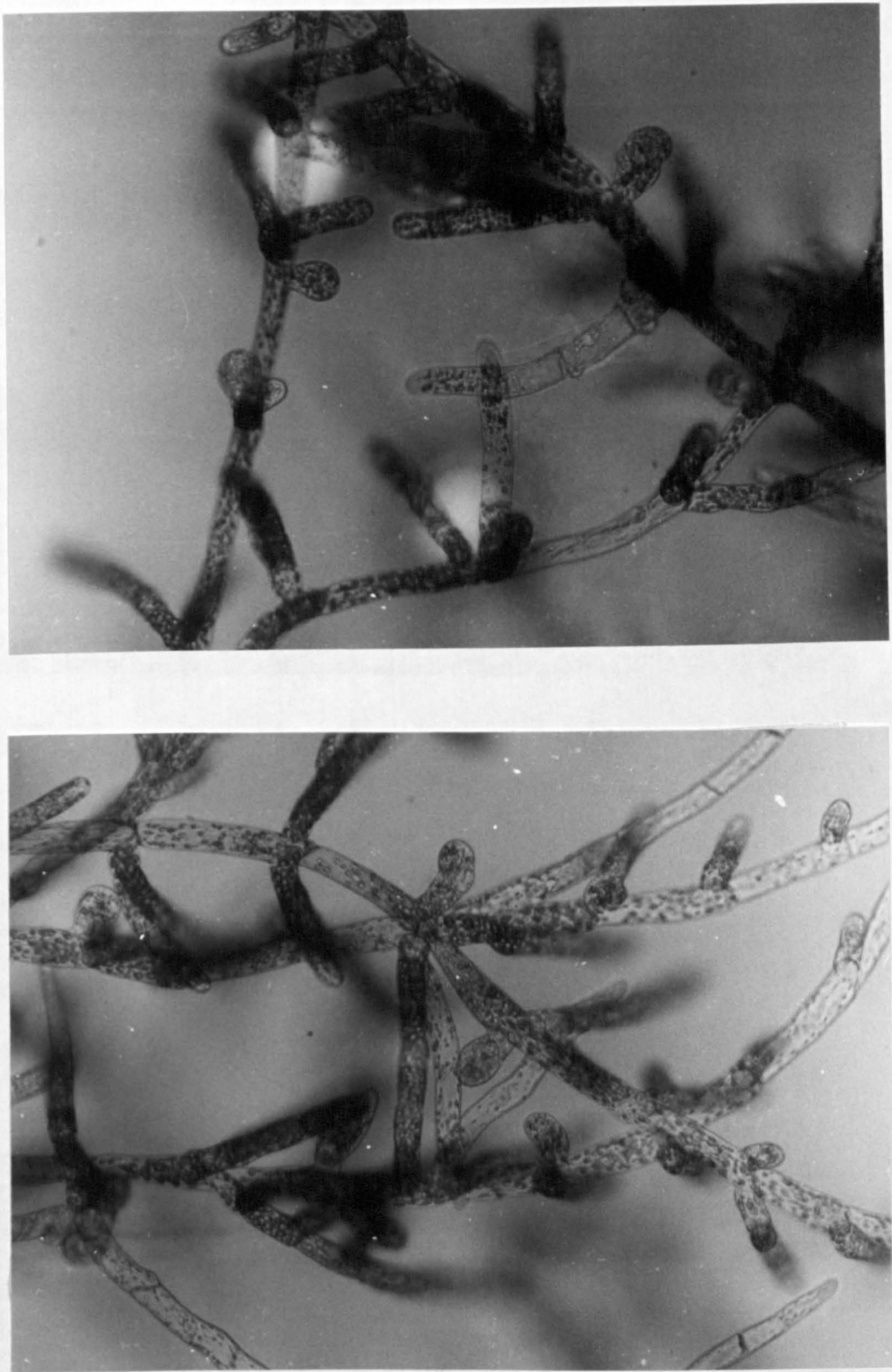


Fig. 4.18 The effect of A23187 (50 $\mu$ M) added to cultures of wild-type *P. patens*. After a 4 day treatment with the ionophore, many side-branch initials have been induced to become buds.



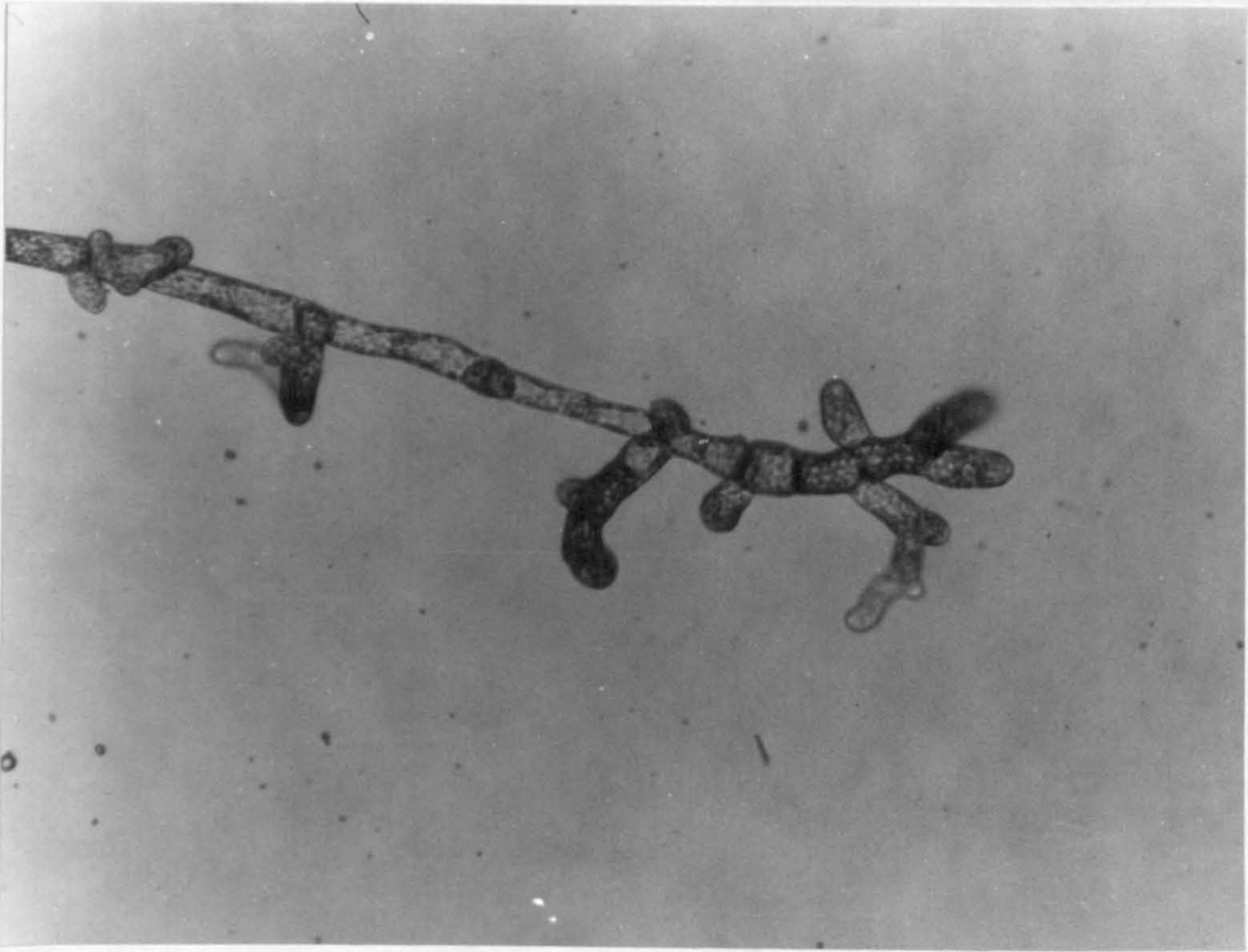


Fig. 4.19 The mutant strain BAR001 treated for 5 days with A23187 (40 $\mu$ M).



Fig. 4.20 The mutant strain BAR576 treated for 5 days with A23187 (40 $\mu$ ).



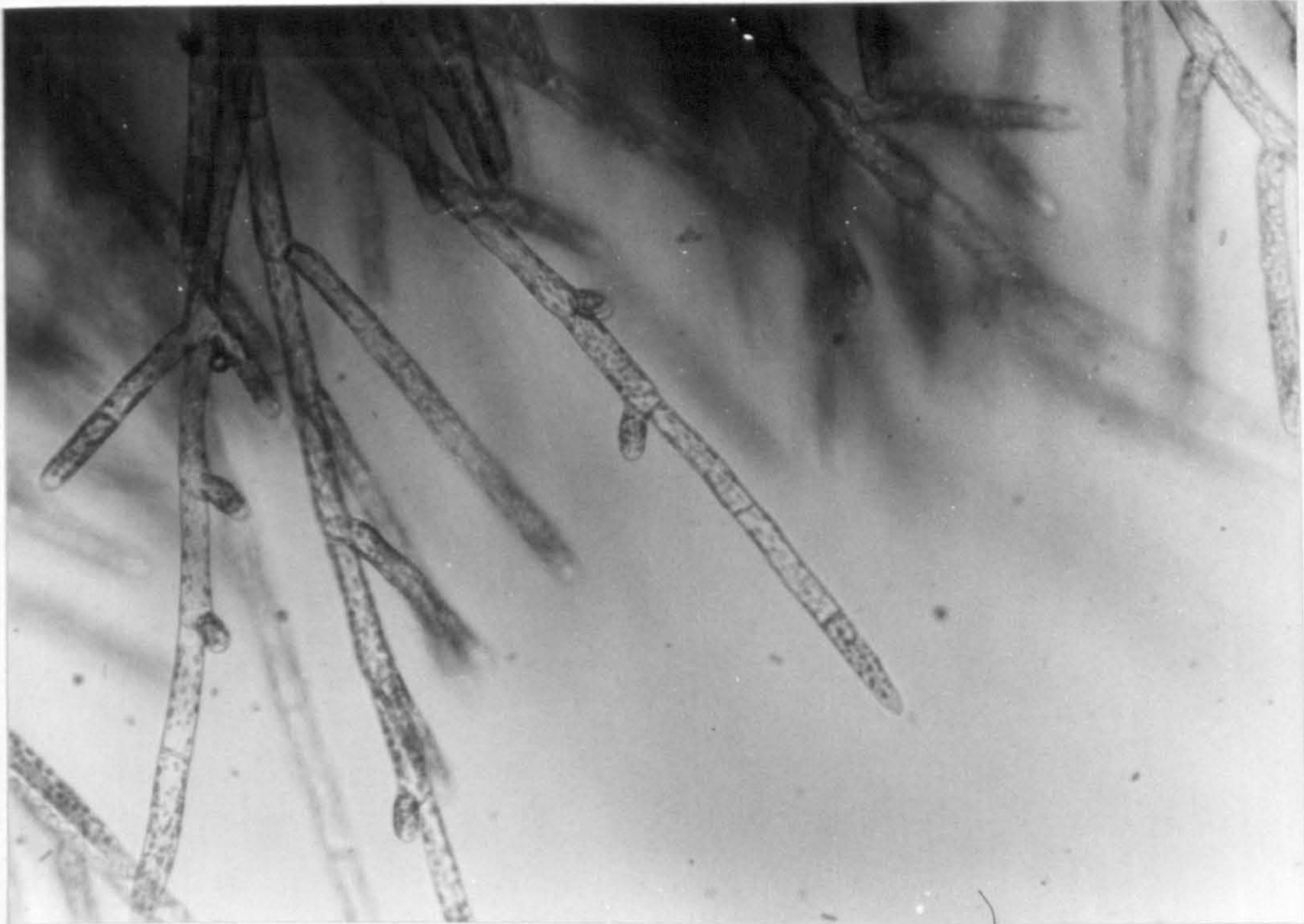


Fig. 4.21 The mutant strain GAM710 treated for 5 days with A23187 (40 $\mu$ M).

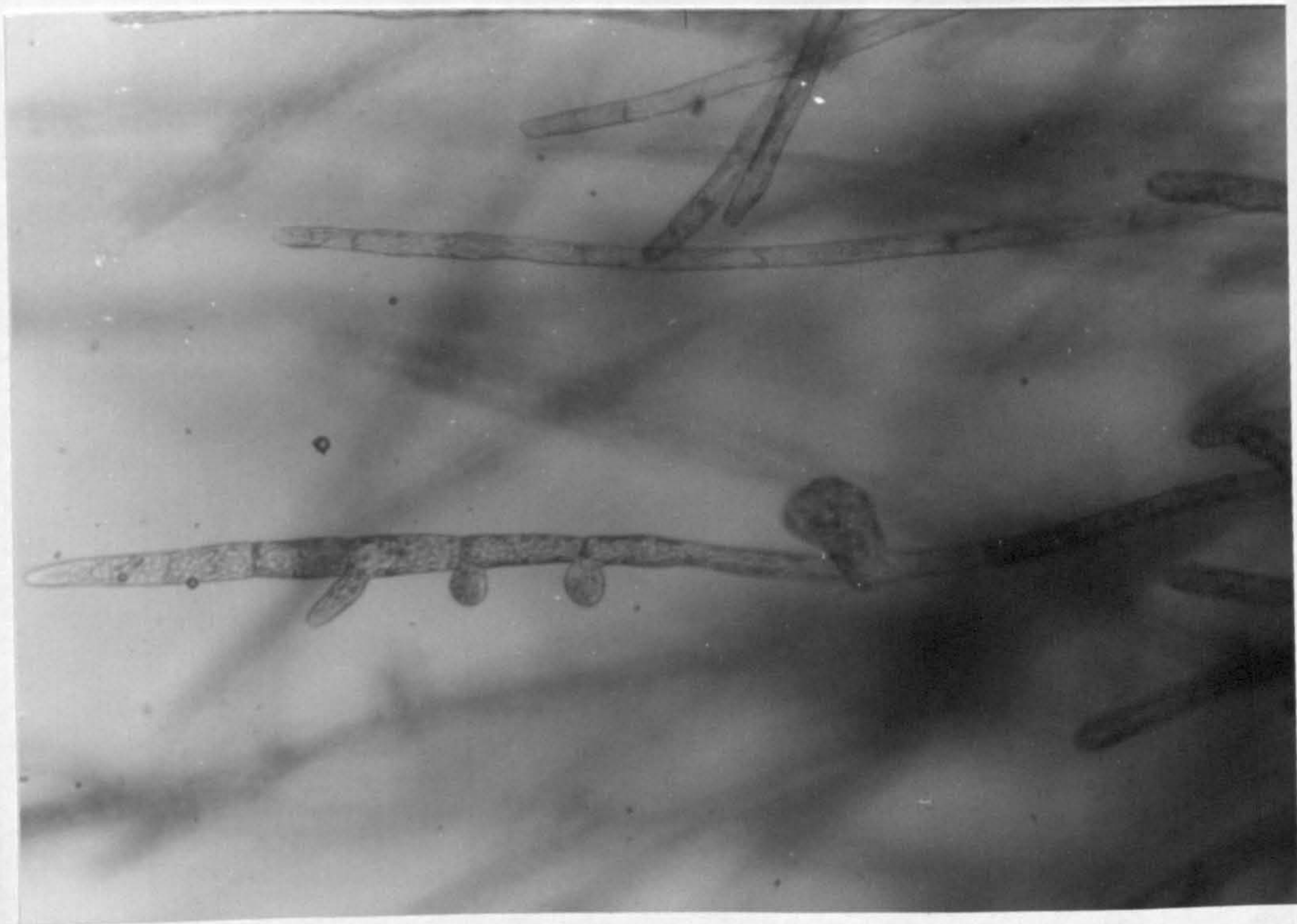


Fig. 4.22 The mutant strain GAM710 treated for 4 days with A23187 (40 $\mu$ M) and BAP (1 $\mu$ M).



inhibitors such as nifedipine and lanthanum have complex effects on protonemal growth which need further investigation before conclusions about the nature of their action can be drawn. An effect of calcium on bud production cannot be discounted, however the production of buds in response to calcium may be via a different mode of action than that of cytokinin.

## CHAPTER V

### CALCIUM IMAGING

#### 5.1 Introduction

It is difficult to detect influxes of small quantities of calcium using classical electrophysiology. However, new methods of imaging calcium will allow the visualisation of increases in intracellular calcium throughout the nanomolar to micromolar range. I have explored two new techniques of imaging calcium, as a further means of examining the putative role of calcium in cytokinin action.

##### 5.1.1 Calcium imaging using fluorescent dyes

The development of a range of fluorescent calcium indicators (Grynkiewicz *et al*, 1985; Tsein and Poenie, 1986), combined with recently developed microscope technologies (fluorescence ratio imaging, confocal scanning laser microscopy), has made it possible to obtain accurate measurements of free calcium in cells (Bush and Jones, 1990). Fluorescent dyes such as Fluo-3, Quin-2, Fura-2 and Indo-1, based on BAPTA or EGTA calcium binding ligands, have a high affinity and selectivity for free calcium ions. Moreover, the latter three dyes exhibit a shift in either the excitation (Quin-2, Fura-2) or emission (Indo-1) spectra upon binding to calcium at physiological calcium concentrations (100-350nM). By taking the ratio of fluorescence intensities at the optimum excitation or emission wavelengths, of the calcium-chelated and the free acid forms, it is possible to estimate the free calcium concentration. The ratio method allows for the correction of many of the optical artefacts which are associated with the use of fluorescent dyes such as Fluo-3, where calcium estimation relies on measurement at a single wavelength. Such artifacts are caused, for example, by uneven cell thickness, unequal dye distribution or variation in



the intensity of illumination (Wahl *et al*, 1990).

The measurement of changes in intracellular calcium using these techniques has proved considerably more straightforward in animal cells (Tsein and Poenie, 1986). Examples of animal cell types in which calcium has been successfully imaged include smooth muscle, lymphocytes, heart muscle, and sea urchin eggs. Many of the problems associated with measuring calcium in plants have been due to difficulties in loading the dyes, and retaining dye in the cytosol once loaded. Few reliable measurements of cytosolic calcium in plants have been published (Trewavas and Gilroy, 1991).

The free dyes are hydrophilic and therefore relatively membrane impermeant. The most widely used method for loading them into animal cells is to incubate the cells with a membrane permeant acetoxymethyl ester derivative. Once inside the cell cytosolic esterases split off the ester groups to leave the free acid trapped in the cytosol. Ester-loading into protoplasts has proved successful in some plant species (Chae *et al*, 1990; Elliott and Petkoff, 1990), but has not been achieved in whole cells. It is not certain whether the cell wall excludes the dye or whether it is only partially hydrolysed inside the cell.

A form of loading dependent on an acid incubating medium has also been successful in the protoplasts of some species (Bush and Jones, 1987; Oparka, 1991; Kiss *et al*, 1991). This method relies on the same principle as hormone transport and depends on the pK of the free acid. With increased acidity enough of the molecules may be in the protonated form to allow passage across the plasma membrane. Once inside the cell the higher cytosolic pH leads to dissociation of the free acid and its retention in the cytosol. Other methods used for introducing the dye into plant cells include microinjection, electroporation, and digitonin permeabilisation (Read *et al*, 1992).

Additional problems encountered using plant cells have been associated with the sequestration of dye into organelles, particularly the vacuole, and dye leakage into the extracellular medium. Some attempts have been made to overcome these problems

using dyes linked to high molecular weight compounds such as dextran, and/or anion-carrier inhibitors such as probenecid. Miller *et al* (1992) visualised a gradient of calcium at the tips of growing pollen tubes by means of pressure microinjecting Fura-2 linked to dextran. However, the use of drugs such as probenecid may have undesirable side-effects. For example, Oparka *et al* (1991) found that probenecid caused the cytoplasm of onion cells to change from an apolar to polar organisation.

Hahm and Saunders (1991), using Indo-1 in conjunction with photometry, reported a threefold increase in  $[Ca^{2+}]_i$ , from 250nM to 750nM, in caulonema subapical cells of *F. hygrometrica* in response to cytokinin. The average rise in  $[Ca^{2+}]_i$  was maintained for up to 30 hours. This increase was not observed in calcium-free medium. However, they found that non-target tip cells and chloronema also responded to cytokinin treatment by a similar rise in  $[Ca^{2+}]_i$ . They concluded that the differential physiological response of the target caulonema subapical cells to hormone stimulation must lie further down the signal transduction chain.

However, the problems associated with this work pose questions about the reliability of the results. The dye was loaded into the cells using the acid incubation method. The resulting signal did not appear to be very strong. The author experienced problems with dye leakage and sequestration into the vacuole and used probenecid to resolve these problems, which may have had an effect on cytoplasmic organisation. The measurements reveal a wide variation around the mean.

The object of the present study was to explore the possibilities for examining the response of the caulonema subapical cell to cytokinin, using the fluorescent dye Indo-1 (fig. 5.1) to image calcium in protonema of *P. patens*. In order to obtain measurements it was necessary to develop a means of loading dye into the protonema.

### 5.1.2 Transformation with recombinant aequorin

Another method of imaging calcium lies with recombinant gene technology.



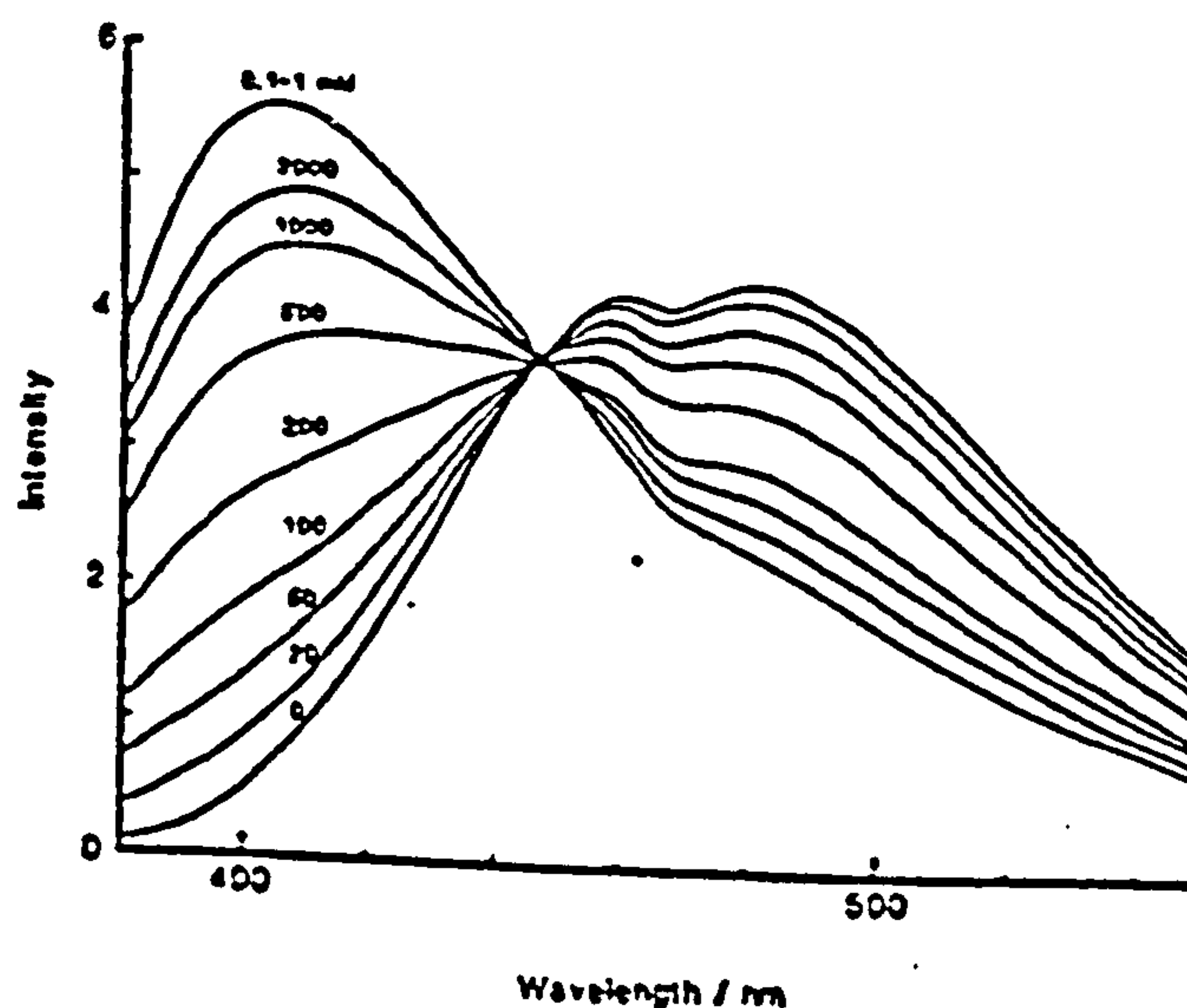
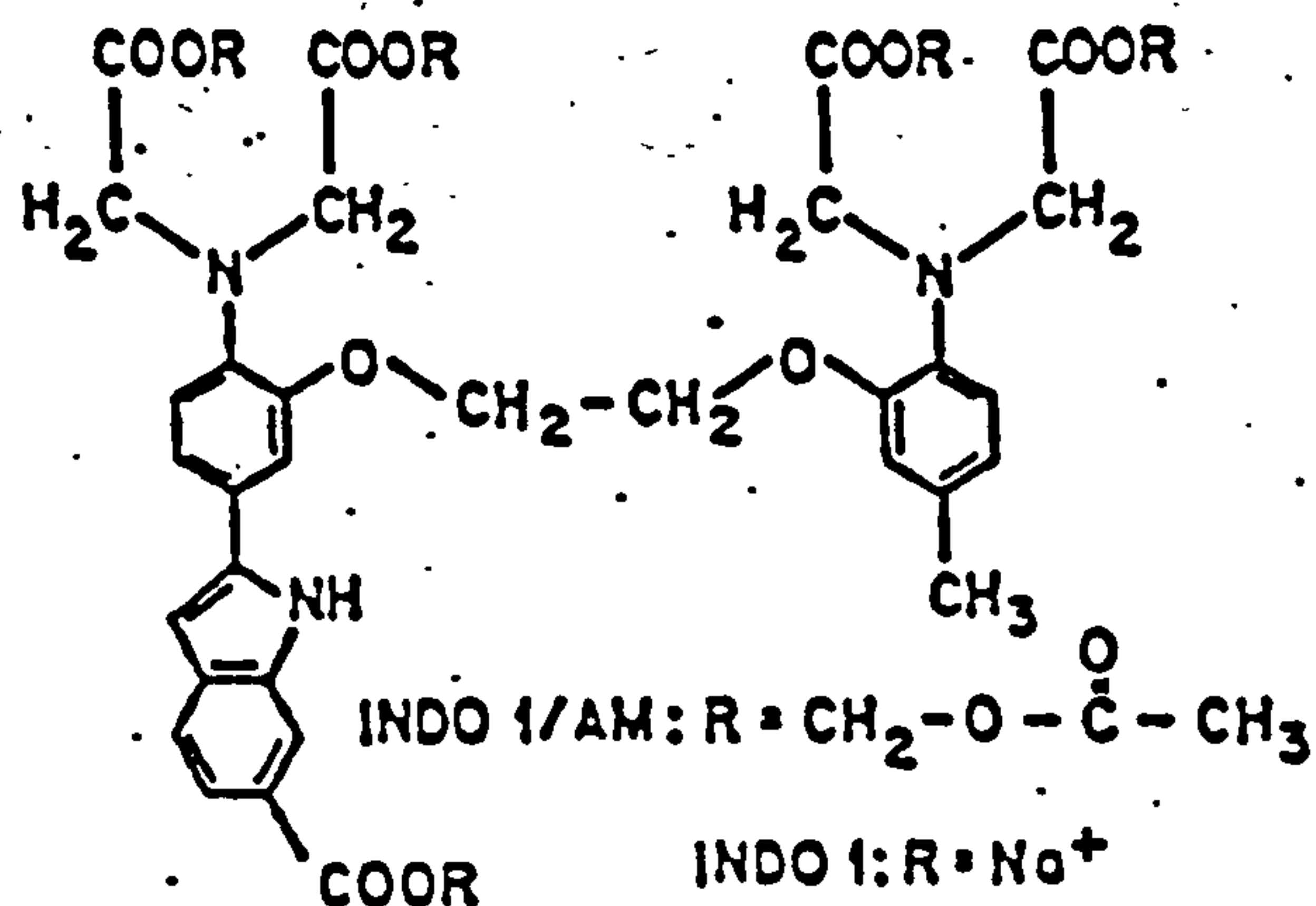


Fig. 5.1 The fluorescent ratio dye Indo-1.

- a) Chemical structure. An EGTA-like tetracarboxylic acid structure is combined with the fluorophore, an Indole group.
- b) Emission spectra as a function of free  $\text{Ca}^{2+}$ . The fluorescence spectra shift to lower wavelengths when the dyes bind calcium relative to the spectra of the  $\text{Ca}^{2+}$ -free form of the dyes.  
 The excitation is set at 355nm.

From: Grynkiewicz *et al*, 1985.

Working with *Nicotiana plumbaginifolia*, Knight *et al* (1991) demonstrated that reconstituted aequorin can report intracellular calcium changes induced by touch, cold shock and fungal elicitors in transformed plants. Aequorin is a calcium-sensitive luminescent protein from the coelenterate *Aequorea victoria*, which responds to free calcium by emitting blue light in a dose-dependent manner (Knight *et al*, 1993). The protein has two components, a 22 Kd polypeptide, apoequorin, and a luminophore, coelenterazine. Tobacco plants transformed with the DNA sequence coding for the 22 Kd polypeptide coupled to the 35s promoter from Cauliflower Mosaic Virus, express apoequorin in every cell. Incubation of transformed plants in the non-cytotoxic coelenterazine (2.5 $\mu$ M) results in the intracellular reconstitution of aequorin. The subsequent growth and development of tobacco plants is not affected by apoequorin, or by incubation in coelenterazine.

Measurements of aequorin luminescence in response to aequorin can be obtained from whole plants using a chemiluminometer. Knight *et al* (1992) have also imaged calcium luminescence in individual *N. plumbaginifolia* cotyledons using an extremely sensitive photon-counting camera in which photons captured by the camera detector were integrated over a 25 second period. Multiple photons were emitted from individual foci over the cotyledon, some of which may represent photons emitted from individual cells. However these methods only provide a qualitative measure of  $[Ca^{2+}]_i$  variation. Using the imaging system, shorter integration can improve spatial resolution. However the light emitted from individual cells is very low and may not be picked up within the time-scale required for good spatial resolution. A range of coelenterazines with differing  $Ca^{2+}$ -sensing and light emitting properties have already been synthesised, with the aim of improving the resolution of this technique.

Moss offers the advantage over multicellular plants of the possibility of imaging calcium in single cells. This system offered a further opportunity of verifying experimentally a role for calcium in cytokinin-induced bud induction in moss.



## 5.2 Materials and methods

### Dye-loading

Stock solutions of the fluorescent dyes Fluo-3 and Indo-1 (Molecular Probes inc., Eugene, Oregon, U.S.A.) were made up by dissolving the pentapotassium forms in DMSO to a concentration of 1mg/ml. The appropriate concentrations were achieved by diluting the stock solution in water (HPLC grade). The dyes were added to cultures in liquid medium to final concentrations of 25, 50 and 100 $\mu$ M. The same concentrations of dye were also added to cultures grown on a thin layer of agar medium. Both the free acid and ester forms of the dyes were tested. Ester loading experiments were carried out at pH 5.0 to 7.0. For loading experiments with the free acid forms of the dyes, cultures were incubated at pH 4.5. Cultures were incubated in the dyes for time-periods of 1 to 16 hours. At the end of each incubation period protonema were washed several times with fresh medium.

### Growth chamber

A growth chamber was prepared by attaching a circular coverslip (No.1, Chance Proper Ltd., Warley, U.K.) to the base of a circular 20mm diameter open perfusion chamber with a thin smear of high vacuum silicon grease around its periphery.

Spores were germinated in liquid culture for up to a week before being plated onto solid agar medium overlain with cellophane. After a further week's growth a small section of cellophane containing spore cultures was cut out and turned upside down into a drop of warm agar placed in the bottom of the growth chamber. As the cellophane was gently lifted, the protonema remained embedded in the solidifying agar. A further drop of hand-warm agar was placed on top of the spore culture to hold the filaments in place.

### Microinjection

Needles were pulled from filament glass electrode tubes (Clark electromedical GC105F, Clark Electromedical Instruments, Reading, Great Britain). The micropipettes (*ca* 0.5 $\mu$ m in diameter) were filled with 50 $\mu$ M Indo-1 for microinjection. Cells were injected by iontophoresis at *ca.* 1 nA for varying time periods, depending on how quickly a signal was achieved. Images were taken at 5 minute intervals after dye loading until the signal was too low. For the incubation experiments, BAP was added to cultures at a concentration of 1 $\mu$ M. Protonema were microinjected 1, 5, 12, 20 and 24 hours after the addition of hormone. Ratios of images taken 10 minutes after a successful microinjection were used for the purpose of comparison.

### The microscope system

The ratio analysis system is based round a modified Nikon Diaphot inverted epifluorescence microscope fitted with a 340nm transmissive optics and a 75W Xenon epifluorescence lamp. A quartz ND2 neutral density filter (Ealing Electro-optics, Watford U.K.) was used to reduce the intensity of the excitation light. The excitation wavelength was determined by a 350nm, 10nm half-bandwidth interference filter (Ealing Electro-optics) mounted in a motor-driven excitation filter wheel (Newcastle Photonic systems, Newcastle-upon-Tyne, U.K.) installed on the front of the Nikon epicondenser. A Nikon 380 nm dichroic mirror allowed fluorescent light from the specimen to pass to the microscope side port.

### Imaging system

A motor-driven emission filter wheel (Newcastle Photonic Systems) was placed on the microscope side-port. Switching between interference filters in the emission light



path was controlled by a computer. Images were recorded using an Extended-ISIS intensified CCD camera (Photonic Science, Kent, U.K) and digitised using a Synapse frame store controlled by the Semper-6-plus image processing language (Synoptics Ltd., Cambridge, U.K.) running on a Dell 310 microcomputer (Dell corp., Berkshire, U.K.). For Indo-1 measurements the filter wheel was switched between a 415nm and 480nm interference filter (both 10nm half-bandwidth, Ealing Electro-optics) for collection of data for ratio calculations and a ND3 ND filter for the corresponding bright field image. Switching between filters and subsequent image capture took approximately 1 second. The 350 nm excitation beam was cut off between each image capture to reduce photobleaching and minimise cell exposure to this wavelength.

### Image processing

Image processing and ratio calculations were performed using the Semper-6-plus image processing system. For each image the autofluorescent value was subtracted. A mask was defined for each image that excluded regions where the final strength was below that known to give reliable ratio results. The grey level value of each pixel in the masked image at 405nm was divided by the value of each corresponding pixel in the masked image at 480nm. The resulting ratio image was colour-coded to represent different calcium concentrations determined after calibration. Floating point arithmetic was used throughout the ratio calculation. Hard copies of the images were produced using a Mitsubishi CP100B video copy processor.

### Transformation

The plasmid pAQNEO1, consisting of the apoaequorin coding region from cDNA clone pAEQ1 (Prasher *et al*, 1985) fused to the cauliflower mosaic virus 35s promoter, linked to the pLGVneo construct, was a gift from Dr. M. Knight,

Edinburgh.

Protoplasts of wild-type *Physcomitrella patens* were transformed with the plasmid pAQNEO 1 (fig. 5.2) using the transformation procedure developed by Schaefer *et al* (1989).

Protoplasts were obtained by incubating 7-day old tissue from the strain pabA3 in Driselase (0.8% w/v) for 40 minutes. Plasmid DNA (24µg) plus PEG solution (300µl) was added to each aliquot of protoplasts. Heat shock (45°C) was applied for 5 minutes and the solutions then allowed to cool for 15 minutes at 15°C before plating on medium containing mannitol (6%).

Five mutant strains of *P. patens*, *bar-1*, *bar-576*, *gam-139*, *gam-710*, *nar-87*, and two different species of moss, *Funaria hygrometrica* and *Ceratodon purpureus*, were also transformed with the plasmid pAQNEO1 using the particle bombardment method (Sawahel *et al*, 1992). Protonemal tissue, 7 to 10 days old, was used for this method.

### Selection

After 3-4 days on mannitol medium the protoplasts of wt *P. patens* were transferred to the medium containing the antibiotic G418. Regeneration was high. However none of the regenerants grew as fast as the wild-type control, suggesting that they were transiently expressing resistance or were unstable transformants. As there were too many regenerants to test individually, the tissue from all plates was mixed and homogenised. Homogenate tissue was grown without antibiotic for 17 days and then transferred to an antibiotic-containing medium for a further 3 weeks. Growth tests were carried out on this tissue by subculturing innocula of tissue onto medium without antibiotic for 14 days and then subculturing back onto plates containing G418. These subcultures now grew as fast in the presence of antibiotic as in its absence and are assumed to be stable transformants.



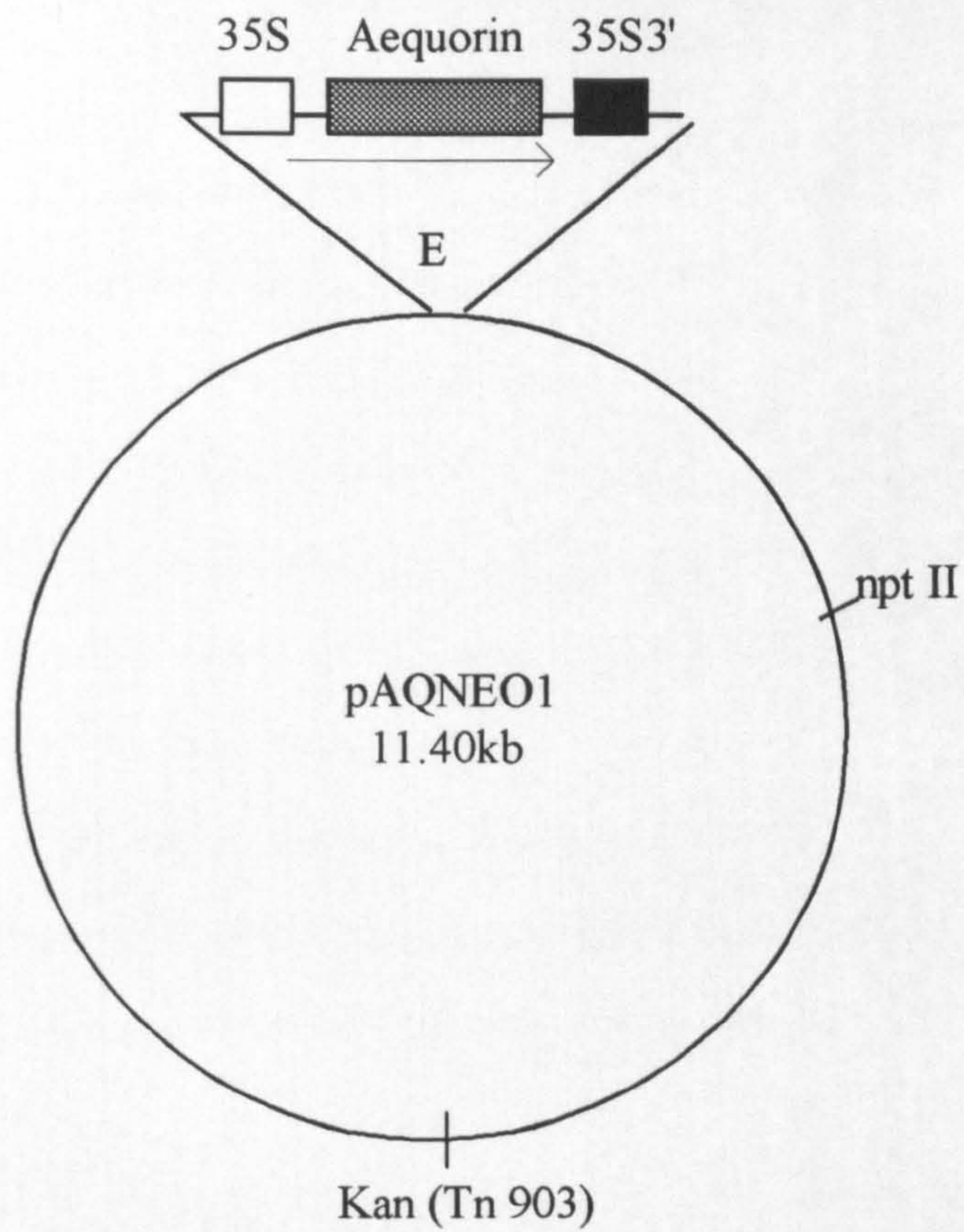


Fig. 5.2 The plasmid pAQNEO1, constructed by Marc Knight, for transformation of *P. patens*. The EcoR1 insert of pCASAQXP consists of the 35S promoter, the aequorin coding sequence and the 35S terminator. This construct is ligated into the EcoR1 site of the plasmid pLGVneo1103 (Hain, R. *et al*, 1985)



### Western analysis

Western analysis was performed for the stable wild-type transformant.

Total protein was extracted from 7-day old tissue (see appendix 1), electrophoresed on a 10% SDS Laemli gel and transferred to a nitrocellulose filter by electroblotting. Protein electrophoresis and electroblotting were according to standard procedures (Towbin *et al*, 1979). After overnight incubation at 4°C in a 1:1000 dilution of mouse primary antibody to aequorin isolated from *Aequorea* (gift from Dr. M. Knight, Edinburgh), the filter was incubated in a 1:500 dilution of horseradish peroxidase conjugated goat anti-mouse antibody for 30 minutes at 37°C. Visualisation was by ECL western blotting reagents (Amersham).

### Reconstitution of aequorin

*In vitro* reconstitution of apoaequorin in *P. patens* was carried out in 0.5M NaCl, 5mM mercaptoethanol, 5mM EDTA, 0.1% gelatin, 10mM Tris-HCl, pH 7.4, 2µM coelenterazine (gift from F. McCapra) in darkness at room temperature. The resulting solution was diluted 1:50 in 200 mM Tris, 0.5mM EDTA, pH 7.0. Reconstituted aequorin was discharged by the addition of an equal volume of 50mM CaCl<sub>2</sub> and the total amount of luminescence produced over 10s measured.

Aequorin was reconstituted in whole plants by incubating cultures in water and 2µM coelenterazine. Before measuring luminescence tissue containing reconstituted aequorin was homogenised in 200mM Tris buffer (as above).

### Measurement of luminescence

Calcium-dependent aequorin luminescence was recorded by a digital luminometer and the output sent to a chart recorder. For luminescence measurements, whole cultures were transferred to plastic cuvettes and placed in the luminometer.



Aequorin luminescence was imaged using a photon counting camera (Photonics, Nottingham).

### Treatment of aequorin transformant with hormones

Prior to the addition of experimental treatments, cultures were incubated in 2.5  $\mu\text{M}$  coelenterazine for a minimum of 6 hours or overnight. NAA and BAP were added in 5 ml aliquots at concentrations of 1, 2 and 10  $\mu\text{M}$  to cultures in the recording cuvettes.

## **5.3 Results and Discussion**

### 5.3.1 Dye-loading

#### a) Ester-Loading

Many attempts were made to load protonema of *P. patens* with dye using the membrane-permeant acetoxymethyl esters of Indo-1 and Fluo-3. Both dyes tended to precipitate out of solution, necessitating the addition of the mild detergent, pluronic. Without pluronic, precipitated dye particles collected around the outside of cells and entered damaged cells to give particulate fluorescence (fig 5.3c). Pluronic (1  $\mu\text{l}$ ) added to 800 mls of 50  $\mu\text{M}$  dye prevented precipitation, and did not lead to any increase in cell damage. The dye was only taken up by damaged cells. In some instances dye could be seen fluorescing brightly in the cell walls in gametophore leaves (fig.5.3a). This suggested that the dye was hydrolysed in the cell walls, before entering the cells.

#### b) Acid-loading

Incubation of protonema in the free acid forms of Indo-1 and Fluo-3 at a pH of 4.5, for periods of up to 16 hours, did not result in dye being taken into the cells at any of the concentrations used. However, the dye was taken up and bound by cell



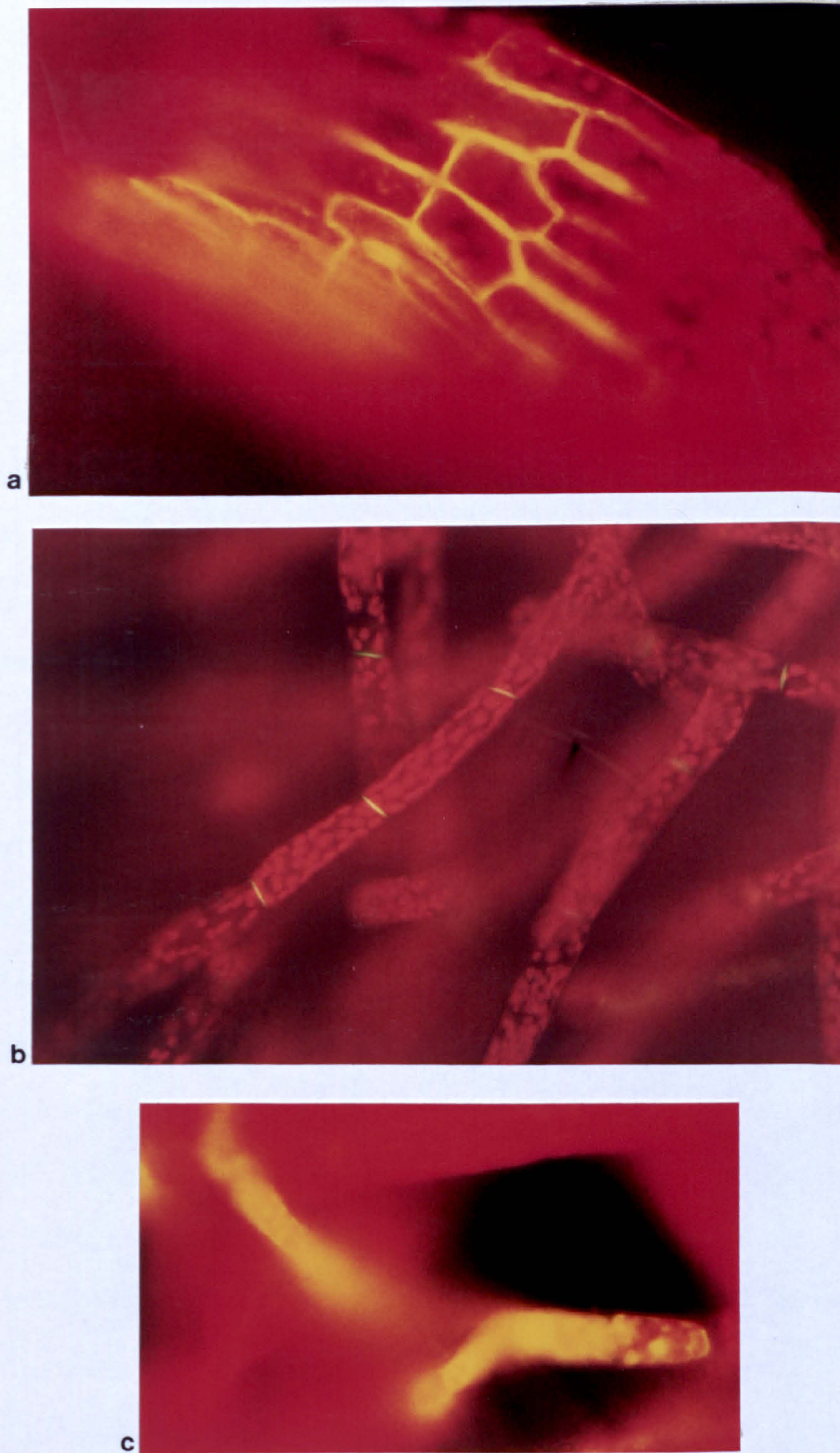


Fig. 5.3 Fluorescence micrographs of *P. patens* cells after incubation in either (a + c) Fluo-3/AM or (b) Fluo-3 pentapotassium salt. (a) Fluo-3/AM fluorescing brightly in the cell walls of gametophore leaves. (b) Fluo-3 binds to the cross walls of protonemata but does not enter undamaged cells. (c) Fluo-3/AM in damaged cells.



walls (fig 5.3b).

### 5.3.2 Microinjection

A method was developed for loading the cells with dye using the technique of iontophoretic microinjection. Initially, difficulties were encountered in transferring filaments to the slide chamber and holding them stably in order to insert microelectrodes. The method which proved best for this purpose was developed over the period of study and is described in 5.2.2. However, it remained difficult to obtain a stable dye signal. Free dye entering the cytosol was rapidly transferred via the plasmadesmata to adjacent cells, particularly into side-branches. There was no visible dye leakage into the surrounding medium, at least for the duration of the visible signal. Dye leaking out of the cell, after withdrawal of the microelectrode, was indicative of a damaged cell. Similarly, dye-leakage into the vacuole was only immediate if the cell was damaged during impalement. If significant amounts of dye were entering the vacuole, this became apparent within 10 minutes by an increased signal in the vacuolar region of the cell compared to other regions (fig 5.6).

A successful impalement resulted in dye entering the cytoplasm and spreading through the cell in a matter of minutes (fig 5.5). If the cell was undamaged, the signal increased in nuclear and side-branch regions (fig 5.7a), and not in the vacuolar regions. In successfully loaded cells the signal remained bright enough for images to be taken for up to half an hour. The signal remained high for longest in the side-branch initials, the target cells for hormone action. The potential of this for analysing the response to cytokinin has not yet been fully explored. Fluorescence could still be visualised under the microscope 24 hours later in dye-loaded cells, but the signal was not intense enough for image analysis. The growth of protonema was not affected by the dye. Apical cells and side-branches continued to grow and divide normally (fig 5.4).



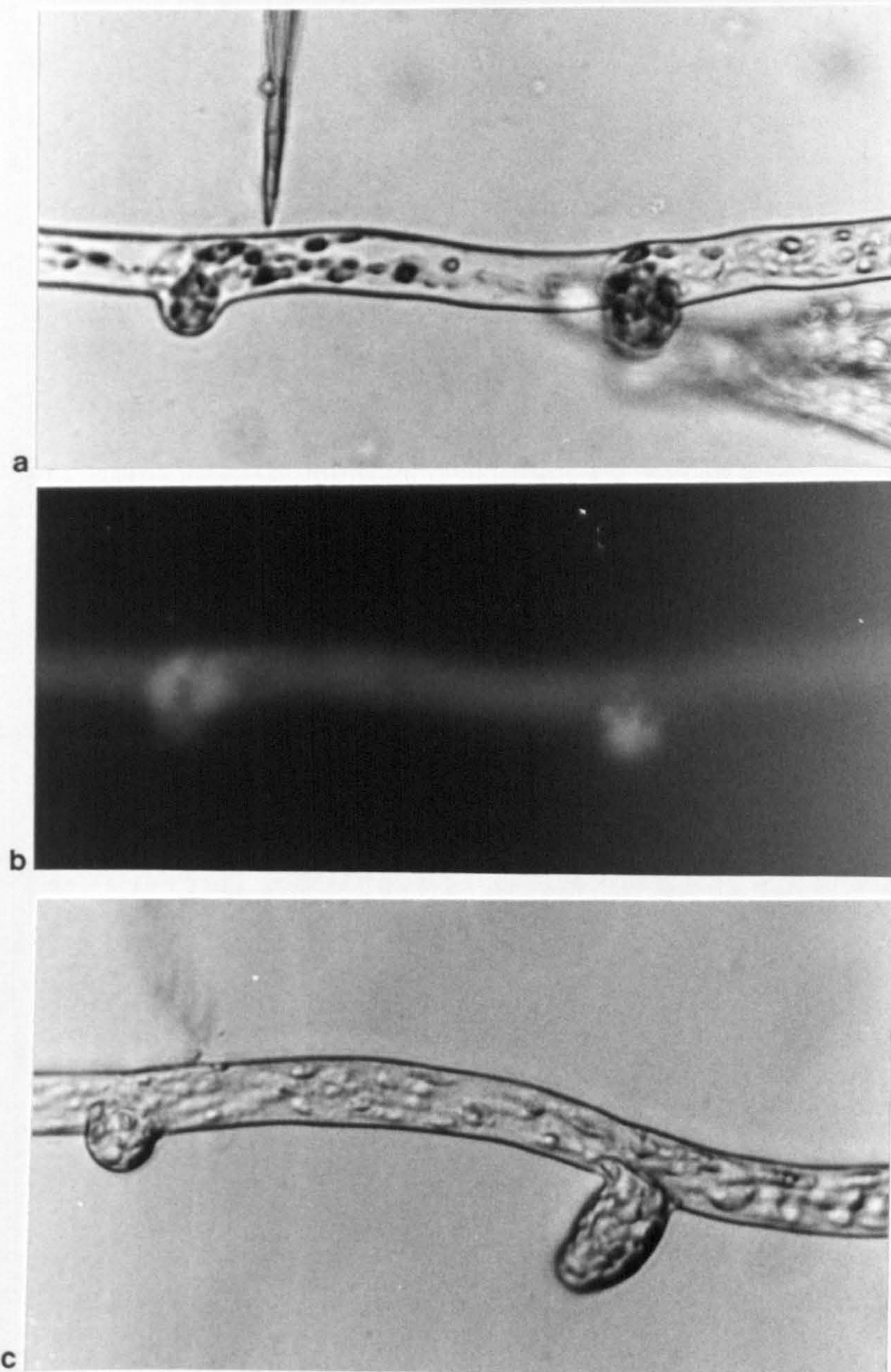


Fig. 5.4 Caulonema filament of *P. patens*. (a) Bright field image showing the caulonema subapical cell immediately prior to microinjection. (b) Indo-1 fluorescence within the cytosol 5 minutes after injection. Dye has moved into adjacent cells on either side of the injected cell, and into the side-branch initials. (c) Differential interference contrast image of the same cell 18h after injection. The cell is healthy and the side-branches are continuing to grow.



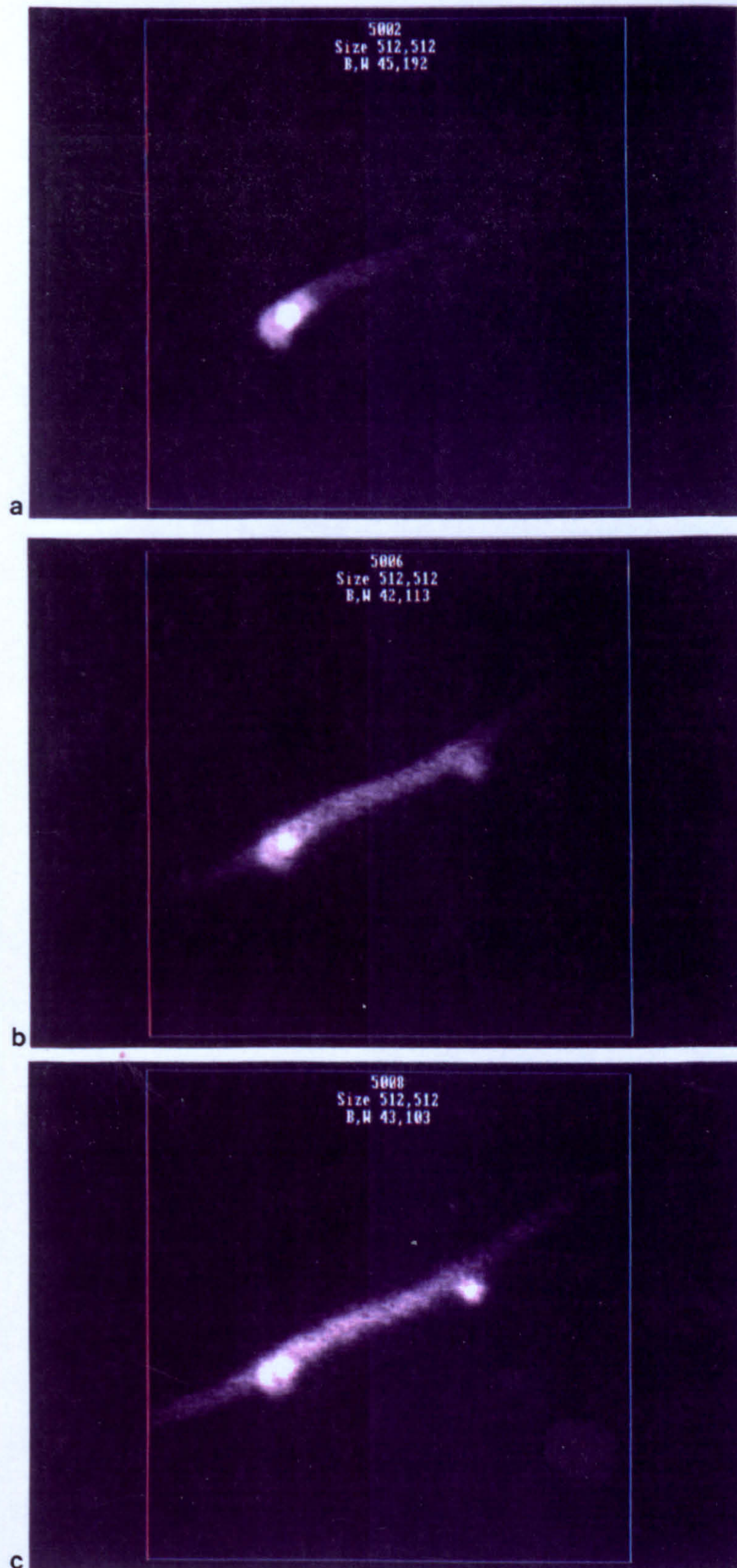


Fig. 5.5 Caulonema subapical cell of *P. patens* immediately (a), 5 minutes (b) and 12 minutes (c) after microinjection. (b) The dye remains concentrated in the nuclear region, but has diffused through the cytoplasm. Some signal has been lost as the dye has moved into adjacent cells. (c) The dye remains concentrated in the nuclear and side-branch regions.



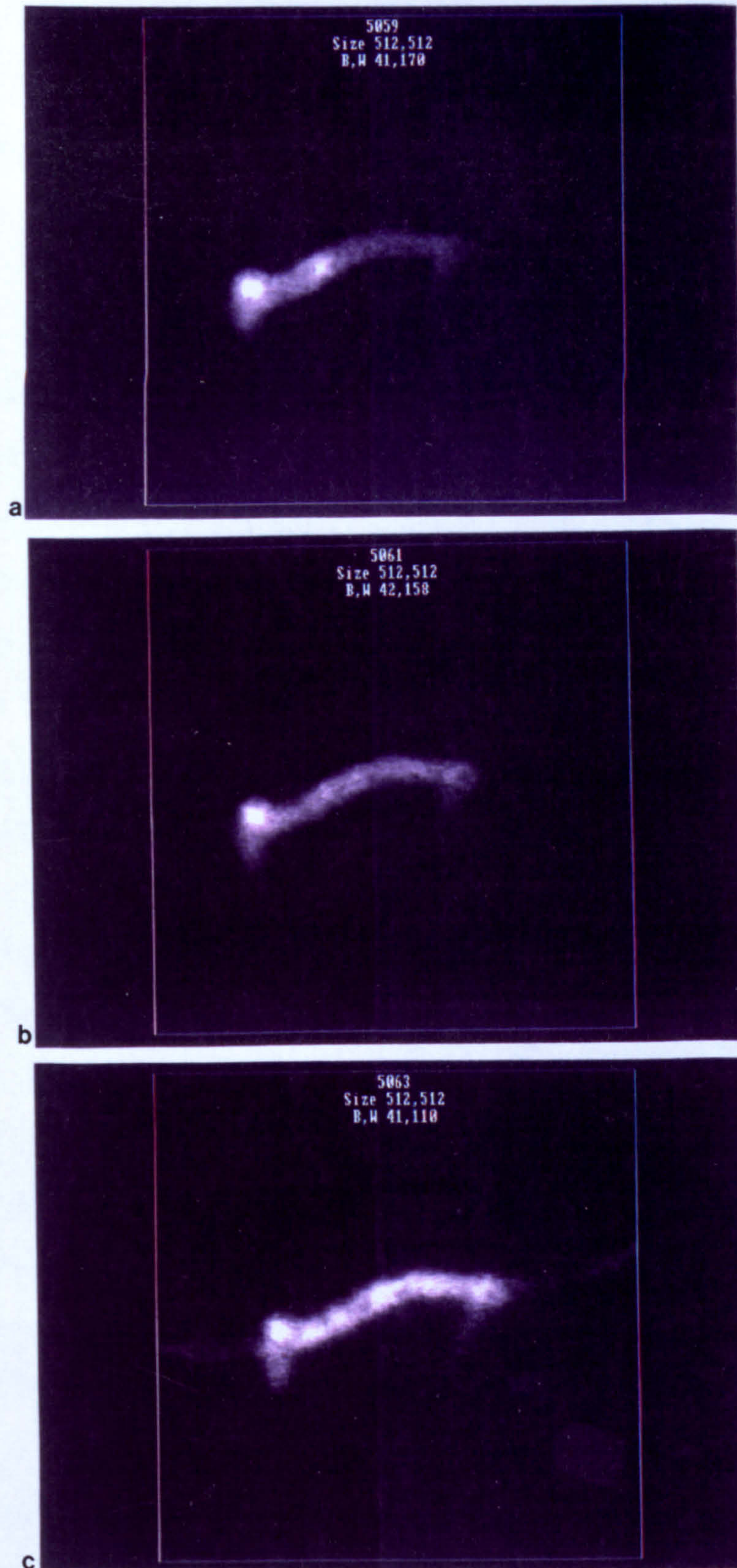


Fig. 5.6 Caulonema subapical cell of *P. patens* 2 minutes (a), 5 minutes (b), and 12 minutes (c) after microinjection. This cell has been damaged by the microelectrode during impalement, and dye has concentrated in the vacuolar region after 10 minutes.



### 5.3.3 Ratio-imaging

Figure 5.7 shows a cell 20 minutes after microinjection, where the dye has concentrated in the nuclear region and developing side-branch initial. Surprisingly the ratio image shows that these regions contain the lowest concentration of free cytosolic calcium. It is possible that regions of high organelle concentration such as developing side branches, due to their greater density relative to the rest of the cell, accumulate a degree of fluorescence that does not reflect the true concentration of cytosolic calcium.

This did not happen in every case. A conflicting result was obtained in fig 5.8 where the ratio image does show the highest calcium concentration to be in the nuclear region, the region of highest dye accumulation. Not enough images were taken to clarify this situation. In each case a different batch of dye was used, at a different time. However, it illustrates the care that is needed in interpreting the results obtained using fluorescent dyes.

#### a) Hormone effects

Attempts to see an immediate increase in the concentration of cytosolic calcium in response to cytokinin were unsuccessful. Cytokinin to a concentration of  $1\mu\text{M}$  was added to a number of successfully loaded subapical caulonema cells. No immediate change in  $[\text{Ca}^{2+}]_i$  was apparent from the ratio analysis. However, as the dye signal was not stable, it was uncertain whether this could be regarded as an accurate result.

An alternative approach was to incubate cultures in cytokinin and compare cytosolic calcium concentrations at different times after the addition of the hormone. The third, fourth or fifth subapical cells were chosen for analysis as target cells for hormone action. Images of successfully microinjected cells were taken for periods of 1, 5, 12, 20 and 24 hours after the addition of hormone. In each case ratios were



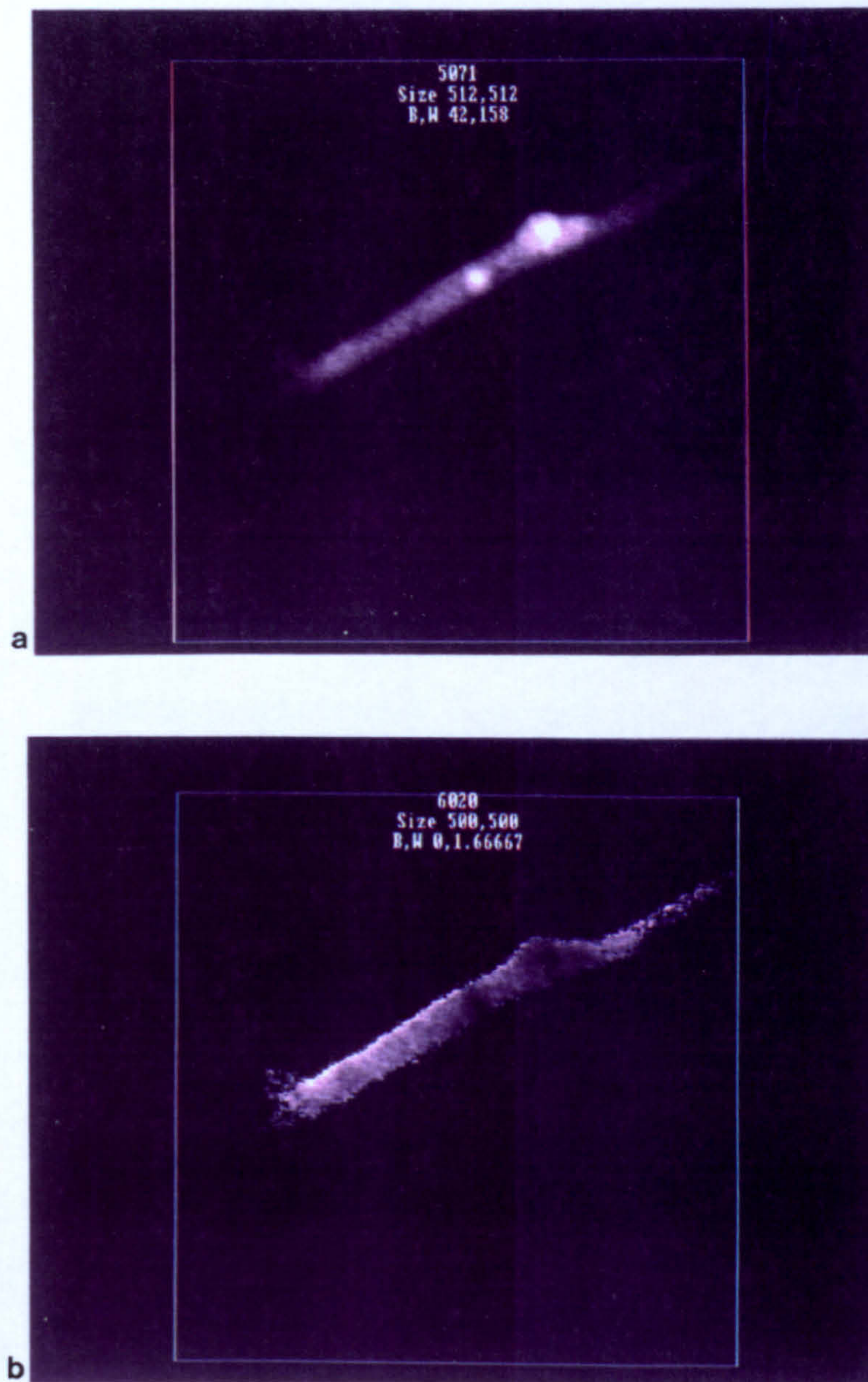


Fig.5.7 Caulonema subapical cell 20 minutes after microinjection. (a) The dye is concentrated in the nuclear regions and in the developing side-branch initial. (b) The ratio image suggests that the regions of brightest fluorescence are not the areas of highest cytosolic calcium.



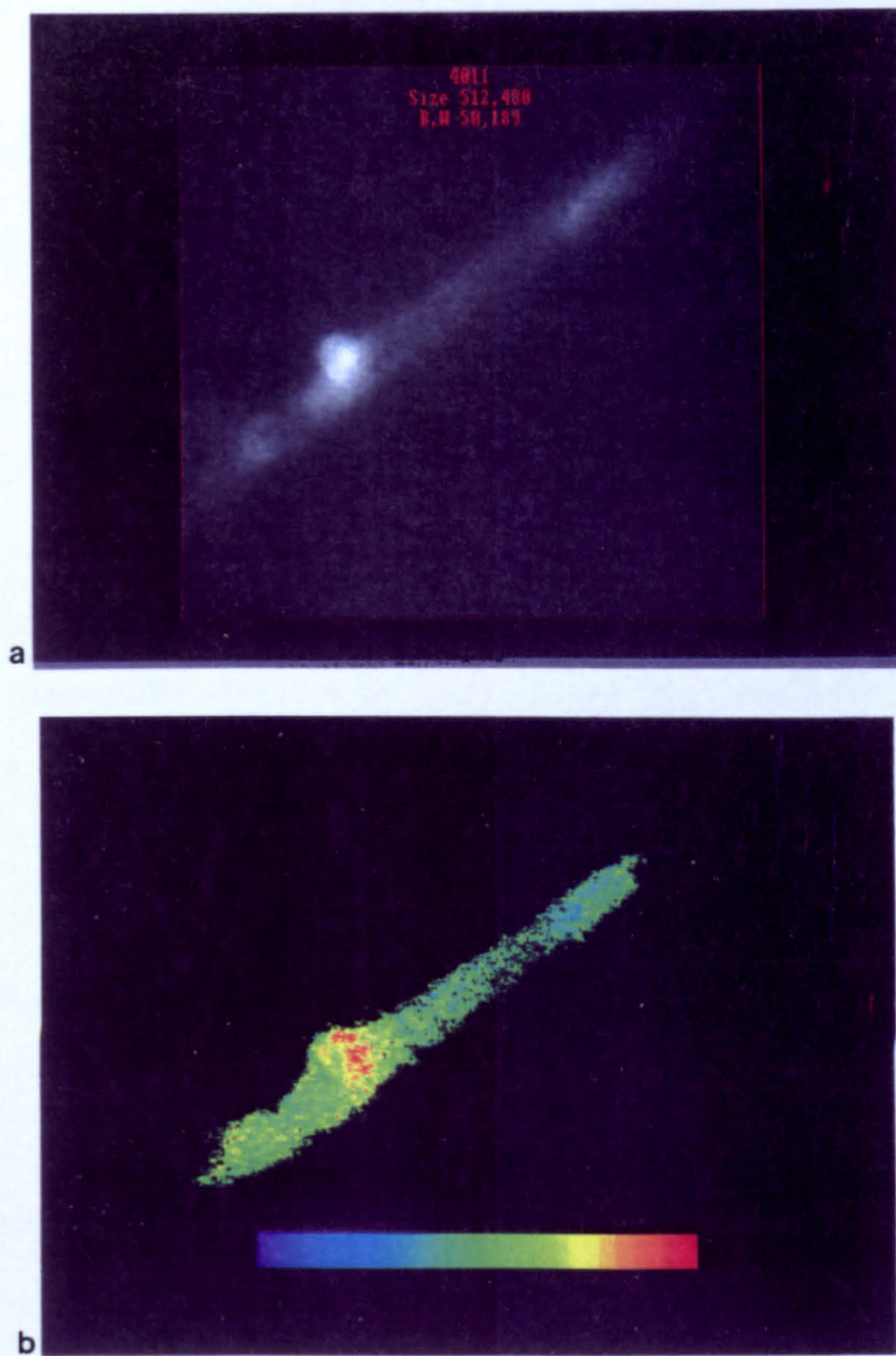


Fig. 5.8 Caulonema subapical cell 20 minutes after microinjection. In this instance the ratio image (b) shows the region of highest calcium concentration to be in the region of the brightest fluorescence (a).



calculated for images 10 to 12 minutes after microinjection. Figure 5.9 shows that in the cells analysed, no noticeable changes in cytosolic calcium levels occurred over a 24 hour period.

#### 5.3.4 Transformation

Wild-type *P. patens* was successfully transformed with the plasmid pAQNEO 1, using the PEG transformation method, and a stable transformant obtained. Fig. 5.10 shows the expression of apoaequorin in *P. patens*. Lane 1 is the control untransformed moss. Lanes 2 to 6 are all transformed tissue. The five mutant strains were also successfully transformed using microprojectile bombardment. Stable transformants were obtained for three of the mutants, *gam-139*, *nar-87* and *bar-576* (fig. 5.11). Unstable transformants of *gam-710* and *bar-1* were maintained on selection media containing G418. The transformation of *F. hygrometrica* and *C. purpureus* was unsuccessful. No regenerants were obtained after the tissue was transferred to medium containing antibiotic.

The moss continued to grow normally during and after incubation in coelenterazine. No signs of toxicity in response to coelenterazine were observed.

The reconstitution of aequorin *in vitro* shows similar kinetics to tobacco (fig 5.12). Near maximum luminescence (released in response to 50mM CaCl) was achieved by 3 hours. The experiment to show *in vivo* reconstitution was unsuccessful. However aequorin clearly is reconstituted *in vivo* as there is a clear response to cold shock both using the luminometer and from imaging (figs 5.13, 5.15). However for some reason, moss cultures did not reconstitute the more sensitive H-coelenterazine, which was successfully reconstituted in tobacco.

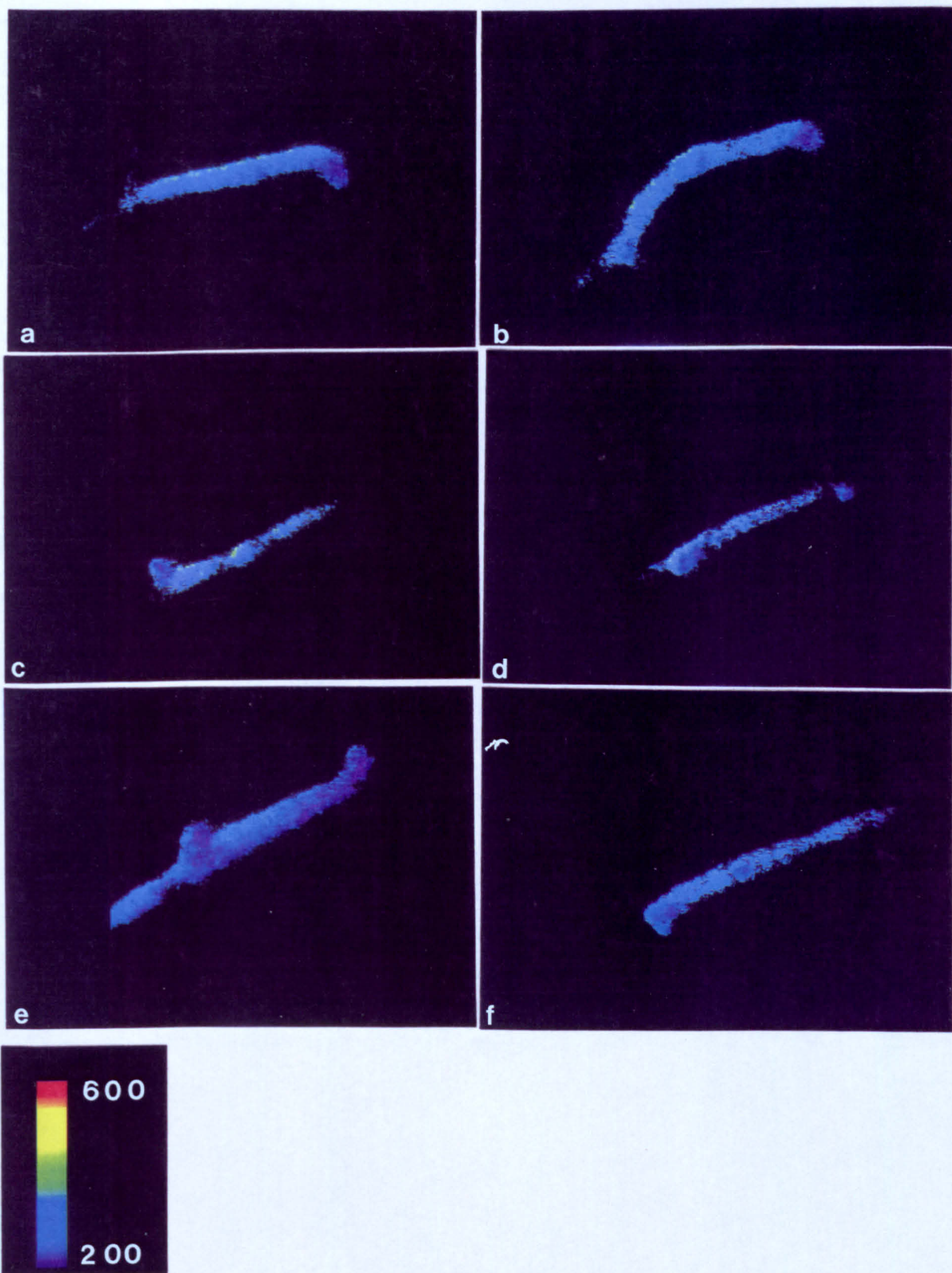
The response of the wild-type moss to cold-shock follows a similar temperature range to that of tobacco, but includes a response to 10°C which tobacco does not respond to (fig. 5.13a). All three mutant strains stably transformed with the gene for apoaequorin responded to cold-shock, but to differing degrees (fig 5.14). The



**Fig. 5.9** Caulonema subapical cells 10-12 minutes after microinjection.

The cells in (c) to (f) have been incubated in BAP ( $1\mu\text{M}$ ) for 1h (c), 5h (d), 12h (e) and 24h (f). The cells in (a) and (b) are control protonema, with no added BAP. The same calibration scale has been applied to all the cells. There does not appear to be any variability in cytosolic calcium concentration over the time-period of incubation with BAP.







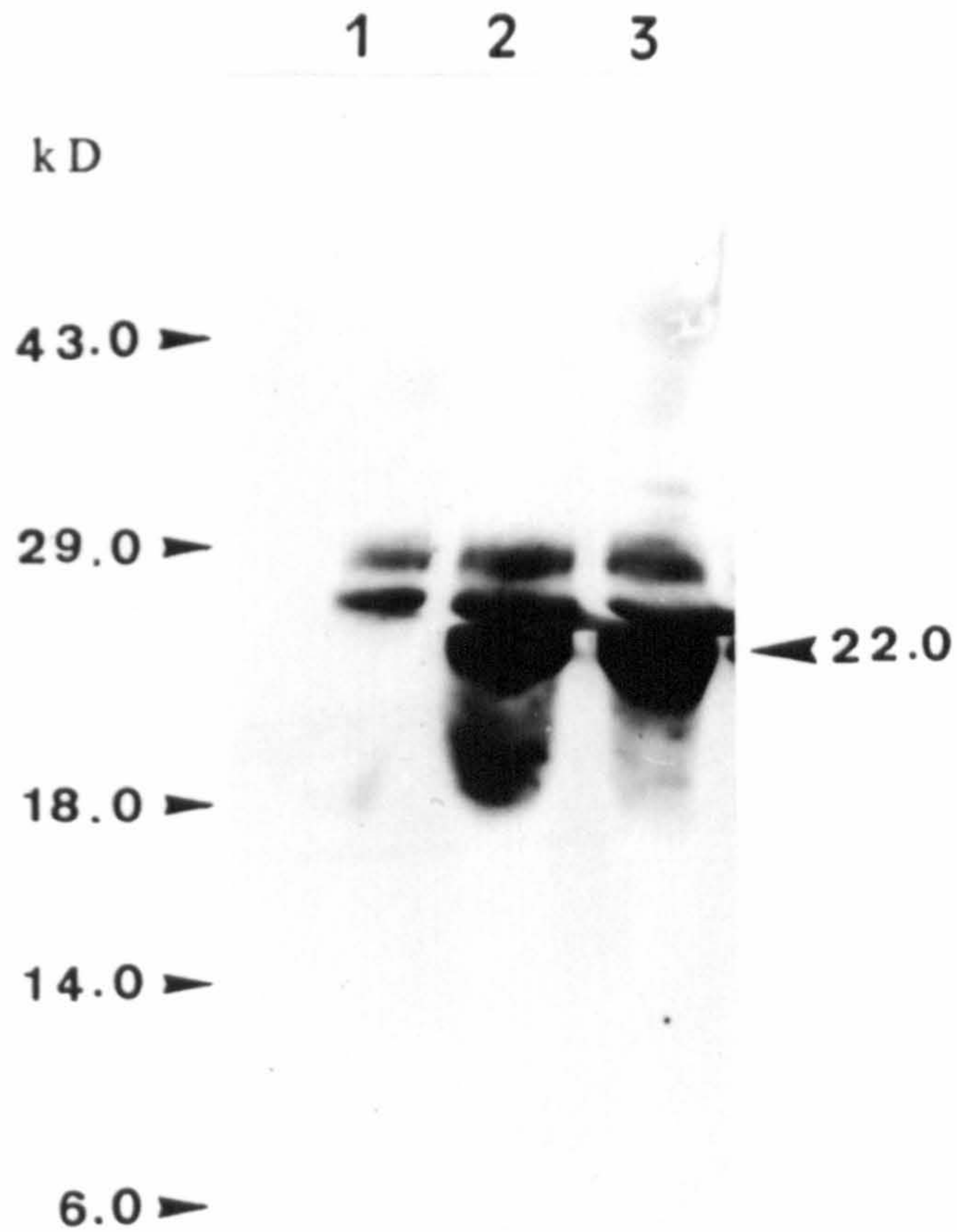


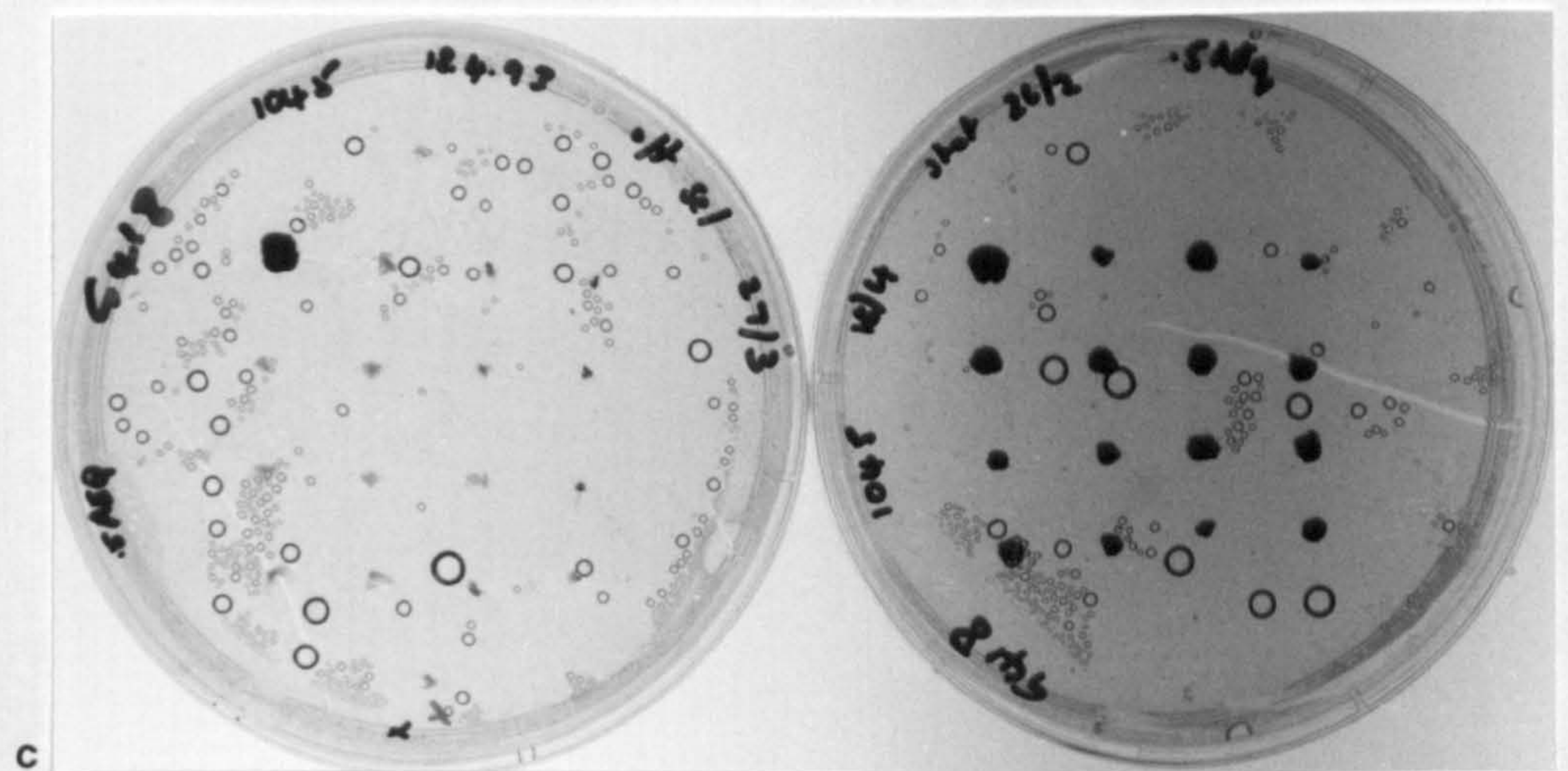
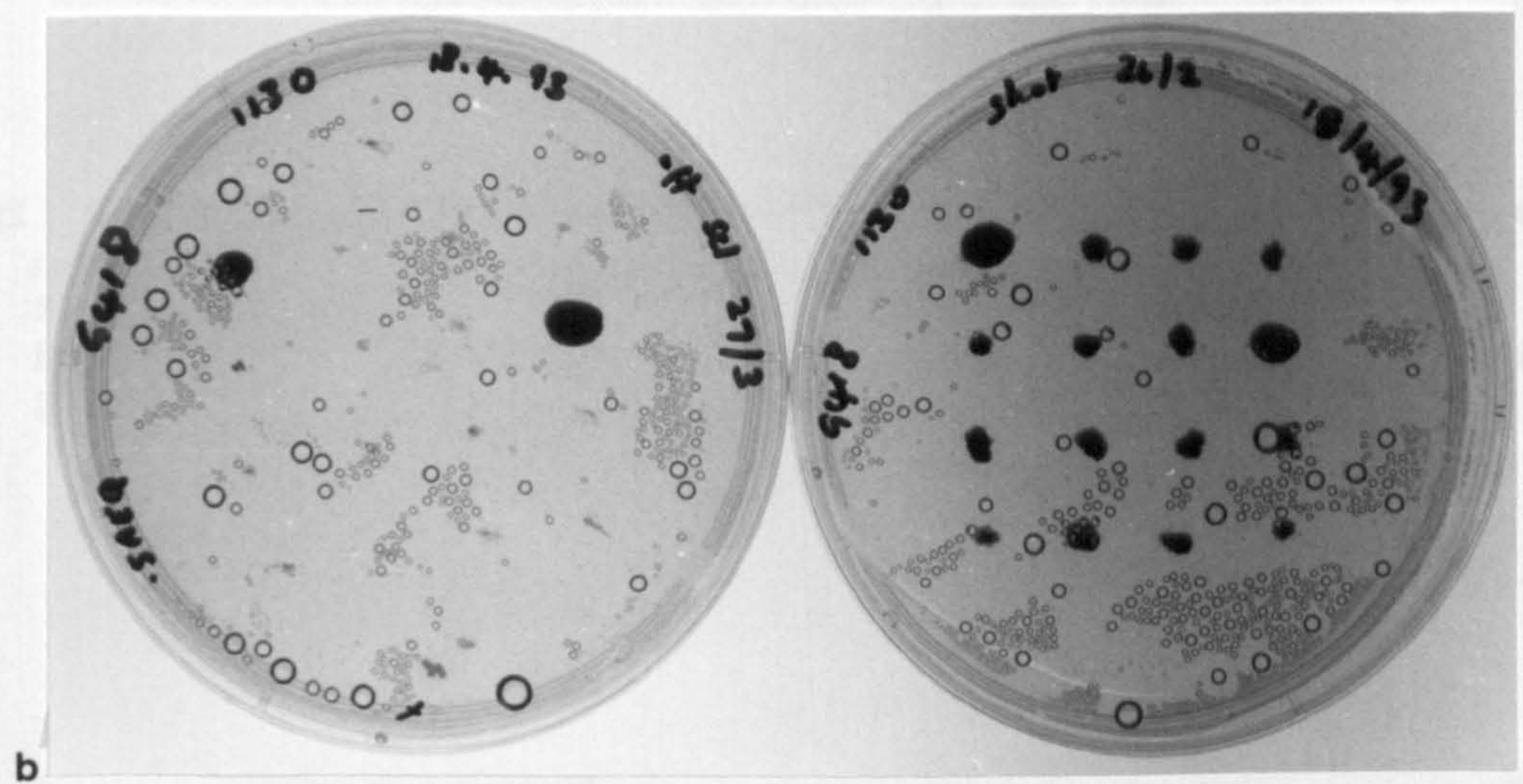
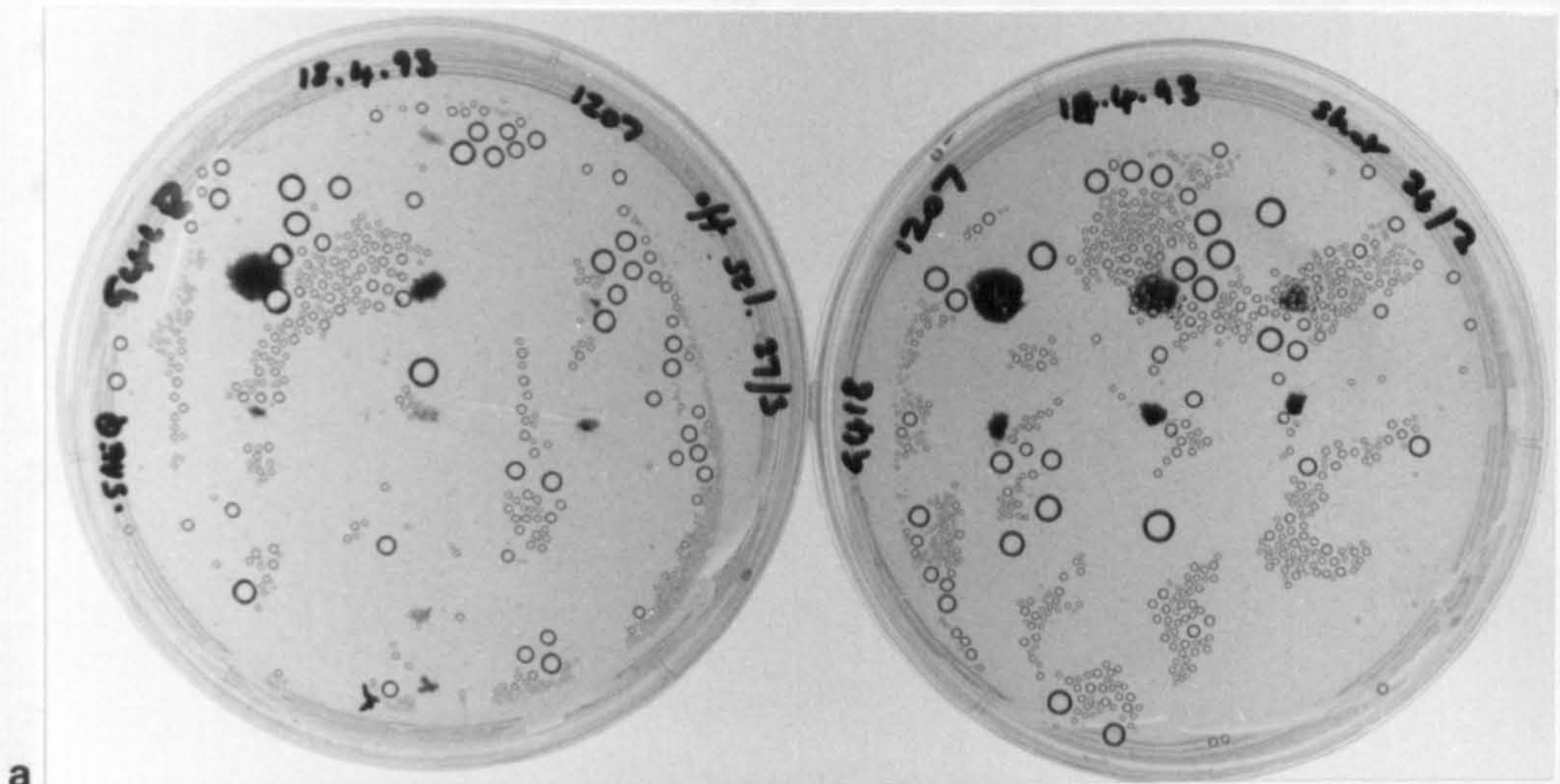
Fig. 5.10. Western blot analysis shows the expression of the 22 kDa protein apoaequorin in transformed wild-type moss.  
Lane 1: untransformed tissue.  
Lanes 2 and 3: moss transformed with apoaequorin.



**Fig. 5.11** Stable mutant strains of *P. patens* growing on medium containing the antibiotic G418 after a 14 day period of growth on non-antibiotic containing medium.

- a) *gam-139*
- b) *bar-576*
- c) *nar-87*







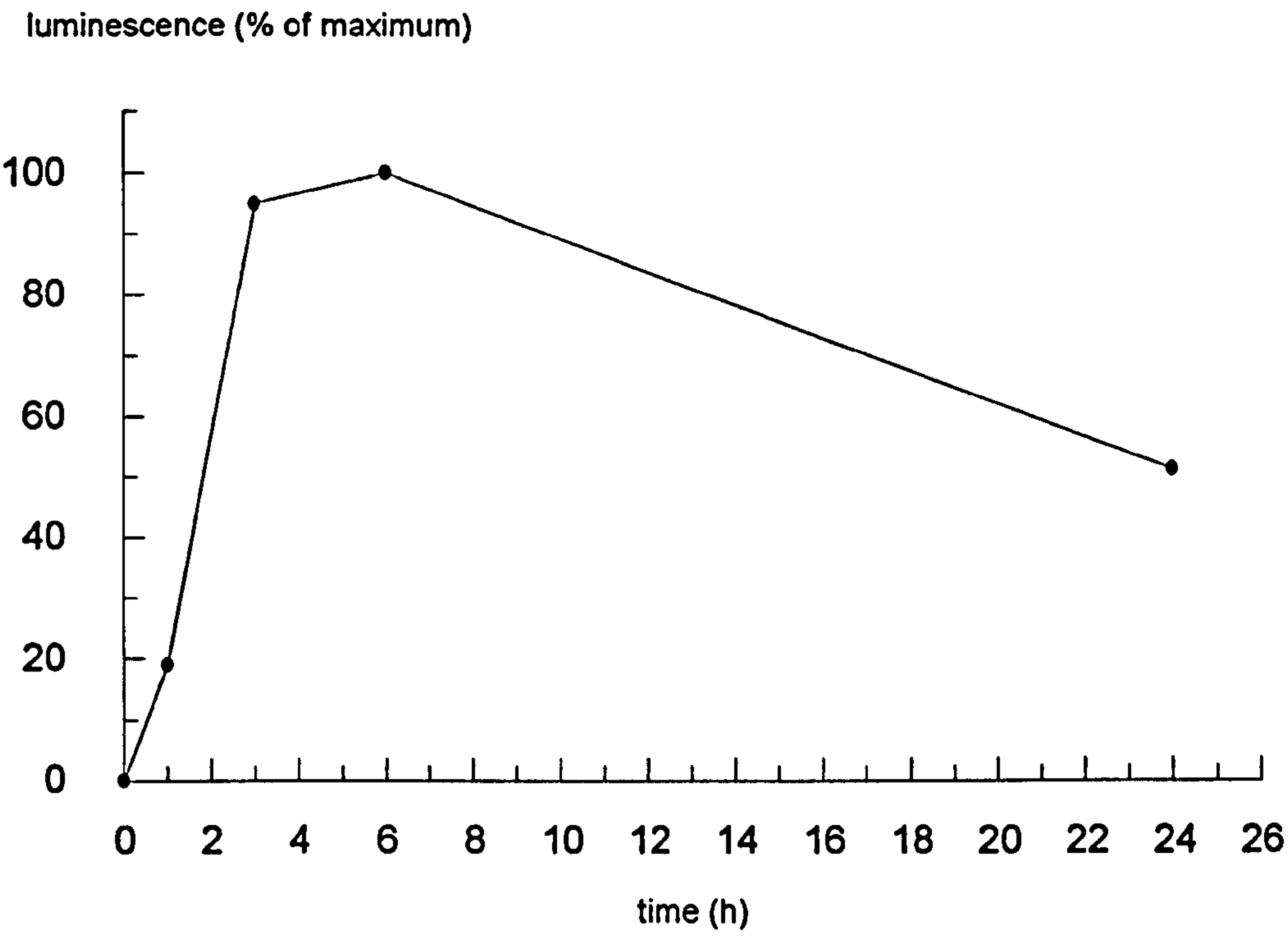


**Fig 5.12** The time-course of reconstitution of aequorin from apoaequorin and coelenterazine in whole cultures of wt *P. patens*. Moss cultures were incubated in water containing coelenterazine at 2.5 $\mu$ M. Reconstituted aequorin was discharged by the addition of 50mM CaCl, and the total amount of luminescence produced over 10s measured.



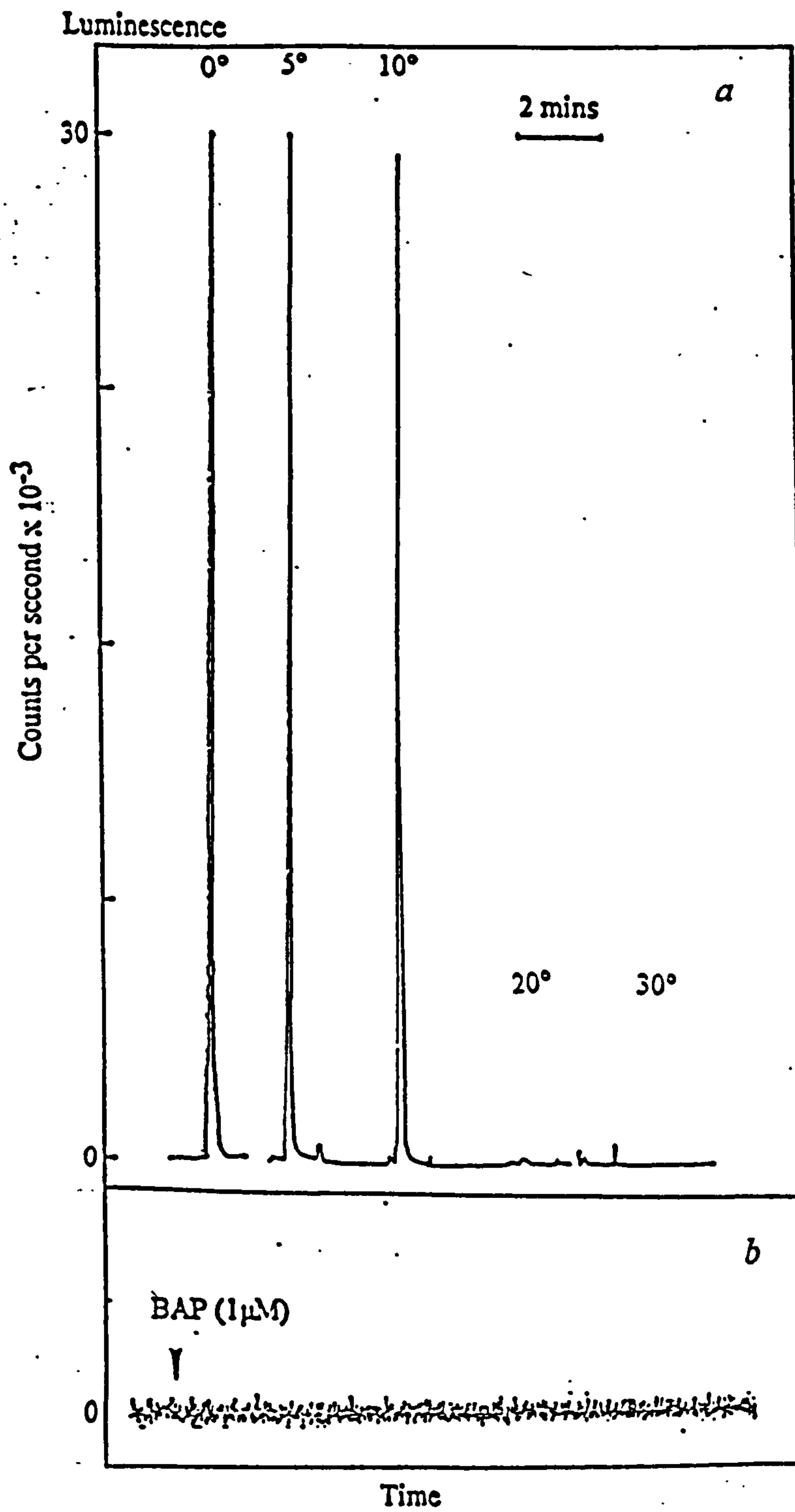


Fig. 5.13 The effect of temperature shock (a) and the hormone cytokinin (b) on calcium dependent aequorin luminescence. Moss gametophyte colonies were incubated in water containing coelenterazine for 6 hours. For luminescence measurements, individual colonies of moss were transferred to plastic cuvettes and placed in a luminometer. Water at temperatures of 0-50°C and benzylaminopurine (1  $\mu$ M) were added to the cultures in the cuvettes.



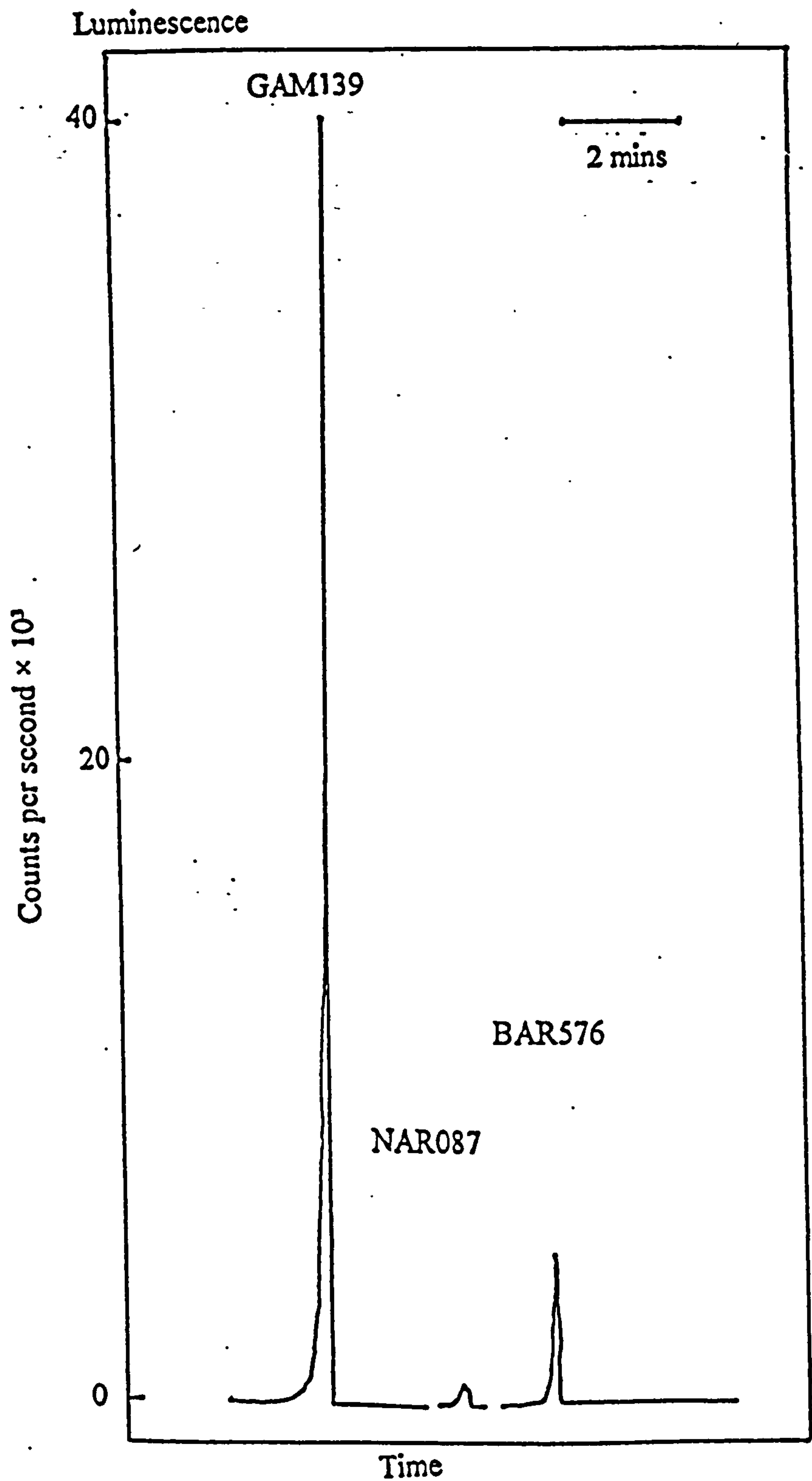


Fig. 5.14 The effect of temperature shock ( $0^{\circ}\text{C}$ ) on calcium-dependent aequorin luminescence in three mutant strains stably transformed with the gene for apoaequorin.



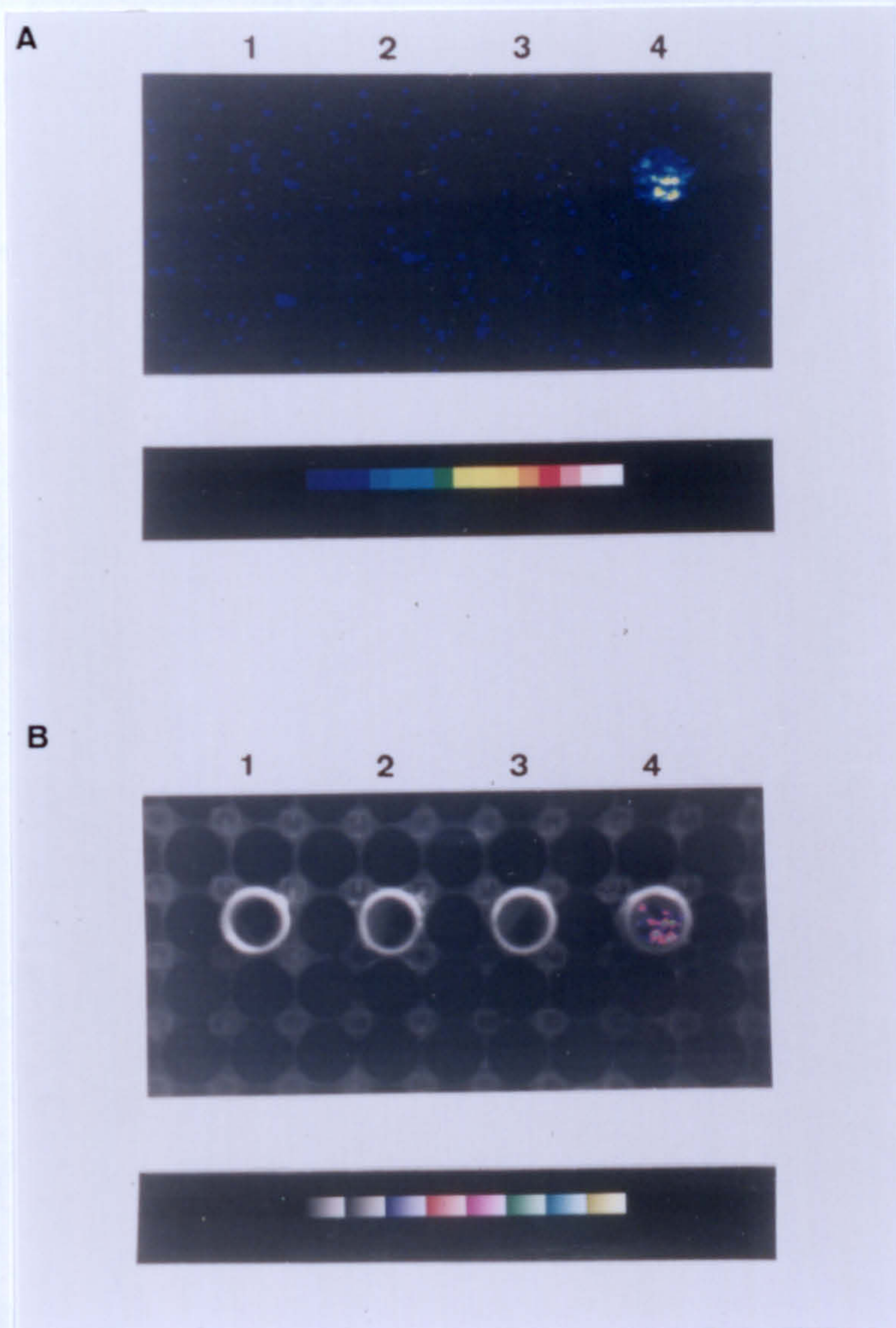


Fig. 5.15 The effect of cold shock on whole cultures of *Physcomitrella*. Transformed and untransformed cultures were placed in microtitre containers and imaged using a photon counting camera.

a) calcium-dependent aequorin luminescence in response to a temperature-shock of 0°C. Photons were integrated over a period of 20s.

b) light image of the experimental set-up superimposed on the luminescence image. Nos.1 and 2 contain untransformed moss. Nos.3 and 4 contain transformed cultures. Iced water was added to nos. 2 and 4.



response of the gametophore-overproducing strain *gam-139* was the closest to the wild-type response. Of the two cytokinin-sensitive mutants, the most sensitive, *nar-87*, showed the smallest response to cold-shock. The response of the less sensitive *bar-576* was between the two.

The three mutants also responded to increased pH by increasing intracellular calcium concentration (fig 5.16). The response of each parallels the response to cold-shock. This result suggests that the two cytokinin-sensitive mutants are defective in some aspect of membrane transport involving calcium release. Their response to the calcium-mobilising agents does not reflect their sensitivity to cytokinin.

The results reported here on the response to an increase in pH contrast to those of Felle (1988), who measured a decrease in cytoplasmic  $\text{Ca}^{2+}$  in response to an increase in external pH from 4.2 to 9.5, and reports that cytoplasmic alkalinization results in a decrease of cytoplasmic free  $\text{Ca}^{2+}$ . It is possible that the initial release of calcium is rapidly compensated for in *P. patens*. However Felle (1988) measured a large increase in cytoplasmic calcium in response to alkalinisation of the vacuole with neutral red, and proposed that an  $\text{H}^+/\text{Ca}^{2+}$  antiporter was located at the tonoplast. It is possible that the change in external pH caused calcium release from the vacuole in this instance. The results are in agreement with those of Bush and Jones (1988) who reported that large changes in cytoplasmic  $\text{Ca}^{2+}$  can be induced in barley aleurone protoplasts by raising external pH.

The addition of the hormones BAP and IAA at 1 and 10  $\mu\text{M}$  to cultures of wild-type *P. patens* incubated overnight in coelenterazine elicited no measurable response (fig. 5.13b). No difference was observed between cultures incubated in coelenterazine plus water and coelenterazine plus calcium-containing medium.

An alternative approach to examining the effect of BAP or auxin on intracellular calcium levels is to incubate cultures in coelenterazine and then add IAA and BAP for a period of incubation. The amount of aequorin left after a long period of incubation in the hormones may provide a measure of the aequorin being used in that time, and may pick up long-term shifts in calcium levels that cannot be picked up on the



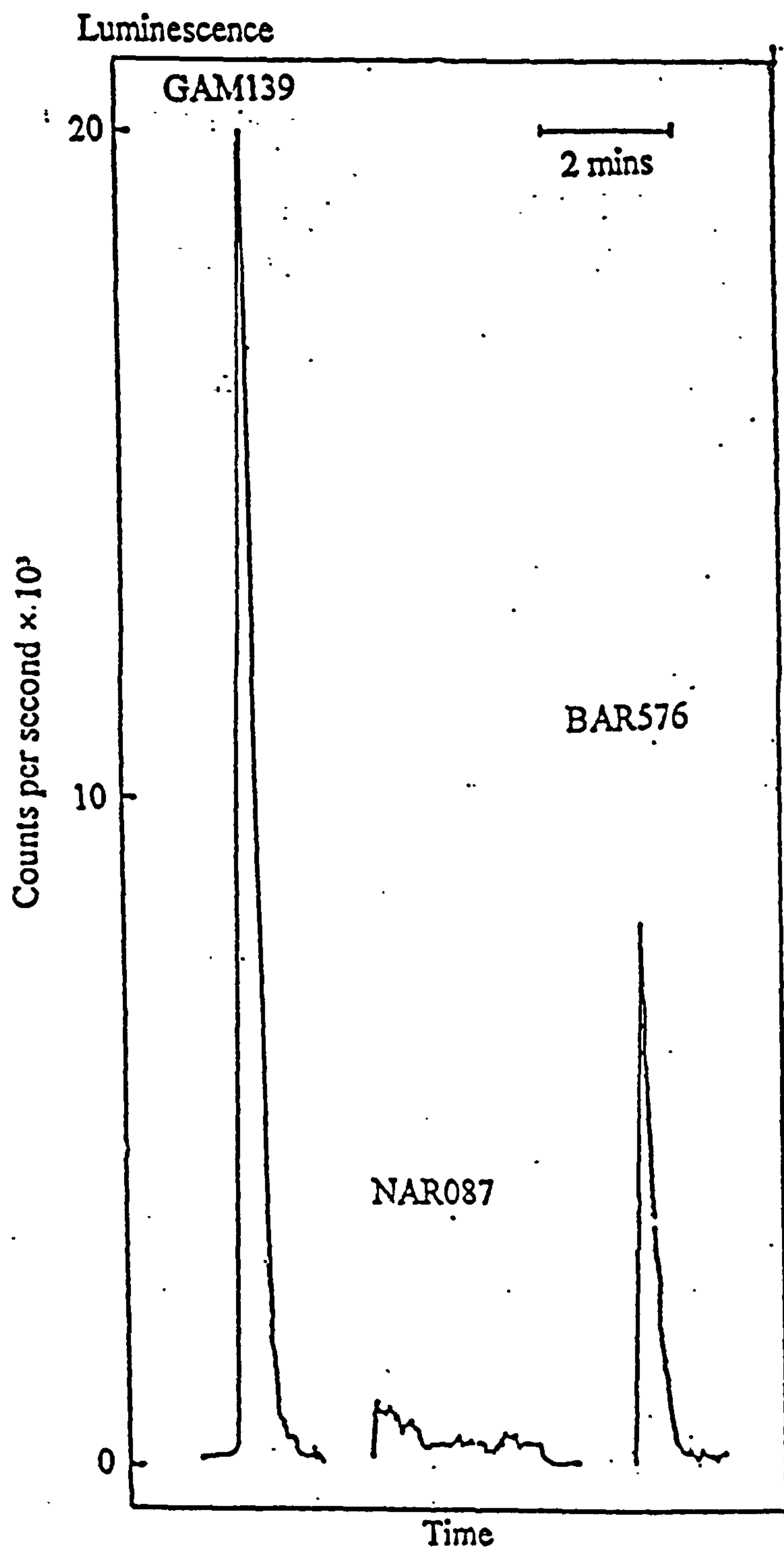


Fig. 5.16 The effect of pH 10.5 on calcium-dependent aequorin luminescence in the mutant strains transformed with apoaequorin.



luminometer. It was not possible to carry out this experiment successfully because of the difficulty experienced in extracting aequorin from the cultures. However no significant difference in the response to cold shock was noted in cultures incubated in BAP and IAA for up to 20 hours.



## CHAPTER VI

### GENERAL DISCUSSION

In this project I have developed methods of analysing growth and development in *Physcomitrella patens*, using time-lapse video microscopy and the quantitative analysis of developmental pattern. Particular attention has been given to the action of the plant hormone cytokinin in inducing buds. I have explored the hypothesis that the mode of action of cytokinin is linked to an influx of calcium, using traditional experimental methods of exogenous applications of hormones and inhibitors, and new imaging technology. In this discussion, I wish to summarise the main results of these experiments, and discuss them with reference to future experimental work.

#### 6.1 Time-lapse microscopy

The use of time-lapse microscopy has clarified many aspects of early protonemal development that were previously unclear, and has provided a more complete picture of the early stages of moss development. The following sections summarise the more significant observations from time-lapse films.

##### 6.1.1 Spore germination and protonemal development

Time-lapse films of spores of *P. patens* have provided a sequence of development from germination to the formation of buds. It has been possible to obtain accurate growth rates of primary and secondary chloronema, to follow the transition from one to the other, and to record the period of time for which primary chloronemal growth continues.

It is interesting to compare the germination of spores and growth of *P. patens* and *F. hygrometrica*, as both species are used in a similar manner in developmental



studies. The two species differ in that spore germination in *P. patens* is less clearly polar than in *F. hygrometrica*. The first cell division appears to occur within the spore in *P. patens*, whereas in *F. hygrometrica* it occurs in the primary filament. This has implications for studies of light-induced polarity in the two species. Polarity of germination can be easily controlled by light in *F. hygrometrica*. The two primary chloronemata of *P. patens* turn towards a unidirectional light source after their initiation, but it is not easy to see if their origin has been influenced by the light direction. The primary chloronema of *F. hygrometrica* does not show the intermittent growth observed in *P. patens*.

Previous work on *P. patens* and *F. hygrometrica* defined a primary chloronemal growth phase of about one week, before the caulonemal phase of growth begins. The time-lapse studies bring into question this simple definition of primary chloronema. In *F. hygrometrica* the spore forms the base of a single filament. All further filamentous growth develops as side-branches from this primary filament. In *P. patens* the two cells from which the primary filaments originate behave as subapical cells and undergo further mitosis to form new filaments, which appear to be originating from the spore, rather than the primary filaments. However, as they occur after the first division of the primary filaments, their exact origin is debatable. At its most limiting definition, primary chloronema refers to one filament in *F. hygrometrica* and two filaments in *P. patens*. Time-lapse microscopy has revealed that primary chloronemal growth in *P. patens* is slow and intermittent, lasting no longer than two or three cell cycles. The distinction between chloronemal and caulonemal phases of growth is blurred from the start. From one of the cells of a *P. patens* spore a filament emerges, in the case of each spore filmed the third filament, which grows faster than the first two filaments from the outset (fig. 2.4). Although this filament has transverse cross walls, it does not grow in the same slow and intermittent manner as the primary chloronema filaments, so that the spore appears to produce a filament that is transitional between chloronema and caulonema from the start. Only one of the two cells produces a



transitional filament. This suggests that the first division of the spore germ cell may create an unequal distribution of resources in the two cells.

The switch from chloronema to caulonema occurs earlier than previously believed, and affects all filaments at approximately the same time, regardless of when they emerged from the primary cells. Four to five days after germination, a spore is surrounded by a radial growth of filaments consisting of the primary filaments which emerged from the spore, and their side-branches. By the sixth day after germination, the primary filaments have either switched to caulonema, or stopped growing. It seems that the earlier filaments to emerge take several cell cycles to undergo the transition to caulonema, whereas the later filaments undergo the switch in a single cell cycle. It does appear, therefore, that a caulonema growth phase is reached at a certain time after germination. Under the standard conditions employed, this phase is reached after 5 days. The wider definition of primary chloronemal growth in *P. patens* could refer to the first four days after spore germination, but take into account the first transitional filament. Primary chloronema can therefore be considered to include all chloronemal growth including chloronema side-branches that arise from primary chloronema before the caulonemal growth phase is reached.

The time-scale in which the transition from chloronema to caulonema occurs has implications for studies on isolating caulonema-specific proteins. If spore germination could be synchronised, which may be possible with regimes of darkness and light, experiments aimed at the possible identification of proteins associated with different developmental stages should be started as early as two days after germination.

The first stages in the transition between chloronema and caulonema have been more fully defined using time-lapse techniques. The first sign that a filament is going to switch to caulonema is an increase in the growth rate of the apical cell, and the appearance of a vacuolated area in the tip of the apical cell. As the growth rate



increases, the cell cycle time decreases, however the length of cells continues to increase until the growth rate has reached the maximum level. The oblique cell wall does not begin to appear in *P. patens* until a growth rate of *ca.* 9 to 12  $\mu\text{m}$  is achieved. Only when the oblique cell wall can be seen can a filament be clearly defined as caulonema. However, extended periods of growth between 4  $\mu\text{m}$  and 10  $\mu\text{m}$  per hour, which define the transitional phase between the two filament types, are not uncommon under certain conditions. Growth rate is frequently quoted as one of the parameters defining chloronema and caulonema. It is debatable whether a filament can still be defined as chloronema once the growth rate has begun to increase over 6  $\mu\text{m}$  per hour, or whether this is the point at which the switch to caulonema has begun and the cell is transcribing some factors specific to caulonema.

#### 6.1.2 Bud formation

Time-lapse recording revealed that the early cell divisions of natural bud formation follow a set pattern and that under standard conditions of growth, this pattern is set before the first cell division. The first division divides the bud initial into two distinctive regions, one of which divides to produce two determinate cells, the stalk cell and first rhizoid. The other region, containing the majority of chloroplasts, divides at the same time, but the two cells produced as a result of this division remain indeterminate. The gametophore, including all three primary leaf initials, and further rhizoids, develops from these two cells. Both cells of this region appear to be meristematic, although from the recordings it is hard to tell if the cell nearer the stalk gives rise only to rhizoids. Previous descriptions of bud formation frequently refer to a three-celled initial with a meristematic tetrahedral apical cell, from which the gametophore develops, (for example, Idzikowska and Nuccitelli, 1974, describing *F. hygrometrica*). One reason for errors such as these is the fact that buds induced by cytokinin are frequently used as a basis for study (see below). Time-lapse recording has shown that bud formation, at least in *P. patens*, is more complex and that the



gametophore develops from a four-celled initial, the pattern of which may be determined at the single cell stage. Filming also revealed that this pattern could be very easily perturbed, both in terms of the spatial arrangement of the first cells, and the timing of the appearance of the first rhizoids and leaf initials. Low light causes a callus bud to develop with many rhizoids. High concentrations of auxin also encourage rhizoid formation (Ashton *et al*, 1979, and personal observation). High concentrations of cytokinin result in the formation of callus buds, but in this case without rhizoids. The addition of lanthanum has been shown to alter the early pattern of cell divisions. However, in this case, the basal cells do produce rhizoids, and an apparently normal bud can result from an abnormal early cell pattern. This suggests that the position of a cell within the initial is important in its subsequent differentiation. Gradients of substances, or morphogens, in the initial may be important in the determination of cell fate, which may include, or be, gradients of auxin and cytokinin.

### 6.1.3 The effects of cytokinin

The recording of the effect of cytokinin on bud production revealed that high concentrations of cytokinin alter the pattern of cell division of bud initials, but not the timing of the divisions, so that cytokinin does not appear to alter the cell cycle time. Each cell in a cytokinin-induced bud acts as an independent unit, responding to cytokinin to produce callus. Rhizoid formation is entirely inhibited. If the determination of stalk, leaf and rhizoid cells is by means of the establishment of morphogen gradients, these would be upset by the addition of high concentrations of any one of the substances.

Other effects of cytokinin were also revealed. At concentrations of 1  $\mu$ M and 100nM, the apical cells of caulonema filaments gradually lose their polarity, and revert to chloronemal growth after *ca.* 3 days. This may be an effect of the



stimulation of chloroplast division. The subapical cell produced by the division of the apical cell at the time of application of the hormone divides to give rise to a bud. Subapical cells produced subsequent to cytokinin application frequently do not divide again, resulting in an unbranched region of several cells. As the amount of cytokinin in the medium may exceed the uptake capacity of the filaments by as much as 40% (Wang *et al*, 1984), it is possible that in the proliferation of buds, a factor necessary for cell division other than cytokinin is used up, so that the subapical cells no longer divide to produce initials. The apical cell continues to grow and divide, so that either different concentrations of the same factor, or different factors, regulate apical cell division and subapical cell division.

## 6.2 Side-branch analysis

Time-lapse microscopy also provides the basis for undertaking an analysis of side-branch fate. The filming of side-branch initials clarified the position at which a particular branch type could be distinguished for the purpose of analysis. The different side-branch types could generally be distinguished at an early stage, by their length before their first cell division. When, as occurs rarely, a caulonema filament develops directly from the division of a subapical cell, it is sometimes possible to detect this developmental pathway before the division of the parent subapical cell is completed. In this case at least, it appears that the developmental fate is determined from the beginning of the development of a protrusion of the subapical cell, and is not therefore an event independent of the state of the parent subapical cell. The analysis of the fate of side-branch pairs however suggests otherwise, in that there does not appear to be any relationship between the developmental fates of side-branches arising from the same subapical cell. Some subapical cells do produce two buds, or two caulonema filaments, however this does not occur more than is compatible with each side-branch fate being independent. Side-branch fate therefore does not appear to depend on the state of the subapical cell. Side-branch initials themselves are clearly



susceptible to various external factors. Bopp (1984) found that initials were responsive to growth substances up to a length of 80 $\mu$ m. High light encourages the developing side-branch to switch to caulonema, low light encourages chloronemal growth, or inhibits side-branch development altogether. The state of the parent subapical cell may therefore be regarded as just one of the factors influencing the developmental fate of the side-branch initial.

Time-lapse recording revealed that the majority of caulonema side-branches, or secondary caulonema, begin as chloronema and switch to caulonema after two or three cell divisions. The inclusion of this class of side-branch fate, which I have called transitional caulonema in the side-branch analysis adds extra complexity to the developmental fates available to the initial. A subapical cell may produce a chloronemal initial, a caulonemal initial, or bud. A chloronemal initial may subsequently remain a chloronema, or switch to produce a caulonema filament. Transitional side-branches appear developmentally similar to the primary filaments of the spore, undergoing a similar progressive increase in growth rate and decrease in cell cycle time over a period of 2 or 3 cell divisions.

This has allowed a fuller branch analysis to be carried out than was previously possible. Fig. 6.1 shows a cell lineage for *P. patens* based on the results of this analysis.

The proportions of each branch type for the wild-type *P. patens* provide a standard control against which to assay the effects of environmental factors, and mutant phenotypes. These proportions differ from a previous analysis in that they differentiate between transitional and non-transitional caulonema. Caulonema that are caulonema from inception were found to be rare, less than 1% of the total. This analysis also differs in that no effect of subapical cell position on branch-type was found, except for transitional caulonema, which could not be identified as such until



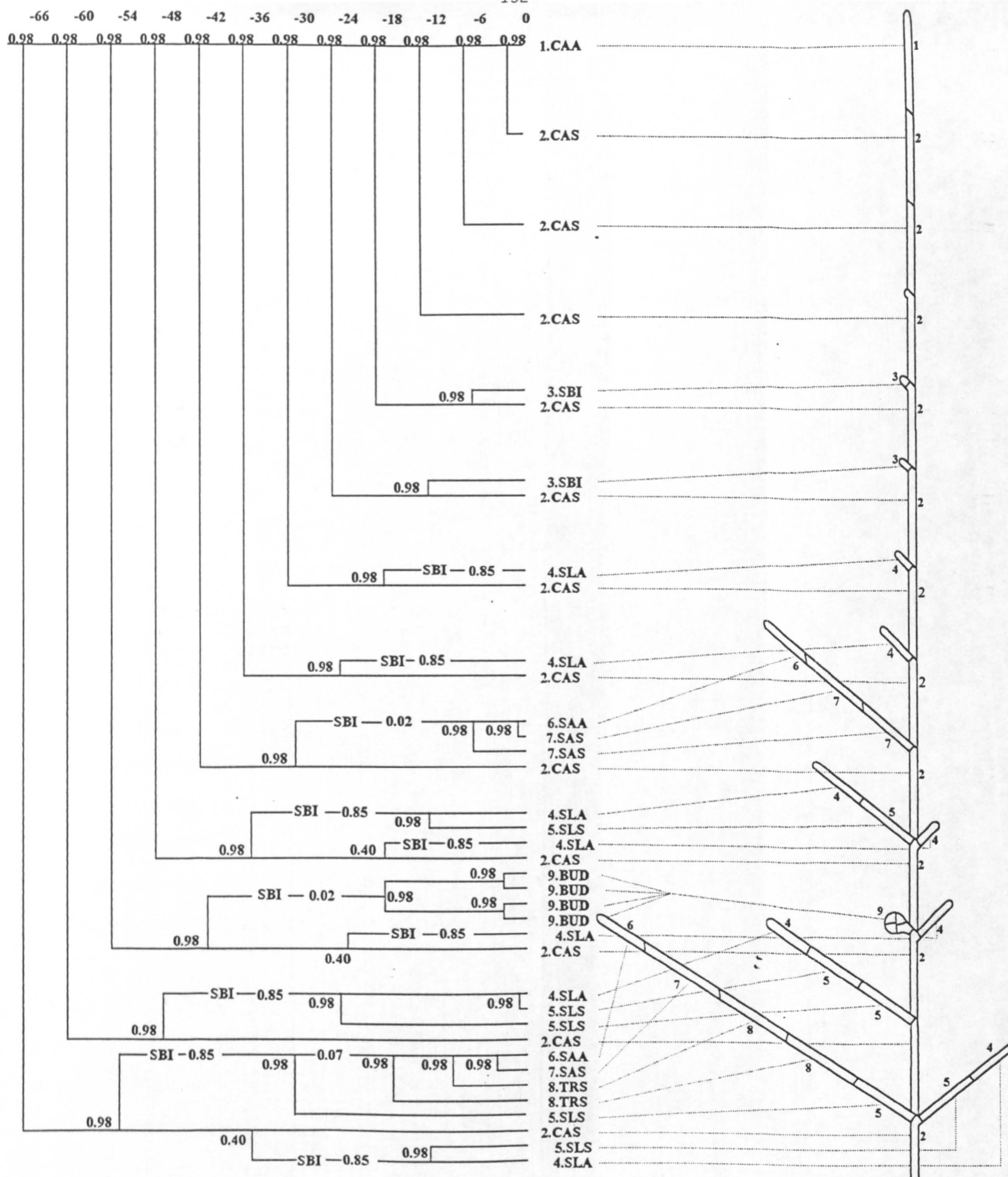


Fig. 6.1

Cartoon of the apical portion of a caulonemal filament (on right) together with the cell lineage which gave rise to it. (on left). Dotted lines connect the lineage to the corresponding cells in the cartoon.

The filament is not a deterministic structure, different caulonemal filaments having different detailed patterns. The cell lineage is therefore probabilistic. The probabilities of each branch point on the cell lineage are given. Where probabilities are in normal type, they are those calculated from observations in chapter 3 of this thesis, where they are in *italic type*, they have been estimated less accurately by others (D.J.Cove, unpublished data). The top row of figures give the time in hours before the observation of the filament as displayed.

Key to cell types:

- |        |                                      |
|--------|--------------------------------------|
| 1. CAA | caulonemal apical                    |
| 2. CAS | caulonemal sub-apical                |
| 3. SBI | side branch initial                  |
| 4. SLA | secondary chloronemal apical         |
| 5. SLS | secondary chloronemal sub-apical     |
| 6. TRS | chl;oronemal/caulonemal transitional |
| 7. BUD | bud/gametophore                      |



they had undergone one or two cell divisions, and therefore only appear from the ninth subapical position onwards. Chloronema, non-transitional caulonema and buds could all be distinguished by the 4th or 5th subapical cell position, when they arose as the first side-branch from a caulonema subapical cell. No evidence for a window of development for side-branch type was found, as was suggested in a previous analysis (McClelland, 1988). Transitional caulonema were the most variable cell type. It would seem that all chloronema side-branches have the potential to switch to caulonema, but that only some do, this proportion being highly dependent on external factors.

All subapical cells have the potential to divide two or three times. Time-lapse has shown that under standard conditions the second cell division of the subapical cell occurs approximately 18 hours after the first, or when the apical cell has undergone a further 3 cell divisions. The results of the analysis show that only around 40% of subapical cells divide to produce a second side-branch. This is a highly variable quantity. The results of the chi-squared test for this part of the analysis showed heterogeneity between the control cultures. Sub-optimum growth conditions, such as phosphate-free medium, or low light levels, affect the ability of subapical cells to divide. The fact that even under optimum growth conditions not all cells divide twice, again suggests the existence of a cell division factor that is limiting. Alternatively, the cells may produce an inhibitor of cell division.

The existence of a cell division factor is further suggested by the analysis of the mutant strain *nar-87*. The high numbers of second and third side-branches in this mutant suggest the overproduction of such a factor. This factor is separate from cytokinin as *nar-87* forms buds in response to the addition of exogenous cytokinin, so is not lacking in cytokinin receptors for bud formation.

An alternative model to explain the phenotype of *nar-87* is the possibility that side-

branch formation and bud formation may depend on different concentrations of cytokinin and therefore different ratios of cytokinin to other factors. The strain *nar-87* has a phenotype consistent with reduced levels of cytokinin. A very low concentration of cytokinin can result in side-branch formation (Markmann-Mulisch and Bopp, 1987), whereas a high concentration can result in the inhibition of side-branch initials (this thesis). A concentration of cytokinin somewhere between these extremes may result in the production of more side-branch initials than the concentration necessary for bud production.

### 6.2.1 Hormones

Detailed observation on the effects of the addition of 1 $\mu$ M NAA to cultures confirmed previously published data, in the overall growth of a culture appears to be reduced. Because there is an inhibition of growth of the apical cell of the main caulonema filament, as well as of chloronema, it is likely that this concentration of auxin has a general toxic effect rather than specifically inhibiting chloronema. While NAA reduced the number of buds, no increase in non-transitional caulonema occurred. Ashton et al (1979) state that production of caulonemata is increased by 2.5 to 50 $\mu$ M NAA, so these results may reflect the lower concentration used in this study.

This method of branch analysis provided a means of assaying the effect of different concentrations of cytokinin. A full branch analysis was carried out for three concentrations of cytokinin (30nM, 100nM and 1 $\mu$ M). An analysis of bud production alone was made for 30nM and 50nM BAP. The results of the analysis differ from previous analyses. Both McClelland (1988), working with *P. patens*, and Bopp (1984), working with *F. hygrometrica* report that increasing the concentration of cytokinin increases the number of responsive cells along a filament. Bopp reports that as the concentration is decreased, the number of cells along a filament that respond by



producing buds decreases until at the lowest concentration, only the sixth cell in a filament responds, so that the most sensitive cell to cytokinin is the subapical cell when it is in the sixth position. In the present analysis, the high concentrations of cytokinin defined the range of sensitive cells. This was found to cover approximately 10 cell positions, including the second initials produced by subapical cells, and agrees with Bopp's report that initials are sensitive until approximately 80µm length (Bopp,1984), which, in *P. patens*, is about the length of a chloronema side-branch when it undergoes its first division. It was found, however, that the lower concentrations of cytokinin affected all cells equally within that range, rather than initials at any particular subapical position. This was also the case with the mutant *bar-576*, which was less sensitive to 1µM BAP. Rather than a lower concentration narrowing the window of sensitivity, these results suggest that all cells in the sensitive region respond equally to low concentrations of cytokinin. The cells most sensitive to cytokinin could be defined more clearly at the higher concentrations, and these were in the four immediately subapical positions at the time of hormone application. At the time of application, two of these cells would have formed initials, and two would not yet have reached that stage. It is difficult to conclude whether the effect in the case of the cells without initials is through an effect on the subapical cell or a later effect on the initials after they have emerged.

The use of this method of branch analysis identified a mutant, previously thought to be unable to produce gametophores, as overproducing buds, the development of which was curtailed at the 4 cell stage. This method of analysis has considerable potential for the detailed characterisation of mutant phenotypes, as already discussed in relation to *nar-87*. The analysis of mutant strains combined with analysis of wild-type moss should allow the identification of key developmental parameters.

### 6.2.2 Bud spacing

The results of the bud spacing analysis show that, when total buds are considered without regard to origin, buds are not formed randomly, but occur in clusters. Buds are not inhibited from forming in regions of the filament which have already produced a bud, rather it seems that buds encourage other buds to form. When more than one bud is produced on a filament, it is more likely to be close to the previous bud, than many cells apart. The question remains whether this is restricted to individual filaments, or to regions of the protonemata i.e. is the transport of bud-forming substances symplastic or extracellular. Colonies may possess foci of cytokinin synthesis, causing a gradual build-up of cytokinin in certain areas of the culture.

### 6.3 Mutant strains

Several existing mutant strains were further characterised in terms of their response to cytokinin, in order to evaluate their potential in studies on cytokinin action. The mutant strains *nar-87*, and *gam-710* were found to have a response to BAP similar to the wild-type moss. Strain *bar-576* exhibited a lower sensitivity to BAP. The strain *bar-1* was insensitive. In view of the putative association of cytokinin action with calcium, the effect of the ionophore A23187 was also tested on these mutants. Strain *bar-1*, resistant to cytokinin, exhibited the highest sensitivity to the ionophore. The response of *nar-87*, *bar-576* and the bud-overproducing strain *gam-139* was similar to that of wild-type moss. The strain *gam-710*, however, which responded normally to cytokinin, exhibited a much lower sensitivity to the ionophore. The influx of calcium did not cause any of the mutants to produce buds. No obvious relationship appeared between sensitivity to cytokinin and sensitivity to the ionophore. The synergistic effect of BAP on the response of *gam-710* to the ionophore needs further investigation. The mutants also exhibited differential responses to the calcium channel blocker lanthanum. Strain *nar-87* exhibited the most sensitive response, stopping



growth entirely at a concentration of 100 $\mu$ M LaCl<sub>3</sub>. The fact that these mutants exhibited different responses to the ionophore and to lanthanum suggests that the mutations affect their ion transport systems, as already discussed in chapter IV. Further experiments are necessary to confirm this. If it proves to be the case, these may be useful mutants for studies of the relationship of cytokinin action to ionic fluxes.

#### 6.4 Calcium and cytokinin action

The mode of action of cytokinin has been linked to rises in intracellular calcium (ch. 1.6). This hypothesis was explored using classical electrophysiology, established calcium channel inhibitors, and two techniques in calcium imaging. The results show that if a relationship between calcium and cytokinin action exists, it is not easy to establish. This is in part due to the nature of plant cells, and the large amounts of calcium stored in the cell wall and vacuolar compartments. On the one hand, it is virtually impossible to achieve a calcium-free external environment. On the other, perturbation of these stores leads to a range of non-specific effects on growth. Working with protoplasts bypasses some of these effects, but renders it impossible to relate a response to a specific developmental event.

##### 6.4.1 Calcium imaging

The results of the calcium imaging experiments are preliminary. Many problems associated with both types of imaging could not be resolved during the period of the study.

Ratio-imaging requires the maintenance of a strong fluorescent signal in the cell. The major problem experienced was the movement of dye into adjacent cells. While fluorescence could frequently be visualised in successfully loaded cells 24 hours after

injection, it did not provide a strong enough signal for ratio-imaging. In general, the signal remained strong enough for at least 30 minutes after introduction of the dye. More experiments need to be performed to establish the potential of this technique. When dye is successfully loaded into subapical cells, it moves quickly into the side-branch initials, the main targets of cytokinin action. This suggests that there is considerable potential for further study using this method.

The incubation method of dye-loading was reported to be successful for *F. hygrometrica* (Hahm and Saunders, 1991). This is the only report of this being the case in cells with walls. Many attempts were made to load *P. patens* with dye using the published incubation methods. In no instance could dye be visualised in undamaged cells.

The advantages of microinjection are that experiments can be performed before the dye has had time to be sequestered into intracellular organelles or the vacuole. The amount of dye entering the cells can be controlled to a greater extent. Filaments are not subject to the damage incurred by the washing necessary before and after incubation. However, the technique of microinjection is time-consuming, and not enough cells were successfully loaded during the period of the study to produce reliable results.

Previously published results of increases in intracellular calcium in response to cytokinin are conflicting. Saunders and Hepler (1981) report that CTC fluorescence becomes high in developing side-branch initials in *F. hygrometrica* approximately 12 hours after treatment with cytokinin and remains high during the first few divisions of the bud. This conflicts with later experimental evidence obtained using a vibrating microelectrode in which Saunders (1986) reports an immediate increase in inward current up to an hour after the application of cytokinin, then a fall back to normal levels with no evidence of increased inward current at the site of the developing



initial. Using Indo-1 loaded into *F. hygrometrica* by means of incubation in acid medium, Hahm and Saunders (1991) once again report a sustained rise in calcium to 750 $\mu$ M throughout all the protonema in calcium-containing medium. This only occurred in protonema incubated in BA with Indo-1, so the cells would have been incubated at least 2 hours in BA. The results published in this paper therefore do not suggest a transient rise in intracellular calcium as a mode of action of cytokinin.

The preliminary results using fluorescent dyes reported in this thesis do not indicate either a transient or sustained rise in calcium in response to BAP. However, because of the mobility of the dye in the cells, more experiments need to be undertaken to be sure of this result. The pressure microinjection of dextran-linked dyes may resolve the problem of dye moving through the plasmodesmata, although this technique has not yet been widely explored in plants (Graziana *et al*, 1993). These experiments could also be complemented by the use of photometry.

The ratio method showed that there is not necessarily a relationship between visual fluorescence intensity and calcium concentration. The greater visual fluorescence intensity in the initial may be due to a greater density of cytoplasm, and the presence of densely packed organelles.

#### 6.4.2 Transformation with aequorin

As in the case of the ratio-imaging, the experiments using moss transformed with aequorin are preliminary. However, they show that moss can be stably transformed with the gene for apoaequorin and aequorin can be reconstituted with no toxic effects.

Some interesting preliminary results were obtained using the transformed mutants. While the gametophore-overproducing strain *gam-139* responded to cold-shock in

the same way as the wild-type moss, the mutant strain *nar-87* consistently showed a much smaller response. This suggests that this mutant may be altered in the cell membrane so as to affect uptake mechanisms, or alternatively, altered in the ability to release bound calcium from internal membranes. Further experiments with this mutant strain are necessary to confirm this, and to attempt to distinguish between these possibilities.

The lack of a release of aequorin luminescence in response to cytokinin confirms the results of classical electrophysiology, where cytokinin action is not accompanied by membrane depolarisation, and thus suggesting that there is no immediate transient rise in intracellular calcium. No calcium luminescence in response to cytokinin was measured over a 20 minute period, so that a sustained rise in intracellular calcium is not immediately apparent either. The results of classical electrophysiology were equivocal, however in experimental work where cytokinin has been found to have an effect on the membrane potential, and therefore ion fluxes, the use of inactive analogues has shown that this effect is not necessarily related to the biological activity (Parsons *et al*, 1989).

As well as examining the effects of cytokinin and other plant hormones, the transformed moss has the potential to allow the effects of other agents on intracellular calcium to be explored. Preliminary experiments have shown that there may be effects of low and high pH on intracellular calcium. This needs to be investigated further, also it may be possible to determine if high concentrations of inhibitors have effects on intracellular calcium. A further experiment would be to quantify the effect of the ionophore A23187, and relate this to biological effects.

### 6.5 Calcium and bud formation

The response of caulonema tip cells to A23187 is initially a slowing or cessation of



growth, followed by a swelling of the apical tip. The appearance of this characteristic growth pattern in response to other agents, such as light, suggests that an influx of calcium has occurred. In some cases, the subapical cell reacts by producing a caulonema side-branch, in response to the loss of apical dominance of the tip cell. In many instances one of the initials produced subsequent to the response develops into a bud.

The response of side-branch initials to cytokinin is a slowing of the growth rate and swelling of the cell apex. Superficially, this is similar to the response of the apical cell to a calcium influx. Conrad and Hepler (1988) perceive the loss of polarity of the tip cells in response to the calcium agonists (+)202-791 and CGP28392, both at concentrations of 100 $\mu$ M, as evidence that "even the tip cells produce buds". However, the two responses are hardly equivalent. Caulonema apical cells do not swell in response to the concentrations of cytokinin that induce buds. They do swell in response to toxic concentrations of inhibitors in a manner analogous their response to A23187. When a sustained rise in intracellular calcium does lead to the production of buds, this is an effect on the subapical parent cell before the initial has been produced. Existing initials are not stimulated to turn into buds. The effect of cytokinin is on existing initials, and subapical cells that form subsequently do not even form side-branch initials. The effect of cytokinin occurs within hours, while the response to calcium influx is over several days.

It has been suggested that only a small percent of the total material imaged using aequorin, or measured using electrophysiology, is cytokinin-sensitive, and that this is a reason for not detecting a response. However, as early as 1978, Erichsen *et al* reported that all cells were able to take up labelled kinetin. The fact that, in phosphate-free medium, where side-branch initial formation is usually absent, cytokinin stimulates the subapical cell to divide, confirms that uptake of cytokinin is throughout the filament, and not just by receptive side-branch initials. The results suggest that this response to cytokinin, which relates to overall uptake, would

therefore appear not to be associated with a calcium influx, contrary to the idea of Markmann-mulisch and Bopp (1987). Hanke *et al* (1990) found that the calcium channel blockers  $\text{La}^{3+}$ , D600 and verapamil did not inhibit cell division in cytokinin-dependent suspension cultures of soybean callus. Neither could the  $\text{Ca}^{2+}$ -ionophore A23187 induce cell division in cells mitotically arrested by cytokinin deprivation. These results support the argument against a role for extracellular calcium in the mode of action of cytokinin. However, the sensitivity of the side-branch initial to higher concentrations of cytokinin may be a different, and a more specific, response. Whether this sensitivity relates to a different and highly localised uptake mechanism, or whether it is due to the retention of localised receptors, cannot be determined. If overall uptake of cytokinin is not accompanied by an influx of calcium, it is hard to imagine that this might occur in a very specific region of the cell, i.e. the tip of the developing side-branch initial before it undergoes the first cell division as a side-branch.

This work confirms earlier work (Kubowicz *et al*, 1982; Kuiper *et al*, 1992) that if there is a relationship between cytokinin and intracellular dynamics, this is indirect, rather than direct. The fact that the budding response is reversible for as long as 24 hours (Brandes and Kende, 1968) is also incompatible with a transient rise in calcium that sets in motion a cascade of irreversible events. Brandes and Kende (1968) state that this shows the hormone does not act as a trigger. This also supports the suggestion by Blowers and Trewavas (1989) that a hydrophobic molecule such as cytokinin does not need a receptor-operated second-messenger system.

However, a role for calcium in bud induction cannot be entirely discounted, as a sustained rise in calcium caused by A23187 can induce buds. Branching pattern analysis shows that this is a different pattern of budding from that induced by cytokinin. Rather than every side-branch initial stimulated to develop into a bud, only a few side-branch initials on each filament develop into buds. These are highly specific



for a certain subapical position, rather than random as at a low concentration of cytokinin. Buds can also be induced by other agents such as light, even nifedipine. It is possible that in a filament competent to produce buds, different agents can induce the budding response via different mechanisms.

## APPENDIX A

Methods and procedures for *Physcomitrella patens*Media and supplements

The medium routinely used for the culture of *P. patens* is a modified Knops medium, containing the following nutrients:

Ca(NO <sub>3</sub> ) <sub>2</sub> .4H <sub>2</sub> O	59mg l <sup>-1</sup>
MgSO <sub>4</sub> .7H <sub>2</sub> O	250mg l <sup>-1</sup>
KH <sub>2</sub> PO <sub>4</sub>	250mg l <sup>-1</sup>
KNO <sub>3</sub>	1.036g l <sup>-1</sup>
FeSO <sub>4</sub> .7H <sub>2</sub> O	10mg l <sup>-1</sup>
Trace element solution (TES)	1ml l <sup>-1</sup>

Trace element solution (Hoagland's A-Z):

H <sub>3</sub> BO <sub>3</sub>	614mg l <sup>-1</sup>
MnCl <sub>2</sub> .4H <sub>2</sub> O	389mg l <sup>-1</sup>
NiCl <sub>2</sub> .6H <sub>2</sub> O	59mg l <sup>-1</sup>
Al <sub>2</sub> (SO <sub>3</sub> ) <sub>3</sub> .K <sub>2</sub> SO <sub>4</sub> .24H <sub>2</sub> O	55mg l <sup>-1</sup>
CoCl <sub>2</sub> .6H <sub>2</sub> O	55mg l <sup>-1</sup>
CuSO <sub>4</sub> .5H <sub>2</sub> O	55mg l <sup>-1</sup>
ZnSO <sub>4</sub> .7H <sub>2</sub> O	55mg l <sup>-1</sup>
Kbr	28mg l <sup>-1</sup>
KI	28mg l <sup>-1</sup>
LiCl	28mg l <sup>-1</sup>
SnCl <sub>2</sub> .2H <sub>2</sub> O	28mg l <sup>-1</sup>



### Nutritional supplements

Mutant strains isolated from auxotrophic backgrounds required the following supplements:

nicotinic acid	1mg $l^{-1}$
p-amino benzoic acid	250 $\mu$ g $l^{-1}$
thiamine-HCl	100 $\mu$ g $l^{-1}$

Medium was solidified by the addition of 15g $l^{-1}$  bacteriological agar No.1 (Sigma or Oxoid).

### Growth in darkness or low light

Sucrose (0.5%, w/v) was added to the medium, either before or after autoclaving.

### Moss strains

All experimental work with *P. patens* was carried out using the wild-type stock (Ashton and Cove, 1977). The following mutant strains were also used for experimental work:

STRAIN	PHENOTYPE	REFERENCE
<i>bar-1, thiA1</i>	BAP resistance	Ashton <i>et al</i> , 1979
<i>bar-576, pabB6 thiA1</i>	BAP resistance	Grimsley, 1978
<i>gam-710, thiA1</i>	leaky <i>gam</i>	Grimsley, 1978
<i>gad-139, pabA3</i>	produces very small buds	Grimsley, 1978
<i>nar-87, thiA1</i>	BAP sensitive	Ashton <i>et al</i> , 1979
<i>ove-405, pabA3</i>	overproduces gametophores	



Spores of *Funaria hygrometrica* were obtained from a capsule from moss collected from a wood. Tissue of *Ceratodon purpurea* was obtained from the laboratory of Dr. F. Sack, Ohio State University.

### Inhibitors

Stock solutions of inhibitors were prepared as follows:

Verapamil and Trifluoperazine were dissolved in water to make  $10^{-2}$ M stock sol<sup>ns</sup>.

Nifedipine was dissolved in DMSO to make a  $10^{-2}$ M stock sol<sup>n</sup>.

A23187 was dissolved in 100% methanol to make a 15mM stock sol<sup>n</sup>.

### Buffers used for Western Analysis

Protein extraction buffer:

10 mM Tris pH 7.5

5mM Mercaptoethanol

One plate of homogenate tissue (*ca* 0.5g dry wt) was ground in 2 mls of buffer in a mortar and pestle. The resulting solution was spun at high power in a bench centrifuge. The supernatant was collected and stored at -20°C.

Laemli loading buffer:

2.3% SDS

10% glycerol

62.5 mM Tris-Cl pH 6.8

5% mercaptoethanol

Bromophenol-blue



Transfer buffer:

20% methanol  
 25 mM Tris  
 192 mM glycine pH 8.3  
 0.1% SDS  
 H<sub>2</sub>O

Transformation of *P. patens* using PEG

1. Protoplasts were isolated by incubating 1 g of 7-day old protonemal tissue in 10ml of 2% (w/v) Driselase (Sigma) / 8% mannitol solution for 40 minutes.
2. A further 10 ml of 8% mannitol was added and the mixture filtered through a 100µm nylon mesh protoplast filter to remove cellular debris.
3. The filtrate was centrifuged for 5 min at 700 rpm. The supernatant was discarded and the pellet resuspended in 20 ml of 8% mannitol. This procedure was repeated twice in order to remove residual driselase.
4. The concentration of protoplasts was estimated by placing a drop of protoplast solution on a haemocytometer and calculating the average average from three counts.
5. After the final wash, the pellet of protoplasts was resuspended in the correct amount of 8% mannitol/MgCl<sub>2</sub>/MES sol<sup>n</sup> to give a final concentration of 1.6.10<sup>6</sup> protoplasts/ml.
6. Aliquots of protoplasts (0.3ml) were placed in 10ml sterile tubes and mixed with plasmid DNA and 300µl PEG sol<sup>n</sup> (2g PEG 6000, 8% mannitol, and 0.1M Ca(NaO<sub>3</sub>)<sub>2</sub>).
7. The DNA/protoplast mixture was subjected to 5 minutes heat shock at 45°C, then placed at 15°C for 15 minutes.
8. Manitol (8%) was added 1ml at a time to dilute the protoplast sol<sup>n</sup> to 10 ml.
9. The solution was spun in a bench centrifuge at 700 rpm for 5 minutes and the supernatant discarded. The pellet was mixed with 10 ml molten top layer agar (6%

mannitol) and divided equally onto 3 plates containing bottom layer agar (8% mannitol) with cellophane overlay.

10. The transformed protoplasts were left to regenerate at 20°C for 3 days before being transferred to medium containing antibiotic.

#### Transformation of *P. patens* using a gun

1. 50 mg of dry tungsten powder (M17 grade, Sylvania, Towanda, PA 18848, USA) was suspended in 300 µl of absolute ethanol in a 1.5 ml Eppendorf tube, mixed vigorously, and then centrifuged at 10,000 x g for 5 minutes.

2. The tungsten was washed by resuspending in 1.5 ml sterile distilled water and centrifuging. This was repeated twice more. After the final wash, the tungsten was resuspended in 1ml of 50%(w/v) sterile glycerol.

3. 25µl of the tungsten suspension was mixed with:

5 µl plasmid DNA

25 µl sterile 2.5 M CaCl<sub>2</sub> solution

10 µl sterile 0.1 M spermidine (free base) solution

The suspension was mixed gently and allowed to stand for 10 minutes. 35 µl of the supernatant was carefully withdrawn and discarded. The mixture was transferred to ice until used.

4. Immediately before use, DNA-tungsten complexes were dispersed by briefly touching the outside of the Eppendorf microfuge tube to a horn-type sonicator probe. Immediately after, 3 µl of suspension was placed in the centre of the front surface of a plastic microprojectile, which was then placed into the barrel of the gun. Protonemal tissue grown for 6 days on cellophane-overlay plates was placed in the chamber without removal from the plate. The lid of the petri dish was removed and a sterile stainless steel mesh (aperture size 1mm x 1mm) was placed over the open plate. The chamber was evacuated to 28 mbar before discharge.

5. The gun used was made to the design of Lonsdale *et al.*, (1990), J. Exp. Bot



41:1161-1165, by Sheerline Precision Engineering Ltd., Cambridge Road, Milton, Cambridge CB4 4AT. Polycarbonate macroprojectiles were obtained from Turner-Richards, Birmingham, England. Blank launcher cartridges were obtained from Winchester Group, East Alton, Il 62024, USA. The best results with this gun are obtained with a distance of 150mm between the stopper plate and the tissue, and with two discharges per petri-dish of tissue (the position of the dish is moved between discharges).

6. Following bombardment the tissue was incubated under standard conditions for 48 h before being homogenised and placed on medium containing the appropriate antibiotic.

## REFERENCES

- Akerman, K.E.O., Proudlove, M.O. & Moore, A.L. (1983). Evidence for a  $\text{Ca}^{2+}$  gradient across the plasma membrane of wheat protoplasts.  
 Biochem. and Biophys. Res. Commun. *113*(1):171-177.
- Ashton, N.W. & Cove, D.J. (1977). The isolation and preliminary characterization of auxotrophic and analogue resistant mutants of the moss *Physcomitrella patens*.  
 Molec. Gen. Genet. *154*:87-95.
- Ashton, N.W., Grimsley, N.H. & Cove, D.J. (1979). Analysis of gametophytic development in the moss *Physcomitrella patens*, using auxin and cytokinin resistant mutants.  
 Planta *144*:427-435.
- Ashton, N.W., Schultz, A., Hall, P. & Bandurski, R.S. (1985). Estimation of Indole-3-acetic acid in gametophytes of the moss, *Physcomitrella patens*.  
 Planta *164*: 142-144.
- Bean, B.P. (1989). Classes of calcium channels in vertebrate cells.  
 Ann. Rev. Physiol. *51*:367-384.
- Berridge, M.J. (1993). Inositol trisphosphate and calcium signalling.  
 Nature *361*:315-325.
- Beutlemann, P. (1973). Untersuchungen zur biosynthese eines cytokinins in calluszellen von laubmoosporophyten.  
 Planta *112*:181-190.
- Bjorkman, T. & Cleland, R.E. (1991). The role of extracellular free-calcium gradients in gravitropic signalling in maize roots.  
 Planta *185*:379-384.
- Blatt, M.R., Thiel, G. & Trentham, D.R. (1990). Reversible inactivation of  $\text{K}^{+}$  *Vicia* stomatal guard cells following the photolysis of caged inositol-1,4,5-triphosphate.  
 Nature *346*:766-769.



Blowers, D.P. & Trewavas, A.J. (1989). Second messengers: their existence and relationship to protein kinases.

In: Second Messengers in Plant Growth and Development, ed. W.F. Boss and D.J. Morre. New York: Alan R. Liss, Inc., 1-28.

Bopp, M. (1961). Morphogenese der laubmoose.  
Biol. Revs. 36:237-280.

Bopp, M. (1980). The hormonal regulation of morphogenesis in mosses.  
In: Plant Growth Substances, ed. F. Skoog. Springer Verlag., 934-944.

Bopp, M. (1983). Developmental physiology of bryophytes.  
In: New Manual of Bryology, ed. R.M. Schuster. Hat. Bot Lab., 276-324.

Bopp, M. (1984). The hormonal regulation of protonema development in mosses II. The first steps of cytokinin action.  
Z. Pflanzenphysiol. 113:435-444.

Bopp, M. (1990). Plant hormones in lower plants.  
In: Plant Growth Substances 1988, ed. R.P. Pharis and S.B. Rood. Berlin, Heidelberg: Springer-Verlag, 1-10.

Bopp, M., Erichsen, U., Nessel, M. & Knoop, B. (1978). Connection between the synthesis of differentiation specific proteins and the capacity of cells to respond to cytokinin in the moss *Funaria*.  
Physiol. Plantarum 42:73-78.

Bopp, M. & Jacob, H.J. (1986). Cytokinin effects on branching and bud formation in *Funaria*.  
Planta 169:462-464.

Boss, W.F. and Morre, D.J. (eds) (1989). Second Messengers in Plant Growth and Development. New York: Alan R. Liss, Inc.

Boss, W.F. (1989). Phosphoinositide metabolism: its relation to signal transduction in plants.  
In: Second Messengers in Plant Growth and Development, ed. W.F. Boss and D.J. Morre, D.J. New York: Alan R. Liss, Inc. 29-56.

Boyd, P.J., Grimsley, N.H. & Cove, D.J. (1988). Somatic mutagenesis of the moss, *Physcomitrella patens*.

Mol. Gen. Genet. 211:545-546.

Brandes, H. (1967). Der wirkungsmechanismus des kinetins bei der Induktion von Knospen am Protonema der Laubmoose.

Planta 74:55-71.

Brandes, H. & Kende, H. (1968). Studies on cytokinin-controlled bud formation in moss protonema.

Plant Physiol. 43:827-837.

Bush, D.S. & Jones, R.L. (1987). Measurement of cytoplasmic calcium in aleurone protoplasts using Indo-1 and Fura-2.

Cell Calcium 8:455-472.

Bush, D.S. & Jones, R.L. (1988). Cytoplasmic calcium and  $\alpha$ -amylase secretion from barley aleurone protoplasts.

Euro. J. Cell Biol. 46:466-469.

Bush, D.S., Biswas, A.K. & Jones, R.L. (1989). Gibberellic-acid stimulated  $\text{Ca}^{2+}$  accumulation in endoplasmic reticulum of barley aleurone:  $\text{Ca}^{2+}$  transport and steady state levels.

Planta 178:411-420.

Bush, D.S. & Jones, R.L. (1990). Measuring intracellular  $\text{Ca}^{2+}$  levels in plant cells using the fluorescent probes Indo-1 and Fura-2. (Review).

Plant Physiol. 93:841-845.

Chae, Q., Park, H.J. & Hong, S.D. (1990). Loading of Quin2 into oat protoplasts and measurement of cytosolic ion changes by phytochrome action.

Biochem. Biophys. Acta, 1051:115-122.

Chen, T.H. & Jaffe, L.F. (1979). Forced calcium entry and polarized growth of *Funaria* spores.

Planta 144:401-406.



Cheung, W.Y. (1982). Calmodulin - an introduction.

In: Calcium and Cell Function, Vol. 1, ed. W.Y.Cheung. New York, London: Academic Press.

Chopra, R.N. & Gupta, U. (1967). Dark-induction of buds in *Funaria hygrometrica* Hedw.

The Bryologist 70:102-104.

Conrad, P.A. & Hepler, P.K. (1988). The effect of 1, 4-dihydropyridines on the initiation and development of gametophore buds in the moss *Funaria*.

Plant Physiol. 86:684-687.

Conrad, P.A., Steucek, G.L. & Hepler, P.K. (1986). Bud formation in *Funaria*: Organelle redistribution following cytokinin treatment.

Protoplasma 131:211-223.

Conrad, P.A. & Hepler, P.K. (1986). The PI cycle and cytokinin-induced bud formation in *Funaria*.

Plant Physiol. 80S: 60.

Cove, D.J. (1984). The role of cytokinin and auxin in protonemal development in *Physcomitrella patens* and *Physcomitrium sphearicum*.

J. Hatt. Bot. Lab. 55:79-86.

Cove, D.J. (1983). Genetics of Bryophyta.

In: New Manual of Bryology, Vol. 1, ed. R.M. Schuster. Hatt. Bot. Lab. 220-232.

Cove, D.J. & Ashton, N.W. (1983). The hormonal regulation of gametophytic development in bryophytes.

In: Experimental Biology of Bryophytes, ed A.F. Dyer & J.G. Duckett). Academic Press. pp177-201.

Cove, D.J., Schild, A., Ashton, N.W. & Hartmann, E. (1978). Genetic and physiological studies of the effects of light on the development of the moss *Physcomitrella patens*.

Photochem. and Photobiol. 27:249-254.

Cove, D. (1992). Regulation of development in the moss *Physcomitrella patens*.

In: Development, ed. V.E.A. Russo, S. Brody, D. Cove & S. Ottolenghi. Berlin, Heidelberg: Springer-Verlag, 179-193.

Cove, D.J. and Knight, C.D. (1993). The moss *Physcomitrella patens*, a model system with potential for the study of plant reproduction.

The Plant Cell 5 (*in press*).

Crowell, D.N., Kadlecek, A.T., John, M.C. & Amasino, R.M. (1990). Cytokinin-induced messenger-RNAs in cultured soybean cells.

Proc. Nat. Acad. Sci. USA 87(22):8815-8819.

Dieter, P. & Marme, D. (1980). Calmodulin activation of plant microsomal  $\text{Ca}^{2+}$  uptake.

Proc. Natl. Acad. Sci. USA 77:7311-7314.

Dieter, P. & Marme, D. (1981). A calmodulin-dependent microsomal ATPase from corn (*Zea mays* L.).

FEBS Lett. 125:245-248.

Doonan, J.H. (1983). Morphogenetic role of the cytoskeleton in *Physcomitrella patens*.

Ph.D thesis. University of Leeds.

Doonan, J.H., Cove, D.J., Corke, F.M.K. & Lloyd, C.W. (1987). The preprophase band of microtubules, absent from tip-growing moss filaments arises in leafy shoots during transition to intercalary growth.

Cell motility and the cytoskeleton 7:138-153.

Elliott, D.C. & Yao, Y. (1989). Cytokinin and fusaric acid effects on calcium transport in *Amaranthus* protoplasts.

Plant Science 67:243-252.

Elliott, D.C. & Petkoff, H.S. (1990). Measurement of cytoplasmic free calcium plant protoplasts.

Plant Science 67:125-131.



Elliott, D.C. & Skinner, J.D. (1986). Calcium-dependent, phospholipid-activated protein kinase in plants.

Phytochem. 25:39-44.

Engel, P.P. (1968). The induction of biochemical and morphological mutants of the moss *Physcomitrella patens*.

Amer. J. Bot. 55:438-446.

Erichsen, J., Knoop, B. & Bopp, M. (1977). On the action mechanism of cytokinins in mosses: caulonemal specific proteins.

Planta 135:161-168.

Erichsen, U., Knoop, B. & Bopp, M. (1978). Uptake, transport and metabolism of cytokinin in moss protonema.

Plant and Cell Physiol. 19:839-850.

Felle, H. (1988). Cytoplasmic free calcium in *Riccia fluitans* L. and *Zea mays* L.: interaction of  $\text{Ca}^{2+}$  and pH?

Planta 176:248-255.

Felle, H. (1989).  $\text{Ca}^{2+}$ -selective microelectrodes and their application to plant cells and tissues. (Review).

Plant Physiol. 91:1239-1242.

Feruichi, T., et al. (1990). Distribution of inositol 1,4,5-triphosphate receptor mRNA in mouse tissues.

FEBS Lett. 267:85-88.

Foissner, I. (1990). Wall appositions induced by ionophore A23187,  $\text{CaCl}_2$ ,  $\text{LaCl}_3$  and nifedipine in characean cells.

Protoplasma 154:80-90.

Futers, T.S. (1984). The mode of action of cytokinin in the moss *Physcomitrella patens*.

Ph.D Thesis. University of Leeds. 174pp

Gilroy, S., Read, W.D. & Trewavas, A.J. (1990). Elevation of cytoplasmic calcium by caged calcium or caged inositol triphosphate initiates stomatal closure.

Nature 346:769-771.

Gorton, B.S. & Eakin, R.E. (1957). Development of the gametophyte in the moss *Tortella caespitosa*.

Botan. gaz. 119:31-38.

Graziana, A., Fosset, M., Ranjeva, R., Hetherington, A.M. & Lazdunski, M. (1988).  $\text{Ca}^{2+}$  channel inhibitors that bind to plant cell membranes block  $\text{Ca}^{2+}$  entry into protoplasts.

Biochemistry 27:764-768.

Graziana, A., Bono, J.J., and Ranjeva, R. (1993). Measurements of cytoplasmic calcium by optical fluorescence in plant systems.

Plant Physiol. Biochem. 31(2):277-281.

Gross, J. & Marme, D. (1978). ATP-dependent  $\text{Ca}^{2+}$ -uptake into plant membrane vesicles.

Proc. Nat. Acad. Sci. USA 75:1232-1236.

Grotha, R. (1983). Chlorotetracycline-binding surface regions in gemmalings of *Riella helicophylla* (Bory et Mont.) Mont.

Planta 158:473-481.

Grynkiewicz, G., Poenie, M. & Tsien, R.Y. (1985). A new generation of  $\text{Ca}^{2+}$  indicators with greatly improved fluorescence properties.

J. Biological Chemistry 260:3440-3450.

Hain, R., Stable, P., Czernilofsky, A.P., Steinbiss H.H., Herrera-Estrella, L., and Schell, J. (1985). Uptake, integration, expression and genetic transmission of a selectable chimaeric gene by plant protoplasts.

Mol. Gen. Genet. 199: 161-168.

Handa, A.K. & Johri, M.M. (1979). Involvement of cyclic adenosine-3',5'-monophosphate in chloronema differentiation in protonema cultures of *Funaria hygrometrica*.



*Planta* 144:317-324.

Hahn, S.H. & Saunders, M.J. (1991). Cytokinin increases intracellular  $\text{Ca}^{2+}$  in *Funaria*: detection with Indo-1.

*Cell Calcium* 12: 675-681.

Hanke, D.E., Davies, H., Biffen, M., Connett, R.J.A. & Freathy, T.C. (1989). Cytokinin mode of action - problems and perspectives.

In: *Plant Growth Substances 1988*, ed. R.P. Pharis & S.B. Rood. Heidelberg: Springer-Verlag.

Hartmann, E. & Pfaffmann, H. (1990). Phosphatidyl, inositol and phytochrome-mediated phototropism of moss protonemal tip cells.

In: *Inositol Metabolism in Plants*, ed. D. J. Morre, W.F. Boss & F.A. Loewus. Wiley-Liss, Inc., 259-275.

Harvey, H.J., Venis, M.A., Trewavas, A.J. (1989). Partial purification of a protein from maize (*Zea mays*) coleoptile membranes binding the  $\text{Ca}^{2+}$ -channel antagonist verapamil.

*Biochem. J.* 257:95-100.

Hepler, P.K. & Wayne, R.O. (1985). Calcium and plant development.

*Ann Rev. Plant Physiol.* 36:397-439.

Hicks, G.R., Rayle, D.L., Jones A.M. & Lomax, T.L. (1989). Specific photo-affinity labeling of the plasma membrane polypeptides with an azido auxin.

*Proc. Nat. Acad. Sci. USA* 86:4944-4952.

Idzikowska, K. & Sweykowska, A. (1978). The ultrastructural aspects of cytokinin-induced bud formation in *Ceratodon purpureus*.

*Protoplasma* 94:41-52.

Jaffe, L.F. (1985). The role of calcium explosions, waves, and pulses in activating eggs.

In: *Biology of Fertilisation*, ed. C.B. Metz & A. Monroy. New York: Academic Press, 127-165.

Jaffe, L.F. & Nuccitelli, R. (1974). An ultrasensitive vibrating electrode for measuring

steady extracellular currents.

J. Cell Biol. 63:614-628.

Jenkins, G.I. & Cove, D.J. (1983b). Phototropism and polarotropism of primary chloronemata of the moss *Physcomitrella patens*: responses of the wild type.

Planta 158:357-364.

Jensen, L.C.W. (1981). Division, growth, and branch formation in the protonema of the moss *Physcomitrium turbinatum*: studies of sequential cytological changes in living cells.

Protoplasma 107:301-317.

Johri, M.M. & Desai, S. (1973). Auxin regulation of caulonema formation in moss protonema.

Nature New Biology 245:223-224.

Kauss, H. (1987). Some aspects of calcium-dependent regulation in plant metabolism.

Ann. Rev. Plant Physiol. 38:47-72.

Kiss, H.G., Evans, M.L. & Johnson, J.D. (1991). Cytoplasmic calcium levels in protoplasts from the cap and elongation zone of maize roots.

Protoplasma 163:181-188.

Knight, C.D. & Cove, D.J. (1988). Time-lapse microscopy of gravitropism in the moss *Physcomitrella patens*. In: Methods in Bryology (Ed. J. Glime).

The Hattori Bot. Lab., Nichinan, Miyazaki. pp127-129.

Knight, C.D., Cove, D.J., Boyd, P.J. & Ashton, N.W. (1988). The isolation of biochemical and developmental mutants in *Physcomitrella patens*.

In: Methods in Bryology, ed. by J.M. Glime. The Hattori Bot. Lab., Nichinan. pp47-58.

Knight, C.D. & Cove, D.J. (1991). The polarity of gravitropism in the moss *Physcomitrella patens* is reversed during mitosis and after growth on a clinostat.

Plant, Cell and Environment 14:995-1001.

Knight, M.R., Campbell, A.R., Smith, S.M. & Trewavas, A.J. (1991). Transgenic plant aequorin reports the effects of touch and cold-shock and elicitors on



cytoplasmic calcium.

Nature 352:524-526.

Knight, M.R., Smith, S.M. & Trewavas, A.J. (1992). Wind-induced plant motion immediately increases cytosolic calcium.

Proc. Nat. Acad. Sci. USA 89:4967-4971.

Knight, M.R., Read, N.D., Campbell, A.K. & Trewavas, A.J. (1993). Imaging calcium dynamics in living plants using semi-synthetic recombinant aequorins.

The J. Cell Biol. 121(1): 83-90.

Knoop, B. (1984). Development in bryophytes. Ch. 7

In: The Experimental Biology of Bryophytes, ed. by A.F. Dyer and J.G. Duckett. London: Academic Press. pp 143-169.

Kubowicz, B.D., Yanderhoeff, L.N. & Hanson, J.B. (1982). ATP-dependent calcium transport in *Plasmalemma* preparations from soybean hypocotyles.

Plant Physiol. 69:187-191.

Kuiper, D., Kuiper, P.J.C., Lambers, H., Schuit, J. & Staal, M. (1989). Cytokinin concentration in relation to mineral nutrition and benzyladenine treatment in *Plantago major* ssp. *pleiosperma*.

Physiol. Plant. 75:511-517.

Kuiper, D., Sommarin, M. & Kylin, A. (1991). The effects of mineral nutrition on and benzyladenine on the plasmalemma ATPase activity from roots of wheat and *Plantago major* ssp *pleiosperma*.

Physiol. Plant. 81: 169-174.

Kuiper, D., Sommarin, M. & Kylin, A. (1992). The modulating effects of pH and benzyladenine on the  $\text{Ca}^{2+}$ -and  $\text{Mg}^{2+}$ -ATPases in the plasmalemma of wheat root cells.

Physiol. Plant. 84:367-373.

Kuhtreiber, M. & Jaffe, L.F. (1990). Detection of extracellular calcium gradients with calcium-specific vibrating electrode.

J. Cell Biology, 110: 1565-1573.

Lazarus, C.M., Napier, R.M., Yu, L.-X., Lynas, C. & Venis, M.A. (1991). Auxin-binding protein - antibodies and genes.

In: *Molecular Biology of Plant Development*, ed. G.I. Jenkins & W. Schuch. SEB, 1991, Cambridge: The Company of Biologists Ltd., 129-148.

Loewus, F.A. & Loewus, M.W. (1983). Myo-inositol: its biosynthesis and metabolism.

*Ann Rev. Plant Physiol.* 34:137-161.

McCauley, M.M. & Hepler, P.K. (1990). Visualisation of the endoplasmic reticulum in living buds and branches of the moss *Funaria hygrometrica* by confocal laser scanning microscopy.

*Development* 109:753-764.

McCauley, M.M. & Hepler, P.K. (1992). Cortical ultrastructure of freeze-substituted protonemata of the moss *Funaria hygrometrica*.

*Protoplasma* 169:168-178.

McClelland, D.J. (1988). Genetical studies of gametophyte development in the moss *Physcomitrella patens*.

Ph.D Thesis. University of Leeds. 268pp.

Markmann-Mulisch, U. & Bopp, M. (1987). The hormonal regulation of protonema development in mosses IV. The role of  $\text{Ca}^{2+}$  as cytokinin effector.

*J. Plant Physiol.* 129:155-168.

Marme, D. (1989). The role of calcium and calmodulin in signal transduction.

In: *Second Messengers in Plant Growth and Development*, ed. W.F. Boss & D.J. Morre. New York: Alan R. Liss, Inc., pp57-80.

Marre, E., Lado, P., Ferroni, A. & Ballarin-Denti, A. (1974). Transmembrane potential increase induced by auxin, benzyladenine and fusaric acid. Correlation with proton extrusion and cell enlargement.

*Plant Sci. Lett.* 2:257-265.

Menon, M.K.C. & Lal, M. (1974). Morphogenetic role of kinetin and abscissic acid in the moss *Physcomitrium*.

*Planta* 115:319-328.



- Messiaen, J., Read, N.D., Cutsem, P. Van & Trewavas, A.J. (1993). Cell wall oligogalacturonides increase cytosolic free calcium in carrot protoplasts.  
J. Cell Sci. 104:365-371.
- Michell, R.H. (1975). Inositol phospholipids and cell surface receptor functions.  
Biochim. Biophys. Acta 415:81-147.
- Miller, D.D., Callaham, D.A., Gross, D.J. & Hepler, P.K. (1992). Free  $\text{Ca}^{2+}$  gradient in growing pollen tubes of *Lilium*.  
J. Cell Sci. 101: 7-12.
- Miyazaki, S. (1988). Inositol 1,4,5-Trisphosphate-induced calcium release and Guanine nucleotide-binding protein-mediated periodic calcium rises in golden hamster eggs.  
J. Cell Biol. 106:345-353.
- Olah, Z., Berczi, A. & Erdei, L. (1983). Benzylaminopurine-induced coupling between calmodulin and Ca-ATPase in wheat root microsomal membranes.  
FEBS Lett. 154: 395-399.
- Oparka, K.J. (1991). Uptake and compartmentation of fluorescent probes by plant cells.  
J. Exp. Bot. 42(238):565-579. (check ref to text).
- Parsons, A., Blackford, S. & Sanders, D. (1989??). Kinetin-induced stimulation of electrogenic pumping in soybean suspension cultures is unrelated to signal transduction.  
Planta 178:215-222.
- Pickard, B.G. (1985) Roles of hormones, protons and calcium in geotropism.  
In: Encyclopaedia of Plant Physiology, New Series, Vol. 11, ed. R.P. Pharisi and D.M. Reid. Berlin, New York:Springer-Verlag, 193-281.
- Prasher, D.C., McCann, R.O., & Cormier, M.J. (1985). Cloning and expression of the cDNA coding for aequorin, a bioluminescent calcium-binding protein.  
Biochem. Biophys. Res. Commun. 126: 1259-1268.

Ranjeva, R., Refeno, G., Boudet, A.M. and Marme, D. (1983). Activation of plant quinate:NAD<sup>+</sup> 3-oxidoreductase by Ca<sup>2+</sup> and calmodulin.

Proc. Nat. Acad. Sci. USA 80:5222-5224.

Ranjeva, R. & Boudet, A.M. (1987). Phosphorylation of proteins in plants: regulatory effects and potential involvement in stimulus/response coupling.

Ann. Rev. Plant Physiol. 38:73-93.

Ranjeva, R., Graziana, A., Mazars C., and Thuleau, P. (1992). Putative L-type calcium channels in plants: biochemical properties and subcellular localisation.

In: Transport and Receptor Proteins: Molecular Structure and Function, ed. D.T. Cooke & D.T. Clarkson. London: Plenum Press, 145-153.

Rasmussen, H., Goodman, D.B.P. & Tenenhouse, A. (1972). The role of cyclic AMP and calcium in cell activation.

CRC critical reviews in biochemistry 1:95-148.

Read, N.D., Allan, W.T.G., Knight, H., Knight, M.R., Malho, R., Russell, A., Shacklock, P.S. and Trewavas, A.J. (1992). Imaging and measurement of cytosolic free calcium in plant and fungal cells.

Journal of Microscopy 166(1):57-86.

Reed, P.W. & Lardy, H.A. (1972). A23187: a divalent cation ionophore.

J. Biol. Chem. 247(21):6970-6977.

Reski, R., Wehe, M., Hader, B., Marienfeld, J.R. & Abel, W.O. (1991). Cytokinin and light quality interact at the molecular level in the chloroplast-mutant PC22 of the moss *Physcomitrella*.

J. Plant Phys. 138:236-243.

Rincon, M. & Boss, W.F. (1987). Myo-inositol trisphosphate mobilises calcium from fusogenic carrot (*Daucus carota* L.) protoplasts.

Plant Physiol. 83:395-398.

Roux, S.J. & Slocum, R.D. (1982). Role of calcium in mediating cellular functions important for growth and development in higher plants.

In: Calcium and Cell Function, Vol. 3, ed. W.Y. Cheung. New York: Academic Press, pp409-453.



Rowler, F. & Bopp, M. (1985). Ethylene synthesis in moss protonema.  
J. Plant Physiol. 117:331-338.

Saunders, M.J. (1986). Cytokinin activation and redistribution of plasma-membrane ion channels in *Funaria*. A vibrating-microelectrode and cytoskeleton-inhibitor study.  
Planta 167:402-409.

Saunders, M.J. (1992). Cytokinin signal transduction through  $\text{Ca}^{2+}$  in mosses.  
In: Progress in Plant Growth Regulation, ed C.M. Karssen, L.C. Van Loon, D. Vreugdenhill. Dordrecht, Boston, London: Kluwer Academic Publ., 1992.

Saunders, M.J. & Hepler, P.K. (1981). Localization of membrane-associated calcium following cytokinin treatment in *Funaria* using chlorotetracycline.  
Planta 152:272-281.

Saunders, M.J. & Hepler, P.K. (1982). Calcium ionophore A23187 stimulates cytokinin-like mitosis in *Funaria*.  
Science 217:943-945.

Saunders, M.J. & Hepler, P.K. (1983). Calcium antagonists and calmodulin inhibitors block cytokinin-induced bud formation in *Funaria*.  
Developmental Biology 99:41-49.

Sawahel, W., Onde, S., Knight, C.D. & Cove, D. (1992). Transfer of foreign DNA into *Physcomitrella patens* protonemal tissue by using the gene gun.  
Plant Molecular Biology Reporter 10(4):315-316.

Schaefer, D., Zryd, J.P., Knight, C.D. & Cove, D.J. (1989). Stable transformation of the moss, *Physcomitrella patens*.  
Molec. gen. Genet.

Scheverlein, R., Schmidt, K., Poenie, M. & Roux, S.J. (1991). Determination of cytoplasmic calcium concentration in *Dryopteris* spores.  
Planta 184:166-174.

Schiefelbein, J.W., Shipley, A. & Rowse, P. (1992). Calcium influx at the tip of growing root-hair cells of *Arabidopsis thaliana*.

*Planta* 187:455-459.

Schmiedel, G. & Schnepf, E. (1979a). Side branch formation and orientation in caulonema of the moss *Funaria hygrometrica*: Normal development and fine structure.

*Protoplasma* 100:367-383.

Schmiedel, G. & Schnepf, E. (1979b). Side branch formation and orientation in caulonema of the moss *Funaria hygrometrica*: Experiments with inhibitors and with centrifugation.

*Protoplasma* 101:47-59.

Schmiedel, G. & Schnepf, E. (1980). Polarity and growth of caulonema tip cells of the moss *Funaria hygrometrica*.

*Planta* 147:405-413.

Schneider, J. & Szweykowska, A. (1974). Changes in enzyme activities accompanying cytokinin-induced formation of gametophore buds in *Ceratodon purpureus*.

*Z. Pflanzenphysiol.* 72:95-106.

Schneider, J., Szweykowska, A. & Spychala, M. (1975). Evidence against mediation of adenosine-3',5'-cyclic monophosphate in the bud-inducing effect of cytokinins in moss protonemata.

*Act. Soc. Bot. Pol.* XLIV:607-614.

Schroeder, J.I. & Thuleau, P. (1991).  $\text{Ca}^{2+}$  channels in higher plant cells.

*The Plant Cell* 3:551-558.

Schroeder, J.I. & Hagiwara, S. (1990) Repetitive increases in cytosolic  $\text{Ca}^{2+}$  of guard cells by abscissic acid activation of non-selective  $\text{Ca}^{2+}$  channels.

*Proc. Natl. Acad. Sci. USA* 87 9305-9309.

Schwuchow, J., Sack, F.D. & Hartmann, E. (1990). Microtubule distribution in gravitropic protonema of the moss *Ceratodon*.

*Protoplasma* 159:60-69.

Sergeeva, L.I., Machackova, I., Eder, J., Konstantinova, T.N., Aksenova, N.P. and



Chailakhyan, M.Kh. (1992). Levels of free cytokinins and IAA in potato plants grown *in vitro* in light of different spectral quality.

In: Physiology and Biochemistry of Cytokinins in Plants, ed. M. Kaminek, D.W.S. Mok and E. Zazimalova. The Hague: SPB Academic Publishing, 365-367.

Shacklock, P.S., Read, N.D. and Trewavas, A.J. (1992). Cytosolic free calcium mediates red light-induced photomorphogenesis.

Nature 358:753-755.

Sharma, S. & Johri, M.M. (1982). Partial purification and characterization of cyclic AMP phosphodiesterases from *Funaria hygrometrica*.

Archives of Biochemistry and Biophysics 217:87-97.

Sharma, S. & Johri, M.M. (1983). Cyclic AMP phosphodiesterases of *Funaria hygrometrica*.

Phytochem. 22:2715-2717.

Sheldrake, A.R. (1971). The occurrence and significance of auxin in the substrata of bryophytes.

New Phytol. 70:519-526.

Shiina, T., & Tazawa, M. (1987). Demonstration and characterisation of  $\text{Ca}^{2+}$  channel in tonoplast-free cells of *Nitellopsis obtusa*.

J. Membr. Biol. 96, 263-276.

Simon, P.E. & Naef, J.B. (1981). Light dependency of the cytokinin-induced bud initiation in protonema of the moss *Funaria hygrometrica*.

Physiol. Plantarum 53:13-18.

Sironval, C. (1947). Experiences sur les stades de developpement de la forme filamenteuse en culture de *Funaria hygrometrica*.

L. Bull. Soc. Bot. Belg. 79:48-69.

Slocum, R.D. & Roux, S.J. (1983). Cellular and subcellular localisation of calcium in gravistimulated oat coleoptiles and its possible significance in the establishment of tropic curvature.

Planta 157: 481-492.

Sutherland, E.W., Robinson, G.A., Butcher, R.W. (1968). Some aspects of the biological role of adenosine 3'-5'-monophosphate (cAMP).

Circulation 37:279-306.

Szweykowska, A., Dornowska, E., Cybulska, A. & Wasiek, G. (1971). The cell division response to cytokinins in isolated cell cultures of the protonema of *Funaria hygrometrica* and its comparison with the bud induction response.

Biochem. Physiol. Pflanzen (BPP) 162:514-525.

Szweykowska, A., Korcz, I., Ja\_kiewicz-mroczkowska, B. & Metelska, M. (1972). The effect of various cytokinins and other factors on the protonemal cell divisions and the induction of gametophores in *Ceratodon purpureus*.

Act. Soc. Bot. Pol. 41:401-409.

Talbot, J. & Saunders, M.J. (1986). Fluctuation of IP<sub>3</sub> concentration during cytokinin-induced bud formation in *Funaria*.

Plant Physiol. 80S: 113.

Tester, M. (1990). Plant ion channels: whole-cell and single-channel studies. Tamsley Review 21.

New Phytol. 114:305-340

Tester, M. & MacRobbie, E.A.C. (1990). Cytoplasmic calcium affects the gating of potassium channels in the plasma membrane of *Chara corallina*: a whole-cell study using calcium-channel effectors.

Planta 180:569-581.

Towbin, H., Staehelin, T. & Gordon, J. (1979). Electrophoretic transfer of proteins from polyacrylamide gels to nitrocellulose sheets: procedure and some applications.

Proc. Nat. Acad. Sci. USA 76: 4350-4354.

Tretyn, A. (1987). Influence of red light and acetylcholine on <sup>45</sup>Ca<sup>2+</sup> uptake by oat coleoptile cells.

Cell Biol. Int. Rep. 11:887-896.

Tretyn, A., Wagner, G. & Felle, H. (1991). Signal transduction in *Sinapsis alba* root hairs: auxins as external messengers.

J. Plant Physiol. 139:187-193.



Trewavas, A.J. & Gilroy, S. (1991). Signal transduction in plant cells.

Trends Genet. 7:356-361.

Tsein, R.Y. & Poenie, M. (1986). Fluorescence ratio-imaging: a new window into intracellular ionic signalling.

TIBS 11:450-455.

Venis, M.A. & Napier, R.M. (1990). Characterisation of auxin receptors.

In: Hormone Perception and Signal Transduction in Plants, ed. J. Roberts, C. Kirk & M. Venis. Cambridge: Company of Biologists, 55-65.

Wacker, I. & Schnepf, E. (1990). Effects of nifedipine, verapamil and diltiazem on tip growth in *Funaria hygrometrica*.

Planta 180:492-501.

Wahl, M., Lucherini, M.J. & Gruenstein, E. (1990). Intracellular  $\text{Ca}^{2+}$  measurement with Indo-1 in substrate-attached cells: advantages and special considerations.

Cell Calcium 11: 487-500.

Wang, T.L., Cove, D.J., Beutelmann, P. & Hartmann, E. (1980). Isopentenyladenine from mutants of the moss, *Physcomitrella patens*.

Phytochemistry 19:1103-1105.

Wang, T.L., Futers, T.S., McGeary, F. & Cove, D.J. (1984). Moss mutants and the analysis of cytokinin metabolism.

In: The Biosynthesis and Metabolism of Plant Hormones, ed. A. Crozier & J.R. Hillman. Cambs. Univ. Press. pp135-164.

Yoshida, K. & Yamamoto, K. (1982). The position of bud differentiation on protonema of the moss *Physcomitrium sphearicum*.

Plant and Cell Physiol. 23:737-743.

Zbell, B., Schwendemann, I. & Bopp, M. (1989). High-affinity GTP-binding on microsomal membranes prepared from moss protonema of *Funaria hygrometrica*.

J. Plant Physiol. 134:639-641.

Zherelova, O.M. (1989) Effect of calmodulin inhibitors on functioning of potential-

dependent calcium channels of the *Nitellopsis obtusa* plasmalemma.  
Sov. Plant Physiol. 35:499-504.